MARMARA MEDICAL JOURNAL

VOLUME: 37 • ISSUE : 2 • MAY 2024
ONLINE ISSN: 1309-9469
PRINT ISSN: 1019-1941

MARMARA UNIVERSITY PRESS

School of Medicine
Marmara Med J

MARMARA
MEDICAL JOURNAL

VOLUME 37 • ISSUE 2 • MAY • 2024

Correspondence and Communications
Seza Arbay
Marmara Üniversitesi Tıp Fakültesi Dekanlığı,
Temel Tıp Bilimleri Binası, 3. Kat, Başıbüyük Mahallesi,
Başıbüyük, Maltepe, İstanbul, Turkey
Tel: +90 216 4144734, Faks: +90 216 4144731
E-mail: mmj@marmara.edu.tr

Publisher
Marmara University Press
Göztepe Kampüsü, Kadıköy 34722 İstanbul, Turkey
Tel. +90 216 777 1400, Faks +90 216 777 1401
E-mail: yayinevi@marmara.edu.tr
Typesetting: Burcu Diker, Burcu Yıldırım, Hakan Temeloğlu

VOLUME 37 • ISSUE 2 • MAY • 2024

Instructions to Authors

About Journal

The Marmara Medical Journal, Marmara Med J, is a multidisciplinary, academic publication of Marmara University, School of Medicine. It is an open access, double blind peer-reviewed journal. It publishes manuscripts that focus on clinical and laboratory medicine, health care policy and medical education, ethics, and related topics. It includes original research papers, case reports, reviews, articles about clinical and practical applications and editorials, short reports, letters to the editor and occcasionally a photo-quiz.

The Marmara Medical Journal is continuously published since 1988 and its archive with full-text manuscripts can be reached under www.dergipark.org.tr/marumj/archive.

Frequency: Three times a year (January, May, October)

Year of first print issue: 1988

Year of first online issue: 2004 (Between 2004 and 2011 the Journal was published solely in an electronic format.)

Language: English
Print ISSN: 1019-1941 **eISSN:** 1309-9469

The manuscripts published in the Marmara Medical Journal are indexed and abstracted in: Thomson Reuters/ Emerging Sources Citation Index (ESCI), EBSCO, SCOPUS, EMBASE/Excerpta Medica, DOAJ (Directory of Open Access Journals), CrossRef, ULRICH'S Database, Google Scholar, The British Library, Turkish Academic Network and Information Center (ULAKBİM)-Turkish Medical Database, TURK MEDLINE–Türk Sağlık Bilimleri (Index of Turkish Health Sciences), Türkiye Makaleler Bibliyografyası (Bibliography of Articles in Turkish Periodicals), Türkiye Klinikleri Tip Dizini (Turkish Citation Index).

Aims and Scope

The Marmara Medical Journal, Marmara Med J, is a peer-reviewed, multidisciplinary academic publication of Marmara University, School of Medicine, which is authored by physicians both nationally and internationally.

The journal aims to publish papers of general interest relating to advances in medical practice and novel treatments that will be of interest to general practitioners, medical students, and senior practitioners and specialists. Marmara Medical Journal also aims to publish all types of research conducted by medical students.

The Marmara Medical Journal is among the most widely read and cited scientific publications for physicians among journals of its kind nationally and increasingly gaining new readers and authors internationally with its English only format since 2016.

The journal consists of manuscripts on recent developments in general and internal medicine and new methods of treatment based on original research. We greatly welcome research papers, case reports, reviews and occasionally a photo-quiz of an interesting medical encounter in English, only.

Each manuscript is strictly assessed by a select Editorial Board. and refereed critically by two or more reviewers, at least one from another institution. The editor reserves the right to reject or to return the manuscript to the author(s) for additional changes.

Special review issues with invited editors are published since 2015 to focus on specific areas of medicine to bring recent data into attention covering multiple aspects of the chosen topic. Marmara Medical Journal welcomes and encourages physicians from all over the world to publish a special review issue on the topic of their preference as an "Invited editor" to collaborate with authors on the same focus area with the aim of increasing scientific collaboration via publishing.

The Marmara Medical Journal has an open access policy. All articles in the journal are permanently available online for all to read.

Author Guidelines

The Marmara Medical Journal publishes original scientific research papers, case reports, manuscripts about clinical and practical applications and editorials, short reports, letters and occasionally a photo-quiz.

Manuscripts submitted under multiple authorship are reviewed on the assumption that all listed authors concur with the submission and that a copy of the final manuscript has been approved by all authors and tacitly or explicitly by the responsible authorities in the laboratories where the work was carried out.

Manuscripts are accepted for review with the understanding that no substantial portion of the study has been published or is under consideration for publication elsewhere.

VOLUME 37 • ISSUE 2 • MAY • 2024

The Marmara Medical Journal is in compliance with the Uniform Requirements for Manuscripts Submitted to Biomedical Journals created by International Committee for Medical Editors (ICMEJ link), the World Association of Medical Editors (WAME), the Council of Science Editors (CSE), the Committee on Publication Ethics (COPE) and the European Association of Science Editors (EASE).

Preparation of the Manuscript

1. Manuscript files must be prepared in Word, WordPerfect, EPS, LaTeX, text, Postscript, or RTF format. Figures/Images should be embedded in the manuscript file or sent as external files in TIFF, GIF, JPG, BMP, Postscript, or EPS format.

2. Manuscripts should be approximately 20-25 pages double-spaced, including references, with margins of 2.5 cm.

Pages should be numbered consecutively and organized as follows:

1. Title Page
2. Abstract
3. Keywords
4. Introduction
5. Materials and Methods
6. Results
7. Conclusion
8. References

1. Title Page

The title page should contain the article title, authors' names and academic or professional affiliations, and the address for manuscript correspondence (including e-mail address, Open Researcher and Contributer ID (ORCID) identifier, telephone and fax numbers).

2. Abstract

Abstract of not more than 200 words must be included. The abstract should be divided into the following sections: Objective, Materials and Methods, Results and Conclusion,

3. Keywords

Three to six keywords should be supplied below the Abstract and should be taken from those recommended by the US National Library of Medicine's Medical Subject Headings (MeSH).

http://www.nlm.nih.gov/mesh/meshhome.html

4. Introduction

State why the investigation was carried out, note any relevant published work, and delineate the objective of the investigation.

5. Materials and Methods

New methods or significant improvements of methods or changes in old methods must be described. Methods for which an adequate reference can be cited are not to be described, except for providing information about the aims of the method. Details regarding animal housing conditions should be given. All clinical studies must contain :

1. A statement that all experimental protocols have been approved by the Ethical Committee of the Institution prior to the commencement of the studies,

2. A statement that all participants gave informed consent.

6. Results

Duplication between the text of this section and material presented in tables and figures should be avoided. Tabular presentation of masses of negative data must be avoided and replaced with a statement in the text whenever possible. The results must be presented clearly, concisely and without comment.

7. Discussion

The discussion should begin with a brief summary of the findings, followed by the following: how this study is similar or different from prior studies with regards to methods and results and limitations of this study. This section must also relate the significance of the work to existing knowledge in the field and indicate the importance of the contribution of this study.

8. References

The style of references is that of the Index Medicus. List all authors when there are six or fewer, when there are seven or more list the first three, then add "et al.". Unpublished results or personal communications should be cited as such in the text. Where a doi number is available it must be included at the end of the citation. Please note the following examples:

i. Yazici D, Taş S, Emir H, Sunar H. Comparison of premeal mixed insulin three times daily and basal – bolus insulin therapy started post-operatively on patients having coronary artery bypass graft surgery. Marmara Med J 2011; 25:16-9.doi: 10.5472/

ii. Walker M, Hull A. Preterm labor and birth. In: Taeusch HW, Ballard RA, eds. Avery's Diseases of the Newborn. Philadelphia: WB Saunders, 1998: 144,153.

iii. Hagström H, Nasr P, Ekstedt M, et al. Fibrosis stage but not NASH predicts mortality and time to development of severe liver disease in biopsy-proven NAFLD. J Hepatol 2017; 67: 1265-73. doi: 10.1016/j.jhep.2017.07.027.

iv. WONCA Ad Hoc Task Force on Tobacco Cessation.

http://globalfamilydoctor.com/publications/new/november/09.htm
(Accessed on …….)

In the text, reference numbers should be placed in square brackets [ ], and placed before the punctuation; for example [1], [1-3] or [1,3]. References must be numbered consecutively in the order they are first mentioned.

Figures, Tables, Units

Diagrams and illustrations should be given Arabic numerals. All figure legends should be grouped and written on a separate page. Each Figure should be in one of the following preferred formats: Tiff, JPEG, PDF, and EPS.Tables should be numbered consecutively with Roman numerals in order of appearance in the text. Type each table double-spaced on a separate page with a short descriptive title directly above and with essential footnotes below.

Units will be in general accordance with the International System (SI) as adopted by the 11th General Conference on Weights and Measures.

Ethical Issues

Compliance with the principles of the last version of the Declaration of Helsinki for humans and the European Community guidelines for the use of animals in experiments is accepted as a policy by the Marmara Medical Journal. Studies involving human or animal subjects should conform to national, local and institutional laws and requirements. Manuscripts which do not properly consider ethical issues for humans or animals will not be accepted for publication.

http://www.wma.net/e/policy/b3.htm

Double-blind Review

This journal uses double-blind review, which means that both the reviewer and author identities are concealed from the reviewers, and vice versa, throughout the review process. To facilitate this, authors need to ensure that their manuscripts are prepared in a way that does not give away their identity.

Plagiarism

Manuscripts are investigated for possible plagiarism once they are accepted for possible publication. If an author receives a plagiarism notice regarding his/her manuscript, the corrections should be made within one month. If the Editorial Board detects any plagiarism on the second check after correction of the manuscript by the authors, the chief editor can reject the manuscript. your article will be checked by the plagiarism detection software iThenticate.

Funding Source

All sources of funding should be declared as an acknowledgment at the end of the text.

Following Documents are Required Prior Publication

Approval of the Institutional Ethics Committee

a) Marmara Medical Journal requires that investigations performed on human subjects have the prior approval of the Institutional Ethics Committee on Human Experimentation. Authors are required to submit a signed statement as to the date and details of the appropriate review. The authors must state that the investigation conforms with the principles of Declaration of Helsinki.

b) When studies involve the use of experimental animals, manuscripts should briefly describe the procedures employed for animal care and handling. Where drugs are used at particular concentrations in intact animal systems, the author should indicate some rationale for selection of the particular concentration.

Copyright Release Form

Copyright Release Form must be read and signed by all authors.

Copyright Release Form pdf

Authorship

It is the responsibility of every researcher listed as an author of a manuscript in Marmara Medical Journal to have contributed in a meaningful and identifiable way to the design, performance, analysis, and reporting of the work and to agree to be accountable for all aspects of the work.

Before publication, each author must sign a statement attesting that he or she fulfills the authorship criteria of the

ICMJE Recommendations.

http://www.icmje.org/recommendations/

Financial Associations/Conflicts of Interest

All participants – not only the corresponding author – must consider their conflicts of interest when fulfilling their roles in the process of article preparation and must disclose all relationships that could be viewed as potential conflicts of interest according to the Committee on Publication Ethics (COPE) Guidelines and/ or Recommendations for the Conduct, Reporting, Editing, and Publication of Scholarly Work in Medical Journals (ICMJE) Recommendations. Disclosure forms filed by all authors alongside the full text of each article is mandatory.

https://publicationethics.org/guidance/Guidelines

http://www.icmje.org/recommendations/

We encourage the authors on using the ICMJE Form for Disclosure of Conflicts of Interest to standardize authors' disclosures.

Conflict of Interest Form.pdf

Statement of Human Rights and Statement ofAnimal Rights

Statement of human rights and statement of animal rights, when necessary, must be signed by all authors prior publication.

Statement of human and animal rights form.pdf

Patient Consent for Publication

Patients have a right to privacy. Identifying information, including patients' names, initials, or hospital numbers, should not be published in written descriptions, photographs or in any kind of patient-related materials. In circumstances where this information is essential for scientific purposes, authors should obtain the patient's (or the legal guardian's) written informed consent prior to the publication.

Patient Consent for Publication pdf

VOLUME 37 • ISSUE 2 • MAY • 2024

Statement of Human Rights

Title:

This is to certify that the procedures and the experiments followed for the manuscript were in accordance with the ethical standards of the …… Ethics Committee on human experimentation and with the ethical standards in the Declaration of Helsinki 2013, as well as the national law.

Author's Name	Signature	Date
…….	……...	…….
…….	……...	……...
……...	…….	…….

Statement of Animal Rights

Title:

This is to certify that the procedures and the experiments were conducted in accord with the highest scientific, humane and ethical principles of the Institutional and National Guide for the Care and Use of Laboratory Animals.

Author's Name	Signature	Date
…….	……...	…….
…….	……...	……...
……...	…….	…….

School of Medicine
Marmara Med J

MARMARA
MEDICAL JOURNAL

VOLUME 37 • ISSUE 2 • MAY • 2024

Contents

Review Articles

Original Articles

VOLUME 37 • ISSUE 2 • MAY • 2024

MARMARA
MEDICAL JOURNAL

Review Article

https://dergipark.org.tr/tr/pub/marumj

SCUBE in human diseases: A systematic review

Hirowati ALI[1]

[1] Department of Biochemistry and Biomedical Laboratory/Center for Integrated Biomedical Research, Faculty of Medicine, Universitas Andalas, Indonesia

Corresponding Author: Hirowati ALI
E-mail: hirowatiali@med.unand.ac.id

Submitted: 16.04.2023 **Accepted:** 01.09.2023

ABSTRACT

The involvement of the Signal peptide-complement components of C1r/C1s, the sea urchin Uegf and Bone Morphogenetic Protein (CUB) domain-Epidermal Growth Factor (EGF)-related (SCUBE) gene in human diseases has been progressively apparent. The SCUBE1 is detectable in platelet-aggregation diseases. The SCUBE2 is reported to have a better cancer survival prognosis. However, SCUBE3 is detected in bone-related diseases. SCUBE gene interacts with Hedgehog (Hh) signaling pathway and epidermal growth factor receptor (EGFR), which has a wide range of biological functions such as cell proliferation, apoptosis, differentiation, and activation of platelet activity.

The current review is a systematic review performed using SCOPUS, Cochrane, and Pubmed/Medline according to The Preferred Reporting Items for Systematic Reviews and Meta-Analysis Protocol (PRISMA-P) guidelines. This review discusses the entanglement of the SCUBE gene's potential role in human diseases. Examining the role of the SCUBE family sheds new light on platelet aggregation-related diseases, cancer prognosis, and their pathogenesis.

Keywords: SCUBE, Human diseases, Hedgehog (Hh) pathway

1. INTRODUCTION

Signal peptide-CUB domain-EGF-related (SCUBE) genes encode a cell surface glycoprotein known to be present in humans, mice, and zebrafish. SCUBE belongs to the EGF superfamily characterized by NH2-terminal signal peptide sequence, nine copies of epidermal growth factor (EGF)-like repeats, spacer region, three cysteine-rich motifs, and one complement C1r/C1s, Uegf, Bmp1(CUB) domain. The CUB domain is an extracellular domain involved in developmental processes and zinc-metalloprotease activities. The EGF has been known as a mitogen for various tissues especially involved in wound healing, cancer, and angiogenesis. Many genes that contain EGF-like repeats are involved in cell lysis, cell movement, signaling molecules, transmembrane receptors, and blood coagulation pathways. Moreover, EGF-like repeats also transform growth factor-α and LDL receptors in cholesterol metabolism [1-3].

Like other genes of the EGF superfamily, SCUBE plays an important role during development, organogenesis, and morphogenesis. Biochemical studies for the SCUBE gene showed that this gene encoded protein SCUBE which is extracellular and membrane-anchored glycoproteins. SCUBE gene has been associated with Hedgehog (Hh) signaling pathway. This gene is known as upstream signaling of the Hh pathway. Mutation in the SCUBE gene was detrimental to organ development, such as delayed dorsal aorta development, the absence of lateral floor plate, and slow muscle development [4-9]. There are three family members of SCUBE genes, which are SCUBE1, SCUBE2, and SCUBE3. Previous studies showed that SCUBE1, SCUBE2, and SCUBE3 were expressed in endothelium and showed unique expression profiles during embryogenesis. SCUBE1 has been found in developing the central nervous system, gonad, anterior surface ectoderm, and limb buds. This gene showed a substantial similarity with other family members, the SCUBE2 gene.

SCUBE1 involves in bone morphogenetic protein (BMP) signaling. SCUBE1 is linked to platelet activated-diseases such as thrombus, atherosclerotic plaque, inflammation, and hypoxia-related disorders. Soluble SCUBE1 is detected in activated platelet and is a promising biomarker in acute coronary syndrome and ischemic stroke. A recent study has shown that the SCUBE1 level is higher in patients who have achieved spontaneous circulation return, implying its role in cellular vitality [10-12]. Interestingly, the SCUBE2 gene is expressed ubiquitously in the lung, heart, and testis, which is not

How to cite this article: Ali H. SCUBE in human diseases: A systematic review. Marmara Med J 2024: 37(2):106-114. doi: 10.5472/marumj.1484448

ISSN: 1309-9469

http://doi.org/10.5472/marumj.1484448
Marmara Med J 2024;37(2): 106-114

expressed in the SCUBE1 gene. SCUBE2 has been reported in various cancer, angiogenesis, and cardiovascular diseases.

Furthermore, the SCUBE3 gene is expressed abundantly in osteoblasts. In humans, SCUBE3 mutations are linked to abnormalities in the growth and differentiation of both bones, further involved in bone-related bones [12-14]. Despite the fact that the SCUBE gene has been identified for decades, the development of research on its biological functions has made significant progress in disclosing the potential mechanism of human diseases, such as cancers, metabolic abnormalities, and cardiovascular diseases. This review highlights recent progress in understanding the SCUBE gene and its role in human disease.

2. METHODS

The literature search strategy for this systematic review was performed using SCOPUS, Cochrane and Pubmed/Medline, according to The Preferred Reporting Items for Systematic Reviews and Meta-Analysis Protocol (PRISMA-P) guidelines [15]. Keywords for English considered papers were SCUBE1, SCUBE2, and SCUBE3 in human diseases such as cancer, cardiovascular, and other inflammations. Selection process according to PRISMA-P guidelines is shown in a flow diagram (Figure 1). Inclusion criteria were screened by titles and abstracts, and published in the English language. Papers excluded if articles were not written in English and not focused on SCUBE1, SCUBE2, SCUBE3 and its effect on human diseases. The articles excluded if the report presented the SCUBE family in animal study.

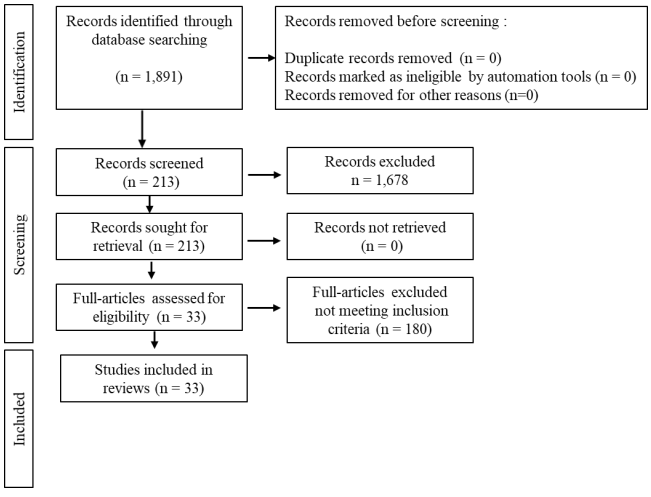

Figure 1. *Selection of papers included in the current review. Relevant papers included SCUBE1, SCUBE2 and SCUBE3 in human studies.*

The review article excluded for the present systematic review. Collected papers were selected from the journals with the SCOPUS impact factors, and organized further analyzed based on the SCUBE family, mechanism in the disease and biological functions. Inclusion criteria in this systematic review (Table I, Table II, Table III).

Table I. *SCUBE1 involves platelet activation leading to thrombosis. The elevated levels of SCUBE1 and sCD40L lead to platelet-aggregating activities*

Type of Disease	Biological function and mechanism	References
Acute Coronary Syndrome	Platelet activation : increased SCUBE1, increased sCD40L	[11,26]
Ischemic Stroke	Platelet activation : increased SCUBE1, increased sCD40L	[26]
Myocardial infraction	Platelet activation : increased SCUBE1, late ST development	[27]
Hypertension	Platelet activation : increased SCUBE1, increased sCD40L	[28]
Gestational Diabetes Mellitus, Diabetic Retinopathy	Platelet activation : increased SCUBE1, increased malondialdehyde (MDA) level	[29-30]
Pulmonary Embolism	Thrombosis : increased SCUBE1	[31-32]
Pulmonary hypertension without the presence of CAD and NICM	Thrombosis : decreased SCUBE1, increased mPAP* and PVR**, RV dysfunction***	[33]
Hashimoto's Thyroiditis	Platelet activation : increased SCUBE1, increased sCD40L, increased LDL-C, triglycerides	[34]
Hyperthyroidism	Platelet activation : increased SCUBE1	[35]
Sepsis	Platelet activation, inflammation : increased SCUBE1, increased CRP, increased platelet count	[36]
COVID-19 with thrombotic complications	Platelet activation: increased SCUBE1	[37]
Psoriasis	Angiogenesis : increased SCUBE1	[38]
Ovarian Torsion	Unknown : increased SCUBE1	[39]
Renal Cancer	Probably thrombosis : increased SCUBE1	[40]
Gastric cancer	Probably thrombosis : increased SCUBE1	[41]

**mPAP= mean pulmonary artery pressure; ** PVR =pulmonary vascular resistance; ***RV dysfunction =right ventricular dysfunction*

Table II. *SCUBE2 gene increased and played a role as a tumor suppressor gene*

Type of Disease	Biological function and mechanism	References
Diabetes Mellitus Type 2, Dyslipidemia	Endothelial dysfunction : increased SCUBE2, increased ET-1	[44]
Nasopharyngeal carcinoma	Tumor suppressor gene : increased SCUBE2	[47]
Glioma	Tumor suppressor gene : increased SCUBE2	[48]
Kaposi's Sarcoma	Inflammation : increased SCUBE2	[49]
Colorectal cancer	Tumor suppressor gene : increased SCUBE2	[50]
Breast cancer prognosis	Tumor related gene : suppression of SCUBE2	[51, 52, 54, 55]
Bladder cancer	Tumor suppressor gene : increased SCUBE2	[53]
Endometrial cancer	Tumor suppressor gene, associated with estrogen receptor and progesterone receptor : increased SCUBE2	[56]

http://doi.org/10.5472/marumj.1484448
Marmara Med J 2024;37(2): 106-114

Table III. *SCUBE3 is highly expressed in bone. In human diseases, SCUBE3 is found in breast cancer, renal carcinoma, and lung disease. Interestingly, one study showed SCUBE3 in a patient with a higher risk of psychiatric disorder.*

Type of Disease	Biological function and mechanism	References
Breast cancer	Tumor suppressor gene : increased SCUBE3, downstream of TGF-β, ER	[65-67]
Renal carcinoma	Tumor methylation : increased SCUBE3, CpG island methylation	[68]
Lung cancer	Tumor related gene : overexpression of SCUBE3	[69]
Psychiatric disorder	Synaptic plasticity : increased SCUBE3, probably extracellular matrix (ECM) production	[70]

3. RESULTS

SCUBE1

The first member of the SCUBE gene family is SCUBE1. In developing mouse embryos, SCUBE1 is detected in the ectoderm, neuroectoderm of the ventral forebrain, infundibulum, dermomyotome, digital mesenchyme, urogenital ridge, and hair follicles. In adult tissues, the SCUBE1 gene is highly expressed in the liver, kidney, lung, small intestine, brain, colon, and spleen. SCUBE1 gene consists of 988 amino acids and contains 9 EGF-like repeats expressed in extracellular matrix protein (ECM) [10-18]. The secretion pathway of SCUBE1 is determined by the spacer region between the EGF-like domain and cysteine-rich repeats and acts as a Ca^{2+}-dependent cell-to-cell adhesion molecule. This gene was co-expressed with platelet-derived growth factor (PDGF)-D, interleukin (IL)-8, or IL-17F. The gene expression profiling study using fluorescent cationic liposomes specific for detecting vascular endothelial cells has shown detectable SCUBE1 expression in endothelial cells of normal lung vasculature. Based on a previous cellular study, SCUBE1 can form homomeric and heteromeric complexes with SCUBE2 through its EGF-like repeats which is critical for SCUBE1 secretion. Moreover, human vein endothelial cells (HUVEC) treated with IL-1β and TNF-α has shown downregulation of SCUBE1 expression. Injection of lipopolysaccharide (LPS) into C57BL/6 mice downregulated SCUBE1 expression as well, implying its response to inflammatory stimulation [19-22].

An immunohistochemical analysis has indicated that the SCUBE1 is mainly expressed to the intravascular platelet-rich thrombus in α-granules upon platelet stimulation. The study of gene expression profiling of lung endothelial cells has exhibited the SCUBE1 expression in endothelial cell fraction as well as the expression of other growth factors and signaling genes such as endothelin, VEGF, VEGFR1, VEGFR2, BMP2, leptin receptor, and many more. This gene is also found in atherosclerotic plaque, co-localized with endothelial cells lining the lesion, and involved in platelet adhesion, suggested for its role in atherosclerosis development [23-25]. This evidence might explain the increased level of plasma SCUBE1 in acute coronary syndrome (ACS) and acute ischemic stroke (AIS). Moreover, SCUBE1 expression showed to increase in several ischemic conditions such as acute mesenteric ischemia, mesenchymal ischemia of the kidney and ileum, ovarian torsion, bowel obstruction, and myocardial infarction as well as elevation of this gene in diabetic diseases and other systemic diseases (Table I).

An elevated level of plasma SCUBE1 in ischemia with the elevation of sCD40L has been found to be significantly correlated, suggesting the role of SCUBE1 in platelet activation [21-30]. In concomitant to previous findings, SCUBE1 has also been detected in patients diagnosed with pulmonary embolism (PE). A higher level of SCUBE1 exhibited specificity and sensitivity for PE diagnosis. This finding suggested early detection of PE to prevent severe complications from this disease [31-32]. Interestingly, in pulmonary arterial hypertension (PAH), the SCUBE1 level was lower in the World Symposium of Pulmonary Hypertension (WSPH) group 1 PAH compared to control healthy and acute lung injury. In the in vitro study of pulmonary artery endothelial cells (PAECs), SCUBE1 knockdown inhibited tube formation, proliferation, and increased apoptosis of PAECs. In contrast, overexpression of SCUBE1 in PAECs exhibited increased proliferation, enhanced tube formation, and decreased apoptosis, suggesting SCUBE1's role as a protective function for pulmonary endothelium, controlling the proangiogenic effect and proliferation capacity.

Interestingly, SCUBE1 knockdown reduced the intracellular SCUBE1 level and decreased the activated and phosphorylated SMAD1/5/9. Conversely, overexpression of SCUBE1 increased the expression of intracellular SCUBE1 and increased the activated and phosphorylated SMAD1/5/9. SCUBE1 appears to be an upstream signaling and mediator of SMAD1/5/9 relevant to BMPR2 but not SMAD 2/3 relevant to TGF-β signaling (Figure 2). Furthermore, this study also indicated that higher SCUBE1 level was found in group 2 PAH than those in group PAH. SCUBE1 level was higher in patients with coronary artery disease (CAD) and ischemic cardiomyopathy (ICM) compared to patients without CAD, suggesting the diagnostic value of SCUBE1 in distinguishing WSPH group 1 PAH from group 2 PH [33].

Moreover, SCUBE1 was reported to be increased in Hashimoto's thyroiditis. Hashimoto's thyroiditis is an autoimmune disease caused by environmental factors such as infections, medicines, smoking, and stress. This disease showed hypercholesterolemia, hypertriglyceridemia, and endothelial dysfunction. In this study, higher SCUBE1 expression was found significantly correlated to higher sCD40L, increased low-density lipoprotein (LDL)-C, triglyceride level, thyroid-stimulating hormone (TSH), T4, and anti-thyroid peroxidase (TPO) level, suggesting for the higher risk for cardiovascular disease in this patients [34-35].

Another evidence of an increased level of SCUBE1 showed that this gene could be a predictive marker for poor sepsis prognosis. SCUBE1 appeared significantly correlated with higher C-reactive protein (CRP), lactate, acute physiology, and chronic health evaluation 2 (APACHE 2) score, and sequential organ failure assessment (SOFA). This study speculated that higher SCUBE1 levels are caused by endothelial damage, platelet activation, and altered microcirculation in sepsis conditions [36]. In a recent study on COVID-19 disease, plasma SCUBE1

level was found to be higher than in the control group. The thrombotic complication has been known to cause higher mortality and morbidity in COVID-19. Plasma SCUBE1 level was significantly higher in patients with thrombotic complications and patients with severe COVID-19 than those with mild and moderate disease. A positive correlation was also found in SCUBE1, D-dimer, and fibrinogen levels. This study suggested that measurement of SCUBE1 early stages of the disease may prevent the disease progression and thrombotic complications in COVID-19 disease [37].

The additional data on SCUBE1 in human disease, a study in psoriasis patients showed an increased level of SCUBE1 and SCUBE3. This higher level of SCUBE1 and SCUBE3 were associated with a higher level of VEGF. The results might reveal the future treatment of psoriasis with anti-VEGFR therapy [38]. A prospective study among patients with ovarian torsion also exhibited a higher SCUBE1 level. Unfortunately, higher SCUBE1 levels did not significantly correlate with oxidative stress parameters such as advanced oxidation protein products (AOPP), the ferric-reducing ability of plasma (FRAP), and glutathione [39].

A limited study of SCUBE1 in cancer showed that this gene appeared to upregulate in renal and gastric cancer. In renal cancer, SCUBE1 expression increased compared to healthy control. Unfortunately, there was no significant correlation between carbonic anhydrase IX and soluble urokinase plasminogen activator receptor, known as a previously known biomarker for renal cancer and contributed to the poor prognosis of cancer. Increased SCUBE1 expression was also detected in patients with gastric cancer, even though this expression was not different among gastric cancer stages [40-41].

SCUBE2

The second member of the SCUBE family is named SCUBE2. During embryogenesis, the SCUBE2 was identified in the dorsal neuroectoderm, the posterior telencephalon, the diencephalon of the forebrain, and the neural tube. In adult tissues, this gene is detected in the heart, lung, and testis [12,13,16,17]. Unlike other SCUBE gene families, SCUBE2 is ubiquitously expressed in highly vascularized tissues, and many studies reported SCUBE2 involvement in the Hedgehog (Hh) signaling pathway, which is required during the development of vertebrates and invertebrates. The study with diabetes mellitus and dyslipidemia patients showed that SCUBE2 expression was upregulated compared to control healthy and statistically correlated to the upregulation of ET-1 in the same group. Deleting the SCUBE2 gene showed an impairment of Hh signaling and alteration of endochondral bone formation during embryogenesis. SCUBE2 contains hydrophobic stretch in the middle of the CUB domain, which is important to increase the secretion of sonic hedgehog (Shh) due to its dual palmitate and cholesterol modifications. The complex binding of SCUBE2-Shh, needs co-receptor CDON/BOC and growth arrest specific-1(GAS1) before being attached to its receptor Patch-1 (PTCH-1). CDON/BOC enhances SCUBE2-Shh recruitment on the cell surface, then further releases SCUBE2 from Shh to bind with Ptch-1 to activate Hh signaling. GAS-1 increases Shh catalyzation from SCUBE2 to bind to Ptch-1 [42-45].

A previous study on a triple-negative breast cancer cell line, MDA-MB-231, revealed that the upregulation of SCUBE2 levels in these cells was concomitantly followed by the upregulation of OCT4, SOX2, and NANOG expression. OCT4, SOX2, and NANOG are known as a marker of breast cancer stem cell (BCSC) phenotype. As postulated, BCSC is a crucial driver for tumor metastases and chemoresistance. This might explain why the upregulation of the SCUBE2 in TNBC showed resistance to paclitaxel chemotherapy in these cells. Furthermore, the SCUBE2 gene appeared to involve the Notch signaling pathway, where the depletion of SCUBE2 exhibited downregulation of the Notch signaling, NICD, jagged1, HEY1, and HES1 [46].

The study of the SCUBE2 showed that this gene is involved in cancer such as breast cancer, bladder cancer, glioma, nasopharyngeal carcinoma, colorectal carcinoma, and Kaposi Sarcoma [47-51]. Retrospective study investigation of 156 breast carcinoma biopsy samples, 86 cases were found to be positive for SCUBE2 protein expression, while 70 cases were negative for SCUBE2 expression. Interestingly, SCUBE2 gene overexpression was associated with better clinical outcomes among patients [51]. Supporting these findings, Liu et al., identified genes in patients with survival breast cancer. This study found that miR-9-5p, known as the SCUBE2, exhibited higher expression of the SCUBE2, associated with shorter survival years, compared to the lower expression of the SCUBE2 [52]. The same results were also shown in the study with bladder cancer. Patients with high-grade stage 1 (HGT1) specimens showed increased SCUBE2 expression strongly associated with higher disease-specific survival (DSS) among patients [53]. In addition to those findings, the SCUBE2 was reported as a plausible biomarker to predict the response of taxane-based neoadjuvant chemotherapy in breast cancer, where this gene expression was found in patients with a response to this chemotherapy [54].

Moreover, gene expression analysis study using human tissue specimens of breast carcinoma, the SCUBE2 is expressed and highly correlated to estrogen receptor and progesterone receptor. This study revealed that SCUBE2 expression was found to be increased among other genes related to tumorigenesis and endocrine-related cancer. SCUBE2 was reported to correlate with ESR1 gene-encoded estrogen receptor (ER) and NAT1, XBP1, and GATA3. A similar analysis also showed that this gene positively correlated with PGR gene-encoded progesterone receptor (PR). The following study reported that SCUBE2 expression was higher in postmenopausal endometrium than in premenopausal endometrium, suggesting its association with ER, PR, and PTEN, a tumor suppressor gene [55-56]. Further study found that overexpression of the SCUBE2 gene suppressed the proliferation activity of the MCF-7 breast cancer cell line in vitro and in vivo. Stable SCUBE2 overexpression in the MCF-7 breast cancer cell line showed lower cell growth than control cells without doxycycline as a SCUBE2 suppressor.

Concomitant to this finding, in vivo study using SCUBE2 overexpression cells in mice exhibited slower tumor growth compared to control mice, and this study suggested that higher

SCUBE2 expression related to lower BMP2 activity [57]. The following study by Lin YC et al., revealed that SCUBE2 was found in the plasma membrane at the cell-to-cell contact site and made a complex with E-cadherin and β-catenin in breast cancer cells. The suppression of the SCUBE2 decreased the expression of E-cadherin and β-catenin, thus suppressing Forkhead Box A1 (FOXA1) [58].

Moreover, the downregulation of SCUBE2 expression appeared to decrease the level of E-cadherin, further decreasing epithelial-to-mesenchymal transition (EMT) events. SCUBE2 suppression effect in breast cancer cell line also exhibits an increase of DNA methyltransferase 1 (DNMT1), which involves DNA methylation catalyzation and methylate the *SCUBE2* CpG site, further inactivates tumor-suppressor gene during TGF-β promoted EMT. The same finding showed in the bladder cancer study. SCUBE2 and FOXA1 were significantly associated with higher DSS in HGT1 cases. Further, SCUBE2 has been reported to involve in angiogenesis. SCUBE2 interacted with vascular endothelial growth factor receptor 2 (VEGFR2) to induce vascular endothelial growth factor (VEGF) specifically through elevated hypoxia-inducible factor (HIF)-1α in hypoxic conditions. A recent study demonstrated that combined therapy of anti-SCUBE2 and anti-VEGF had a beneficial effect in inhibiting tumor growth in xenograft human tumors [57-58].

SCUBE3

The third member of the SCUBE family is SCUBE3. This gene expression is high in human osteoblasts and low expression in human umbilical vein endothelial cells (HUVEC) and coronary smooth muscle cells. In tissue, this gene is highly expressed in the humerus, femur, kidney, adrenal gland, and heart. During embryogenesis, the SCUBE3 gene was detected in the neuroectoderm, particularly in the ventral rhombencephalon, caudal neuropore, neural folds, and trunk. At the later stages of embryogenesis, this gene is highly expressed in cartilaginous condensations of the peripheral skeleton such as limbs, ribs, vertebra, glomerular of the kidney, tooth germ, and hair follicle [12-14]. The human disease data mapped SCUBE3 resides in the chromosome 6p21 region, which was identified as the locus of a rare human disease, Paget's Disease of Bone (PDB). A previous study found that PDB was caused by the mutation in the receptor activator of the nuclear factor-kB (RANK) and the RANK-induced NF-kB signaling pathway. The fact that the SCUBE3 gene resides in the PDB locus, there is a possibility that this gene is also involved in PDB or other bone-related diseases [59]. Furthermore, transfection of human SCUBE3 in HEK-293T cells showed that SCUBE3 is a cell surface protein and underwent N-glycosylation with tunicamycin treatment. This study also reported that SCUBE3 exhibited proteolytic cleavage in the presence of protease in fetal bovine serum (FBS) [60,61].

A further study on the SCUBE3 revealed that this gene was an inhibitor for fibroblast growth factor (FGF) signaling. SCUBE3 suppressed the expression of fibroblast growth factor receptor (FGFR) 4, but not FGFR1, EGF receptor, and platelet-derived growth factor (PDGF)-α. A previously reported study exhibited that FGFR4 is involved in skeletal muscle development and myogenic differentiation through FGF8 signaling. This study showed that the knockdown of SCUBE3 decreased myosin heavy chain (HC) expression and reduced the myofibers formation [62]. Concomitant results to the previous study, SCUBE3 mutation mice, showed the defect in skeletal bone development and bone metabolism abnormalities. These mice showed low mineral bone density and hyper-ossification in the center and pedicles of the thoracic, lumbar, and sacral vertebrae regions. Ossification in those regions was more fused and closed. In addition, these mice exhibited an increase in plasma urea, creatinine, and potassium level and an increase in α-amylase activity, implying that SCUBE3 defect may cause the alteration of renal function. The SCUBE3 mutant mice also showed a decrease in interventricular septum width, left ventricular posterior wall thickness, left ventricular mass, diastolic ventricular dimension, and respiration rate followed by prolonged QRS interval duration even though no alteration was detected in heart function and conduction [63]. However, the study by Yang et al., 2007, showed that overexpression of SCUBE3 mice exhibited cardiac hypertrophy and higher atrial natriuretic factor (ANF) expression. Interestingly, in overexpression, SCUBE3 mice also showed simultaneously upregulated TGF-β1 in cardiomyocytes [64].

Unlike SCUBE2, known as a tumor suppressor gene, the SCUBE3 gene oppositely showed a poor prognosis in cancer. This gene was reported to involve breast cancer, small lung carcinoma, and renal carcinoma [65-69]. In a recent study in HER-2 positive breast cancer patients, the SCUBE3 appeared to be upregulated through the TGF-β1 signaling pathway, and the TWIST1 gene further indicated poor prognosis [65-67].

Conclusion

The molecular mechanism of the SCUBE gene has been progressively studied. SCUBE family involvement in the Hh signaling pathway during embryogenesis and in diseases has been extensively reported. However, the mechanism of how this gene induced the proliferation of cells involved in cell-to-cell contact, angiogenesis, platelet activation, and EMT via Hh signaling remains to be elucidated. Each SCUBE member appears to involve in a different pattern of disease development. SCUBE1 plays a role in platelet activity. It is thus primarily reported in platelet aggregation and thrombosis-induced diseases such as myocardial infarction, ACS, stroke, hypertension, diabetes, pulmonary embolism, and sepsis. Little is known about this gene's involvement in cancer.

SCUBE2 has been reported in cancer, particularly breast cancer. This gene has been known as the tumor suppressor gene in cancer. SCUBE2 has shown upstream signaling of Hh, where it binds with Shh upon activation and binds to its receptor Patch-1. The lower expression of the SCUBE2 has been linked to the downregulation of E-Cadherin and β-catenin, further lowering the EMT event in cancer progression. Interestingly, higher expression of SCUBE2 in TNBC showed a BCSC phenotype and its association with the Notch signaling pathway.

Moreover, a third family member of the SCUBE family, SCUBE3, is reported to be highly expressed in osteoblast, and this gene

http://doi.org/10.5472/marumj.1484448
Marmara Med J 2024;37(2): 106-114

resides in the locus of bone diseases such as PDB. A limited report on the SCUBE3 gene role in human diseases remained to be explored, such as SCUBE3 involvement in suicidal behavior. Note that the SCUBE3 expressed in inhibitory neurons of the middle temporal gyrus may lead to further exploration of this gene in the genetic trait of psychiatric disorder [70].

Taken together, the SCUBE family has been reported in many human diseases, especially in cancer, and it is known that this gene involved in Hh signaling, Notch signaling, and TGF-β signaling in disease development remains to be elucidated because each SCUBE member, SCUBE1, SCUBE2, and SCUBE3 seems to play a different pattern in cell signaling to induce cell proliferation, cell migration, and cell differentiation as well (Figure 2).

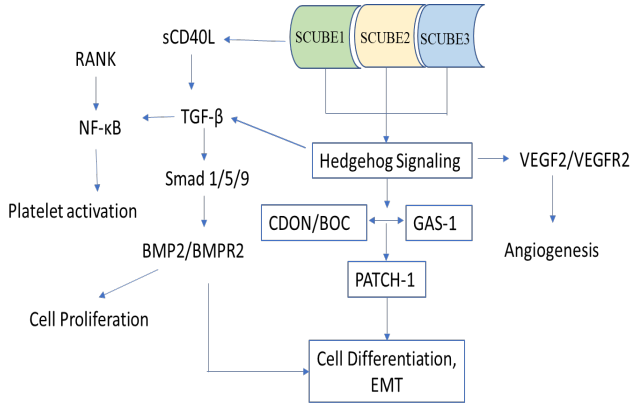

Figure 2. *The SCUBE is known to be associated with Hh signaling pathway. Molecular mechanisms in vitro and in vivo studies show that this gene is also correlated with TGF-β/Smad signaling, Notch signaling, and NF-κB signaling in inducing cell proliferation, angiogenesis, and EMT event. SCUBE1 acts as an upstream signal for the Hh signaling pathway and TGF-β pathway, further inducing angiogenesis through VEGF activation and sCD40L for platelet aggregation.*

Future perspective

In recent years, the molecular mechanism of the SCUBE has been progressively precise. However, in the human study, the expression of SCUBE1, SCUBE2, and SCUBE3 is still limited. The signal transduction of these genes with other signaling pathways in disease development remains to be elucidated. The current review shows that SCUBE is crucial in cancer, cardiovascular diseases (CVD), and inflammation. SCUBE gene revealed as upstream signaling of Hedgehog signaling, but the connection of SCUBE, Hedgehog signaling, TFG-β/Smad signaling, Notch signaling, and inducing VEGF for angiogenesis are needed to be assessed. More intense experimental, translational, and clinical research evidence is needed to validate the SCUBE gene as a potential therapeutic target for cancer and CVD.

Compliance with Ethical Standards

Funding: This work was supported by Faculty of Medicine, Andalas University, Biomedical Laboratory, and Graduate School of Biomedical Sciences, Andalas University, West Sumatra, Indonesia.

Conflict of interest: The author declares no conflicts of interest.

Author contribution: The author confirms sole responsibility for the following: study conception and design, data collection, analysis and manuscript preparation.

REFERENCES

[1] Tsao KC, Tu CF, Lee SJ, Yang RB. Zebrafish scube1 (Signal Peptide-CUB (Complement ProteinC1r/C1s, Uegf, and Bmp1)-EGF (Epidermal Growth Factor) Domain-containing Protein 1) is involved in primitive hematopoiesis. J Biol Chem 2013;288:5017-26. doi: 10.1074/jbc.M112.375196

[2] Bork P, Beckmann G. The CUB domain. A widespread module in developmentally regulated proteins. J Mol Biol 1993; 231: 539-45. doi: 10.1006/jmbi.1993.1305

[3] Campbell ID, Baron M, Cooke RM, et al. Structure-function relationships in epidermal growth factor (EGF) and transforming growth factor – alpha (TGF-a). Biochem Pharmacol 1990;40:35-40. doi: 10.1016/0006-2952(90)90175-k

[4] Groenen LC, Nice EC, Burgess AW. Structure-function relationships for the EGF/TGF-a family of mitogens. Growth Factors 1994;235-57. doi: 10.3109/089.771.99409010997

[5] Grimmond S, Larder R, Van Hateren N, et al. Clonning, mapping, and expression analysis of a gene encoding a novel mammalian EGF-related protein (SCUBE1). Genomics 2000;15: 74-81. doi: 10.1006/geno.2000.6370

[6] Woods IG, Talbot WS. The you gene encodes an EGF-CUB protein essential of hedgehog signaling in zebrafish. PLoS Biol 2005;3:e66. doi: 10.1371/journal.pbio.0030066

[7] Kawakami A, Nojima Y, Toyoda A, et al. The zebrafish-secreted matrix protein You/SCUBE2 is implicated in long-range regulation of hedgehog signaling. Curr Biol 2005;15:480-88. doi: 10.1016/j.cub.2005.02.018

[8] Johnson JLFA, Hall TE, Dyson JM, et al. SCUBE Activity is necessary for hedgehog singal transduction in vivo. Dev Biol 2012;368:193-202. doi: 10.1016/j.ydbio.2012.05.007

[9] Grimmond S, Larder R, Van Hateren N, et al. Cloning, mapping, and expression analysis of a gene encoding a novel mammalian EGF-related protein (SCUBE1). Genomics 2000;70: 74-81. doi: 10.1006/geno.2000.6370

[10] Lin YC, Sahoo BK, Gau SS, Yang RB. The biology of SCUBE. J Biomed Sci 2023;30:33. doi: 10.1186/s12929.023.00925-3

[11] Yılmaz C, Gülen B, Sönmez E, et al. Serum SCUBE-1 Levels and return of spontaneous circulation following cardiopulmonary resucitation in adult patients. Avicenna J Med 2022; 12:148-53. doi: 10.1055/s-0042.175.5389

[12] Kumar S, Prajapati KS, Gupta S. The multifaceted role of signal peptide-cub-egf domain containing protein (SCUBE) in cancer. Int J Mol Sci 2022;23:10577. doi: 10.3390/ijms231810577

[13] Grimmond S, Larder R, Van Hateren N, et al. Expression of a novel mammalian epidermal growth factor-related gene

during mouse neural development. Mech. Dev 2001; 102: 209-11. doi: 10.1016/s0925-4773(00)00586-4

[14] Haworth K, Smith F, Zoupa M, Seppala M, Sharpe PT, Martyn T Cobourne. Expression of the *Scube3* epidermal growth factor-related gene during early embryonic development in the mouse. Gene Expr Patterns 2007;7: 630-4. doi: 10.1016/j.modgep.2006.12.004

[15] G. Urrútia, X. Bonfill. PRISMA declaration: a proposal to improve the publication of systematic reviews and meta-analyses. Med Clin 2010;135:507-11. doi: 10.1016/j.medcli.2010.01.015

[16] Tu CF, Yan YT, Wu SY, et al. Domain and functional analysis of a novel platelet-endothelial cell surface protein, SCUBE1. J Biol Chem 2008; 283:12478-488. doi: 10.1074/jbc.M705872200

[17] Yang RB, Ng CK, Wasserman SM, et al. Identification of novel family of cell-surface proteins expressed in human vascular endothelium. J Biol Chem 2002;277:46364-73. doi: 10.1074/jbc.M207410200

[18] Wu BT, Su YH, Tsai MT, Wasserman SM, Topper JN, Yan RB. A novel secreted, cell-surface glycoprotein containing multiple epidermal growth factor-like repeats and one CUB domain is highly expressed in primary osteoblasts and bones. J Biol Chem 2004;37485-90. doi: 10.1074/jbc.M405912200

[19] Tu CF, Yan YT, Wu SY, et al. Domain and functional analysis of a novel platelet-endothelial cell surface protein, SCUBE1. J Biol Chem 2008;12478-88. doi: 10.1074/jbc.M705872200

[20] Tu CF , Su YH, Huang YN, et al. Localization and characterization of a novel secreted protein SCUBE1 in human platelets. Cardiovasc Res 2006;71:486-495. doi: 10.1016/j.cardiores.2006.04.010

[21] Turkmen S, Eryigit U, Karaca U, et al. Diagnostic value of plasma signal peptide-Cub-Egf domain-containing protein-1 (SCUBE-1) in an experimental model of acute ischemic stroke. Am J Emerg Med 2015;33:262-5. doi: 10.1016/j.ajem.2014.11.051

[22] Cekic AB, Cekic OG, Aygun A, et al. The diagnostic value of ischemia-modified albumin (IMA) and signal peptide-CUB-EGF domain-containing protein-1 (SCUBE-1) in an experimental model of strangulated mechanical bowel obstruction. J Invest Surg 2022;35:450-6. doi: 10.1080/08941.939.2020.1847218

[23] Aköz A, Türkdoğan KA, Çetin NK, et al. Predicting critical duration and reversibility of damage in acute mesenteric ischemia: an experimental study. Ulu Travma Acil Cerrahi Derg 2018;24:507-13. doi: 10.5505/tjtes.2018.69710

[24] Sancaktar NC, Altınbaş A, Çekiç B. Protective role of dexmedetomidine on ileum and kidney damage caused by mesenchymal ischaemia in rats. Turk J Anaesthesiol Reanim 2018;46:470-77. doi: 10.5152/TJAR.2018.46244

[25] Favre CJ, Mancuso M, Maas K, McLean JW, Baluk P, McDonald DM. Expression of genes involved in vascular development and angiogenesis in endothelial cells of adult lung. Am J Physiol Heart Circ Physiol 2003;285: H1917-38. doi: 10.1152/ajpheart.00983.2002

[26] Dai DF, Thajeb P, Tu CF, et al. Plasma concentration of SCUBE1, a novel platelet protein, is elevated in patients with acute coronary syndrome and ischemic stroke. J Am Coll Cardiol 2008;51:2173-80. doi: 10.1016/j.jacc.2008.01.060

[27] Bolayır HA, Kıvrak T, Güneş H, Akaslan D, Şahin O, Bolayır A. The role of SCUBE1 in the development of late stent thrombosis presenting with ST-elevation myocardial infarction. Rev Port Cardiol 2018;37:375-81. doi: 10.1016/j.repc.2017.07.015

[28] Guzel M, Dogru MT, Simsek V, et al. Influence of circadian blood pressure alterations on serum sCUBE1 and soluble CD40 ligand levels in patients with essential hypertension. Am J Cardiovasc Dis 2019;9: 42-8.

[29] Tekin YB, Erin KB, Yilmaz A. Evaluation of SCUBE1 Levels as a placental dysfunction marker at gestational diabetes. Gynecol Endocrinol 2020;36:417-20. doi: 10.1080/09513.590.2019.1683537

[30] Icel E, Icel A, Mertoglu C, et al. Serum SCUBE-1 levels in patients with diabetic retinopathy. Int Opthalmol 2020;40:859-65. doi: 10.1007/s10792.019.01249-8

[31] Turkmen S, Sahin A, Gunaydin M, et al. The value of signal peptide-CUB-EGF domain-containing protein – 1 (SCUBE1) in the diagnosis of pulmonary embolism: A preliminary study. Acad Emerg Med 2015;22: 922-26. doi: 10.1111/acem.12721

[32] Dirican N, Duman A, Sağlam G, et al. The diagnostic significance of signal peptide-complement C1r/C1s, Uegf, and Bmp1-epidermal growth factor domain-containing protein-1 levels in pulmonary embolism. Ann Thorac Med 2016;11:277-82. doi: 10.4103/1817-1737.191876

[33] Sun W, Tang Y, Tai YY, et al. SCUBE1 controls BMPR2-relevant pulmonary endothelial function: implications for diagnostic marker development in pulmonary arterial hypertension. JACC Basic Transl Sci 2020;5:1073-92. doi: 10.1016/j.jacbts.2020.08.010

[34] Bilir B, Soysal-Atile N, Bilir BE, et al. Evaluation of SCUBE-1 and sCD40L biomarkers in patients with hypothyroidism due to Hashimoto's thyroiditis: A single-blind, controlled clinical study. Eur Rev Med Pharmacol Sci 2016;20:407-13.

[35] Erem C, Civan N, Coskun H, et al. Signal peptide-CUB-EGF domain-containing protein 1 (SCUBE1) levels in patients with overt and subclinical hyperthyroidism: effects of treatment. Clin Endocrinol 2016;84:919-24. doi: 10.1111/cen.12955

[36] Erdoğan M, Findikli HA, Teran IO. A novel biomarker for predicting sepsis mortality SCUBE-1. Medicine 2021;100:e24671. doi: 10.1097/MD.000.000.0000024671

[37] Toprak K, Kaplangoray M, Palice A, et al. SCUBE1 is associated with thrombotic complications, disease severity, and in-hospital mortality in COVID-19 patients. Thromb Res 2022;220:100-6. doi: 10.1016/j.thromres.2022.10.016

[38] Capkin AA, Demir S, Mentese A, Bulut C, Ayar A. Can signal peptide-CUB-EGF domain-containing protein (SCUBE) levels be a marker of angiogenesis in patients with psoriasis? Arch Dematol Res 2017;309: 203-7. doi: 10.1007/s00403.017.1722-7

[39] Uyanikoglu H, Hilali NG, Yardimciel M, Koyuncu I. A new biomarker for the early diagnosis of ovarian torison:

SCUBE-1. Clin Exp Reprod Med 2018;45:94-9. doi: 10.5653/cerm.2018.45.2.94

[40] Karagüzel E, Menteşe A, Kazaz IO, et al. SCUBE1: a promising biomarker in renal cell cancer. Int Braz J Urol 2017:43:638-43. doi: 10.1590/S1677-5538.IBJU.2016.0316

[41] Mentese A, Fidan E, Sumer AU, et al. Is SCUBE 1 a new biomarker for gastric cancer? Cancer Biomark 2012; 11: 191-95. doi: 10.3233/CBM-2012-00285

[42] Tsai MT, Cheng CJ, Lin YC, et al. Isolation and characterization of a secreted, cell-surface glycoprotein SCUBE2 from humans. Biochem J 2009;422:119-28. doi: 10.1042/BJ20090341

[43] Lin YC, Roffler SR, Yan YT, Yang RB. Disruption of SCUBE2 impairs endochondral bone formation. J Bone Miner Res 2015;30:1255-67. doi: 10.1002/jbmr.2451

[44] Ali H, Rustam R, Aprilia D, Arizal C, Gusadri IB, Utami PR. Upregulation of SCUBE2 expression in dyslipidemic type 2 diabetes mellitus is associated with endothelin-1. diabetes Metab Syndr 2019;13:2869-72. doi: 10.1016/j.dsx.2019.07.058

[45] Cheng CJ, Lin YC, Tsai MT, et al. SCUBE2 Suppresses breast tumor cell proliferation and confers a favorable prognosis in invasive breast cancer. Cancer Res 2009;69:3634-41. doi: 10.1158/0008-5472.CAN-08-3615

[46] Chen JH, Kuo KT, Bamodu OA, et al. Upregulated SCUBE2 expression in breast cancer stem cells enhances triple negative breast cancer aggression through modulation of notch signaling and epithelial-to-mesenchymal transition. Exp Cell Res 2018;370:444-53. doi: 10.1016/j.yexcr.2018.07.008

[47] Chen Y, Zhou C, Li H, Li H, Li Y. Identifying key genes for nasopharyngeal carcinoma by prioritized consensus differentially expressed genes caused by aberrant methylation. J Cancer 2021;12:874-84. doi: 10.7150/jca.49392

[48] Guo E, Liu H, Liu X. Overexpression of SCUBE2 inhibits proliferation, migration, and invasion in glioma cells. Oncol Res 2017;25:437-44. doi: 10.3727/096504016X147.473.35734344

[49] Rinne SJ, Sipilä LJ, Sulo P, et al. Candidate Predisposition Variants in Kaposi Sarcoma as Detected by Whole-Genome Sequencing. Open Forum Infect Dis 2019;6:ofz337. doi: 10.1093/ofid/ofz337

[50] Song Q, Li C, Feng X, et al. Decreased Expression of SCUBE2 is Associated with Progression and Prognosis in Colorectal Cancer. Oncol Rep 2015;33:1956-64. doi: 10.3892/or.2015.3790

[51] Cheng CJ, Lin YC, Tsai MT, et al. SCUBE2 suppresses breast tumor cell proliferation and confers a favorable prognosis in invasive breast cancer. Cancer Res 2009;69:3634-41. doi: 10.1158/0008-5472.CAN-08-3615

[52] Liu M, Zhou S, Wang J, et al. Identification of Genes Associated with Survival of Breast Cancer Patients. Breast Cancer 2019;26:317-25. doi: 10.1007/s12282.018.0926-9

[53] Ottley EC, Pell R, Brazier B, et al. Greater Utility of Molecular Subtype Rather Than Epithelial-to-Mesenchymal Transition (EMT) Markers for Prognosis in High-Risk Non-Muscle-Invasive (HGT1) Bladder Cancer. J Patho Clin Res 2020;6:238-51. doi: 10.1002/cjp2.167

[54] Kallarackal J, Burger F, Bianco S, Romualdi A, Schad M. A 3-Gene Biomarker Signature to Predict Response to Taxane-Based Neoadjuvant Chemotherapy in Breast Cancer. PLoS One 2020;15:e0230313. doi: 10.1371/journal.pone.0230313

[55] Andres SA, Wittliff JL. Co-expression of Genes with Estrogen Receptor – α and Progesterone Receptor in Human Breast Carcinoma Tissue. Horm Mol Biol Clin Investig 2012;12:377-90. doi: 10.1515/hmbci-2012-0025

[56] Skrzypczak M, Lattrich C, Häring J, Schüler S, Ortmann O, Treeck O. Expression of SCUBE2 Gene Declines in High Grade Endometrial Cancer and Associates with Expression of Steroid Hormone Receptors and Tumor Suppressor PTEN. Gynecol Endocrinol 2013;29:1031-35. doi: 10.3109/09513.590.2013.829441

[57] Lin YC, Lee YC, Li LH, Cheng CJ, Yang RB. Tumor Suppressor SCUBE2 Inhibits Breast-Cancer Cell Migration and Invasion Through the Reversal of Epithelial–Mesenchymal Transition. J Cell Sci 2014;127:85-100. doi: 10.1242/jcs.132779

[58] Lin YC, Liu CY, Kannagi R, Yang RB. Inhibition of Endothelial SCUBE2 (Signal Peptide-CUB-EGF Domain-Containing Protein 2), a Novel VEGFR2 (Vascular Endothelial Growth Factor Receptor 2) Coreceptor, Suppresses Tumor Angiogenesis. Arterioscler Thromb Vasc Biol 2018;38:1202-15. doi: 10.1161/ATVBAHA.117.310506

[59] Wu BT, Su YH, Tsai MT, Wasserman SM, Topper JN, Yang RB. A Novel Secreted, Cell-Surface Glycoprotein Containing Multiple Epidermal Growth Factor-like Repeats and One CUB Domain Is Highly Expressed in Primary Osteoblasts and Bones. J Biol Chem 2004;37485-90. doi: 10.1074/jbc.M405912200

[60] Xavier GM, Economou A, Guimarães ALS, Sharpe PT, Cobourne MT. Characterization of a Mouse Scube3 Reporter Line. Genesis 2010;684-92. doi: 10.1002/dvg.20678

[61] Liu X, Wang LG, Zhang LC, et al. Molecular Cloning, Tissue Expression Pattern, and Copy Number Variation of Porcine SCUBE3. Genet Mol Res 2016;15:gmr7010. doi: 10.4238/gmr.15017010

[62] Tu CF, Tsao KC, Lee SJ, Yang RB. SCUBE3 (Signal Peptide-CUB-EGF Domain-containing Protein 3) Modulates Fibroblast Growth Factor Signaling during Fast Muscle Development. J Biol Chem 2014;289:18928-42. doi: 10.1074/jbc.M114.551929

[63] Fuchs H, Sabrautzki S, Przemeck GKH, et al. The First Scube3 Mutant Mouse Line with Pleiotropic Phenotypic Alterations. G3 (Bethesda) 2016;6:4035-46. doi: 10.1534/g3.116.033670

[64] Yang HY, Cheng CF, Djoko B, et al. Transgenic Overexpression of The Secreted, Extracellular EGF-CUB Domain-containing Protein SCUBE3 Induces Cardiac Hypertrophy in Mice. Cardiovasc Res 2007;75:139-147. doi: 10.1016/j.cardiores.2007.03.014

[65] Yang X, Hu J, Shi C, Dai J. Activation of TGF-b1 Pathway by SCUBE3 Regulates TWIST1 Expression and Promotes Breast Cancer Progression. Cancer Biother Radiopharm 2020;35:120-28. doi: 10.1089/cbr.2019.2990

[66] Gao C, Zhuang J, Li H, et al. Development of a Risk Scoring System for Evaluating the Prognosis of Patients with Her2-positive Breast Cancer. Cancer Cell Int 2020;20:121. doi: 10.1186/s12935.020.01175-1

[67] Huo Q, He X, Li Z, et al. SCUBE3 Serves as An Independent Poor Prognostic Factor in Breast Cancer. Cancer Cell Int 2021;21:268. doi: 10.1186/s12935.021.01947-3

[68] Morris MR, Ricketts CJ, Gentle D, et al. Genome-wide Methylation Analysis Identifies Epigenetically Inactivated Candidate Tumour Suppressor Genes in Renal Cell Carcinoma. Oncogene 2011;30:1390-1401. doi: 10.1038/onc.2010.525

[69] Zhao C, Qin Q, Wang Q, et al. SCUBE3 Overexpression Predicts Poor Prognosis in Non-Small Cell Lung Carcinoma. Biosci Trends 2013;7:264-69

[70] Wendt FR, Pathak GA, Levey DF, et al. Sex-stratified Gene-by-Environment Genome-Wide Interaction Study of Trauma, Posttraumatic-Stress, and Suicidality. Neurobiol Stress 2021;14:100309. doi: 10.1016/j.ynstr.2021.100309

MARMARA
MEDICAL JOURNAL

Review Article

https://dergipark.org.tr/tr/pub/marumj

Non-alcoholic fatty liver disease: pathogenesis and assessing the impact of dietary bioactive compounds on the liver

Esma OGUZ[1], Berna KARAKOYUN[2]

[1] Department of Nutrition and Dietetics, Faculty of Health Sciences, Institute of Health Sciences, Marmara University, Istanbul, Turkey
[2] Department of Physiology, Hamidiye School of Medicine, University of Health Sciences, Istanbul, Turkey

Corresponding Author: Esma OGUZ
E-mail: esmaoguz34@gmail.com

Submitted: 15.06.2023 **Accepted:** 10.02.2024

ABSTRACT

Non-alcoholic fatty liver disease (NAFLD) is a pathological condition ranging from simple steatosis to non-alcoholic steatohepatitis, cirrhosis, and liver cancer. NAFLD is a complex disease mediated by metabolic, environmental, and genetic mechanisms. Many factors such as insulin resistance, lipotoxicity, inflammation, mitochondrial dysfunction, endoplasmic reticulum stress, circadian rhythm, genetics, epigenetics, dietary factors, and gut microbiota play a crucial role in the pathogenesis of NAFLD. Lifestyle changes such as healthy diet, physical activity, avoiding alcohol and smoking are involved in the NAFLD treatment. Dietary bioactive compounds including curcumin, resveratrol, catechins, quercetin, sulforaphane, epigallocatechin-3-gallate, alkaloids, vitamins, and peptides have many health promoting effects such as antioxidant, anti-inflammatory, antihypertensive, chemopreventive, and hepatoprotective. In this review, the pathophysiology of NAFLD and the effects of dietary bioactive compounds on this disease will be discussed in detail with updated information.

Keywords: Non-Alcoholic Fatty Liver Disease, Pathogenesis, Dietary Bioactive Compounds

1. INTRODUCTION

Non-alcoholic fatty liver disease (NAFLD) is defined as the pathological spectrum of the liver that can progress from simple steatosis to non-alcoholic steatohepatitis (NASH), cirrhosis, and liver cancer [1]. Histopathologically, the absence of necroinflammatory activity is accepted as simple steatosis; however, the presence of a fibrosis caused by portal inflammation, ballooning and hepatocyte damage together with fatty liver is called NASH [2].

Non-alcoholic fatty liver disease has been accepted as a global public health issue, affecting 6 to 45% of the general population, increasing to 70% in patients with type 2 diabetes mellitus and up to 90% in morbidly obese patients [3].

Although, there is no licensed pharmacotherapy for NAFLD, antidiabetic drugs, drugs affecting the bile acid system and lipid-lowering agents are given for treatment according to the accompanying diseases. The most important treatment is mainly based on lifestyle changes such as healthy diet, body weight control, physical activity, smoking cessation and avoiding alcohol [4]. Diet is affordable and effective and does not have any adverse effects. Also, it does not include the metabolic burden that medications load on the body systems. In this respect, many different dietary components are being studied for their possible pharmacological activity in several pathophysiological conditions [5].

The most widely accepted definition of bioactive compounds is 'compounds which have the ability to interact with one or more component(s) of living tissue by presenting a wide range of probable effects [6]. Bioactive compounds which mainly include curcumin, resveratrol, catechins, quercetin, sulforaphane, epigallocatechin-3-gallate, alkaloids, vitamins, and peptides, are particullary present in small quantities in fruits, vegetables, whole grains, beverages and milk products. These bioactive compounds have anti-inflammatory, antioxidant and hepatoprotective properties [7]. In this review, we discussed the pathophysiology of NAFLD and the effects of dietary bioactive compounds on this disease.

How to cite this article: Oguz E, Karakoyun B. Non-alcoholic fatty liver disease: pathogenesis and assessing the impact of dietary bioactive compounds on the liver. Marmara Med J 2024: 37(2):115-120. doi: 10.5472/marumj.1479280

ISSN: 1309-9469

http://doi.org/10.5472/marumj.1479280
Marmara Med J 2024;37(2): 115-120

2. PATHOGENESIS

Non-alcoholic fatty liver disease is considered as a multifactorial disease and mediated by metabolic, environmental, and genetic mechanisms. Many factors such as insulin resistance, lipid metabolism, inflammation, mitochondrial dysfunction, endoplasmic reticulum stress, circadian rhythm, genetics, epigenetics, dietary factors, and gut microbiota play a crucial role in the pathogenesis of NAFLD (Figure 1).

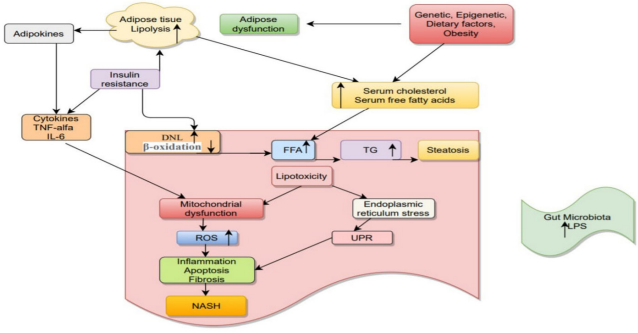

Figure 1. *The multi-hit hypothesis of non-alcoholic fatty liver disease (NAFLD) pathogenesis. The insulin resistance and lipid metabolism dysregulation lead to the development of simple steatosis and render hepatocytes susceptible to "multi-hit", which includes gut-derived bacterial toxins(lipopolysaccharides), adipocytokine imbalance, mitochondrial dysfunction, reactive oxygen species, endoplasmic reticulum stress, apoptosis, activation of pro-fibrogenic factors and pro-inflammatory mediators ultimately leading to non-alcoholic steatohepatitis (NASH). IL: Interleukin; TNF: Tumor necrosis factor; ROS: Reactive oxygen species; DNL: de novo lipogenesis; UPR: Unfolded protein response; TG: Triglyceride; FFA: Free fatty acids; LPS: lipopolysaccharides*

Insulin resistance

Insulin resistance has critical role in the activation of lipotoxicity, oxidative stress, and inflammatory processes in NAFLD and its progression to NASH [8]. Insulin resistance is associated with lipolysis in adipose tissue, it causes an increase in circulating free fatty acids (FFAs) and their uptake by the liver [9].

Increased glucose and insulin levels inhibit mitochondrial β-oxidation, suppress apolipoprotein B100 synthesis, and increase *de novo* lipogenesis (DNL) in the liver through glycolysis [10]. Hepatic DNL could be increased by activation of transcription factors such as sterol regulatory element binding protein (SREBP)-1, carbohydrate response element binding protein (ChREBP), and peroxisome proliferator activated receptor (PPAR). SREBP-1c which regulates DNL, is stimulated by insulin [11]. ChREBP is activated by glucose and increases DNL, it also provides more substrate for triglyceride and FFAs synthesis [12]. In general, PPARs are involved in glucose and fat metabolism as well as in immune response, inflammation, apoptosis, and cell proliferation [13].

Lipid metabolism

Fat accumulates in the liver of NAFLD patients in the form of triglycerides [11]. FFAs are obtained from diet, adipose tissue by lipolysis and/or liver by DNL. In hepatocytes, FFAs undergo acyl-CoA synthesis and form fatty acyl-CoAs that enter esterification or β-oxidation pathways [14]. Increased levels of FFAs in the liver lead to lipid peroxidation, which causes the release of inflammatory cytokines such as tumor necrosis factor (TNF)-α, interleukin (IL)-1, IL-6, and reactive oxygen species (ROS). Inflammation and oxidative stress resulting from the release of these molecules, cause cellular damage and inflammation seen in NASH [15].

Oxidative stress plays an important role in the beginning of hepatic and extrahepatic injuries. Increased levels of FFAs cause oxidative stress by increasing ROS production [16].

Inflammation

Lipotoxicity, insulin resistance, peripheral adipose tissue dysfunction, and gut-derived endotoxins due to increased levels of FFAs induce production and secretion of pro-inflammatory cytokines both systemically and locally in the liver. Also, adipose tissue produces pro-inflammatory cytokines such as IL-6 and TNF-α, which are responsible for the inflammatory and fibrogenic profile of the liver [16].

Adipokines (e.g. leptin, adiponectin) are hormones derived from adipose tissue that contribute to steatosis, NASH, cirrhosis, and carcinogenesis. Adipokines are in balance in healthy and normal weight individuals, but this balance is impaired in NAFLD [17]. Leptin appears to show an anti-steatotic effect in early stage of the NAFLD, but it can trigger hepatic inflammation and fibrosis when the disease progresses [18]. On the other hand, adiponectin, which has anti-steatotic, anti-inflammatory and anti-fibrotic effects, inhibits pro-inflammatory cytokines and stimulates anti-inflammatory cytokines, thus reduces oxidative stress and fibrogenesis [19].

Mitochondrial dysfunction

Structural and functional changes in mitochondria contribute to the pathogenesis of NAFLD. While structural changes occur with the reduction of mitochondrial DNA, functional changes include respiratory chain and mitochondrial β-oxidation [20]. ROS stimulate oxidative stress through the activation of inflammatory pathways and mitochondrial damage; together with oxidized LDL particles they activate Kupffer cells and hepatic stellate cells which lead to inflammation and fibrosis [21].

Endoplasmic reticulum stress

The accumulation of FFAs leads to endoplasmic reticulum stress by triggering an unfolded protein response (UPR). The factors which induce UPR include hyperglycemia, mitochondrial damage, hypercholesterolemia, and oxidative stress in NAFLD [22]. UPR activates c-jun terminal kinase, which is an activator of inflammation and apoptosis [23].

http://doi.org/10.5472/marumj.1479280
Marmara Med J 2024;37(2): 115-120

Circadian rhythm

Animal studies have shown that there is a link between circadian rhythm genes and NAFLD pathogenesis. Environmental factors such as circadian disruption (jet lag or night shift work) and high fat diet (HFD) increase the risk of NAFLD in animal knockout models of circadian locomotor output cycles kaput (clock) and PPAR-α [24]. Treatment with PPAR agonists or melatonin could potentially prevent progression of NAFLD and even cause regression of the disease [25].

Genetics and epigenetics

Genetic variants affect the development and progression of NAFLD by playing a central role in different ways such as single nucleotide polymorphism, lipogenesis, lipoprotein transport, oxidation of FFAs, oxidative stress, and cytokine production by endotoxin [26]. Patatin-like phospholipase-3 (PNPLA3) gene encodes enzymes which are involved in lipid metabolism [27]. The PNPLA3 protein, which is also known as adiponutrin, exerts a lipolytic activity on triglycerides [27]. However, the role of genetics in NAFLD is needed to study more to understand the pathogenesis of the disease.

Epigenetic modifications include DNA methylation, histone modifications, and the activity of microRNAs (miRNAs) without altering the primary DNA sequence. These modifications exhibit a high degree of developmentally and environmentally oriented plasticity, and contribute to cell homeostasis [28].

Dietary factors

Dietary composition and high energy intake have important effects on NAFLD pathogenesis. High energy intake and fat accumulation that are associated with insulin resistance, result in the increase of inflammatory cytokines and fatty acids in the circulation [29]. In general, NAFLD is characterized by high intake of saturated fats, simple carbohydrates, foods containing fructose, cholesterol, and low intake of antioxidants, fiber, and omega-3 fatty acids [30].

In NAFLD pathogenesis, fructose has been suggested to increase DNL, inhibit β-oxidation, increase inflammation, and alter gut microbiota which potentially causes dysbiosis. It has been also shown that fructose is an important factor for increasing intestinal permeability and endotoxins in the portal blood [31].

Mediterranean diet which can reduce liver fat, has been recommended for the treatment of NAFLD by the EASL-EASD-EASO Clinical Practice Guideline and the European Society of Clinical Nutrition and Metabolism (ESPEN) Guidelines [4, 32].

Gut microbiota

Microbiota is thought to play an important role in the pathogenesis of NAFLD. Several mechanisms have been suggested for the role of microbiota in NAFLD including gut permeability, microbiome-induced regulation of gut barrier, inflammatory factors, and metabolites produced or altered by the microbiota such as bile acids, short chain fatty acids, and ethanol [33].

Intestinal bacterial overgrowth leads to a leaky mucosal barrier which allows bacterial translocation and increases microbial products such as lipopolysaccharides. These products, particularly pathogen-associated molecular pattern molecules, interact with receptors found not only on inflammatory cells but also on other cell types such as hepatic stellate cells and endothelial cells [34].

3. THE IMPACT OF DIETARY BIOACTIVE COMPOUNDS ON NAFLD

Dietary bioactive compounds are being investigated intensively to complement therapeutic strategies of many diseases including NAFLD [35]. They show many health-promoting effects such as antioxidant, anti-inflammatory, antihypertensive, chemopreventive, and hepatoprotective [36].

Some dietary bioactive compounds showing antioxidant and/or anti-inflammatory effects, and their mechanism of actions on NAFLD are summarized in Table I.

Table I. *The impact of dietary bioactive compounds in NAFLD*

Nutrient/Bioactive compound	Effects	Mechanism of action
Caffeine	Antioxidant	Weight gain ⇓ Oxidative stress ⇓
Epigallocatechin gallate	Antioxidant	Weight gain ⇓ Oxidative stress ⇓ Lipid accumulation ⇓
Probiotic	Anti-inflammatory	Lipid accumulation ⇓ Steatosis ⇓ Serum lipids ⇓
Omega-3	Anti-inflammatory Antioxidant	Steatosis ⇓ Lipid peroxidation ⇓
Prebiotic	Anti-inflammatory Antioxidant	β-oxidation ⇓ Lipogenesis ⇓ Serum lipids ⇓
Astaxanthin	Anti-inflammatory Antioxidant	Pro-inflammatory cytokines ⇓ Inhibition of lipogenesis
Quercetin	Anti-inflammatory Antioxidant	Pro-inflammatory cytokines ⇓ Inhibition of lipogenesis
Curcumin	Anti-inflammatory Antioxidant	Intestinal barrier function ⇓ Endotoxin ⇓ Toll-like receptor (TLR)4 / nuclear factor (NF)-κB inflammation ⇓
Resveratrol	Anti-inflammatory Antioxidant	Oxidative stress ⇓ Inflammation ⇓ Serum lipids ⇓

Yang et al., found that the co-administration of epigallocatechin-3-gallate and caffeine in low doses improved obesity and NAFLD in obese rats, suggesting the possible role of epigallocatechin-3-gallate and caffeine co-administration in reducing body weight, oxidative stress and inflammatory cytokines and improving serum lipid profiles [37].

http://doi.org/10.5472/marumj.1479280
Marmara Med J 2024;37(2): 115-120

A study included 20 male and 20 female participants, aged between 19 and 64 years and diagnosed with NAFLD. Among them, those who consumed ≥250 mg/day of caffeine showed elevated ALT and AST levels, as well as a decrease in high-density lipoprotein cholesterol (HDL-C) levels [38].

Consumption of 50 mg green tea tablets containing 500 mg of standardized total polyphenols three times daily for three months was effective in reducing liver fat accumulation, attenuating fatty liver grading and improving liver function in 52 patients diagnosed with NAFLD aged 10 to 16 years [39].

Administration of both probiotic and omega-3 supplements to obese mice caused a significant reduction in hepatic steatosis and hepatic lipid accumulation [40]. Similarly, another study showed the beneficial effects of omega-3 fatty acids treatment in a mouse model of NAFLD by decreasing plasma cholesterol, plasma triglycerides, fasting plasma glucose and liver lipid peroxidation levels [41]. Patients diagnosed with NAFLD were given omega-3 fatty acids supplementation, improvements in hepatic steatosis were seen in contrast to those who received placebo. Omega-3 fatty acid supplementation resulted in a reduction in triglyceride and total cholesterol levels as well as a decrease in body mass index (BMI), while also increasing HDL-C concentrations among individuals with NAFLD [42].

It has been shown that prebiotic and synbiotic (prebiotic and probiotic) supplementation improved hepatic changes due to hypercholesterolemia in adult rats [43]. These changes appear to be mediated by altered gene expressions such as SREBP-1c and PPAR-α which are associated with β-oxidation and lipogenesis. Thus, prebiotic supplementation can modulate and decrease SREBP-1c expression in lipogenesis [43].

Behrouz et al., conducted a study investigating the effects of probiotics and prebiotics on individuals NAFLD. The results showed reductions in AST, ALT, triglycerides, and total cholesterol; however, there were no changes observed in inflammation biomarkers such as C-reactive protein. It is important to note that the trial had a relatively short duration, making it challenging to guarantee the sustained reduction of metabolic parameters. Moreover, the study did not include assessments for liver fibrosis to examine the severity and progression of liver disease [44].

Hernandez-Ortega et al. and Shen et al., found that hepatic marker levels such as alanine aminotransferase and aspartate aminotransferase were reduced by adding astaxanthin and quercetin to the diets of mice with liver fibrosis [45,46]. Also, decrease in pro-inflammatory cytokines (TNF-α, IL-6 and IL-1β) in serum and liver tissue and antifibrotic effects have been associated with their anti-inflammatory capacities. In addition, quercetin and astaxanthin contribute to the improvement of lipid metabolism by inhibiting lipogenesis and stimulating fatty acid oxidation by affecting PPAR-α and adiponectin [45,46].

Administration of curcumin protects against HFD-induced hepatic steatosis in ApoE−/− mice by modulating intestinal barrier function and reducing endotoxin and toll-like receptor (TLR)4/nuclear factor (NF)-κB inflammation [47]. In a study involving 55 NAFLD individual, it was observed that administering a daily dose of 500 mg of curcumin resulted in a reduction in the serum concentrations of inflammatory cytokines such as TNF-α and interleukins [48].

In a 12-week clinical trial that randomized 90 participants aged 20 to 60 years with NAFLD, the subjects were divided into three distinct groups: the calorie-restricted (CR) diet group (n = 30), the resveratrol group (n = 30) receiving a daily dose of 600 mg pure trans-resveratrol, and the placebo group (n = 30) receiving placebo capsules. Findings from the trial demonstrated that the CR diet induced significant reductions in weight (4.5%), BMI, waist circumference, waist-to-hip ratio, as well as ALT, AST, and lipid profiles, surpassing the outcomes observed in both the resveratrol and placebo groups [49].

Conclusion

Non-alcoholic fatty liver disease has high morbidity and mortality rates worldwide as it has become the major cause of end-stage liver disease and liver transplantation. The pathogenesis of NAFLD is a complex process with multiple factors such as gut microbiota, insulin resistance, hormones secreted from adipose tissue, increased levels of FFAs, endoplasmic reticulum stress, mitochondrial dysfunction, inflammation, circadian rhythm, genetic and epigenetic factors. Dietary bioactive compounds, which modulate lipogenesis, lipid oxidation and lipid peroxidation, reduce endotoxin and inflammation and improve intestinal barrier function, represent a new attractive therapeutic approach for NAFLD. Further studies could provide insights into the role of dietary bioactive compounds in NAFLD treatment.

Compliance with Ethical Standards

Financial support: The authors have no relevant financial information to disclose.

Conflict of interest: No potential conflict of interest was reported by the authors.

Authors' contributions: Both authors contributed equally to this manuscript as mentioned in copyright form. Preparation, creation, and/or presentation of the published work by those from both authors, specifically critical review, commentary, or revision – including pre-or postpublication stages.

REFERENCES

[1] Cohen JC, Horton JD, Hobbs HH. Human fatty liver disease: old questions and new insights. Science 2011; 332:1519-23. doi:10.1126/science.1204265.

[2] Çolak Y, Tuncer İ. Nonalkolik karaciğer yağlanması ve steatohepatit. İst Tıp Fak Derg 2010; 73:85-9.

[3] Fazel Y, Koenig AB, Sayiner M, Goodman ZD, Younossi ZM. Epidemiology and natural history of non-alcoholic fatty liver disease. Metab 2016; 65:1017-25. doi: 10.1016/j.metabol.2016.01.012.

[4] EASL-EASD-EASO Clinical Practice Guidelines for the management of non-alcoholic fatty liver disease. J Hepatol 2016; 64:1388-402. doi: 10.1016/j.jhep.2015.11.004.

[5] Cecchini M, Sassi F, Lauer JA, Lee YY, Guajardo – Barron V, Chisholm D. Tackling of unhealthy diets, physical inactivity, and obesity: health effects and cost-effectiveness. Lancet 2010; 376:1775-84. doi:10.1016/S0140-6736(10)61514-0.

[6] Guaadaoui A, Benaicha S, Elmajdoub N, Bellaoui M, Hamal A. What is a bioactive compound? A combined definition for a preliminary consensus. Int J Nutr Food Sci 2014; 3:74-9. doi: 10.11648/j.ijnfs.20140303.16.

[7] Gil-Chavez JG, Villa JA, Ayala-Zavala JF, et al. Technologies for extraction and production of bioactive compounds to be used as nutraceuticals and food ingredients: An overview. Compr Rev Food Sci Food Saf 2013; 12:5-23. doi: 10.1111/1541-4337.12005.

[8] Peverill W, Powell LW, Skoien R. Evolving concepts in the pathogenesis of NASH: beyond steatosis and inflammation. Int J Mol Sci 2014; 15:8591-638. doi: 10.3390/ijms15058591.

[9] Fabbrini E, Mohammed BS, Magkos F, Korenblat KM, Patterson BW, Klein S. Alterations in adipose tissue and hepatic lipid kinetics in obese men and women with nonalcoholic fatty liver disease. Gastroenterology 2008; 134:424-31. doi: 10.1053/j.gastro.2007.11.038.

[10] Angulo P. Nonalcoholic fatty liver disease. N Engl J Med 2002; 346:1221-31. doi: 10.1056/NEJMra011775.

[11] Schultz JR, Tu H, Luk A, et al. Role of LXRs in control of lipogenesis. Genes Dev 2000; 14:2831-8. doi: 10.1101/gad.850400.

[12] Musso G, Gambino R, Cassader M. Cholesterol metabolism and the pathogenesis of non-alcoholic steatohepatitis. Prog Lipid Res 2013; 52:175-91. doi: 10.1016/j.plipres.2012.11.002.

[13] Tyagi S, Gupta P, Saini AS, Kaushal C, Sharma S. The peroxisome proliferator-activated receptor: A family of nuclear receptors role in various diseases. J Adv Pharm Technol Res 2011; 2:236. doi: 10.4103/2231-4040.90879.

[14] Ferramosca A, Zara V. Modulation of hepatic steatosis by dietary fatty acids. World J Gastroenterol 2014; 20:1746-755. doi: 10.3748/wjg.v20.i7.1746.

[15] Farrell GC, Larter CZ. Nonalcoholic fatty liver disease: from steatosis to cirrhosis. Hepatology 2006; 43:99-112. doi: 10.1002/hep.20973.

[16] Puntarulo S. Iron, oxidative stress and human health. Mol Aspects Med 2005; 26:299-312. doi: 10.1016/j.mam.2005.07.001.

[17] Adolph TE, Grander C, Grabherr F, Tilg H. Adipokines and non-alcoholic fatty liver disease: multiple interactions. Int J Mol Sci 2017; 18:1649. doi: 10.3390/ijms18081649.

[18] Polyzos SA, Kountouras J, Mantzoros CS. Leptin in nonalcoholic fatty liver disease: a narrative review. Metabolism 2015; 64:60-78. doi: 10.1016/j.metabol.2014.10.012.

[19] Saxena NK, Anania FA. Adipocytokines and hepatic fibrosis. Trends Endocrinol Metab 2015; 26:153-61. doi: 10.1016/j.tem.2015.01.002.

[20] Pessayre D, Fromenty B. NASH: a mitochondrial disease. J Hepatol 2005; 42:928-40. doi: 10.1016/j.jhep.2005.03.004.

[21] Begriche K, Igoudjil A, Pessayre D, Fromenty B. Mitochondrial dysfunction in NASH: causes, consequences and possible means to prevent it. Mitochondrion 2006; 6:1-28. doi: 10.1016/j.mito.2005.10.004.

[22] Seki S, Kitada T, Sakaguchi H. Clinicopathological significance of oxidative cellular damage in non-alcoholic fatty liver diseases. Hepatol Res 2005; 33:132-4. doi: 10.1016/j.hepres.2005.09.020.

[23] Yung, JHM, Giacca, A. Role of c-Jun N-terminal kinase (JNK) in obesity and type 2 diabetes. Cells 2020; 9:706. doi: 10.3390/cells9030706.

[24] Mazzoccoli G, De Cosmo S, Mazza T. The biological clock: A pivotal hub in non-alcoholic fatty liver disease pathogenesis. Front Physiol 2018; 9:1-16. doi: 10.3389/fphys.2018.00193.

[25] Ip E, Farrell G, Hall P, Robertson G, Leclercq I. Administration of the potent PPAR alpha agonist, Wy-14,643, reverses nutritional fibrosis and steatohepatitis in mice. Hepatology 2004; 39:1286-96. doi: 10.1002/hep.20170.

[26] Anstee QM, Daly AK, Day CP. The Genetics of Nonalcoholic Fatty Liver Disease: Spotlight on *PNPLA3* and *TM6SF2*. Semin Liver Dis 2015; 35:270-90. doi: 10.1055/s-0035.156.2947.

[27] Anstee QM, Day CP. The genetics of NAFLD. Nat Rev Gastroenterol Hepatol 2013; 10:645-55. doi: 10.1038/nrgastro.2013.182.

[28] Zeybel M, Mann DA, Mann J. Epigenetic modifications as new targets for liver disease therapies. J Hepatol 2013; 59:1349-53. doi: 10.1016/j.jhep.2013.05.039.

[29] Dongiovanni P, Valenti LA. Nutrigenomic approach to nonalcoholic fatty liver disease. Int J Mol Sci 2017; 18:1534. doi: 10.3390/ijms18071534.

[30] Musso G, Gambino R, De Michieli F, et al. Dietary habits and their relations to insulin resistance and postprandial lipemia in nonalcoholic steatohepatitis. Hepatology 2003; 37:909-16. doi: 10.1053/jhep.2003.50132.

[31] Zelber-Sagi S, Nitzan-Kaluski D, Goldsmith R, et al. Long term nutritional intake and the risk for non-alcoholic fatty liver disease (NAFLD): A population based study. J. Hepatol 2007; 47:711-7. doi:10.1053/jhep.2003.50132.

[32] Bischoff SC, Bernal W, Dasarathy S, et al. ESPEN practical guidline: Clinical nutrition in liver disease. Clin Nut 2020; 39:3533-62. doi: 10.1016/j.clnu.2020.09.001.

[33] Bashiardes S, Shapiro H, Rozin S, Shibolet O, Elinav E. Non-alcoholic fatty liver and the gut microbiota. Mol Metab 2016; 5:782-94. doi: 10.1016/j.molmet.2016.06.003.

[34] Chakaroun RM, Massier L, Kovacs P. Gut microbiome, intestinal permeability, and tissue bacteria in metabolic disease: perpetrators or bystanders? Nutrients 2020; 12:1082. doi: 10.3390/nu12041082.

[35] Suárez M, Boqué N, Del Bas JM, Mayneris-Perxachs J, Arola L, Caimari A. Mediterranean Diet and Multi-Ingredient-Based Interventions for the Management of Non-Alcoholic Fatty Liver Disease. Nutrients 2017; 9:1052. doi: 10.3390/nu9101052.

[36] Ortega AMM, Campos MRS. Bioactive compounds as therapeutic alternatives. In: Bioactive compounds, Cambridge, England: Woodhead Publishing, 2019:247-64. ISBN: 978.012.8147757.

[37] Yang Z, Zhu MZ, Zhang YB, et al. Coadministration of epigallocatechin-3-gallate (EGCG) and caffeine in low dose ameliorates obesity and nonalcoholic fatty liver disease in obese rats. Phytother Res 2019;33:1019-1026. doi: 10.1002/ptr.6295.

[38] Uçar K, Kahramanoğlu K, Göktaş Z. Association between caffeine intake and liver biomarkers in non-alcoholic fatty liver disease. Cukurova Med J 2023; 48:177-86. doi: 10.17826/cumj.1171396.

[39] Rostampour N, Kasiri KA, Hashemi-Dehkordi E, et al. Therapeutic effects of green tea on nonalcoholic fatty liver disease in 10 – 16-year-old children. J Clin Diagn Res 2019; 13:4-7. doi: 10.7860/JCDR/2019/35236.12986.

[40] Kobyliak N, Falalyeyeva T, Bodnar P, Beregova T. Probiotics supplemented with omega-3 fatty acids are more effective for hepatic steatosis reduction in an animal model of obesity. Probiotics Antimicrob Proteins 2017; 9:123-30. doi: 10.1007/s12602.016.9230-1.

[41] Popescu LA, Vîrgolici B. Lixardu D, et al. Effect of diet and omega-3 fatty acids in NAFLD. Rom J Morphol Embryol 2013;54:785-90.

[42] Lee CH, Fu Y, Yang SJ, Chi CC. Effects of omega-3 polyunsaturated fatty acid supplementation on non-alcoholic fatty liver: A systematic review and meta-analysis. Nutrients 2020;12:9. doi: 10.3390/nu12092769.

[43] Alves CC, Waitzberg DL, de Andrade LS, et al. Prebiotic and synbiotic modifications of beta oxidation and lipogenic gene expression after experimental hypercholesterolemia in rat liver. Front Microbiol 2017; 8:2010. doi:10.3389/fmicb.2017.02010.

[44] Behrouz V, Aryaeian N, Zahedi MJ, Jazayeri S. Effects of probiotic and prebiotic supplementation on metabolic parameters, liver aminotransferases, and systemic inflammation in nonalcoholic fatty liver disease: A randomized clinical trial. J Food Sci 2020; 85: 3611-17. doi: 10.1111/1750-3841.15367.

[45] Hernandez-Ortega LD, Alcantar-Diaz BE, Ruiz-Corro LA, et al. Quercetin improves hepatic fibrosis reducing hepatic stellate cells and regulating pro-fibrogenic/anti-fibrogenic molecules balance. J Gastroenterol Hepatol 2012; 27:1865-72. doi:10.1111/j.1440-1746.2012.07262.x

[46] Shen M, Chen K, Lu J, et al. Protective effect of astaxanthin on liver fibrosis through modulation of TGF-beta1 expression and autophagy. Mediators Inflamm 2014; 2014:954502. doi: 10.1155/2014/954502.

[47] Feng Dan, Zou J, Mai H, et al. Curcumin prevents high-fat diet-induced hepatic steatosis in ApoE−/− mice by improving intestinal barrier function and reducing endotoxin and liver TLR4/NF-κB inflammation. Nutr Metab 2019; 16:79. doi: 10.1186/s12986.019.0410-3.

[48] Saberi-Karimian M, Keshvari M, Ghayour-Mobarhan M, et al. Effects of curcuminoids on inflammatory status in patients with non-alcoholic fatty liver disease: a randomized controlled trial. Complement Ther Med 2020; 49:102322. doi: 10.1016/j.ctim.2020.102322.

[49] Asghari S, Asghari-Jafarabadi M, Somi MH, Ghavami SM, Rafraf M. Comparison of calorie-restricted diet and resveratrol supplementation on anthropometric indices, metabolic parameters, and serum sirtuin-1 levels in patients with nonalcoholic fatty liver disease: a randomized controlled clinical trial. J Am Coll Nutr 2018; 37:223-33 doi: 10.1080/07315.724.2017.1392264.

MARMARA
MEDICAL JOURNAL

Original Article

https://dergipark.org.tr/tr/pub/marumj

Impact of fragmented QRS on in-hospital mortality in emergency coronary artery bypass grafting for STEMI: A retrospective analysis

Mehmet ALTUNOVA[1], Gul CAKMAK[2]

[1]Cardiology Clinic, Mehmet Akif Ersoy Thoracic and Cardiovascular Surgery Training and Research Hospital, Istanbul, Turkey
[2]Department of Anesthesiology and Reanimation, School of Medicine, Marmara University, Istanbul, Turkey

Corresponding Author: Mehmet ALTUNOVA
E-mail: dr.mehmetaltunova@gmail.com

Submitted: 18.12.2023 **Accepted:** 23.02.2024

ABSTRACT

Objective: Fragmented QRS complex (fQRS) is associated with increased morbidity and mortality, sudden cardiac death, and recurrent cardiovascular events. The role of coronary artery bypass grafting (CABG) in the primary treatment of acute myocardial infarction remains controversial. In this study, we aimed to assess the predictive value of fQRS in-hospital mortality among acute segment elevation myocardial infarction (STEMI) patients undergoing emergency CABG for primary revascularization.

Patients and Methods: Between 2010 and 2020, we retrospectively included 99 consecutive STEMI patients who were not eligible for primary percutaneous intervention and required emergency CABG. The study population was divided into two groups: survivors and non-survivors. We compared the two groups regarding demographic, clinical, and operative characteristics.

Results: fQRS was identified as an independent predictor of in-hospital mortality ($p = 0.037$). Additionally, left ventricular ejection fraction (LVEF) was an independent predictor of in-hospital mortality ($p = 0.028$). Glomerular filtration rate (GFR), glucose levels, and Killip class ≥ III were significantly associated with in-hospital mortality ($p = 0.002$), ($p = 0.001$) and ($p < 0.001$).

Conclusion: fQRS emerged as an independent predictor of in-hospital mortality among patients undergoing emergency CABG for primary revascularization in cases of STEMI.

Keywords: Fragmented QRS, ST-elevation myocardial infarction, Coronary artery bypass grafting, Mortality

1. INTRODUCTION

Segment elevation myocardial infarction (STEMI) is an acute and potentially fatal condition typically managed through primary percutaneous coronary intervention (pPCI) or thrombolytic therapy [1]. The guidelines for determining when coronary artery bypass grafting (CABG) surgery should be considered in STEMI patients remain somewhat ambiguous. Generally, CABG is regarded as a secondary option in current guidelines, to be pursued when PCI is not technically feasible, fails, or in cases of cardiogenic shock with acute myocardial infarction (AMI) accompanied by mechanical complications. Nevertheless, there is a limited body of research investigating the outcomes of emergent CABG treatment in STEMI patients [2,3].

Fragmented QRS (fQRS) is a depolarization abnormality that reflects delayed ventricular conduction around myocardial scar tissue and has been linked to various cardiac conditions [4-7]. In STEMI patients, fQRS has been demonstrated to be associated with in-hospital mortality, reperfusion failures, and it may serve as an independent predictor for major adverse cardiac events (MACEs) [8,9]. Furthermore, significant correlations have been identified between fQRS and in-hospital MACEs, as well as prognostic factors like hospitalization duration and long-term MACEs in patients undergoing CABG [10]. However, there is a paucity of data concerning the prognostic value of fQRS in patients undergoing emergent CABG.

In this study, we aimed to assess the predictive potential of fQRS in determining in-hospital mortality in STEMI patients undergoing emergent CABG. This study represents the first investigation into the relationship between fQRS and in-hospital mortality in STEMI patients undergoing emergent CABG for primary revascularization.

How to cite this article: Altunova M, Cakmak G. Impact of fragmented QRS on in-hospital mortality in emergency coronary artery bypass grafting for STEMI: A retrospective analysis. Marmara Med J 2024: 37(2):121-128. doi: 10.5472/marumj.1485355

ISSN: 1309-9469

http://doi.org/10.5472/marumj.1485355
Marmara Med J 2024;37(2): 121-128

2. PATIENTS and METHODS

Study population

A total of 125 patients, who were admitted to the catheter laboratory with a diagnosis of STEMI from the emergency department between 2010 and 2020, and for whom pPCI was either unsuitable or unsuccessful, underwent CABG within 6 hours of their emergency admission and were included in our study. This retrospective screening involved the following exclusion criteria: patients undergoing elective CABG after balloon dilation or stent implantation to the culprit lesion (n=7), patients deemed inoperable due to diffuse vascular disease (n=2), patients necessitating simultaneous valve intervention (n=3), acute STEMI patients with mechanical complications (n=1), individuals with chronic kidney and liver failure (n=3), presence of left or right bundle branch block (BBB) (n=4), patients with a pacemaker rhythm (n=1), patients who were receiving type I and III antiarrhythmic drugs (n=1), patients whose electrocardiogram (ECG) was unsuitable for evaluation (n=3), and patients receiving treatment for a previous cerebrovascular disease (n=1). Following the application of these exclusion criteria, a total of 99 patients were included in the study. Demographic data, laboratory findings, and outcomes were obtained from hospital records, file reviews, and telephone interviews. Our study was conducted per the principles of the Declaration of Helsinki and received approval from Mehmet Akif Ersoy Thoracic and Cardiovascular Surgery Training and Research Hospital Ethics Committee with decision number 2023.04-46. Due to the nature of the study, informed consent was not obtained from the patients.

Patient characteristics and definitions

A complete blood count, serum creatinine, total cholesterol, low-density lipoprotein cholesterol (LDL-C), high-density lipoprotein cholesterol (HDL-C), triglycerides (TG), and serum electrolyte levels were assessed. Blood samples were collected during the patients' hospitalization in the emergency room. The Killip class was evaluated upon admission and defined as follows: Killip class 1, AMI without heart failure; Killip class 2, AMI with mild heart failure; Killip class 3, AMI with pulmonary edema; and Killip class 4, AMI with cardiogenic shock [11]. Cardiogenic shock was defined as patients exhibiting pulmonary edema or a cardiac index <2.2 l/min/m2 in the absence of vasopressor or inotrope therapy, or systolic arterial pressure <90 mm Hg or mean arterial pressure (MAP) <65 mm Hg without the administration of a vasopressor agent or the need for vasopressor therapy to correct hypotension. It was also defined as pulmonary artery occlusion pressure >15 mm Hg or echocardiographic evidence of high pressure, or at least evidence of tissue hypoperfusion (e.g., skin mottling, oliguria, elevated lactate level, altered consciousness) [11]. Regarding smoking habits, individuals were categorized as "current smokers" or "non-smokers." Hypertension (HT) was defined as systolic arterial pressure >140 mmHg and/or diastolic arterial pressure >90 mmHg or if the patient was currently using antihypertensive medication [12]. Diabetes mellitus (DM) was defined as having at least two fasting plasma glucose levels ≥ 126 mg/dL or postprandial plasma glucose levels ≥ 200 mg/dL, or the use of anti-diabetic medication. Hyperlipidemia (HL) was defined as having serum total cholesterol ≥ 200 mg/dL, serum triglycerides ≥ 150 mg/dL, low-density lipoprotein cholesterol ≥ 130 mg/dL, a previous diagnosis of hyperlipidemia, or the use of lipid-lowering medication. Chronic renal failure was characterized as an estimated glomerular filtration rate of ≤ 60 mL/min. Chronic liver disease was defined as conditions requiring hospitalization due to cirrhosis or liver-related events.

Furthermore, all patients underwent echocardiographic imaging immediately before CABG. The echocardiographic examinations were conducted using an echocardiography device (GE Vingmed Ultrasound AS, Horten, Norway) equipped with a 3.2 MHz adult probe, and measurements were performed in accordance with the guidelines of the American Society of Echocardiography [13].

Segment elevation myocardial infarction was diagnosed based on the following criteria: ST-segment elevation ≥2.5 mm in men under 40 years of age, ≥2 mm in men aged 40 or older, or ≥1.5 mm in women in leads V2–V3, and/or ≥1 mm in the other leads, all measured at the J point in two contiguous leads [10]. Reperfusion failure during coronary intervention was characterized by the following criteria: less than 50% ST-segment regression within 90 minutes of the initial elevation and a thrombolysis in myocardial infarction (TIMI) flow grade of 0 observed in the infarct-related artery following pPCI or thrombolytic therapy [14]. In-hospital mortality was defined as any cause of death occurring from the time of admission to CABG in patients diagnosed with STEMI.

Fragmented QRS

Upon admission to the emergency department, 12-lead electrocardiograms (ECG) of all patients were recorded with the following settings: a filter range of 0.16–100 Hz, a paper speed of 25 mm/s, and an amplitude of 10 mm/mV. FQRS was defined as follows: the presence of an additional R wave (R') or notching in the nadir of the S wave, or the presence of more than one R' (fragmentation) in two contiguous leads, corresponding to a major coronary artery territory [15]. This definition excluded cases with a typical BBB pattern and incomplete right BBB (Figure 1). The interpretation of all ECG findings was conducted independently by two experienced cardiologists who were blinded to the clinical outcomes. The intra – and inter-observer differences for fQRS were both less than 5%.

Statistical Analysis

The data analysis was conducted utilizing the Statistical Package for the Social Sciences version 26.0 (SPSS Inc., Chicago, Illinois, USA). To assess the distribution of variables, both visual methods (histograms, probability curves) and analytical methods (Kolmogorov–Smirnov or Shapiro–Wilk tests) were employed. Numerical variables that exhibited a normal distribution were presented as mean ± standard deviation, while those not conforming to a normal distribution were expressed as median (interquartile range). Categorical variables were

http://doi.org/10.5472/marumj.1485355
Marmara Med J 2024;37(2): 121-128

reported as percentages (%). To compare numerical variables between the two groups, Student's t-test and Mann–Whitney U test were employed, depending on the distribution. Categorical variables were compared using the Chi-square or Fisher's exact test. Event-free survival curves were constructed utilizing the Kaplan–Meier method and were subjected to comparison using the log-rank test. For calculating hazard ratios (HRs) and their corresponding 95% confidence intervals (95% CI) concerning clinical endpoints, both univariate and multivariate Cox proportional hazards models were applied. In this study, a P-value less than 0.05 was considered statistically significant.

3. RESULTS

This study included a total of 99 patients who presented with acute STEMI and underwent CABG. Among these patients, 59.6% were male, and the mean age was 56 ± 11.2 years. During their hospital admission, 11 (11.1%) patients succumbed to their conditions. Specifically, eight patients died due to low cardiac output syndrome (LCOS), two patients experienced malignant arrhythmias (ventricular fibrillation and tachycardia-resistant LCOS), and two patients passed away as a result of sepsis with accompanying LCOS.

The patients were categorized into two groups: hospital survivors and non-survivors. The baseline demographics, clinical characteristics, and laboratory findings of these study groups are summarized in Table I. While the two groups exhibited similarities in demographics, clinical features, and laboratory characteristics, certain clinical traits such as Killip class > III ($p < 0.001$), cardiogenic shock ($p < 0.001$), and preoperative cardiopulmonary resuscitation ($p < 0.001$) were more prevalent in the non-survivor group. Furthermore, the non-survivor group displayed a higher Thoracic Surgery Society (STS) score ($p < 0.001$). White Blood Cells (WBC) count ($p < 0.001$), glucose levels ($p = 0.001$), and troponin levels ($p = 0.032$) were elevated in the non-survivor group, whereas glomerular filtration rate (GFR; $p = 0.001$) and left ventricular ejection fraction (LVEF) were higher in the survivor group. Additionally, the rate of fQRS ($p < 0.001$) (Figure 1), QRS duration ($p = 0.001$), and heart rate ($p < 0.001$) were greater in the non-survivor group compared to the survivor group.

Table II presents the distribution of responsible lesions, as well as intraoperative and postoperative characteristics of the study groups. The non-survivor group exhibited longer ICU length of stay ($p < 0.001$) and ventilation time ($p < 0.001$), whereas aortic cross-clamp (ACC) duration ($p = 0.049$) was prolonged and the use of internal mammary artery (IMA) ($p = 0.031$) was more common in the survivor group.

Table III provides the results of univariate and multivariate regression analyses aimed at identifying predictors of in-hospital mortality. In the univariate regression analysis, LVEF, GFR, glucose levels, Killip class ≥ III, and fQRS were significantly associated with in-hospital mortality. In the multivariate regression analysis, both LVEF ($p = 0.028$) and fQRS ($p = 0.037$) emerged as independent predictors of in-hospital mortality.

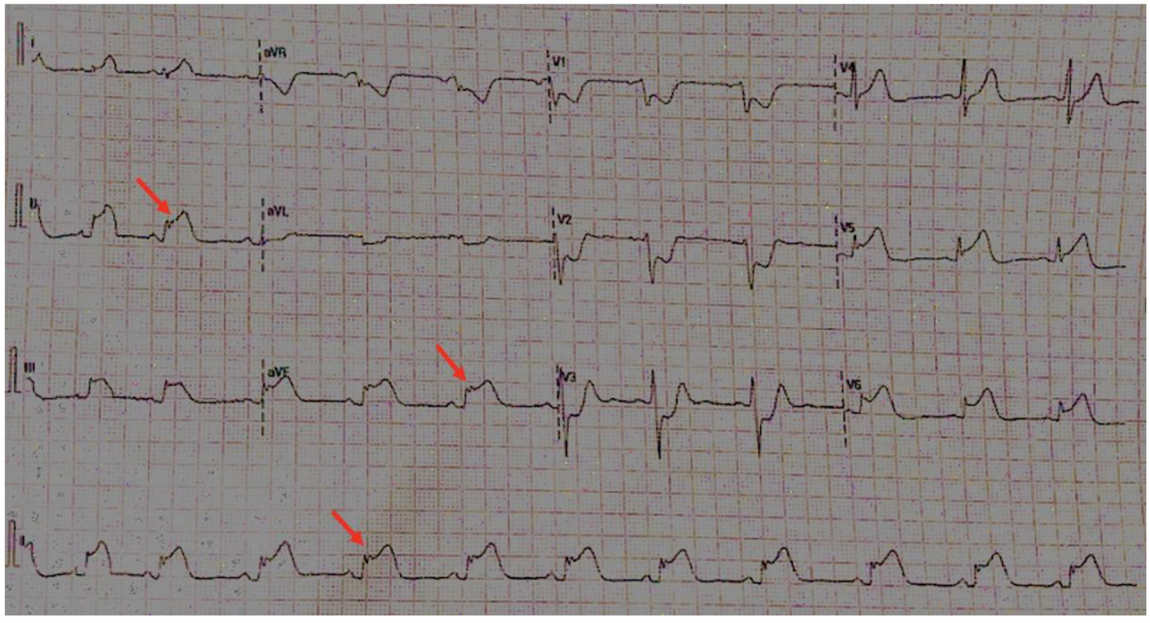

Figure 1. *An exemplary electrocardiogram shows the presence of fragmented QRS in derivatives of DII and AVF in inferior myocardial infarction.*

http://doi.org/10.5472/marumj.1485355
Marmara Med J 2024;37(2): 121-128

Table I. *The baseline demographics, clinical and laboratory characteristics of the study groups*

N = 99	Survivors (n = 88)	Non-survivors (n = 11)	P value
Age, years	55.6 ± 10.6	60 ± 15.1	0.267
Gender (male), n (%)	52 (59.1)	7 (63.6)	0.772
Hypertension, n (%)	25 (28.4)	4 (36.4)	0.585
PAD, n (%)	13 (14.8)	2 (18.2)	0.766
CVD, n (%)	7 (8)	1 (9.1)	0.896
COPD, n (%)	14 (15.9)	2 (18.2)	0.847
Atrial fibrilation, n (%)	4 (4.5)	1 (9.1)	0.516
Smoking, n (%)	27 (30.7)	3 (27.3)	0.817
WBC, 10^6 /L	12.3 ± 4.3	18.7 ± 11.2	**<0.001**
Hemoglobin, g/dL	12.5 ± 2.7	11 ± 1.5	0.087
Platelets, 10^3/uL	236.6 ± 85.8	245.7 ± 94.9	0.744
Glucose, mg/dl	169.2 ± 56.8	238.1 ± 103.5	**0.001**
Total cholesterol, mg/dL	188.1 ± 40.1	184.5 ± 20.1	0.769
LDL-C, mg/dL	126 ± 34	121.2 ± 17.5	0.645
HDL-C, mg/dL	37.8 ± 7.9	40 ± 6.9	0.371
Triglyceride, mg/dL	175.1 ± 93.2	158.7 ± 59.2	0.573
Troponin, ng/mL	0.120 (0.036-0.256)	0.283 (0.127-0.450)	**0.032**
GFR, mL/min	87.5 ± 22.3	62 ± 34.8	**0.001**
LV Ejection Fraction, %	45.4 ± 6.8	35 ± 5.9	**<0.001**
fQRS	21 (23.9)	9 (81.8)	**< 0.001**
Q wave on ECG	18 (20.5)	5 (45.5)	0.064
QRS duration, ms	87.6 ± 13	101.6 ± 15.2	**0.001**
Heart rate, beats / min	82.8 ± 14.4	101.9 ±9.3	**<0.001**
Correct QT duration, ms	439.2 ± 37.6	450.8 ± 44.1	0.344
Previous PCI, n (%)	11 (12.5)	3 (27.3)	0.185
Failed PCI, n (%)	16 (18.2)	5 (45.5)	0.037
Previous stent thrombosis, n (%)	12 (13.6)	1 (9.1)	0.674
CPR before surgery, n (%)	2 (2.3)	3 (27.3)	**<0.001**
Killip class, n (%) I II ≥III	 80 (90.9) 2 (2.3) 6 (6.8)	 3 (27.3) 2 (18.2) 6 (54.5)	**<0.001**
CAD 1 vessel 2 vessels 3 vessels ≥4 vessels	 8 (9.1) 31 (35.2) 29 (33) 20 (22.7)	 3 (27.3) 2 (18.2) 4 (36.4) 2 (18.2)	0.274
Cardiogenic shock, n (%)	3 (3.4)	4 (36.4)	**<0.001**
STS score	5.2 (4.2-6.4)	11.2 (9.4-15.3)	**<0.001**

Data are expressed as percentage, mean±standard deviation, or median (inter – quartile range).

Abbreviations: CAD, coronary artery disease; COPD, chronic obstructive pulmonary disease; CPR, cardiopulmonary resuscitation; CVD, cerebrovascular disease; ECG: electrocardiograms; GFR: glomerular filtration rate; HDL-C: High-density lipoprotein cholesterol; LDL-C: Low-density lipoprotein cholesterol; LVEF: left ventricular ejection fraction; PAD, peripheral artery disease; PCI: percutaneous coronary intervention; STS, Society of Thoracic Surgeons; WBC, White Blood Cells.

http://doi.org/10.5472/marumj.1485355
Marmara Med J 2024;37(2): 121-128

Table II. *The distribution of culprit lesion, intraoperative and postoperative characteristics of study groups*

N = 99	Survivors (n = 88)	Non-survivors (n = 11)	P value
Culprit lesion			0.779
LMCA	24 (27.3)	4 (36.4)	
LAD	63 (71.6)	7 (63.6)	
LCX	1 (1.1)	0 (0)	
RCA	0 (0)	0 (0)	
Intraoperative characteristics			
ACC time (min)	47.7 ± 18.7	36 ± 15.5	**0.049**
CPB time (min)	83.8 ± 35.3	93.8 ± 38	0.381
Grafts per patient (n)	2.74 ± 1.01	2.45 ±1.13	0.388
IMA use	54 (61.4)	3 (27.3)	**0.031**
Complete revascularization (n)	81 (92)	5 (45.5)	**<0.001**
Postoperative characteristics			
Drainage (ml)	640.5 ± 162.4	689.1 ± 188.1	0.360
Hospital stay (days)	7.5 ± 3.7	9.2 ± 6.7	0.195
IABP support	30 (34.1)	7 (63.6)	0.056
ICU stay (days)	2.52 ± 1.8	9.18 ± 6.71	**<0.001**
Ventilation time (h)	9 (6.3-12)	24 (14-214)	**<0.001**

Abbreviations: ACC, aortic cross-clamp; CPB, cardiopulmonary bypass; IABP, intra-arterial balloon pump; ICU, intensive care unit; IMA, internal mammary artery; LAD, left anterior descending artery; LCX, left circumflexartery; LMCA, left main coronary artery; RCA, right coronary artery.

Table III. *Univariate and multiple cox regression analyses to determine predictors of in-hospital mortality*

	Univariate analysis			Multivariate analysis		
	Hazard ratio	95%CI (lower–upper)	P value	Hazard ratio	95%CI (lower–upper)	P value
Age	1.031	0.978-1.088	0.257			
HT	1.427	0.418-4.875	0.571			
COPD	1.168	0.252-5.406	0.843			
PAD	1.266	0.274-5.861	0.763			
CVD	1.107	0.142-8.648	0.923			
LVEF	0.781	0.693-0.879	**<0.001**	0.862	0.755-0.985	**0.028**
GFR	0.958	0.933-0.984	**0.002**	0.983	0.957-1.011	0.231
Glucose[a]	1.010	1.004-1.016	**0.001**	1.001	0.994-1.008	0.717
Troponin[b]	1.708	0.592-4.927	0.322			
Smoking	0.857	0.227-3.231	0.820			
Killip class ≥III	11.016	3.332-36.417	**<0.001**	0.971	0.183-5.161	0.973
ACC timec	0.959	0.919-1.001	0.055			
IABP support	3.267	0.956-11.166	0.059			
fQRS	11.429	2.467-52.957	**0.002**	6.337	1.122-35.800	**0.037**

Abbreviations: ACC, aortic cross-clamp; CAD: coronary artery disease; CI, confidence interval; COPD: chronic obstructive pulmonary disease; CVD: cerebrovascular disease; GFR, glomerular filtration rate; HT: hypertension; IABP, intra-arterial balloon pump; LVEF, left ventricular ejection fraction; OR, odds ratio; PAD: peripheral artery disease.

[a]For each 1 mg/dl increase the odds ratio for mortality.

[b]For each 1 ng/ml increase the odds ratio for mortality.

[c]For each 1 minute increase the odds ratio for mortality.

http://doi.org/10.5472/marumj.1485355
Marmara Med J 2024;37(2): 121-128

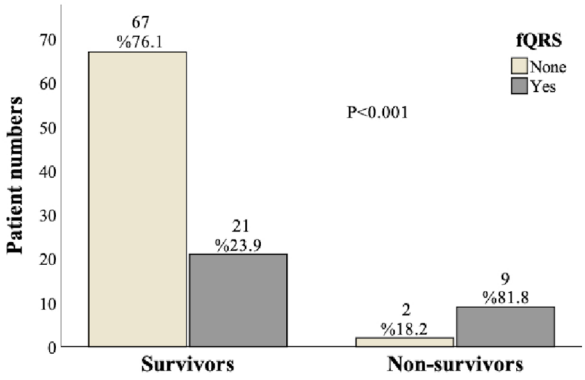

Figure 2. *Distribution of fQRS in-hospital survivors and non-survivors groups.*

4. DISCUSSION

This study sheds light on a significant clinical issue within our clinical practice, and its main findings can be summarized as follows: I) fQRS is strongly associated with in-hospital mortality in patients undergoing CABG for STEMI. II) fQRS and low LVEF were identified as independent predictors of in-hospital mortality.

Primary percutaneous coronary intervention is the standard treatment for STEMI patients, with only a small proportion (5% or less) requiring emergency CABG surgery [16]. Patients with STEMI may have an increased risk of early CABG, which suggests that if patients are hemodynamically stable, delaying surgical revascularization for at least 24 hours might yield better short-term and long-term outcomes [17]. However, patients experiencing ongoing myocardial ischemia may necessitate emergency CABG when PCI is not feasible or has failed. Prior studies on mortality among patients undergoing emergency CABG for STEMI have primarily focused on the duration of the procedure. For example, Voisine et al., reported a mortality rate of 19.2% in patients operated on within 6 hours, although, they did not account for factors necessitating emergency CABG [18]. Axelsson et al., reported an in-hospital mortality rate of 13% in patients who underwent CABG within 24 hours after STEMI [19], while Uygur et al. found a rate of 10.8% in their study [20], and Lemaire et al. reported an 8.2% mortality rate [21]. In our study, which included patients operated on within 6 hours of symptom onset, the in-hospital mortality rate was 11.1%, consistent with the literature.

Risk assessment of patients before surgery is crucial for guiding clinical decisions. Various risk classification scores such as EuroSCORE, STS score, and ACEF score are well-established and widely used in clinical practice [22,23]. In our study, higher Killip class 3 and STS scores were associated with higher in-hospital mortality, in line with the literature. Thielmann et al., demonstrated that preoperative cardiac troponin I (cTnI) levels can predict the risk of in-hospital mortality in patients undergoing emergency CABG for STEMI [24]. Although, troponin levels were elevated in the non-survivor group in our study, it was not identified as an independent predictor in the regression analysis. This may be due to the fact that patients in our study underwent CABG early. Moreover, while high glucose levels were not found to be an independent predictor of in-hospital mortality in our study, they appeared to be a risk factor for such mortality. The role of elevated glucose levels as an independent risk factor for operative mortality after CABG remains controversial in the literature [25,26].

None of the aforementioned risk scores take into account simple ECG findings. fQRS is an ECG finding associated with ventricular conduction disorders observed in various cardiac conditions. The frequency of fQRS on ECG can be as high as 35% in STEMI patients undergoing PCI [27]. In our patient group, the fQRS rate was 30.3%, consistent with the literature. Recent studies have indicated that STEMI patients with fQRS have a significantly higher in-hospital mortality rate and can be used as a risk stratification tool for STEMI patients [28]. It has also been linked to low cardiac output syndrome and in-hospital mortality in patients undergoing CABG surgery [29]. In our study, fQRS was shown to be an independent predictor of in-hospital mortality in STEMI patients who underwent emergency CABG.

Additionally, in previous studies, left ventricular (LV) dysfunction has been identified as an independent risk factor for postoperative complications and mortality in CABG surgery [30]. In line with the literature, low LVEF was found to be an independent risk factor for in-hospital mortality in our patient group.

The presence of cardiogenic shock or preoperative cardiopulmonary resuscitation (CPR) in patients undergoing CABG is associated with a high rate of periprocedural mortality and morbidity [31]. In our study, cardiogenic shock or preoperative CPR was statistically more significant in relation to mortality, which is consistent with the literature. The use of intra-aortic balloon pump (IABP) reflects the acuity level and the presence of cardiogenic shock, often associated with poor left ventricular output, and has been linked to in-hospital mortality [32]. Although, IABP was more frequently used in the non-survivor group in our study, it was not identified as an independent predictor of mortality. Patients in our study underwent urgent procedures, and complete revascularization was achieved in 86.9% of them. Additionally, patients underwent an average of 2.7 distal anastomoses, and the internal mammary artery (IMA) was used less frequently (57%) compared to elective CABG (90-95%) [33].

To our knowledge, this study is the first to evaluate the utility of a simple ECG finding in predicting in-hospital mortality in acute STEMI patients undergoing primary revascularization with CABG and to demonstrate the prognostic power of fQRS.

Study limitations

This study has several limitations that should be acknowledged. Firstly, it was a single-center retrospective study, which may

http://doi.org/10.5472/marumj.1485355
Marmara Med J 2024;37(2): 121-128

limit the generalizability of the findings. Secondly, the non-survivor group had a relatively small sample size, which could impact the statistical power and generalizability of the results. Thirdly, the study did not employ other quantitative methods such as myocardial perfusion scanning or magnetic resonance imaging to confirm myocardial ischemia or scar formation in the study's patients. Additionally, the study lacked long-term follow-up data to assess future cardiovascular events.

In essence, this study demonstrated the effectiveness and utility of fQRS on ECG as an indirect method for predicting in-hospital mortality in patients undergoing emergency CABG for STEMI.

Conclusion

As a marker of myocardial fibrosis, fQRS has the potential to serve as a valuable non-invasive risk assessment tool for patients undergoing emergency CABG for STEMI. This study has demonstrated a clear relationship between in-hospital mortality and the presence of fQRS in such patients. The evaluation of fQRS can aid in identifying individuals at higher risk of developing in-hospital mortality among this patient population. This information can be valuable for clinicians in making informed decisions and optimizing care for these high-risk patients.

Compliance with Ethical Standards

Ethical approval: Our study was conducted per the principles of the Declaration of Helsinki and received approval from Mehmet Akif Ersoy Thoracic and Cardiovascular Surgery Training and Research Hospital Ethics Committee with decision number 2023.04-46.

Funding: This study did not receive any specific grants from funding agencies in the public, commercial, or not-for-profit sector.

Conflict of interest: Both authors have no conflict of interest to declare.

Authors' contributions: Both authors contributed to the understanding and design of the study. MA: Material preparation and data collection, statistical analysis, GC: Language assistance, MA:Writing of the first draft of the article, GC: Commented on previous versions of the article. MA and GC: Proof reading of the article. Both authors have read and approved the final version of the article.

REFERENCES

[1] Ibanez B, James S, Agewall S, et al.. ESC Scientific Document Group. 2017 ESC Guidelines for the management of acute myocardial infarction in patients presenting with ST-segment elevation: The Task Force for the management of acute myocardial infarction in patients presenting with ST-segment elevation of the European Society of Cardiology (ESC). Eur Heart J 2018 7;39:119-77. doi: 10.1093/eurheartj/ehx393.

[2] Rohn V, Grus T, Belohlavek J, Horak J. Surgical revascularisation in the early phase of ST-segment elevation myocardial infarction: Haemodynamic status is more important than the timing of the operation. Heart Lung Circ 2017;26:1323-29. doi: 10.1016/j.hlc.2017.01.009.

[3] Khan AN, Sabbagh S, Ittaman S, et al. Outcome of early revascularization surgery in patients with ST-elevation myocardial infarction. J Interv Cardiol 2015;28:14-23. doi: 10.1111/joic.12177.

[4] Das MK, Saha C, El Masry H, et al. Fragmented QRS on a 12-lead ECG: a predictor of mortality and cardiac events in patients with coronary artery disease. Heart Rhythm 2007;4:1385-92. doi: 10.1016/j.hrthm.2007.06.024.

[5] Gungor B, Ozcan K S, Karatas M B, Sahin I, Ozturk R, Bolca O. (2016). Prognostic value of QRS fragmentation in patients with acute myocardial infarction: a meta-analysis. Ann Noninvasive Electrocardiol 2016;21:604-12. doi:10.1111/anec.12357

[6] Rosengarten J A, Scott P A, Morgan J M. 2015). Fragmented QRS for the prediction of sudden cardiac death: a meta-analysis. Europace 2025; 17: 969-77. doi:10.1093/europace/euu279

[7] Altunova M, Püşüroğlu H, Karakayalı M, et al. Relationship between fragmented QES complex and long-term cardiovascular outcome in patients with essential hypertension. Anatol J Cardiol. 2022;26:442-9. doi: 10.5152/AnatolJCardiol.2022.1322.

[8] Kewcharoen J, Trongtorsak A, Kittipibul V, et al. Fragmented QRS predicts reperfusion failure and in-hospital mortality in ST-Elevation myocardial infarction: a systematic review and meta-analysis. Acta Cardiol 2020 ;75:298-311. doi: 10.1080/00015.385.2019.1584696.

[9] Xia W, Feng XY. Fragmented QRS (fQRS) complex predicts adverse cardiac events of st-segment elevation myocardial infarction patients undergoing percutaneous coronary intervention and thrombolysis. Med Sci Monit 2018;24: 4634-40. doi: 10.12659/MSM.908712.

[10] Çiçek Y, Kocaman SA, Durakoğlugil M, et al. Relationship of fragmented QRS with prognostic markers and long-term major adverse cardiac events in patients undergoing coronary artery bypass graft surgery. J Cardiovasc Med (Hagerstown) 2015;16:112-7. doi: 10.2459/01.JCM.000.043.5615.40439.68.

[11] Levy B, Clere-Jehl R, Legras A, et al. Epinephrine versus norepinephrine for cardiogenic shock after acute myocardial infarction. J Am Coll Cardiol 2018;72:173-82. doi:0.1016/j.jacc.2018.04.051.

[12] Karakayali M, Artac I, Omar T, et al. The association between frontal QRS-T angle and reverse dipper status in newly diagnosed hypertensive patients. Blood Press Monit 2023;28:96-102. doi: 10.1097/MBP.000.000.0000000637.

[13] Lang RM, Badano LP, Mor-Avi V, et al. Recommendations for cardiac chamber quantification by echocardiography in adults: an update from the American Society of Echocardiography and the European Association of Cardiovascular Imaging. J Am Soc Echocardiogr 2015;28:1-39.

[14] de Lemos JA, Morrow DA, Gibson CM, et al. TIMI 14 Investigators. Thrombosis in myocardial infarction. Early noninvasive detection of failed epicardial reperfusion after

fibrinolytic therapy. Am J Cardiol 2001;88:353-8. doi: 10.1016/s0002-9149(01)01678-2.

[15] Das MK, Khan B, Jacob S, Mahenthiran J. Significance of a fragmented QRS complex versus a Q wave in patients with coronary artery disease. Circulation 2006;113:2495-501. doi: 10.1161/CIRCULATIONAHA.105.595892.

[16] Gu YL, van der Horst IC, Douglas YL, Svilaas T, Mariani MA, Zijlstra F. Role of coronary artery bypass grafting during the acute and subacute phase of ST-elevation myocardial infarction. Neth Heart J 2010;18:348-54. doi: 10.1007/BF03091790.

[17] Lang Q, Qin C, Meng W. Appropriate timing of coronary artery bypass graft surgery for acute myocardial infarction patients: A meta-analysis. Front Cardiovasc Med 2022;9:794925. doi: 10.3389/fcvm.2022.794925.

[18] Voisine P, Mathieu P, Doyle D, et al. Influence of time elapsed between myocardial infarction and coronary artery bypass grafting surgery on operative mortality. Eur J Cardiothorac Surg 2006;29:319-23. doi: 10.1016/j.ejcts.2005.12.021.

[19] Axelsson TA, Mennander A, Malmberg M, Gunn J, Jeppsson A, Gudbjartsson T. Is emergency and salvage coronary artery bypass grafting justified? The Nordic Emergency/Salvage coronary artery bypass grafting study. Eur J Cardiothorac Surg 2016;49:1451-6. doi: 10.1093/ejcts/ezv388.

[20] Uygur B, Demir AR, Guner A, Iyigun T, Uzun N, Celik O. Utility of logistic clinical SYNTAX score in prediction of in-hospital mortality in ST-elevation myocardial infarction patients undergoing emergent coronary artery bypass graft surgery. J Card Surg 2021;36:857-63. doi: 10.1111/jocs.15308.

[21] Lemaire A, Vagaonescu T, Ikegami H, Volk L, Verghis N, Lee LY. Delay in coronary artery bypass grafting for STEMI patients improves hospital morbidity and mortality. J Cardiothorac Surg 2020;15:86. doi: 10.1186/s13019.020.01134-x.

[22] Ranucci M, Castelvecchio S, Menicanti L, Frigiola A, Pelissero G. Risk of assessing mortality risk in elective cardiac operations: age, creatinine, ejection fraction, and the law of parsimony. Circulation 2009 ;119:3053-61. doi: 10.1161/CIRCULATIONAHA.108.842393.

[23] Nashef SA, Roques F, Sharples LD, et al. EuroSCORE II. Eur J Cardiothorac Surg 2012;41:734-44. doi: 10.1093/ejcts/ezs043

[24] Thielmann M, Massoudy P, Neuhauser M, et al. Prognostic value of preoperative cardiac troponin I in patients undergoing emergency coronary artery bypass surgery with non-ST-elevation or ST-elevation acute coronary syndromes. Circulation 2006;114(1 Suppl):I448-53. doi: 10.1161/CIRCULATIONAHA.105.001057.

[25] Antunes PE, de Oliveira JF, Antunes MJ. Coronary surgery in patients with diabetes mellitus: a risk-adjusted study on early outcome. Eur J Cardiothorac Surg 2008;34:370-5. doi: 10.1016/j.ejcts.2008.05.008.

[26] Leavitt BJ, Sheppard L, Maloney C, Clough RA, Braxton JH, Charlesworth DC et al.; Northern New England Cardiovascular Disease Study Group. Effect of diabetes and associated conditions on long-term survival after coronary artery bypass graft surgery. Circulation. 2004 Sep 14;110(11 Suppl 1):II41-4. doi: 10.1161/01.CIR.000.013.8197.07051.e7.

[27] Kanjanahattakij N, Rattanawong P, Riangwiwat T, et al. Fragmented QRS and mortality in patients undergoing percutaneous intervention for ST-elevation myocardial infarction: Systematic review and meta-analysis. Ann Noninvasive Electrocardiol 2018 ;23:e12567. doi: 10.1111/anec.12567. Epub 2018 Jun 22

[28] Kewcharoen J, Trongtorsak A, Kittipibul V, et al. Fragmented QRS predicts reperfusion failure and in-hospital mortality in ST-elevation myocardial infarction: a systematic review and meta-analysis. Acta Cardiol 2020 ;75:298-311. doi: 10.1080/00015.385.2019.1584696.

[29] Erdoğan T, Çetin M, Kocaman SA, et al. Relationship of fragmented QRS with prognostic markers and in-hospital MACE in patients undergoing CABG. Scand Cardiovasc J 2012;46:107-13. doi: 10.3109/14017.431.2011.651485.

[30] Vickneson K, Chan SP, Li Y, et al. Coronary artery bypass grafting in patients with low ejection fraction: what are the risk factors? J Cardiovasc Surg (Torino) 2019;60:396-405. doi: 10.23736/S0021-9509.19.10670-2.

[31] Sergeant P, Meyns B, Wouters P, Demeyere R, Lauwers P. Long-term outcome after coronary artery bypass grafting in cardiogenic shock or cardiopulmonary resuscitation. J Thorac Cardiovasc Surg 2003 ;126:1279-86. doi: 10.1016/s0022-5223(03)01289-3.

[32] Poirier Y, Voisine P, Plourde G, et al. Efficacy and safety of preoperative intra-aortic balloon pump use in patients undergoing cardiac surgery: a systematic review and meta-analysis. Int J Cardiol 2016;207:67-79. doi: 10.1016/j.ijcard.2016.01.045.

[33] Gong B, Li Z. Total mortality, major adverse cardiac events, and echocardiographic-derived cardiac parameters with fragmented qrs complex. Ann Noninvasive Electrocardiol 2016;21:404-12. doi: 10.1111/anec.12325.

MARMARA
MEDICAL JOURNAL

Original Article

https://dergipark.org.tr/tr/pub/marumj

The impact of right ventricular energy failure on the results of pulmonary endarterectomy and balloon pulmonary angioplasty in patients with chronic thromboembolic pulmonary hypertension

Redwan Seid BUSERY[1], Bulent MUTLU[1], Dursun AKASLAN[2], Emre ASLANGER[3], Bedrettin YILDIZELI[4], Halil ATAS[1]

[1] Department of Cardiology, School of Medicine, Marmara University, Pendik Training and Research Hospital, Istanbul, Turkey
[2] Cardiology Clinic, Antalya City Hospital, Antalya, Turkey
[3] Cardiology Clinic, Başakşehir Pine and Sakura City Hospital, Istanbul, Turkey
[4] Thoracic Surgery, School of Medicine, Marmara University, Pendik Training and Research Hospital, Istanbul, Turkey

Corresponding Author: Redwan Seid BUSERY
E-mail: redwan.900@gmail.com

Submitted: 25.03.2024 **Accepted:** 07.05.2024

ABSTRACT

Objective: We aimed to investigate the effect of right ventricular energy failure (RVEF) on hemodynamic and clinical outcomes in patients diagnosed with chronic thromboembolic pulmonary hypertension (CTEPH) undergoing pulmonary endarterectomy (PEA) surgery or balloon pulmonary angioplasty (BPA).

Patients and Methods: A total of 100 CTEPH patients planned for PEA or BPA were included in the study. Based on the presence of RVEF during diagnosis, patients divided into two groups. Hemodynamic data from right heart catheterization (RHC) were compared before and after procedures in 3-6 months follow up period.

Results: Patients with RVEF revealed a decrease in mean pulmonary artery pressure (mPAP) from 54.67±12.27 mmHg to 36.12±11.76 mmHg (p:<0.001), mean right atrial pressure (mRAP) from 13.40±4.08 mmHg to 9.76±4.56 mmHg (p:0.003), and pulmonary vascular resistance (PVR) from 11.36±5.15 Wood Units (WU) to 5.46±3.30 WU (p <0.001). In the non-RVEF group, mPAP decreased from 38.82±12.61 mmHg to 30.81±10.57 mmHg (p:<0.001), mRAP from 7.09±3.02mmHg to 7.15±3.07mmHg (p: 0.917), and PVR from 6.33±3.65 WU to 4.09±2.31 WU (p:<0.001).

Conclusion:The presence of RVEF at the time of diagnosis in CTEPH patients does not have a negative impact on early perioperative and 3-month postoperative outcomes following PEA or BPA. This high-risk patient group demonstrated significant hemodynamic and clinical benefits from both PEA and BPA.

Keywords: Chronic thromboembolic pulmonary hypertension, Right ventricular energy failure, Pulmonary endarterectomy, Pulmonary balloon angioplasty

1. INTRODUCTION

Chronic thromboembolic pulmonary hypertension (CTEPH) is a rare and progressive disease that occurs as a result of the occlusion of the pulmonary arteries by organized blood clots. The diagnosis of CTEPH is established by the presence of filling defects in two or more segments on ventilation-perfusion scintigraphy (V/Q), visualization of obstructive or flow-limiting material in the pulmonary arteries using computed tomography pulmonary angiography (CTPA) and/or selective pulmonary angiography with digital subtraction angiography (DSA). A diagnosis of CTEPH is made when, after at least 3 months of effective anticoagulation therapy for pulmonary embolism (PE) diagnosis, the mean pulmonary artery pressure (mPAP) is greater than 20 mmHg on the right heart catheterization (RHC), the pulmonary capillary wedge pressure (PCWP) is less than 15 mmHg, and the pulmonary vascular resistance (PVR) is greater than 2 Wood Units (WU). If imaging methods demonstrate the disease but pulmonary hypertension is not detected on RHC, a diagnosis of chronic thromboembolic pulmonary disease (CTEPD) is made [1].

The treatment algorithm for CTEPH includes a multimodal approach consisting of pulmonary endarterectomy (PEA) targeting anatomical lesions, balloon pulmonary angioplasty (BPA), and combinations of medical therapies. PEA is the

How to cite this article: Busery SR, Mutlu B, Akaslan D, Aslanger E, Yildizeli B, Atas H. The impact of right ventricular energy failure on the results of pulmonary endarterectomy and balloon pulmonary angioplasty in patients with chronic thromboembolic pulmonary hypertension. Marmara Med J 2024: 37(2):129-136. doi: 10.5472/marumj.1484403

ISSN: 1309-9469

http://doi.org/10.5472/marumj.1484403
Marmara Med J 2024;37(2): 129-136

preferred and gold standard treatment method significantly improving pulmonary hemodynamics and functional capacity in CTEPH patients with accessible lesions [2].

Balloon pulmonary angioplasty has become a treatment option that improves right heart function and exercise capacity in patients who are not suitable for PEA surgery due to technical reasons or comorbidities, or in those who develop pulmonary hypertension after PEA due to residue CTEPH [3,4].

In pulmonary hypertension and CTEPH patients, an increased PVR in the pulmonary vascular bed leads to workload on the right ventricle, eventually resulting in right heart failure. Clinical manifestations and mortality in patients are primarily driven by the development of right heart failure, which has prognostic implications. Right ventricular energy failure (RVEF) is defined by a ratio of left atrial (or PCWP) pressure to right atrial pressure <1, which provides more specific information about the patient's RV systolic performance related to their own pulmonary vascular status, independent of volume status, PVR, and RV systolic dysfunction levels [5-7].

In previous studies RVEF was defined as the RA pressure to PCWP ratio and has been investigated as predictor of long term mortality and 1 year survival rate in group 1 PH patients [7]. RVEF in CTEPH patients is similarly used in our study and to our knowledge there is no prospectively studied data on hemodynamic outcome after PEA and BPA procedure. The aim of this study is to investigate the impact of presence of right ventricular energy failure, at the time of diagnosis on the outcomes of PEA surgery and BPA.

2. PATIENTS and METHODS

Study design

This study was conducted at Marmara University, Pendik Training and Research Hospital, a tertiary center for pulmonary hypertension (PH) by the Department of Cardiology. Ethical approval for the study was obtained from the Clinical Research Ethics Board (18.04.2023 approval number: 09.2023.309), and the study was conducted in accordance with the Helsinki Declaration. Patients referred to our center with a diagnosis of CTEPH between February 2023, and October 2023 with a plan for PEA surgery or BPA intervention were included in the study. Post procedural findings were collected prospectively.

All patients were evaluated by a multidisciplinary team, including an experienced cardiothoracic surgeon specialized in PEA, an interventional cardiologist specialized in BPA, a pulmonologist, a rheumatologist, and a radiologist experienced in pulmonary hypertension. A comprehensive examination included transthoracic echocardiography, multislice computed tomographic angiography, ventilation/perfusion scintigraphy, right heart catheterization, and selective pulmonary angiography when necessary. All patients were evaluated for the diagnosis and management of CTEPH according the European Society of Cardiology/European Respiratory Society (ESC/ERS) guidelines for PH [1,8].

Inclusion and exclusion criteria

Patients aged 18 and above, diagnosed with CTEPH, and deemed suitable for surgical or BPA procedures who consented to participate were included in the study. Pulmonary endarterectomy and BPA procedures were conducted at Marmara University Pendik Training and Research Hospital. Patients diagnosed with CTEPH but having significant valve disease (except functional tricuspid regurgitation), left ventricular systolic dysfunction (EF < 50%), and those with a prior diagnosis of atrial fibrillation were excluded from the study.

Study protocol

Clinical and hemodynamic assessment

In this cohort study, initial baseline assessment with detailed medical history, comorbidities and past treatment modalities, namely anticoagulant use and pulmonary vasodilator drug classes were documented. Follow-up findings were evaluated prospectively at 3 to 6 months after the completion of the appropriate treatment strategy.

Demographic findings were recorded in a previously prepared case follow-up forms. Blood samples were collected from all patients for complete blood count, renal function tests, liver function tests, and serum N-terminal pro-brain natriuretic peptide (NT-proBNP) levels. A 6-minute walk distance test (6MWT) was conducted by an experienced nurse, and all information was added to the case follow-up form.

Patients who underwent PEA or BPA received pre-procedural hemodynamic assessment via right heart catheterization (RHC) conducted by an interventional cardiologist specialized in this field. A 7-F Swan-Ganz catheter (Edwards Lifesciences) was inserted through femoral or jugular venous approach for RHC. Measurements included mean right atrial pressure (mRAP), right ventricular (RV) pressure, systolic pulmonary artery pressure (sPAP), diastolic pulmonary artery pressure (dPAP), mean pulmonary artery pressure (mPAP), mean pulmonary artery wedge pressure (mPAWP),

Patient's height, weight, and hemoglobin levels were noted, and using pulmonary artery and systemic saturations, cardiac output (CO), cardiac index (CI), pulmonary vascular resistance (PVR) and systemic vascular resistance (SVR) measurements were calculated via the Fick method. RVEF assessment utilized mRAP and PCWP. Right ventricular energy failure was defined as a ratio of mean PCWP to mean RA pressure ≤1.

All pressure tracings were visually inspected for physiological accuracy, and expiratory end pressure values were recorded. RHC reports were generated using a database program that records the findings of pulmonary hypertension patients within our institution and all parameters were reassessed during diagnosis and repeated 3-6 months after treatment.

Right ventricular energy failure (RVEF)

Right ventricular energy failure (RVEF) is a condition where the heart's right ventricle cannot effectively pump blood, leading

http://doi.org/10.5472/marumj.1484403
Marmara Med J 2024;37(2): 129-136

to various cardiac and pulmonary issues. This condition often results from increased pulmonary vascular resistance causing high pressure in the right ventricle, leading to right ventricular failure.

Right ventricular energy failure is typically evaluated by measuring parameters from right heart catheter findings mainly mean pulmonary artery pressure (mPAP) and mean right atrial pressure (mRAP). A defining feature of RVEF is the ratio of mPCWP to mRAP, and a ratio ≤1 indicates energy failure [7,9].

Utilizing RHC findings for patients diagnosed with CTEPH, the mPCWP and mRAP ratio were calculated for all patients, and based on the obtained value, patients were categorized into two groups: those with RVEF and those with no RVEF. The pre – and post-treatment RHC, 6MWT, NT-proBNP, and functional capacities of both groups were compared.

Statistical Analysis

The data were analysed using IBM SPSS statistics (version 26.0; SPSS Inc., Chicago, Illinois). The distribution of variables was evaluated according to the Kolmogorov-Smirnov criteria. Continuous variables were presented as mean ± standard deviation (SD) or median (interquartile range, IQR). Categorical variables were expressed as numbers and percentages.

Depending on the presence of subgroups of RVEF, the chi-square test, Student's t-test, and Mann-Whitney U test were used for comparisons of baseline parameters before and after the appropriate treatment accordingly. Two-way correlation analysis was performed using the Pearson test for normally distributed data and the Spearman test for non-normally distributed data. Statistical analyses with a p-value below 0.05 were considered significant.

3. RESULTS

Demographic data

A total of 128 CTEPH patients were included in the study. 67 patients were evaluated as suitable for PEA through a multidisciplinary approach, and PEA was planned. Simultaneous coronary artery bypass graft surgery was performed in 3 of these patients. 3 patients declined PEA. Eight patients died, with 1 during PEA surgical preparation and 7 during the intensive care follow-up after the surgical procedure. A total of 12 patients could not undergo surgery due to technical reasons or unfavorable risk/benefit ratios. Among them, 4 had previously undergone PEA and were being followed for residual CTEPH. These patients were re-evaluated in the CTEPH council, and 2 were treated with BPA. The remaining 2 patients with residual CTEPH and the remaining 8 patients were followed with medical treatment only.

After selective pulmonary angiography and a comprehensive evaluation, BPA was decided as a treatment option for 43 patients. A total of 218 BPA sessions were performed on these patients and RHC and clinical evaluations were performed 3-6 months after the last BPA session. Of these, 100 patients were included in the final analysis of our study, 27 (27%) had RVEF, and 73 (73%) did not. The mean age of patients with RVEF was 47.96 ± 15.12 years, while the non-RVEF group had a mean age of 56.14 ± 13.97 years. In the RVEF group, 13 (48.1%) were male, while the non-RVEF group consisted of 35 (47.9%) males.

The NT-ProBNP values were 2297.48 ± 2881.93 ng/L and 1436.59 ± 1737.21 ng/L, respectively, for the RVEF and non-RVEF groups, and the 6MWT distances were 297.11 ± 122.35 m and 281.2 ± 114.0 m, respectively.

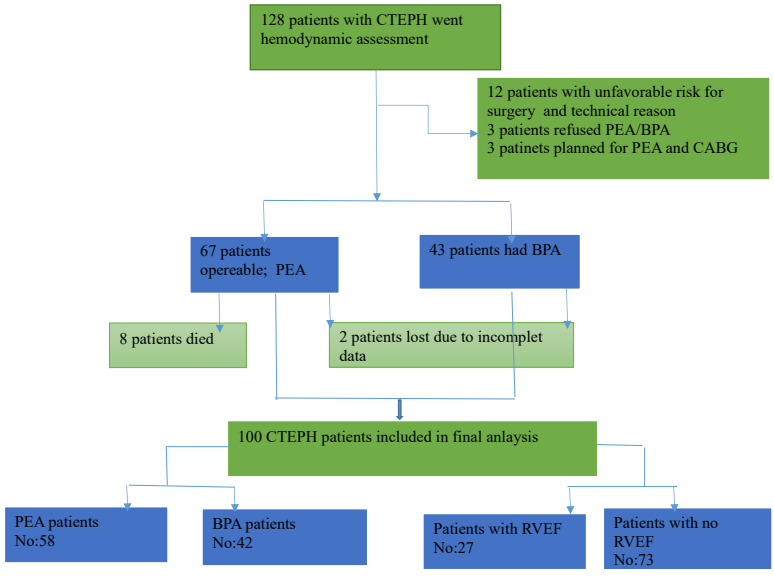

Figure 1. *Patient selection and disposition*
BPA: Balloon Pulmonary Angioplasty; CABG: Coronary Artery Bypass Graft; CTEPH: Chronic Thromboembolic Pulmonary Hypertension; PEA: Pulmonary Endarterectomy; RVEF: Right Ventricular Energy Failure

http://doi.org/10.5472/marumj.1484403
Marmara Med J 2024;37(2): 129-136

In the RVEF group, 8 (29.6%) patients had controlled hypertension (HT), and 3 (11.1%) had controlled diabetes mellitus (DM). In the non-RVEF group, there were 42 (57.5%) with HT and 12 (16.4%) with DM. A history of coronary artery disease was found at 2 (7.4%) in the RVEF group and 7 (9.6%) in the non-RVEF group. All patients were on anticoagulant therapy. Of these, 42% were on warfarin, 33% on rivaroxaban, 20% on enoxaparin, and the remaining 5% were on other direct oral anticoagulant treatment (Table I).

Table I. *Hemodynamic findings according to patients' demographic characteristics and the presence of RVEF.*

Variables	RVEF present (27)	RVEF absent (73)	P value
Demographic data			
Age, years	47.96 ±15.12	56.14±13.97	0.013
Gender, male n(%)	13(48.1%)	35(47.9%)	0.096
BMI, kg./m2	25.57±7.37	28.15±5.32	0.056
Hb, g/dl	12.96±2.37	13.23±1.65	0.534
NT-Probnp, ng/L *	2052.50 (393.75 – 6017.85)	1005.0 8(886.40 – 2082.14)	0.072
Creatinin, mg/dl	0.84±032	0.81±0.23	0.666
6MWT, m	297.11±122.35	281.2±114.0	0.547
Coomorbidities			
HT	8 (29.6%)	42(57.5%)	0.023
DM	3 (11.1%)	12(16.4%)	0.753
Thyroid disorder	5(18.5%)	17(23.3%)	0.787
CAD	2(7.4%)	7(9.6%)	1.000
COPD	5(18.5%)	8(11%)	0.329
DVT	10(37%)	21(28%)	0.470
Hemodynamic parameters			
PA systolic, mmhg	91.38±20.36	65.32±22.15	**<0.001**
PA diastolic, mmhg	32.54±10.64	23.88±8.93	**<0.001**
PA mean, mmhg	54.92±11.80	38.77±12.75	**<0.001**
Ao BP mean,mmhg	93.37±17.14	95.71±18.90	0.558
RA mean, mmhg	13.37±3.93	7.15±2.99	**<0.001**
CI, L/min/m2	2.28±0.54	2.63±0.63	**0.010**
PVR, woods	11.48±5.15	6.13±3.44	**<0.001**
SaPO2 (%)	93.27±3.80	93.53±4.05	0.778
Pa O2 (%)	58.82±10.81	65.25±6.92	0.001

Values are mean ± standard deviation or number (percentage), unless specified otherwise.
** median (interquartile range, IQR)*
6MWT: six-minute walk test distances; Ao: Aortic; BMI: Body Mass Index; BNP: B-type Natriuretic Peptide; BP: Blood Pressure; CI: Cardiac Index; DM: Diabetes Mellitus; DVT: Deep Vein Thrombosis; Hb: Hemoglobin; HT: Hypertension; COPD: Chronic Obstructive Pulmonary Disease; mPAP: Mean Pulmonary Artery Pressure; NT-proBNP: N-terminal pro-B-type Natriuretic Peptide; PA: Pulmonary Artery; PAWP: Pulmonary Artery Wedge Pressure; PVR: Pulmonary Vascular Resistance; PaO2: Arterial Oxygen Partial Pressure; RA: Right Atrium; RV: Right Ventricle; SaO2: Arterial Oxygen Saturation; sPAP: Systolic Pulmonary Artery Pressure; SVR: Systemic Vascular Resistance.

RHC Hemodynamic findings

When looking at the RHC data obtained from patients with and without RVEF, the mean pulmonary artery pressure (mPAP) of patients with RVEF was 54.92 ± 11.80 mmHg, mean right atrial pressure (mRAP) was 13.37 ± 3.93 mmHg, pulmonary capillary wedge pressure (PAWP) was 9.96 ± 2.60 mmHg, and pulmonary vascular resistance (PVR) was 11.48 ± 5.15 WU.

For patients without RVEF, mPAP was 38.77 ± 12.75 mmHg, mRAP was 7.15 ± 2.99 mmHg, and PVR was 19.66 ± 6.20 WU.

Hemodynamic and clinical response to PEA surgery and BPA procedure according to presence of RVEF is shown in Table II. Patients with RVEF showed an increase in 6MWT after the procedure from 297.77 ± 124.72m to 370.12 ± 109.66m ($p < 0.001$) and a decrease in NT-proBNP values from 2280 ± 2937.63 , ng/L to 824 ± 941, ng/L ($p = 0.016$).

When examining the hemodynamic data of patients with RVEF, a statistically significant decrease was observed in mPAP from 54.67 ± 12.27mmHg to 36.12 ± 11.76mmHg, mRAP from 13.40 ± 4.08mmHg to 9.76 ± 4.56mmHg, PVR from 11.36 ± 5.15 WU to 5.46 ± 3.30 WU.

In patients without RVEF, a decrease in NT-proBNP values (from 1384.32 ± 1760.29 to 501.97 ± 722.16) and an increase in the 6MWT from 300.92 ± 104.96m to 348.63 ± 97.91m were observed after the procedure. This difference was found to be statistically significant for both parameters ($p < 0.001$) (Table II).

http://doi.org/10.5472/marumj.1484403
Marmara Med J 2024;37(2): 129-136

Table II. *Response to PEA surgery and BPA procedure in patients with RVEF and without RVEF.*

Variables	Patients with RVEF			Patients without RVEF		
	Pre procedure	Post procedure (PEA/ BPA)	P values	Pre procedure	Post procedure (PEA/BPA)	P values
Hb, g/dl	12.85±2.33	12.82±2.05	0.923	13.25 ±1.63	13.65±1.44	0.101
NT-Pro Bnp, ng/L *	908.5 (361.3 – 3326.2)	377.5 (131.2 – 1610.48)	**0.016**	510.0 (290.8 – 2790.8)	296.0 (95.5 8 – 1223.71)	**<0.001**
6MWT, m	297.77 ±124.72	370.12 ±109.66	**<0.001**	300.92±104.96	348.63±97.91	**<0.001**
PA systolic, mmhg	91.17±21.18	62.75±20.27	**<0.001**	66.03±22.42	51.57±18.573	**<0.001**
PA diastolic, mmhg	31.83±10.76	21.83±7.29	**0.002**	23.85±9.31	19.34±7.25	**<0.001**
PA mean, mmhg	54.67±12.27	36.12±11.76	**<0.001**	38.82±12.61	30.81±10.57	**<0.001**
Ao BP mean, mmhg	90.40±13.66	87.04±16.69	0.381	95.57±19.15	93.72±17.93	0.426
RA mean, mmhg	13.40±4.08	9.76±4.56	**0.003**	7.09±3.02	7.15±3.07	0.917
PCWP, mmhg	9.96±2.60	11.32±3.65	0.055	11.23±3.52	11.49±2.95	0.413
CI, L/min/m2	2.29±0.52	2.71±0.67	**0.025**	2.62±0.64	2.65±0.59	0.767
PVR, woods	11.36±5.15	5.46±3.30	**<0.001**	6.33±3.65	4.09±2.31	**<0.001**
SaPO2, %	93.08±3.67	93.50±3.64	0.491	93.63±3.81	94.78±3.54	0.028
PaO2, %	58.41±11.13	65.29±8.48	0.004	65.68±6.85	65.83±7.29	0.896

Values are mean ± standard deviation or number, unless specified otherwise.
** median (interquartile range, IQR)*
Ao: Aortic; BMI: Body Mass Index; BNP: B-type Natriuretic Peptide; BP: Blood Pressure; CI: Cardiac Index; Hb: Hemoglobin; mPAP: Mean Pulmonary Artery Pressure; NT-proBNP: N-terminal pro-B-type Natriuretic Peptide; PA: Pulmonary Artery; PAWP: Pulmonary Artery Wedge Pressure; PVR: Pulmonary Vascular Resistance; PaO2: Arterial Oxygen Partial Pressure; RA: Right Atrium; RV: Right Ventricle; SaO2: Arterial Oxygen Saturation; sPAP: Systolic Pulmonary Artery Pressure; SVR: Systemic Vascular Resistance.

Table III. *Demographic and hemodynamic findings of CTEPH patients undergoing PEA surgery and BPA procedure*

	Patients undergoing PEA (total 58)			Patients undergoing BPA (total 42)		
Variables	**With RVEF (12)**	**Without RVEF (46)**	**P Value**	**With RVEF (15)**	**Without RVEF (27)**	**P Value**
Demographic values						
Age, years	50.5(39.77-56.67)	59.0(50.36-61.1)	0.064	46.50(36.7-59.88)	57.0(46.5-67.22)	0.185
BMI, kg./m2	27.7(24.54-28.76)	28.7(27.14-31.18)	0.610	24.97(18.47-30.95)	27.68(26.09-31.06)	0.590
Hb, g/dl	12.05(10.26-14.91)	13.15(12.46-13.7)	0.623	13.05(11.60-13.66)	13.1(12.46-14.05)	0.393
NT-Probnp, ng/L	2052.5(393.7-6017.8)	1005.0(886.4-2082.1)	0.264	908.5(361.31-3326)	510(290.81-2790.8)	0.208
Creatinin, mg/dl	0.775(0.63-0.99)	0.795(0.68-0.88)	0.417	0.80(0.66-1.38)	0.8(0.52-1.35)	0.517
NT-proBNP	287.5(233.3-344.6)	272.5(236.6-302.9)	0.417	266.0(293.25-392.85)	266(221.58-342.79)	0.534
Hemodynamic parameter						
PA mean, mmhg	57.5(42.13-67.07)	32.5(31.52-42.27)	**0.001**	55.5(50.69-60.48)	40.0(35.28-44.95)	**<0.001**
Ao BP mean,mmhg	92.5(87.69-97.71)	95(94.84-106.83)	0.914	93.5(83.96-102.21)	95(80.77-104.05)	0.864
RA mean, mmhg	13.0(9.58-16.01)	6.0(5.96-8.56)	**<0.001**	14.0(12.1-17.05)	8.0(6.04-9.01)	**<0.001**
PCWP, mmhg	9.50(7.86-13.22)	11.0(10.05-16.6)	0.080	9.50(7.26-13.7)	10.0(9.1-13.46)	0.097
CI, L/min/m2	2.17(1.96-2.72)	2.43(2.28-2.73)	0.351	2.75(1.92-2.48)	2.15(2.44-3.11)	**0.017**
PVR, woods	11.80(7.51-14.72)	4.69(4.31-7.27)	**0.002**	10.36(6.21-14.20)	5.90(4.12-9.68)	**0.008**
SaPO2 (%)	95.5(91.89-96.91)	95(93.28-95.86)	0.999	92.0(90.1-96.24)	93.0(91.44-96.50)	0.879
PaO2 (%)	63.0(54.54-67.85)	66.0(62.93-68.13)	0.886	59.0(55.25-66.38)	66.0(58.40-68.44)	0.10

Values are median (interquartile range, IQR), mean ± standard deviation, or number unless specified otherwise.
Ao: Aortic; BMI: Body Mass Index; BNP: B-type Natriuretic Peptide; BP: Blood Pressure; CI: Cardiac Index; Hb: Hemoglobin; HT: Hypertension; COPD: Chronic Obstructive Pulmonary Disease; mPAP: Mean Pulmonary Artery Pressure; NT-proBNP: N-terminal pro-B-type Natriuretic Peptide; PA: Pulmonary Artery; PAWP: Pulmonary Artery Wedge Pressure; PVR: Pulmonary Vascular Resistance; PaO2: Arterial Oxygen Partial Pressure; RA: Right Atrium; RV: Right Ventricle; SaO2: Arterial Oxygen Saturation; sPAP: Systolic Pulmonary Artery Pressure; SVR: Systemic Vascular Resistance.

http://doi.org/10.5472/marumj.1484403
Marmara Med J 2024;37(2): 129-136

Demographic and hemodynamic findings of patients undergoing PEA surgery and BPA procedure according to presence of RVEF is discussed separately in Table III.

There was no significant difference found in NT-proBNP levels and 6MWT between both groups undergoing PEA. When examining hemodynamic parameters of patients undergoing PEA, in the group with RVEF, mPAP was 57.5 mmHg (42.13-67.07), while in the group without RVEF, it was 32.55 mmHg (31.52-42.27) (p: 0.001). PVR was 11.80 woods (7.51-14.72) in the RVEF group, whereas it was 4.69 WU (4.31-7.27) in the group without RVEF (p: 0.002); the mRAP was 13.0 mmHg (9.58-16.01) in the RVEF group, whereas it was 6.0 mmHg (5.96-8.56) in the group without RVEF (p: <0.001).

In patients undergoing BPA, there were no significant differences found in demographic data, NT-proBNP levels, and 6-minute walking distance between both groups, whether they had RVEF or not. However, when examining hemodynamic parameters, significant differences were observed in mPAP, mRAP and PVR in the RVEF group compared to those without RVEF (Table III).

4. DISCUSSION

In patients with chronic thromboembolic pulmonary hypertension (CTEPH), increased pulmonary vascular resistance leads to high pressure in the right ventricle, resulting in right ventricular failure. RVEF refers to the inability of the right ventricle to transfer its mechanical energy to stroke volume during contraction. This occurs as energy is dissipated through pulmonary vascular resistance during the trans pulmonary flow of blood. Increased pulmonary vascular resistance is associated with the development of RVEF. Despite correction for many established risk factors, right ventricular energy failure is associated with a two fold increase in PH mortality [9]. This concept was initially studied in the left ventricle but also adapted in PH patients [10,11] and its clinical use has been proposed as non-invasive substitute [12,13].

In our study, a more favourable hemodynamic response was observed in patients with RVEF compared to those without RVEF following pulmonary endarterectomy (PEA) surgery or balloon pulmonary angioplasty (BPA) procedure. Surgical candidates, despite having proximal and adequate amounts of thromboembolic material accessible for surgery, still indicate a higher risk due to the presence of RVEF, which demonstrates the severity of right heart failure and their higher risk profile.

In a retrospective study with a follow-up period of lasting 5 years and comprising a total of 549 pulmonary hypertension patients, with 343 (62%) being patients with CTEPH, RVEF was observed in 146 (26.6%) patients and was shown to predict long-term mortality independently [7]. Our study had a similar frequency of RVEF presence (27%) compared to frequency of RVEF rates reported in previous studies.

In a study conducted by Stefan Guth and his friends between January 2010 and March 2016, prospectively examining the PEA outcomes of 664 CTEPH patients, significant improvement was observed in RHC parameters, WHO Functional Class, and symptoms following PEA. This improvement was shown to persist for one year [14].

Another large prospective study from the United Kingdom national cohort obtained dynamic risk stratification of long term outcome in 880 PEA patients. Significant functional improvement following surgery with 85% of patients in either Functional Class I or II, only 28% of patients had an mPAP ≤20 mm Hg, whereas 51% had an mPAP ≥25 mm Hg when measured by right heart catheterization at 3 to 6 months post-PEA. The majority of deaths following the immediate postoperative period were not attributable to right ventricular failure [15]. Identifying patients with RVEF initially prior to PEA with hemodynamic measurements could be interpreted as high risk patients and this would help to better establish CTEPH related clinical deterioration and the need for reassessment during follow up.

In a cohort study conducted by Reesink et al., between May 2000 and August 2009, evaluating the effects of PEA on 74 patients, the 6MWT was shown to be associated with parameters reflecting the clinical and hemodynamic severity of CTEPH. The average 6MWT was 389 meters initially, which increased to 480 meters at one year of follow-up following PEA [16]. When looking at 6MWT and NT-ProBNP levels used in risk classification of CTEPH patients, an increase in 6MWT distance and a decrease in NT-ProBNP levels were found to be statistically significant. The correlation observed in both groups, those with and without RVEF, supported the findings of previous studies and similar hemodynamic improvements were observed in our study, consistent with previous findings.

In a prospective study evaluating the effect of PEA on pulmonary hemodynamics in 32 CTEPH patients, right heart catheterization findings were assessed 12 months post-PEA, showing a lower mPAP (20±3 vs. 17±3 mmHg; p=0.008) and a decrease in PVR from 3.6±0.8 WU preoperatively to 2.7±0.7 WU post-PEA (p=0.004) [17].

In another study, a cohort study conducted in the United Kingdom involving 880 CTEPH patients, during the 3-6 month assessment following PEA, it was observed that 28% had mPAP < 20 mm Hg and 21% had mPAP 21-24 mm Hg, and this decrease was found to be statistically significant [18].

Pulmonary endarterectomy surgery and BPA procedures have been shown to result in a significant decrease in right ventricular afterload and contribute to the improvement of right ventricular function, while also positively impacting right ventricular contractile function. In our study, both groups exhibited positive improvement in hemodynamic parameters; however, patients with RVEF experienced higher risks associated with the procedure but at the same time benefited more when compared to patients without RVEF.

Additionally, patients with RVEF showed a significant increase in cardiac output (CO) and cardiac index (CI) (p: 0.030 and p: 0.025 respectively), whereas in the non-RVEF group, although, an increase was observed, it did not reach statistical significance. This could be due to the relatively near normal and better values observed in patients without RVEF group already before PEA or BPA procedure.

http://doi.org/10.5472/marumj.1484403
Marmara Med J 2024;37(2): 129-136

In many European centers, a study examining the results of BPA procedures revealed that the decrease in mPAP is generally below 30%, and according to recently published global registry data, a 41.5% reduction in PVR was observed in Europe. In two centers in Germany, a total of 266 BPA sessions were conducted in 56 patients, resulting in an 18% decrease in mPAP and a 26% decrease in PVR. The results in our study were consistent with the findings of previous studies yet another study conducted in Japan with 7 BPA centers reported a higher BPA effectiveness with a 47.9% decrease in mPAP [19].

The significant decrease in mean pulmonary artery pressure and pulmonary vascular resistance, regardless of the presence of RVEF, indicates a reduction in right heart pressure load. However, there were differences observed in CO and CI depending on the presence of RVEF. In our study, there was no significant difference in the non-RVEF group after PEA and BPA procedures, which contradicts previous studies. Mizoguchi et al., examined the results of BPA procedures in Japan and reported significant improvement in CO and CI [20].

A relatively short duration of follow up period in our study may not adequately reflect the effect of PEA and BPA procedures on CO and CI. The discrepancy finding in our study may be explained by the relatively normal range of CO and CI values in the non-RVEF group (CO, 4.86 ± 1.29 L/min and CI, 2.62 ± 0.64 L/min/m2).

Study limitations

Although, our study conducted at a tertiary center specialized in CTEPH, being a single – center is the primary limiting factor. Variations in follow-up periods occurred due to some patients unable to reach hospital after follow-up visit schedule was arranged. Some patients who underwent BPA had previously undergone pulmonary endarterectomy but were complex cases that did not respond to treatment; therefore, only a limited number of interventions could be performed, and these patients were excluded from the study. Finally, larger and with a longer period of follow-up prospective studies are needed to effectively establish the significance of RVEF in the hemodynamic and long term clinical outcome after treatment in this group.

Conclusion

In conclusion, the presence of RVEF, a high-risk factor for long-term survival and development of heart failure in pulmonary hypertension, did not negatively affect the outcomes of PEA or BPA procedures. A significant hemodynamic and clinical improvement during the medium-term follow-up was achieved without increasing risk of complication in the perioperative early period and this improvement was consistently observed in patients undergoing both treatment strategies.

Compliance with Ethical Standards

Ethical approval: Ethical approval for the study was obtained from the Clinical Research Ethics Board (18.04.2023 approval number: 09.2023.309), and the study was conducted in accordance with the Helsinki Declaration.

Funding: The authors declared that this study has received no financial support.

Conflict of interest: The authors declare that they have no conflict of interest.

Author contributions: RSB, HA and EG: Conceived the original idea. This was also discussed with BM, DA and BY. All authors discussed and agreed with the main focus and idea of this paper. The main ideas behind this paper were conceived by HA, EA and RSB with many helpful suggestions from BM.

BY together with BM conceptualized this study, generated population and contriubed data and analysis tool. Data was mainly collected by RSB and HA helped in performing data analysis. The main text of the paper was written by RSB and subsequently improved by HA and DA helped edit the manuscript.

REFERENCES

[1] Brida, Jørn Carlsen, Andrew J S Coats, et al ESC/ERS Scientific Document Group , 2022 ESC/ERS Guidelines for the diagnosis and treatment of pulmonary hypertension; Eur Heart J 2022;43:3618-731. doi:10.1093/eurheartj/ehac237

[2] Madani MM, Auger WR, Pretorius V, et al. Pulmonary endarterectomy: recent changes in a single institution's experience of more than 2,700 patients. Ann Thorac Surg 2012;94:97-103.

[3] Tsugu T, Murata M, Kawakami T, et al. Changes in right ventricular dysfunction after balloon pulmonary angioplasty in patients with chronic thromboembolic pulmonary hypertension. Am J Cardiol 2016;118. doi:10.1016/j.amjcard.2016.07.016

[4] Inami T, Kataoka M, Yanagisawa R, et al. Long-term outcomes after percutaneous transluminal pulmonary angioplasty for chronic thromboembolic pulmonary hypertension. Circulation 2016;134:2030-2. doi:10.1161/Circulationaha.116.024201

[5] Viray MC, Bonno EL, Gabrielle ND, et al. Role of pulmonary artery wedge pressure saturation during right heart catheterization: a prospective study. Circ Heart Fail 2020;13:e007981.

[6] Rosenkranz S, Howard SL, Gomberg-Maitland M, Hoeper MM. Systemic consequences of pulmonary hypertension and right-sided heart failure. Circulation 2020;141:678-93. doi: 10/1161/CIRCULATIONAHA.116.022362

[7] Aslanger E, Akaslan D, Atas H, Kocakaya D, Yıldızeli B, Mutlu B, Right ventricular energy failure predicts mortality in patients with pulmonary hypertension. Am J Cardiol 2023;193:19-27. doi:10.1016/j.amjcard.2023.01.046

[8] Delcroix M, Torbicki A, Gopalan D, et al. ERS statement on chronic thromboembolic pulmonary hypertension. Eur Respir J 2020;57:2002828.

[9] Fares WH, Bellumkonda L, Tonelli AR, et al Right atrial pressure/pulmonary artery wedge pressure ratio: a more specific predictor of survival in pulmonary arterial hypertension. J Heart Lung Transplant 2016;35:760-7.

[10] Claessen G, La Gerche A, Dymarkowski S, Claus P, Delcroix M, Heidbuchel H. Pulmonary vascular and right ventricular reserve in patients with normalized resting hemodynamics after pulmonary endarterectomy. J Am Heart Assoc 2015;4:e001602. doi: 10.1161/JAHA.114.001602.

[11] McCabe C, White PA, Hoole SP, et al Right ventricular dysfunction in chronic thromboembolic obstruction of the pulmonary artery: a pressure-volume study using the conductance catheter. J Appl Physiol 2014; 116: 355-63.

[12] Hsu S, Houston BA, Tampakakis E, et al Right ventricular functional reserve in pulmonary arterial hypertension. Circulation 2016; 133: 2413-22.

[13] S. Miyamoto, N. Nagaya, T. Satoh, et al. Clinical correlates and prognostic significance of six-minute walk test in patients with primary pulmonary hypertension. Comparison with cardiopulmonary exercise testing. Am J Respir Crit Care Med 2020;161:487-92.

[14] Guth S, Wiedenroth CB, Rieth A, et al. Exercise right heart catheterisation before and after pulmonary endarterectomy in patients with chronic thromboembolic disease. Eur Respirat J 2018; 52: 1800458; doi: 10.1183/13993.003.00458-2018

[15] Cannon JE, Su L, Kiely DG, et al. Dynamic risk stratification of patient long-term outcome after pulmonary endarterectomy: results from the United Kingdom National Cohort. Circulation 2016;133:1761-71. doi: 10.1161/Circulationaha.115.019470.

[16] Vriz O, Veldman G, Gargani L, et al. Age-changes in right ventricular function-pulmonary circulation coupling: from pediatric to adult stage in 1899 healthy subjects. The RIGHT heart international NETwork (RIGHT-NET).Int J Cardiovasc Imaging. 2021; 37: 3399-411.

[17] Gorter TM, van Veldhuisen DJ, Voors AA, et al. . Right ventricular-vascular coupling in heart failure with preserved ejection fractio and pre – vs. post-capillary pulmonary hypertension. Eur Heart J Cardiovasc Imaging 2018; 19: 425-32.

[18] Ruigrok D, Handoko ML, Meijboom LJ, et al. Noninvasive follow-up strategy after pulmonary endarterectomy for chronic thromboembolic pulmonary hypertension. ERJ Open Res 2022;8:00564-2021. doi: 10.1183/23120.541.00564-2021.

[19] Brenot P, Jaïs X, Taniguchi Y, et al. French experience of balloon pulmonary angioplasty for chronic thromboembolic pulmonary hypertension. Eur Respir J 2019;53:1802095. doi: 10.1183/13993.003.02095-2018

[20] Mizoguchi H, Ogawa A, Munemasa M, Mikouchi H, Ito H, Matsubara H. Refined balloon pulmonary angioplasty for inoperable patients with chronic thromboembolic pulmonary hypertension. Circ Cardiovasc Interv 2012 ;5:748-55. doi: 10.1161/Circinterventions.112.971077.

MARMARA
MEDICAL JOURNAL

Original Article

https://dergipark.org.tr/tr/pub/marumj

The effect of fetal renal artery Doppler ultrasound on neonatal outcomes in fetuses with ureteropelvic junction type obstruction

Ilkin Seda CAN CAGLAYAN[1], Ceren Eda CAN[2], Ibrahim KALELIOGLU[3], Alkan YILDIRIM[3]

[1] Department of Obstetrics and Gynecology, School of Medicine, Cumhuriyet University, Sivas, Turkey
[2] Department of Statistics, Faculty of Science, Hacettepe University, Ankara, 06800, Turkey
[3] Department of Obstetrics and Gynecology, Istanbul School of Medicine, Istanbul University 34093 Istanbul, Turkey

Corresponding Author: Ilkin Seda CAN CAGLAYAN
E-mail: ilkinsedacan@hotmail.com

Submitted: 21.08.2023 **Accepted:** 19.12.2023

ABSTRACT

Objective: Fetal urinary tract dilatation (UTD) is one of the common fetal problems with remarkable difficulties in diagnosis and management in the antenatal and postnatal periods. This study aimed to determine the value of Doppler ultrasound assessment of the renal arteries in fetuses with ureteropelvic junction type hydronephrosis (UPJO) for the prediction of neonatal outcomes of infants.

Materials and Methods: Fetal renal artery Doppler values were evaluated in pregnant women between 28-32 weeks. Measurements were taken for Doppler values and the fetal obstruction and were classified through the utilization of UTD classification. Based on postnatal ultrasound, these infants were grouped by UTD classification.

Results: There was a statistically significant difference between the left renal artery Systolic/Diastolic (S/D) Ratio and bilateral renal artery Peak Systolic Velocity (PSV) values of the control and patient groups, ($p<0.05$). PSV values were higher in the patient group. The difference between the pulsality index, resistive index, and right renal artery S/D values of the control and patient groups was not statistically significant ($p>0.05$).

Conclusion: Fetal renal artery Doppler is not effective in predicting the degree of hydronephrosis and renal damage in postnatal follow-up of fetuses with a diagnosis of UPJO.

Keywords: Renal artery, Fetal pyelectasis, Hydronephrosis, Doppler ultrasound

1. INTRODUCTION

Urinary obstructions are a common prenatal diagnosis, and its findings vary from clinically insignificant conditions to in-utero fetal death. Clinically significant urinary tract obstructions occur in 1 in 500 live births and are associated with elevated morbidity and mortality [1]. These abnormalities may be stratified to obstruct the upper and lower urinary tract. Common causes of obstruction of the upper urinary tract include ureteropelvic junction type obstruction (UPJO), obstruction of the ureterovesical junction, duplication of the collection system, polycystic dysplastic kidney, ureterocele/ectopic ureter as well as pelvic tumor. Of these causes, UPJO and associated hydronephrosis are the most common clinical conditions [1].

The characteristic of the upper urinary tract obstruction is the dilatation of the collector system and potential kidney damage [2]. Renal pelvic dilatation is most commonly seen in fetal renal abnormalities, and there is an estimated prevalence between 2 and 5.5% of all pregnancies [3]. The prognosis for each case depends on the underlying cause and severity of the obstruction and whether there are other findings. In fetal diseases where renal function is affected, the amount of amniotic fluid measured by ultrasound can be used as an indicator of fetal kidney function regarding urine production [5].

A group of urologists, radiologists, and nephrologists proposed a classification of UTD used before and after birth. In a study comparing this classification system with the Society of Fetal Urology (SFU) classification system, it was shown that both methods have the same prognostic capacity to detect the resolution of prenatal hydronephrosis [6]. In a study comparing researchers using the UTD and SFU classification systems, it was found that using UTD was more difficult and had a lower rate of agreement [7]. The UTD classification system is stratified according to six ultrasound findings in total, according to whether it is in the antenatal, postnatal period or the week of gestation [2].

For the assessment of fetal hemodynamics, Doppler ultrasonography is a suitable non-invasive modality when there is a need to obtain additional information about fetal health in

How to cite this article: Caglayan Can SI, Can EC, Kalelioglu I, Yildirim A. The effect of fetal renal artery Doppler ultrasound on neonatal outcomes in fetuses with ureteropelvic junction type obstruction. Marmara Med J 2024: 37(2):137-143. doi: 10.5472/marumj.1484442

ISSN: 1309-9469

http://doi.org/10.5472/marumj.1484442
Marmara Med J 2024;37(2): 137-143

many pregnant women. Renal artery Doppler parameters can potentially be a good indicator of fetal kidney function [7-10]. Although, with ultrasound follow-up, the course of UTD can be monitored, counseling families about the long-term outcome of these anomalies requires additional information; and for this purpose, assessment of fetal hemodynamics with Doppler ultrasonography of the renal arteries may provide additional data about the condition [12]. In a renal artery Doppler study conducted on fetuses with congenital renal tract anomalies, the Pulsality Index (PI) was found to be significantly higher than mild hydronephrosis, especially in cases with severe hydronephrosis [13]. There are not enough studies in the literature that determine the extent to which Doppler ultrasonography can be useful in diagnosing and monitoring fetal upper urinary system obstructions and evaluating their postnatal outcome. This study aimed to determine the value of Doppler ultrasound assessment of the renal arteries in fetuses with UPJO for the prediction of long-term outcomes of infants.

2. PATIENTS and METHODS

The study protocol was reviewed by Istanbul University, Istanbul Faculty of Medicine, Clinical Research Ethics Committee with the file number 2015/785 and accepted at the meeting on 24.04.2015 with the number 08. Our study was created by examining the patients who applied to the Obstetrics Outpatient Clinic of Istanbul University Istanbul Medical Faculty Hospital between May 2015 and September 2015. The inclusion criteria were singleton pregnancy between 28 weeks and 32 weeks. Fetal renal artery Doppler ultrasound was performed on 125 healthy fetuses and 57 fetuses in the patient group. Ultrasound examination was performed only in the prenatal period in the control group and a total of 2 ultrasound examinations were performed (prenatal and postnatal) in the group with UPJO. All ultrasounds were performed by the same person and using the same device in our perinatology unit. The ultrasound examination was performed with the General Electrics Voluson 730 Expert brand Ultrasonography Device (General Electric Medical Systems , Istanbul, Turkey) and the 2.7 MHz transabdominal curvilinear probe. Fetus number, amniotic fluid volume, fetal heart activity, fetal presentation, placental structure/location, and fetal anatomy were evaluated. In addition to standard fetal biometric measurements, bilateral renal artery Doppler indices were taken, and kidney sizes, parenchymal thicknesses, and parenchymal echogenicity were also evaluated after these examinations. Patients with multiple pregnancies, diagnosed with preeclampsia, and with a medical record of diabetes mellitus were excluded. We also excluded subjects with extra-renal anomaly, chromosomal anomaly, and intrauterine growth retardation. Demographic and baseline clinical characteristics were collected as follows: maternal age, gravidity, parity, abortion, and history of previous pregnancy.

For sampling the renal arteries, the optimized image is the coronal plane of the fetal abdomen, which, like both kidneys, also allows viewing of the aorta in the longitudinal plane. During the ultrasound, the pregnant woman was placed in left lateral position was placed and the coronal axial abdominal appearance of the fetus was taken. Doppler measurement was performed at 1/3 proximal to the separation point of the renal artery from the aorta. The pulsed Doppler cursor was reduced to 0.5-1 mm in order to prevent contamination with proximal veins, and at least three clear waveforms were obtained.

The insonation angle was taken as small as possible and always below 30 degrees, and at least three clear waveforms were seen. Average values were used for analysis. Recordings were taken during fetal apnea periods. The Peak Systolic Velocity (PSV), PI, Systolic/Diastolic Ratio (V max), and Resistive Index (RI) values were measured in the fetal renal artery. Measurements of renal artery Doppler parameters were made by measuring renal blood flow on the affected side for fetuses in each classification in the patient group. Renal artery blood flow measurements of the healthy kidney were not calculated. To calculate bladder and kidney volume, the formula depth x width x length x 0.523 was used. Kidney volumes included the renal pelvis. A postnatal renal ultrasound was performed by the researchers and newborn examination was performed by pediatricians. Ultrasound, biochemical tests, urine analysis and in necessary cases, dimercaptosuccinic acid (DMSA) examination were performed for renal function evaluation. An antibiotic requirement in postnatal follow-ups was evaluated according to renal function and UTD classification grade.

Prenatal diagnosis was confirmed by post-natal ultrasound. In the present study, renal pathologies were classified according to the UTD Classification System. The UTD Classification System is a retrospective grading system based on a review, consolidation, and a summary of the available literature [2]. It aims to bring together all the important abnormal urinary system findings including kidney, ureter, and bladder, to cover all types of urinary system problems and determine the risk level for the infant with hydronephrosis[14]. In the UTD classification system, patients are first divided into two main groups as antenatal (A) and postnatal (P), then as subgroups according to different ultrasound findings[2, 14]. Due to the difficulties of intrauterine ultrasonographic evaluation, there are three antenatal categories (normal, A1 [mild abnormality], and A2-3 [more severe findings]), although there are four postnatal categories (P0 [normal], P1 [mild], P2 [moderate], and P3 [severe]). The anterior-posterior renal pelvic diameter (APRPD) is used to characterize the severity of prenatal UTD. A1 UTD is described as an APRPD of 7 to <10 mm with or without central calyceal dilation, A2-3 UTD as an APRPD of >10 mm, peripheral calyceal dilation, renal parenchymal or bladder abnormalities (28–32 weeks). P1 UTD is defined as a normal urinary tract with APRPD 10 to <15 mm and/or central calyceal dilation. P2 UTD describes APRPD ≥ 15 mm or peripheral calyceal dilation. P3 UTD describes additional ureteral dilation, abnormal renal echogenicity, cysts or bladder abnormalities regardless of APRPD measurement [2].

Statistical Analysis

In the present study, all statistical analyses of the data obtained from 125 healthy fetuses and 57 patient fetuses were performed

http://doi.org/10.5472/marumj.1484442
Marmara Med J 2024;37(2): 137-143

with the SPSS 23 Statistical Package for the Social Sciences, version 23 (SPSS 23). The frequency distributions and column percentages are given for categorical variables. The Chi-Square Independence Tests were used to determine whether there was a statistically significant relationship between the degree of fetal renal pyelactasia and categorical variables. The Fisher's Exact Test was used when more than 20% of the cells had an expected frequency value of less than 5 in the crosstabs for categorical variables. Also, column ratios were compared in all crosstabs created for categorical variables. Where the column ratios did not differ statistically at the 95% Confidence Interval, they were marked with the same superscript. The assumption of normality was checked with the Shapiro-Wilk Test for all quantitative variables according to the degree of fetal renal pyelactasia. The Kruskal Wallis H Test, which is one of the non-parametric statistical methods, was used to test the significance of the difference between the means of quantitative variables according to the degree of renal pyelactasia of the fetus because the assumption of normality was not provided. In case of statistically significant differences between the group means as a result of the Kruskal Wallis H Test, the group averages were compared by using the Mann-Whitney U-Test, which is one of the non-parametric tests. No statistically significant differences were detected between the means of the groups marked with the same superscript at the 95% Confidence Interval. All statistical analyses were performed at a 95% Confidence Interval. $p<0.05$ was considered significant [15].

3. RESULTS

Table I shows the clinical and ultrasonographic characteristics of the study population with numbers and percentages. The medians and interquartile ranges are given for the maternal age, gravidity, parity, miscarriage, gestational age, and estimated fetal weight according to the degree of fetal renal pyelectasis. The frequency distributions and column percentages are also presented for the gender, presentation, placental location, and amniotic fluid status for the controls, the A1 mild and the A2-3 severe pyelectasis groups. The rates of the male gender are significantly higher in the A1 mild and A2-3 severe pyelectasis groups compared to the controls ($p<0.05$). The rate of oligo – and an-hydramnios are significantly higher in the A2-3 severe pyelectasis group compared to the other groups ($p<0.05$).

Table 1. *Clinical and ultrasonographic characteristics of the study population*

Quantitative Caracteristics[III]	Controls (n=125)	A1 Mild pyelectasis (n=21)	A2-3 Severe pyelectasis (n=36)	p-value[T]
Age (y), median (IQR)	28 (25-33.5)[a]	29 (25-34)[a]	28 (25-33.8)[a]	0.996
Gravidity, median (IQR)	2 (1-3)[a]	2 (1-3)[a]	2 (1.3-3)[a]	0.315
Parity, median (IQR)	1 (0-1)[a]	0 (0-1)[a]	1 (0-1.8)[a]	0.450
Miscarriage, median (IQR)	0 (0-1)[a]	0 (0-0)[a]	0 (0-1)[a]	0.594
Gestational age (w), median (IQR)	31 (30-32)[a]	29 (29-31)[a]	31 (30-32)[a]	0.089
Estimated fetal weight (g), median (IQR)	1906 (1665-2181.5)[a]	1872 (1130-1929.5)[a]	1786.5 (1208.3-2657.3)[a]	0.060
Qualitative Characteristics[T]				p-value
Gender (n, %)				
Female	62 (49.6%)[a]	6 (28.6%)[b]	8 (22.2%)[b]	0.006*
Male	63 (50.4%)[a]	15 (71.4%)[b]	28 (77.8%)[b]	
‡Presentation (n, %)				
Vertex	84 (67.2%)[a]	16 (76.2%)[a]	31 (86.1%)[a]	0.221
Breech	35 (28%)[a]	5 (23.8%)[a]	5 (13.9%)[a]	
Transverse	6 (4.8%)[a]	0[a]	0[a]	
‡Placental location (n, %)				
Anterior	57 (45.6%)[a]	8 (38.1%)[a]	25 (69.4%)[b]	
Posterior	57 (45.6%)[a]	11 (52.4%)[a]	11 (30.6%)[a]	0.093
Right lateral	10 (8%)[a]	2 (9.5%)[a]	0[a]	
Left lateral	1 (0.8%)[a]	0[a]	0[a]	
‡Amniotic fluid status (n, %)				
Normal	125 (100%)[a]	20 (95.2%)[b]	32 (88.9%)[b]	
Oligo – and Anhydramnios	0[a]	0[a]	2 (5.6%)[b]	0.003*
Polyhydramnios	0[a]	1 (4.8%)[b]	2 (5.6%)[b]	

[T] P-value was determined by the Kruskal Wallis H test.

† P-value was determined by the Chi-square test.

[‡] More than 20% of the cells have expected counts less than 5, therefore p-value was calculated by Fisher's Exact test through the Exact Tests option in SPSS.

** p<0.05.*

[T] When the column proportions do not differ significantly from each other at the 0.05 significance level, the proportions are marked with the same superscript letter (p>0.05).

[a,b] When there was no significant difference between the study groups, the variables are marked with the same letter (p<0.05).

http://doi.org/10.5472/marumj.1484442
Marmara Med J 2024;37(2): 137-143

Table II. *Findings of urinary ultrasonography and Doppler ultrasonography in the study population*

Quantitative Characteristics[III]	Controls (n=125)	A1 Mild pyelectasis (n=21)	A2-3 Severe pyelectasis (n=36)	p-value[Ŧ]
Right kidney volume (mm^3), median (IQR)	3681.9(1652.2-7358.6)[a]	5672.5(2381-8305.2)[a]	12878.4(7699.1-22990.3)[b]	<0.001*
Left kidney volume (mm^3), median (IQR)	3987.9(1893.3-6536.1)[a]	6160.9(3540.4-9544.8)[b]	10052.1(5836.7-15604.8)[c]	<0.001*
Right renal pelvis diameter (mm), median (IQR)	3(2-4)[a]	4.8(4.2-5.8)[b]	10(4-15.8)[c]	<0.005*
Left renal pelvis diameter (mm), median (IQR)	3(2.6-3.3)[a]	6(5-8)[b]	10.5(7.7-14.8)[c]	<0.001*
Bladder volume (mm3), median (IQR)	3200.8(932-7257.7)[a]	4184(1518.3-13890.9)[b]	7102.9(3263.5-12417.7)[b]	0.001*
Bladder wall thickness (mm), median (IQR)	1.3(1-1.5)[a]	1.4(1.2-1.5)[a]	1.5(1.3-1.8)[b]	0.001*
Right renal PI, median (IQR)	2(1.7-2.2)[a]	1.9(1.8-2.1)[a]	2.1(1.8-2.3)[a]	0.101
Left renal PI, median (IQR)	2(1.7-2.2)[a]	2.1(1.9-2.3)[a]	2.1(1.8-2.2)[a]	0.285
Right renal RI, median (IQR)	0.9(0.9-1)[a]	0.9(0.9-1)[a]	0.9(0.9-1)[a]	0.148
Left renal RI, median (IQR)	0.9(0.9—1)[a]	1(0.9-1)[a]	0.9(0.9-1)[a]	0.526
Right renal S/D, median (IQR)	18(8-37)[a]	20(8.5-37.5)[a]	15(8-29)[a]	0.678
Left renal S/D, median (IQR)	16(8-30.5)[a]	27(11.5-42.5)[b]	15(6-29.8)[a]	0.049*
Right renal PSV, median (IQR)	40(32-50)[a]	40(26-54.5)[a]	50(34.3-59.5)[b]	0.035*
Left renal PSV, median (IQR)	40(30-48)[a]	47(38.5-57.5)[b]	48(37-59.3)[b]	0.002*
Qualitative Characteristics[T]				p-value[†]
[‡]Urinary tract malformation (n, %)				
No	125 (100%)[a]	0[b]	0[b]	<0.001*
Bilateral pyelectasis		15 (71.4%)[b]	4 (11.1%)[c]	
Unilateral pyelectasis		6 (28.6%)[b]	1 (2.8%)[a]	
Bilateral hydronephrosis		0[a]	14 (38.9%)[b]	
Unilateral hydronephrosis		0[a]	17 (47.2%)[b]	
[‡]Calyceal dilatation (n, %)				
No	125 (100%)[a]	14 (66.7%)[b]	6 (16.7%)[c]	<0.001*
Unilateral		6 (28.6%)[b]	19 (52.8%)[b]	
Bilateral		1 (4.8%)[a]	11 (30.6%)[a]	

[Ŧ]P-value was determined by the Kruskal Wallis test

†P-value was determined by the Chi-square test.

[‡]More than 20% of the cells have expected counts less than 5, therefore p-value was calculated by Fisher's Exact test through the Exact Tests option in SPSS

** p<0.05.*

[T]When the column proportions do not differ significantly from each other at the 0.05 significance level, the proportions are marked with the same superscript letter (p>0.05).

[III]When there is no significant difference at the 0.05 significance level between the groups, the group medians are marked with the same superscript letter (p>0.05)

PI: Pulsatility Index; RI: Resistive Index; S/D: Systolic/Diastolic Ratio; PSV: Peak Systolic Velocity; IQR: Interquartile range; (IQR)=(Q1 – Q3), Q1: First quartile, Q3: Third quartile

[a,b,c] When there was no significant difference between the study groups, the variables are marked with the same letter (p<0.05).

Table II presents the urinary ultrasonography and Doppler ultrasonographic findings of the controls, A1 mild and A2-3 severe pyelectasis groups. Dilatation is studied as bilateral and unilateral pyelectasis. In the unilateral pyelectasis group of the urinary tract malformation variable, 1 patient has the right and 6 patients have the left pelviectasis. While 1 of the patients with unilateral pelviectasis on the left side is in the A2-3 group, 5 of them are in the A1 group. A patient with unilateral pelviectasis on the right side is in the A1 group. In the unilateral hydronephrosis group, 7 patients had hydronephrosis on the right side and 10 patients on the left side. All those with unilateral hydronephrosis are in groups A2-3. Renal artery blood velocity waveforms were obtained from the control group (250 kidneys), A1 mild pyelectasis group (42 kidneys), and A2-3 severe pyelectasis group (72 kidneys). There is no statistically significant difference at a 0.05 significance level among the study groups regarding the right renal artery PI, the left renal artery PI, the right renal artery RI and the left renal artery RI (p>0.05). The S/D ratio of the left renal artery in the A1 mild pyelectasis group is significantly different from the control and A2-3 severe pyelectasis groups (p<0.05). There is no significant difference between healthy and mild pyelectasis kidneys regarding the right renal artery PSV values (p>0.05). However, the right renal artery PSV values in severe pyelectasis kidneys are significantly higher than those in healthy and mild pyelectasis kidneys (p<0.05). The left renal artery PSV values in mild and severe pyelectasiskidneys are significantly higher than those in the healthy kidneys (p<0.05).

Table III shows the postnatal findings of the study population. There is no significant difference among the A1 mild pyelectasis, and A2-3 severe pyelectasis groups concerning the gestational age and birth weight (p>0.05). There is a significant association between the degree of fetal renal pyelectasis and the mode of delivery, neonatal intensive care unit (NICU) admission, urinary tract dilation (UTD) assessed by the postnatal US on day 2, other fetal malformations, postnatal karyotyping, UTD grade after birth, postnatal treatment, renal function, prophylactic antibiotic (p<0.05). The rate of vaginal deliveries for the A2-3 severe pyelectasis group is significantly higher than those for the A1 mild pyelectasis groups (p<0.05). This statistically significant increase in the cesarean section rate in the A1 mild pyelectasis group was due to the individual and fetal characteristics of the patients (other than fetal anomaly)—for example, previous cesarean section, fetal malpresentation, labor dystocia, abnormal or indeterminate (formerly, nonreassuring) fetal heart rate tracing, failed induction (labor induction), arrest of labor, cephalopelvic disproportion, etc. Additionally, since our study was conducted in a university hospital, the average cesarean section rate in our hospital is around 70%. The rate of neonatal death in the A2-3 severe pyelectasis group is significantly higher than in those of the control and A1 mild pyelectasis groups (p<0.05). The rate of impaired renal function in the A2-3 severe pyelectatis group is significantly higher than in those of the control and the A1 mild pyelectasis groups (p<0.05). Considering the postnatal outcomes of the other 10 fetuses with A1 mild pyelectasis (UTD A1 group) in the prenatal period; there were mild pyelectasis (UTDP1) (15%) in 3 cases, moderate pyelectasis (UTD P2) in 6 cases (30%) and severe pyelectasis (UTDP3) in 1 case (5%). As for the UTD A2-3 group, the postnatal UTD grade of 3 fetuses was observed as normal. In fact, the rate of UTDP0 cases in the UTD A2-3 group is significantly lower than in those of the control and UTD A1 groups. According to the postnatal outcomes of the other 32 fetuses with A2-3 severe pyelectasis (UTD A2-3 group) in the prenatal period; there was mild pyelectasis (UTDP1) (17.1%) in 6 cases, moderate pyelectasis (UTD P2) in 23 cases (65.7%) and severe pyelectasis (UTDP3) in 3 cases (8.6%). The rate of UTDP2 cases in the UTD A2-3 group is significantly higher than in those of the control and UTD A1 groups. The rate of both UTDP1 and UTDP3 cases does not differ significantly from UTD A1 and UTD A2-3 groups.

As a result, the mean of left renal S/D in the A1 mild pyelectasis group is significantly higher than the mean of the control and A2-3 severe pyelectasis groups. The mean of the right renal PSV in the A2-3 severe pyelectasis group is higher than in those of the control and A1 mild pyelectasis groups. There is no significant difference between the A1 mild and the A2-3 severe pyelectasis groups regarding the mean of the left renal PSV. Loss of renal function was observed in 4 infants (1 in the UTD A1 group, and 3 in the UTD A2-3 group). Impaired renal function was observed only in 5 infants in the UTD A2-3 group. There were 2 (5.7%) neonatal deaths in the UTD A2-3 group and pregnancy termination was performed in one patient in each group.

Table III. *Postnatal findings of the study population*

Quantitative Characteristics[III]	A1 Mild pyelectasis (n=21)	A2-3 Severe pyelectasis (n=36)	p-value[Ŧ]
Gestational age at birth (gw), median (IQR)	38(37-39)[a]	38(36.25-40)[a]	0.596
Birth weight (g), median (IQR)	3360(2785-3500)[a]	3200(2822-3500)[a]	0.785
Qualitative Characteristics[T]			p-value[†]
[‡]Mode of delivery (n, %)			
Vaginal	7 (33.3%)[a]	21 (58.3%)[b]	0. 009*
Cesarean	14 (66.7%)[a]	15 (41.7%)[b]	
[‡]NICU admission (n, %)[Ŧ]			
No	16 (80%)[b]	29 (82.9%)[b]	<0.001*
Yes	4 (20%)[b]	6 (17.1%)[b]	
[‡]UTD assessed by the postnatal US on day 2 (n, %)[Ŧ]			
Normal	8 (40%)[b]	6 (17.1%)[b]	<0.001*
Less than the first visit	4 (20%)[b]	9 (25.7%)[b]	
More than the first visit	3 (15%)[b]	10 (28.6%)[b]	
Same	5 (25%)[b]	10 (28.6%)[b]	
[‡]Other fetal malformations (n, %)			
Absent	21 (100%)[a]	29 (80.6%)[b]	<0.001*
VSD		3 (8.3%)[b]	
Short femur		1 (2.8%)[a]	
Hyperechogenic cardiac focus		2 (5.6%)[b]	
Cardiac or neurologic anomaly		1 (2.8%)[a]	
[‡]Postnatal karyotyping (n, %)			
Absent	16 (76.2%)[b]	31 (86.1%)[b]	<0.001*
Normal	5 (23.8%)[b]	4 (11.1%)[b]	
Abnormal	0[a]	1 (2.8%)[a]	
[‡]UTD grade after birth (n, %)[Ŧ]			
P0	10 (50%)[b]	3 (8.6%)[c]	<0.001*
P1	3 (15%)[b]	6 (17.1%)[b]	
P2	6 (30%)[b]	23 (65.7%)[c]	
P3	1 (5%)[b]	3 (8.6%)[b]	
[‡]Postnatal treatment (n, %)[Ŧ]			
No	18 (90%)[b]	26 (74.3%)[b]	<0.001*
Surgery	2 (10%)[b]	9 (25.7%)[b]	
[‡]Renal function (n, %)[Ш]			
Normal	19 (95%)[b]	25 (75.8%)[b]	<0.001*
Impaired	0[a]	5 (15.2%)[b]	
Loss of function	1 (5%)[b]	3 (9.1%)[b]	
[‡]Prophylactic antibiotic (n, %)[Ŧ]			
No	17 (85%)[b]	20 (57.1%)[b]	<0.001*
"Yes	3 (15%)[b]	15 (42.9%)[b]	
[‡]Termination (n, %)			
No	20 (95.2%)[b]	35 (97.2%)[b]	0.097
Yes	1 (4.8%)[b]	1 (2.8%)[b]	
[‡]Neonatal death (n, %)[Ŧ]			
No	20 (100%)[a]	33 (94.3%)[b]	0.051
Yes	0[a]	2 (5.7%)[b]	

[Ŧ]P-value was determined by the Mann-Whitney U test

†P-value was determined by the Chi-square test.

[‡]More than 20% of the cells have expected counts less than 5, therefore P-value was calculated by Fisher's Exact test through the Exact Tests option in SPSS.

** p<0.05.*

[T]When the column proportions do not differ significantly from each other at the 0.05 significance level, the proportions are marked with the same superscript letter (p>0.05).

[III]When there is no significant difference at the 0.05 significance level between the groups, the group medians are marked with the same superscript letter (p>0.05)

gw: gestational week; NICU: Neonatal Intensive Care Unit; UTD: Urinary Tract Dilation; US: Ultrasound; VSD: Ventricular Septal Defect; IQR: Interquartile range; (IQR)=(Q1 – Q3), Q1: First quartile, Q3: Third quartile

[a,b] When there was no significant difference between the study groups, the variables are marked with the same letter (p<0.05).

http://doi.org/10.5472/marumj.1484442
Marmara Med J 2024;37(2): 137-143

4. DISCUSSION

In this study, we assessed the relationship between fetal renal arterial parameters with perinatal outcomes of pregnancies with fetal upper UTD. The PSV value of the right renal artery was higher in the fetuses with severe pyelectasis than in the healthy fetuses and fetuses with mild pyelectasis. The PSV value of the left renal artery was higher in the fetuses with mild and severe pyelectasis than in the healthy fetuses. In the first postnatal ultrasonography of the fetuses with mild pyelectasis, a decrease in renal pelvis diameter was found in most of the fetuses. In the first postpartum ultrasound findings of the fetuses with severe pyelectasis, we observed that the diameters of the renal pelvis increased or remained similar in most of them. We observed that fetuses with severe pyelectasis had a higher risk of kidney failure in the postnatal years compared to fetuses with mild pyelectasis.

One of the most common causes of renal pyelectasis in the antenatal period is ureteropelvic junction stenosis [14,16]. Approximately, half of the urinary tract anomalies in the neonatal period are ureteropelvic junction strictures. In general, unilateral and sporadic strictures can be seen due to abnormal collagen or fibrous bands that may occur at the ureteropelvic junction (90% of cases) [17]. Fetal ultrasound shows a renal pelvic dilation with or without renal calyx dilation, and the degree of dilation depends on the type and severity of the obstruction [14,16].

Wang et al., also reported that fetuses with bilateral hydronephrosis, increased renal pelvis anteroposterior diameter, or higher SFU grade required a longer spontaneous regression period [18]. In our study, we reached results that support the findings of this study. Another study conducted by Ismaili et al., investigated the presence of renal pelvis dilatation in fetuses. They found that minor degrees of renal pelvis dilatation occurred in 4.5% of the fetuses [19].

Bates and Irving emphasized in their study that when they performed renal artery Doppler examination on 29 patients with renal pelvis dilatation, the PI value could not confirm any anomaly in these fetuses. [20]. In the study in which postnatal follow-up of fetuses with hydronephrosis due to UPJO was performed, it was recommended to perform a color Doppler examination in fetuses with antepartum hydronephrosis, since obstruction due to crossing vessels was detected in 11 of 100 operated patients. [21] Benjamin et al. investigated the effect of gestational age on urological outcomes in fetuses with hydronephrosis and concluded that late preterm/early-term deliveries lead to worse postnatal outcomes in the short term [22]. In a study, it was shown that the degree of UTD in the antenatal period is associated with spontaneous regression in the postpartum period, the risk of developing uropathies, urinary tract infection, and surgery, but no relationship has been regarding renal dysfunction.[23]. We found similar results in this study.

The validation of the UTD Classification System was evaluated in the study of Zhang et al.[14]. When fetuses that had isolated hydronephrosis classified as UTD in the antenatal period were evaluated postnatally, postnatal normal ultrasonic urinary tract findings were detected in 24 infants with UTD A1. It was also found that postnatal hydronephrosis persisted in 10 cases with UTD A2-3, and the postnatal UTD classification of these 10 cases was reported as UTD P1 (6 cases), UTD P2 (2 cases), and UTD P3 (2 cases), respectively.

As a result, it was reported that the UTD Classification System is an effective system for both antenatal and postnatal periods in the validation evaluation. In the present study, similar results were found in the validation study, showing that postnatal prognosis may be worse, especially in fetuses with UTD A2-3 Classification.

Conclusion

Based on the data we obtained from our study, an increase in renal echogenicity, oligohydramnios and loss of corticomedullary differentiation are among the poor prognostic factors in terms of renal function in the postnatal period. Periodic follow-up of pregnant women with ultrasound and evaluation with the UTD classification system is significant for the management of the prenatal and postnatal periods. As a final comment, in this study, sample size estimation was not possible despite the retrospective nature of the study because there was not enough data in the literature.

Acknowledgments: We are grateful to Prof. Ali Cetin, M.D. from Cumhuriyet University School of Medicine, Department of Obstetrics and Gynecology for his contributions to the statistical analysis and language editing, and assistance with this project.

Compliance with Ethical Standards Ethical approval

Ethical approval: The study protocol was reviewed by Istanbul University, Istanbul Faculty of Medicine, Clinical Research Ethics Committee with the file number 2015/785 and accepted at the meeting on 24.04.2015 with the number 08.

Conflict of interest: The authors reported no conflict of interest related to this article.

Funding: This research was not funded or supported.

Authors' contributions: ISCC and IK: Planning the study, ISCC, IK and AY: Literature search, ISCC: Collected the data, ISCC and CEC: Analysis and interpretation of data, ISCC and CEC: Drafting of the manuscript, IK and AY: Critical revision of the manuscript for important intellectual content, ISCC, CEC, IK and AY: Final approval of the version to be published.

REFERENCES

[1] Loardi C, Signorelli M, Gregorini M, et al. Moderate and severe fetal pyelectasis: Correlation between prenatal aspects and postnatal outcome. J Neonatal Perinatal Med 2020;13:1-6. doi: 10.3233/NPM-180071

[2] Nguyen H, Benson CB, Bromley B, et al. Multidisciplinary consensus on the classification of prenatal and postnatal urinary tract dilation (UTD classification system). J Pediatr Urol 2014; 10: 982-98. doi:10.1016/j.jpurol.2014.10.002

[3] Kumar S, Walia S, Ikpeme O, et al. Postnatal outcome of prenatally diagnosed severe fetal renal pelvic dilatation. Prenat Diagn 2012; 32 : 519-22. doi: 10.1002/pd.2893

[4] Chalouhi GE, Millischer AE, Mahallati H, et al. The use of fetal MRI for renal and urogenital tract anomalies. Prenat Diagn 2020; 40: 100-9. doi: 10.1002/pd.5610

[5] Braga LH, McGrath M, Farrokhyar F, Jegatheeswaran K, Lorenzo AJ. Society for Fetal Urology Classification vs Urinary Tract Dilation Grading System for prognostication in prenatal hydronephrosis: A time to resolution analysis. J Urol 2018; 199: 1615-21. doi: 10.1016/j.juro.2017.11.077

[6] Nelson CP, Lee RS, Trout AT, et al. Interobserver and Intra-Observer Reliability of the Urinary Tract Dilation Classification System in Neonates: A multicenter study. J Urol 2019; 201: 1186-92. doi: 10.1097/JU.000.000.0000000026

[7] Contag S, Patel P, S. Payton, Crimmins S, Goetzinger KR. Renal artery Doppler compared with the cerebral placental ratio to identify fetuses at risk for adverse neonatal outcome. J J Matern-Fetal Neonatal Med 2021; 34: 532-40. doi: 10.1080/14767.058.2019.1610735

[8] Figueira CO, Surita FG, Dertkigil MSJ, et al. Longitudinal reference intervals for Doppler velocimetric parameters of the fetal renal artery correlated with amniotic fluid index among low-risk pregnancies. Int J Gynecol Obstet 2015; 131: 45-8. doi: 10.1016/j.ijgo.2015.05.010

[9] Jain JA, Gyamfi-Bannerman C, Simpson LL, Miller RS. Renal artery Doppler studies in the assessment of monochorionic, diamniotic twin pregnancies with and without twin-twin transfusion syndrome. Am J Obstet Gynecol MFM 2020; 2: 100167. doi: 10.1016/j.ajogmf.2020.100167

[10] Seravalli V, Miller JL, Block-Abraham D, McShane C, Millard S, Baschat A. The relationship between the fetal volume-corrected renal artery pulsatility index and amniotic fluid volume. Fetal Diagn Ther 2019; 46: 97-102. doi:10.1159/000491749

[11] Benzer N, Tazegül Pekin A, Yılmaz SA, Seçilmiş Kerimoğlu Ö, Doğan NU, Çelik Ç. Predictive value of second and third trimester fetal renal artery D oppler indices in idiopathic oligohydramnios and polyhydramnios in low-risk pregnancies: A longitudinal study. J Obstet Gynaecol Res 2015; 41: 523-8. doi:10.1111/jog.12601

[12] Wladimiroff JW, Heydanus R, Stewart PA, Cohen-Overbeek TE, Brezinka C. Fetal renal artery flow velocity waveforms in the presence of congenital renal tract anomalies. Prenat Diagn 1993; 13: 545-9. doi:10.1002/pd.197.013.0702

[13] Onen A. Grading of hydronephrosis: an ongoing challenge. Front Pediatr 2020; 8: 458. doi:10.3389/fped.2020.00458

[14] Zhang H, Zhang L, Guo N. Validation of 'urinary tract dilation' classification system: Correlation between fetal hydronephrosis and postnatal urological abnormalities. Medicine (Baltimore) 2020; 99:18707. doi:10.1097/MD.000.000.0000018707

[15] Aktaş Altunay S, Yılmaz EA, Bahçecitapar M, Bakacak Karabenli L. SPSS ve R uygulamalı kategorik veri çözümlemesi. 1. baskı. Ankara: Seçkin Yayıncılık, 2021.

[16] Dighe M, Moshiri M, Phillips G, Biyyam D, Dubinsky T. Fetal genitourinary anomalies: a pictorial review with postnatal correlation. Ultrasound Q 2011; 27: 7-21.doi: 10.1097/RUQ.0b013e31820e160a

[17] Wang J, Ying W, Tang D, et al. Prognostic value of three-dimensional ultrasound for fetal hydronephrosis. Exp Ther Med 2015; 9: 766-72. doi: 0.3892/etm.2015.2168

[18] Ismaili K, Hall M, Donner C, Thomas D, Vermeylen D, Avni FE. Results of systematic screening for minor degrees of fetal renal pelvis dilatation in an unselected population. Am J Obstet Gynecol 2003; 188: 242-6. doi: 10.1067/mob.2003.81.

[19] Bates JA, Irving HC. Inability of color and spectral Doppler to identify fetal renal obstruction. J Ultrasound Med 1992; 11: 469-72. doi:10.7863/jum.1992.11.9.469

[20] Rooks VJ, Lebowitz RL. Extrinsic ureteropelvic junction obstruction from a crossing renal vessel: demography and imaging. Pediatr Radiol 2001; 31: 120-4.doi: 10.1007/s002.470.000366

[21] Benjamin T, Amodeo RR, Patil AS, Robinson BK. The impact of gestational age at delivery on urologic outcomes for the fetus with hydronephrosis. Fetal Pediat Pathol 2016; 35: 359-68. doi: 10.1080/15513.815.2016.1202361

[22] Bratina P, Levart TK. Clinical outcome is associated with the Urinary Tract Dilatation Classification System grade. Croat Med J 2020; 61: 246-51. doi: 10.3325/cmj.2020.61.246.

MARMARA
MEDICAL JOURNAL

Original Article

https://dergipark.org.tr/tr/pub/marumj

A study on brain asymmetry in temporal lobe epilepsy

Edibe BILISLI KARA[1,2], Zeynep FIRAT[3], Aziz M ULUG[4,5], Gazanfer EKINCI[3], Umit Suleyman SEHIRLI[6]

[1] Department of Anatomy, Faculty of Medicine, Yeditepe University, Istanbul, Turkey
[2] Institute of Health Sciences, Marmara University, Istanbul,Turkey
[3] Department of Radiology, Faculty of Medicine, Yeditepe University, Istanbul, Turkey
[4] Cortechs Labs, Inc., San Diego, CA, United States.
[5] Institute of Biomedical Engineering, Bogazici University, Istanbul, Turkey
[6] Department of Anatomy, School of Medicine, Marmara University, Istanbul, Turkey

Corresponding Author: Edibe BILISLI KARA
E-mail: edibilisli@gmail.com

Submitted: 27.11.2023 **Accepted:** 26.12.2023

ABSTRACT

Objective: Temporal lobe epilepsy (TLE) accompanied by hippocampal sclerosis (HS) is the most common type of focal epilepsies. Hemispheric asymmetry is a feature of brain organization in both invertebrates and vertebrates and may be the key to some neurodegenerative diseases. In this context, we aimed to investigate the volumetric asymmetry difference in cerebral structures between TLE patients and the healthy control group, based on magnetic resonance imaging (MRI) data that may be used as a new neuroimaging marker for TLE cases.

Patients and Methods: In this retrospective study the cranial MRIs of fourteen clinically manifesting, radiologically HS-identified, and diagnosed TLE patients and fourteen healthy individuals from the Radiology Department of Yeditepe University Hospital were evaluated. Volume measurements and asymmetry index (AI) calculations in the total brain, hippocampus, temporal lobe, amygdala, thalamus, nucleus accumbens (NAc), premotor cortex, primary and somatosensory cortices were performed using the medical NeuroQuant® software. A negative AI value represented asymmetry towards the right due to reduced left hemispheric volume; a positive AI value represented asymmetry towards the left due to reduced right hemispheric volume. Subsequently, differences in volume and asymmetric patterns were investigated among TLE subgroups (right and left-sided TLE) and controls.

Results: The left-sided TLE patients showed significant bilateral total brain volume reduction compared to the control group. Significant ipsilateral volumetric declines were also detected in the premotor cortex, the temporal lobe, and NAc with remarkable asymmetry to the right side. No significant changes were detected in right-sided TLE patients compared to the other groups.

Conclusion: Overall, findings suggest that TLE patients had volumetric alterations with symmetry changes beyond the mesial temporal structures. With further investigations, the asymmetry measures can provide additional knowledge for TLE diagnosis.

Keywords: Brain asymmetry, Temporal lobe epilepsy, Asymmetry index, Nucleus accumbens

1. INTRODUCTION

Epilepsy is one of the most common neurological diseases, accounting for over 0.5% of the global burden of disease affecting over 70 million people worldwide. It is characterized by abnormal electrical activity in the brain, causing seizures or unusual behavior, sensations, and loss of awareness [1]. The classification of epilepsy has an important role in evaluating individuals who have seizures. According to the International League Against Epilepsy (ILAE) classification tool, temporal lobe epilepsy (TLE) is a focal type of epilepsy with or impaired awareness both in adults and children with most of the cases being symptomatic [2]. The causes of TLE can vary with hippocampal sclerosis being the most common cause but extrahippocampal abnormalities are also frequently observed [3,4].

The clinical context, features of the seizure, and proper interpretation of the imaging are the keys to the diagnosis. Magnetic resonance imaging (MRI) has equal importance to the electroencephalogram (EEG) as a part of assessing epileptic patients. The challenge is to require optimized protocols suitable for epilepsy cases. MRI is critical in evaluating TLE, allowing characterization and detection of structural changes, especially hippocampal sclerosis. Imaging displays the anatomy and structural abnormalities of mesiotemporal structures including the hippocampus, amygdala [5], parahippocampal gyrus [6], entorhinal cortex [7], and temporal pole [8]. On T1-weighted images, the most common features associated with hippocampal sclerosis are hippocampal atrophy [9-12] and reduction of

How to cite this article: Kara Bilişli E, Fırat Z, Ulug MA, Ekinci G, Sehirli SU. A study on brain asymmetry in temporal lobe epilepsy. Marmara Med J 2024: 37(2):144-151. doi: 10.5472/marumj.1487475

ISSN: 1309-9469

http://doi.org/10.5472/marumj.1487475
Marmara Med J 2024;37(2): 144-151

internal features of the hippocampus [13-15]. On T2-weighted images, the presence of increased signals from the hippocampus with atrophy can be detected [16, 17]. Several volumetric studies showed volume changes in the insula, thalamus, putamen, pallidum, and cortical thickness in TLE patients [18-23]. The diffusion tensor imaging (DTI) study focusing on the changes in grey and white matter showed alterations in the corpus callosum, corona radiata, cingulum, uncinate fasciculus, external and internal capsule in TLE patients [24].

From an evolutionary aspect, even though both the left and right hemispheres of the brain develop symmetrically, the subsequent existence of structural and functional differences between the two hemispheres indicates asymmetry in both humans and animals. For many years, brain asymmetry and lateralization have been investigated, and correlated with handedness [25], and associated with some neurodegenerative diseases [26-28]. Some studies support the critical role of brain asymmetry with schizophrenia [29]. In Alzheimer's disease, a relationship was found between hippocampal asymmetry and the severity of the diagnosis [30]. Epileptic resting-state functional MRI (rs-fMRI) studies showed functional asymmetry in the hippocampus and amygdala which is evident in the hemisphere ipsilateral to the lesion in mesial temporal lobe patients [31, 32].

Due to the importance of the asymmetric characteristics of the human brain, we focused on the structural asymmetry patterns of epileptic brains. Therefore, in this retrospective study, we evaluated the MRI of healthy controls and TLE patients to define the changes in volume and symmetry patterns of the groups. The comparison was not only between the patient and control groups but also considering the side of the epileptic focus, hemispheric comparisons were made in the right and left-sided TLE patients.

2. PATIENTS and METHODS

Patient selection

In this retrospective study, patients who were followed at the Neurology Clinic of the Yeditepe University Hospital underwent cranial MRI in the Radiology Department between 2017-2021 and were diagnosed with TLE by an experienced neurologist, according to the criteria defined by the ILAE [33] were included. Patients with the following criteria were excluded: a significant medical history of acute encephalitis or ischemic encephalopathy, meningitis, severe head trauma, or any suspicious epileptogenic lesions like tumors, or dysplasia.

Healthy individuals who consulted the Neurology department due to headaches, and had a cranial MRI that was "normal" were included in the study as the control group. Individuals in the control group are included based on the following criteria: no history of neurological or psychiatric diseases; and no medication of central nervous system agents.

All patients and controls underwent a comprehensive clinical evaluation including interviews, neurological examination, neuropsychological assessment, and neurophysiological monitoring. All individuals were right-handed. Participant consent and ethical permissions were obtained. The study was approved by Marmara University's Clinical Research Ethics Committee on 05.03.2021 with the protocol number 09.2021.322.

Effect size and alpha error probability were taken as 1.1 and 0.05, respectively. 14 individuals in each group were evaluated and the power of the study (1-β error prob.) was planned to be 0.80. Totally fourteen patients were diagnosed by a specialist with unilateral TLE, (male/female, 5:9; right / left-sided TLE patients, 8:6), and fourteen age – and sex-matched controls (male/female, 8:6) were included in this study. There was no statistically significant difference in gender or mean age (Control/right and left-sided TLE; 35.86 ± 15.58: 35.75 ± 9.55: 36.33 ± 1308; p=0.99) between subjects.

MRI data acquisition

We obtained MRI data from all individuals. Scanning details were as follows: The MRI was performed on a 3.0-T MR system (GE DISCOVERY MR750w 3.0-T MR scanner. GE HealthCare Technologies, Inc., Chicago, Illinois.) with 16-channel head and neck coils.

Routine MRI examination with the following protocols was made: three-dimensional (3D) sagittal T1-weighted magnetization [TR/TE: 8.6/3.2 ms; matrix 230 × 230, 23 × 23 cm FOV; thickness 1.0 mm with – 0.5 mm gap; 310-330 slices; acquisition time 4:30 sec] and 3D CUBE fluid-attenuated inversion recovery (FLAIR) images [TR/TE 6000/113.5 ms; inversion time 1749 ms; matrix 224 × 224, 23 × 23 cm FOV; thickness 1.4 mm with – 0.7 mm gap; 220-230 slices; acquisition time 5:30 sec].

Images were transferred to FDA-cleared "NeuroQuant®" medical software tool (https://www.cortechs.ai/products/neuroquant/) to assess the volumes and asymmetry index values based on the 3D T1-weighted images for all groups. Automated volumetric analysis and asymmetry calculation of the brain regions for both groups were performed. The brain regions of interest that were executed and evaluated were the total brain, hippocampus, temporal lobe, amygdala, thalamus, nucleus accumbens (NAc), premotor cortex, primary were somatosensory cortices.

Evaluation of the asymmetry index values

An asymmetry index (*AI*) quantifies the differences between the right and left hemispheres. In the literature, cerebral asymmetry is generally reported by a "laterality index" measure. A commonly used formula is the R – L difference in ROI sizes divided by the sum of R + L ROI sizes [34]. Additionally, another "asymmetry index" formula often used in fMRI studies is mentioned in the literature [35].

In our study, the calculation was made by the Neuroquant® software. Our reference formula for AI is 200*(Left-Right volumes)/(Left+Right volumes). The formula divides the hemispheric volume difference by the mean hemisphere volume and reports the percentage. The interpretation of AI is shown in Table I with an example. Negative AI represents the volume decrease in the left hemisphere, interpreted as symmetric changes in the right hemisphere; positive AI value represents the volume decrease in the right hemisphere, interpreted as symmetric changes in the left hemisphere.

http://doi.org/10.5472/marumj.1487475
Marmara Med J 2024;37(2): 144-151

Table I. *Asymmetry Index (AI) and volumetric measurments*

Group and Region	Hippocampus Right Volume	Hippocampus Left Volume	AI	Interpretation according to: AI = 200*(Left – Right)/(Left+Right)
Healthy Control	3.99	3.60	-10.22	Negative AI indicates asymmetry to the right
Right-sided TLE patient	3.12	4.14	28.07	Positive AI indicates asymmetry to the left
Left-sided TLE patient	4.14	3.38	-20.09	Negative AI indicates asymmetry to the right

TLE: Temporal lobe epilepsy, AI: Asymmetry index

Statistical Analysis

Statistical analyses of MR images among the groups were performed using GraphPad Prism 8 software. The variables were investigated by using the Shapiro-Wilk test to determine whether they were normally distributed or not. Descriptive analyses were presented using means and standard deviations for normally distributed volume and asymmetry index measures. The one-way analysis of variance (ANOVA) test was performed to compare the volumes and the asymmetry index values among three groups (control, right-sided TLE, and left-sided TLE). In binary comparison, the unpaired t-test was used. A p-value <0.05 was considered to indicate a significant difference. Pairwise posthoc tests were performed using Tukey's test when significance was observed.

3. RESULTS

This study compared the volumetric measurements and AI values of the brain regions between the TLE patient and the control groups. AI values were compared to define brain asymmetry patterns in groups. Our results showed diverse patterns of structural asymmetries in TLE patients compared to the control group.
In the first step, descriptive analysis (mean and standard deviation calculations) of the AI values and volumetric measurements of the total brain, hippocampus, temporal lobe, amygdala, thalamus, NAc, premotor cortex, primary and somatosensory cortices for each group (right and left-sided TLE and control) were conducted.

Table II. *Mean ± SD total volumes of the brain regions among the three groups (healthy; right-sided TLE and left-sided TLE)*

Structure and Group	Healthy Controls (n=14)	TLE Patients (n=14)		
		Right TLE (n=8)	Left TLE (n=6)	
	Mean ± SD	Mean ± SD	Mean ± SD	p-val.
Amygdala	*3.70* ± 0.68	3.78 ± 0.62	3.46 ± *0.71*	Ns (0.65)
Hippocampus	8.77 ± 0.91	8.44 ± 1.22	8.22 ± 1.14	Ns (0.54)
Nucleus Accumbens	1.45 ± *0.31*	1.47 ± *0.34*	1.18 ± *0.13*	Ns (0.15)
Premotor Cortex	13.71 ± *2.50*	13.07 ± 2.06	11.22 ± 1.24	Ns (0.08)
Primary Motor Cortex	28.46 ± 5.73	25.49 ± 4.41	25.09 ± 4.50	Ns (0.28)
Somatosensory Cortex	22.79 ± *5.26*	21.03 ± *4.35*	20.43 ± 4.29	Ns (0.53)
Temporal Lobe	136.5 ± 20.53	135.4 ± 12.52	119.6 ± *13.62*	Ns (0.13)
Thalamus	16.47 ± 2.83	15.54 ± *1.89*	14.17 ± *1.47*	Ns (0.15)
Total Brain	1262 ± *142.5*	1205 ± 86.02	1085 ± 87.96	**0.0486***

*Bold font denotes the significance of the analysis. * p<0.05 by post hoc comparisons. Ns=not significant*

Volume interpretation: As shown in Table II, the left-sided TLE patients showed significant total brain volume reduction compared to the control group but not with the right-sided TLE group. For other brain regions not mentioned, no significant difference was found between the study groups based on total volume comparisons.

The comparisons of the hemispheric volumes in control and patient groups are presented in Table III. In the left-sided TLE group, remarkable right and left hemispheric volume reductions were observed, consistent with total brain atrophy compared to the controls (Figure 1). Significant volume decreases in the left temporal lobe, left NAc, and left premotor cortex were detected in the left-sided TLE group compared to the controls (Figure 2). However, no significant difference in volume was revealed in the right-sided TLE patient group compared to other groups.

Table III. *Mean ± SD hemispheric volumes of the regions, control vs left-sided TLE patient group*

Structure	Group		p val.
	Healthy (n=14)	Left TLE (n=6)	
Left Amygdala	1.86 ± 0.39	1.69 ± 0.32	Ns
Left Hippocampus	4.23 ± 0.6	3.73 ± 0.80	Ns
Left Nucleus Accumbens	0.76 ± 0.15	0.57 ± 0.071	**0.0126***
Left Premotor Cortex	7.02 ± 1.47	5.34 ± 0.75	**0.0176***
Left Primary Motor Cortex	14.06 ± 2.85	12.57 ± 3.24	Ns
Left Somatosensory Cortex	11.64 ± 2.78	10.54 ± 3.35	Ns
Left Temporal Lobe	66.85 ± 9.83	57.19 ± 7.54	**0.0465***
Left Thalamus	8.10 ± 1.41	6.99 ± 0.81	Ns
Left Hemisphere	614.3 ± 77.63	534,2 ± 45.88	**0.0312***
Right Amygdala	1.84 ± 0.35	1.76 ± 0.4	Ns
Right Hippocampus	4.53 ± 0.47	4.48 ± 0.46	Ns
Right Nucleus Accumbens	0.68 ± 0.17	0.6 ± 0.07	Ns
Right Premotor Cortex	6.68 ± 1.31	5.86 ± 0.78	Ns
Right Primary Motor Cortex	14.40 ± 3.32	12.51 ± 1.52	Ns
Right Somatosensory Cortex	11.16 ± 2.77	9.89 ± 1.13	Ns
Right Temporal Lobe	69.61 ± 10.85	62.44 ± 6.88	Ns
Right Thalamus	8,36 ± 1.5	7.17 ± 0.74	Ns
Right Hemisphere	627.4 ± 79.3	551.1 ± 42.78	**0.0411***

*Bold font denotes the significance of the analysis. * p<0.05 by post hoc comparisons. Ns=not significant*

http://doi.org/10.5472/marumj.1487475
Marmara Med J 2024;37(2): 144-151

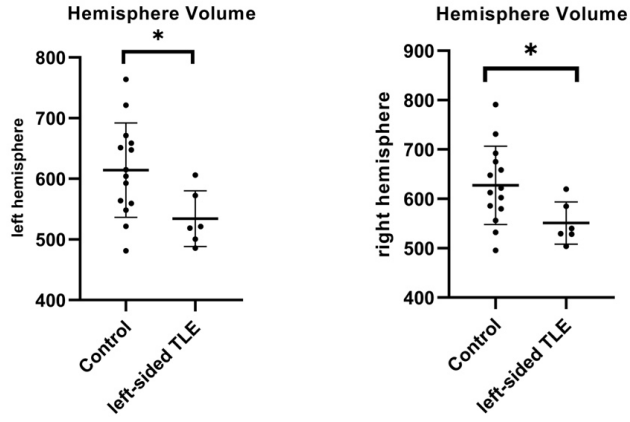

Figure 1. *Significant hemispheric volume reduction in the left-sided TLE group compared to the control group*

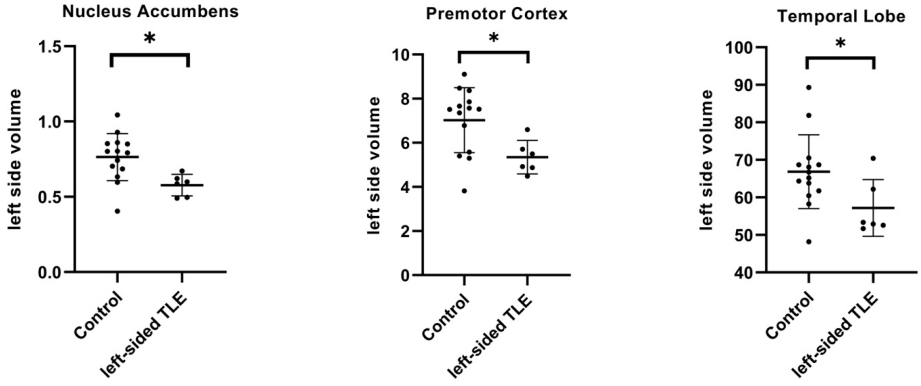

Figure 2. *Significant regional (nucleus accumbens, premotor cortex, and temporal lobe) ipsilateral volume reduction in the left-sided TLE group compared to the control group*

Asymmetry interpretation*:* Comparisons of AI values among the control group, right-sided TLE, and left-sided TLE patients are shown in Table IV. Following the comparisons, there were no significant symmetry differences for the total brain, amygdala, hippocampus, premotor, primary and somatosensory cortices, temporal lobe, and thalamus among the groups. Conversely, the left-sided TLE patients showed significant right asymmetry (contralateral to the lesion side) with negative AI value in the NAc compared to the controls (Figure 3). There were no symmetry changes in the right-sided TLE group compared to other groups. Besides, significant symmetry differences in the amygdala (p=0.0091), hippocampus (p=0.0173), and temporal lobe (p=0.0208) were observed between the patient groups.

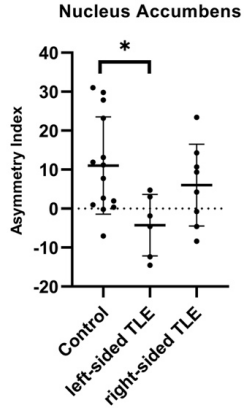

Figure 3. *Significance in asymmetry index value changes of the nucleus accumbens in the left-sided TLE patient group compared to the right-sided TLE and control groups*

Table IV. *Mean ± SD asymmetry index values of the brain regions among the three groups (healthy and subgroups of the patients)*

Structure and Group	Healthy Controls (n=14)	TLE Patients (n=14) Right TLE (n=8)		Left TLE (n=6)	
	Mean ± SD	Mean ± SD	p-val.	Mean ± SD	p-val.
Amygdala AI	0.94 ± 17.30	14.53 ± 10.15	0.1061	-3.16 ± 11.08	0.8309
Hippocampus AI	-7.03 ± 14.10	10.49 ± 22.1	0.0744	-19.35 ± 16.66	0.3230
Nucleus Accumbens AI	11.05 ± 12.46	6.03 ± 10.52	0.5746	-4.25 ± 7.89	**0.0245***
Premotor Cortex AI	4.30 ± 18.71	-2.16 ± 19.36	0.7075	-9.25 ± 15.40	0.2992
Primary Motor Cortex AI	-1.91 ± 15.52	0.18 ± 9.62	0.9408	-1.41 ± 16.04	0.9972
Somatosensory Cortex AI	4.50 ± 16.65	4.46 ± 14.42	>0.9999	3.18 ± 19.77	0.9858
Temporal Lobe AI	-3.84 ± 4.22	0.12 ± 4.22	0.2296	-8.91 ± 8.37	0.1457
Thalamus AI	-3.01 ± 9.17	1.84 ± 8.03	0.4254	-2.65 ± 7.95	0.9961
Total Brain AI	-2.11 ± 1.37	-0.62 ± 2.24	0.1874	-3.16 ± 2.28	0.4861

*Bold font denotes the significance of the analysis. * p<0.05 by post hoc comparisons.*

4. DISCUSSION

Temporal lobe epilepsy is the most common and well-defined localized epilepsy type with HS characterized by neuronal loss as primary pathological evidence. MRI has been one of the most valuable neuroimaging techniques to identify structural changes and epileptogenic foci in epileptic patients. In this study, we aimed to compare the findings of TLE patients versus healthy individuals on changes in volume and symmetry patterns of the total brain, hippocampus, temporal lobe, amygdala, thalamus, NAc, premotor, primary, and somatosensory cortices.

Reduction in total brain volume was observed in left-sided TLE patients compared to the control group in our study. These results are compatible with the meta-analysis that states widespread grey matter volume reduction in unilateral TLE patients [36]. Additionally, the results from our study revealed hemispheric volume reductions in both ipsilateral and contralateral to the lesion in the left-sided TLE group.

The comprehensive surface-based analysis of mesiotemporal and neocortical morphology study displayed marked ipsilateral mesiotemporal atrophy as cortical thinning that was bilateral in the TLE patients versus the controls [37]. Similarly, our results revealed significant volume reduction in the ipsilateral temporal lobe, NAc, and premotor cortex in the left-sided TLE group.

No significant difference was observed in the right-sided TLE patient group in any region compared to other left-sided TLE and control groups. This result is not congruent with the study that detected more expressed structural abnormalities in the right-sided TLE subgroup [38]. Our findings suggest that these results may be consistent with the dominant side of the brain but require more comprehensive research with detailed clinical findings.

The volume reduction of the left temporal lobe in the left-sided TLE group in our results is compatible with voxel-base morphological studies showing atrophy in the temporal regions predominantly ipsilateral to the seizure focus in TLE patients [21, 22, 39-41]. Our findings are also supported by an MRI study showing an asymmetric reduction in cortical surface area in the ipsilateral mesial and anterior temporal lobe subregions in mesial TLE patients [42].

The premotor cortex is highly connected to other brain parts and the elementary motor signs especially arise from precentral and premotor regions in frontal lobe epilepsy patients [43], for temporal region-originated epilepsies the premotor cortex is understudied. The volume reduction in the premotor cortex in our study may provide a new contribution to the literature.

The NAc, an extension of the ventral striatum, is the key nucleus in mediating emotional and motivational processes. Recent studies have shown that NAc participates in the process of epileptic seizures of patients and animal models with TLE thus NAc has been suggested as a target for the treatment in some epilepsy cases [28, 44, 45]. Evidence from both human and animal studies showed that detecting NAc volume reduction can provide valuable data for further investigations on TLE cases.

Hemispheric asymmetry is an important feature of the healthy human brain and reflects the structural and functional differences in the right and left hemispheres. The meta-analysis of the ENIGMA consortium revealed widespread asymmetries at both hemispheric and regional levels in healthy individuals predominantly in the left hemisphere [46]. As shown in previous studies, altered brain asymmetry has also been linked to psychiatric diseases and substance dependence [47, 48].

In our study, we discussed asymmetry patterns concerning TLE and investigated asymmetrical changes in epileptic patients using asymmetry index data calculated by the volumetric measures from the NeuroQuant® software. We detected significant volume asymmetry in the nucleus accumbens with a negative asymmetry index value in left-sided TLE patients compared to the control group. Interestingly, the prior study indicated remarkable whole-brain volumetric asymmetry and blood perfusion in TLE with high AI values [49], the difference between this study and our results was mainly methodological.

Ipsilateral volume decrease and contralateral symmetry deviation of the NAc in the left-sided TLE group could be related to an anatomical injury such as neuronal damage or degeneration in the lesion side. Functional connection changes

http://doi.org/10.5472/marumj.1487475
Marmara Med J 2024;37(2): 144-151

of the NAc subregions have been studied by using the DTI connectivity-based parcellation method and detected the distinct structural connectivity patterns that provide anatomical evidence to support the role of NAc subregions in seizures [50]. The latest study using rs-fMRI pointed out the decrease in functional connectivity between NAc and other brain regions in left-sided TLE patients suggesting that NAc plays an important role in mesial TLE [51]. The small sample size of our study may limit the evaluation of the NAc changes and their relation in TLE patient brains and should be verified in future studies.

In conclusion, researchers have focused on neuroimaging findings in TLE for a long time. Despite the small study group size, the results can provide insight into the morphological changes in TLE patients and symmetry deviation related to the side of the seizure focus. Since the relationship between epileptogenic focus and functional lateralization has been a matter of curiosity recently, asymmetry index results with volume alterations can be considered and implicated in the diagnosis protocols and it may shed light on the correct intervention to the epileptogenic focus treatment like resective surgery for TLE cases.

Compliance with Ethical Standards

Ethical approval: The study was approved by Marmara University, School of Medicine, Clinical Research Ethics Committee on 05.03.2021 with the protocol number 09.2021.322. Participant consent and ethical permissions were obtained.

Funding: This research was not funded or supported.

Conflict of interest: The authors reported no conflict of interest related to this article.

Author Contribution: EBK: Conceived and designed the analysis, made the research and prepared the original draft, ZF: Collected the study data, AMU: Performed data analysis with contributed analysis tool, GE: Supervisor – reviewed the draft, USS: Supervisor – reviewed and edited the draft. All authors approved the final version of the article to be published.

REFERENCES

[1] Epilepsy W. A public health imperative. Geneva, Switzerland: WHO, 2019.

[2] Scheffer IE, Berkovic S, Capovilla G, et al. ILAE classification of the epilepsies: position paper of the ILAE Commission for Classification and Terminology. Zeitschrift Fur Epileptologie 2018; 31:296-306. doi:10.1007/s10309.018.0218-6.

[3] Blumcke I, Thom M, Aronica E, et al. International consensus classification of hippocampal sclerosis in temporal lobe epilepsy: a Task Force report from the ILAE Commission on Diagnostic Methods. Epilepsia 2013; 54:1315-29. doi:10.1111/epi.12220.

[4] Alvarez-Linera J: Temporal lobe epilepsy (TLE) and neuroimaging. In: Barkhof F, Jäger HR, Thurnher MM, Rovira À eds. Clinical Neuroradiology: The ESNR Textbook. Cham: Springer International Publishing, 2019: 891-914.

[5] Watson C, Andermann F, Gloor P, et al. Anatomic basis of amygdaloid and hippocampal volume measurement by magnetic resonance imaging. Neurology 1992; 42:1743-50. doi:10.1212/wnl.42.9.1743.

[6] Bernasconi N, Bernasconi A, Caramanos Z, Antel SB, Andermann F, Arnold DL. Mesial temporal damage in temporal lobe epilepsy: a volumetric MRI study of the hippocampus, amygdala and parahippocampal region. Brain 2003; 126(Pt 2):462-9. doi:10.1093/brain/awg034.

[7] Bernasconi N, Natsume J, Bernasconi A. Progression in temporal lobe epilepsy: differential atrophy in mesial temporal structures. Neurology 2005; 65:223-8. doi:10.1212/01.wnl.000.016.9066.46912.fa.

[8] Caboclo LO, Garzon E, Oliveira PA, et al. Correlation between temporal pole MRI abnormalities and surface ictal EEG patterns in patients with unilateral mesial temporal lobe epilepsy. Seizure 2007; 16:8-16. doi:10.1016/j.seizure.2006.09.001.

[9] Berkovic SF, Andermann F, Olivier A, et al. Hippocampal sclerosis in temporal lobe epilepsy demonstrated by magnetic resonance imaging. Ann Neurol 1991; 29:175-82. doi:10.1002/ana.410290210.

[10] Cascino GD, Jack CR, Jr., Parisi JE, et al. Magnetic resonance imaging-based volume studies in temporal lobe epilepsy: pathological correlations. Ann Neurol 1991; 30:31-6. doi:10.1002/ana.410300107.

[11] Cendes F, Andermann F, Gloor P, et al. MRI volumetric measurement of amygdala and hippocampus in temporal lobe epilepsy. Neurology 1993; 43:719-25. doi:10.1212/wnl.43.4.719.

[12] Jack CR, Jr., Sharbrough FW, Twomey CK, et al. Temporal lobe seizures: lateralization with MR volume measurements of the hippocampal formation. Radiology 1990; 175:423-9. doi:10.1148/radiology.175.2.2183282.

[13] Moghaddam HS, Aarabi MH, Mehvari-Habibabadi J, et al. Distinct patterns of hippocampal subfield volume loss in left and right mesial temporal lobe epilepsy. Neurol Sci 2021; 42:1411-21. doi:10.1007/s10072.020.04653-6.

[14] Thom M. Review: Hippocampal sclerosis in epilepsy: a neuropathology review. Neuropathol Appl Neurobiol 2014; 40:520-43. doi:10.1111/nan.12150.

[15] Van Paesschen W, Revesz T, Duncan JS, King MD, Connelly A. Quantitative neuropathology and quantitative magnetic resonance imaging of the hippocampus in temporal lobe epilepsy. Ann Neurol 1997; 42:756-66. doi:10.1002/ana.410420512.

[16] Bernhardt BC, Bernasconi A, Liu M, et al. The spectrum of structural and functional imaging abnormalities in temporal lobe epilepsy. Ann Neurol 2016; 80:142-53. doi:10.1002/ana.24691.

[17] Van Paesschen W. Qualitative and quantitative imaging of the hippocampus in mesial temporal lobe epilepsy with hippocampal sclerosis. Neuroimaging Clin N Am 2004; 14:373-400, vii. doi:10.1016/j.nic.2004.04.004.

[18] Bernasconi N, Duchesne S, Janke A, Lerch J, Collins DL, Bernasconi A. Whole-brain voxel-based statistical analysis of gray matter and white matter in temporal lobe

epilepsy. Neuroimage 2004; 23:717-23. doi:10.1016/j.neuroimage.2004.06.015.

[19] Dreifuss S, Vingerhoets FJ, Lazeyras F, et al. Volumetric measurements of subcortical nuclei in patients with temporal lobe epilepsy. Neurology 2001; 57:1636-41. doi:10.1212/wnl.57.9.1636.

[20] Li J, Zhang Z, Shang H. A meta-analysis of voxel-based morphometry studies on unilateral refractory temporal lobe epilepsy. Epilepsy Res 2012; 98:97-103. doi:10.1016/j.eplepsyres.2011.10.002.

[21] Riederer F, Lanzenberger R, Kaya M, Prayer D, Serles W, Baumgartner C. Network atrophy in temporal lobe epilepsy: a voxel-based morphometry study. Neurology 2008; 71:419-25. doi:10.1212/01.wnl.000.032.4264.96100.e0.

[22] Santana MT, Jackowski AP, da Silva HH, et al. Auras and clinical features in temporal lobe epilepsy: a new approach on the basis of voxel-based morphometry. Epilepsy Res 2010; 89:327-38. doi:10.1016/j.eplepsyres.2010.02.006.

[23] Whelan CD, Altmann A, Botia JA, et al. Structural brain abnormalities in the common epilepsies assessed in a worldwide ENIGMA study. Brain 2018; 141(2):391-408. doi:10.1093/brain/awx341.

[24] Scanlon C, Mueller SG, Cheong I, Hartig M, Weiner MW, Laxer KD. Grey and white matter abnormalities in temporal lobe epilepsy with and without mesial temporal sclerosis. J Neurol 2013; 260:2320-9. doi:10.1007/s00415.013.6974-3.

[25] Guadalupe T, Willems RM, Zwiers MP, et al. Differences in cerebral cortical anatomy of left – and right-handers. Front Psychol 2014; 5:261. doi:10.3389/fpsyg.2014.00261.

[26] Kuo F, Massoud TF. Structural asymmetries in normal brain anatomy: A brief overview. Ann Anat 2022; 241:151894. doi:10.1016/j.aanat.2022.151894.

[27] Lubben N, Ensink E, Coetzee GA, Labrie V. The enigma and implications of brain hemispheric asymmetry in neurodegenerative diseases. Brain Commun 2021; 3(3):fcab211. doi:10.1093/braincomms/fcab211.

[28] Zuo Z, Ran S, Wang Y, et al. Asymmetry in cortical thickness and subcortical volume in treatment-naive major depressive disorder. Neuroimage Clin 2019; 21:101614. doi:10.1016/j.nicl.2018.101614.

[29] Oertel-Knochel V, Knochel C, Stablein M, Linden DE. Abnormal functional and structural asymmetry as biomarker for schizophrenia. Curr Top Med Chem 2012; 12(21):2434-51. doi:10.2174/156.802.612805289926.

[30] Sarica A, Vasta R, Novellino F, et al. MRI Asymmetry Index of Hippocampal Subfields Increases Through the Continuum From the Mild Cognitive Impairment to the Alzheimer's Disease. Front Neurosci 2018; 12:576. doi:10.3389/fnins.2018.00576.

[31] Pereira FR, Alessio A, Sercheli MS, et al. Asymmetrical hippocampal connectivity in mesial temporal lobe epilepsy: evidence from resting state fMRI. BMC Neurosci 2010; 11:66. doi:10.1186/1471-2202-11-66.

[32] Pittau F, Grova C, Moeller F, Dubeau F, Gotman J. Patterns of altered functional connectivity in mesial temporal lobe epilepsy. Epilepsia 2012; 53:1013-23. doi:10.1111/j.1528-1167.2012.03464.x.

[33] Fisher RS, Cross JH, D'Souza C, et al. Instruction manual for the ILAE 2017 operational classification of seizure types. Epilepsia 2017; 58:531-42. doi:10.1111/epi.13671.

[34] Bullmore E, Brammer M, Harvey I, Ron M. Against the Laterality Index as a Measure of Cerebral Asymmetry. Psychiatry Research-Neuroimaging 1995; 61:121-24. doi:Doi 10.1016/0925-4927(95)02618-8.

[35] Zhao X, Kang H, Zhou Z, et al. Interhemispheric functional connectivity asymmetry is distinctly affected in left and right mesial temporal lobe epilepsy. Brain Behav 2022; 12:e2484. doi:10.1002/brb3.2484.

[36] Li Z, Kang J, Gao Q, et al. Structural brain assessment of temporal lobe epilepsy based on voxel-based and surface-based morphological features. Neurol Neurochir Pol 2021; 55:369-79. doi:10.5603/PJNNS.a2021.0042.

[37] Liu M, Bernhardt BC, Bernasconi A, Bernasconi N. Gray matter structural compromise is equally distributed in left and right temporal lobe epilepsy. Hum Brain Mapp 2016; 37:515-24. doi:10.1002/hbm.23046.

[38] Pail M, Brazdil M, Marecek R, Mikl M. An optimized voxel-based morphometric study of gray matter changes in patients with left-sided and right-sided mesial temporal lobe epilepsy and hippocampal sclerosis (MTLE/HS). Epilepsia 2010; 51:511-8. doi:10.1111/j.1528-1167.2009.02324.x.

[39] Jber M, Habibabadi JM, Sharifpour R, et al. Temporal and extratemporal atrophic manifestation of temporal lobe epilepsy using voxel-based morphometry and corticometry: clinical application in lateralization of epileptogenic zone. Neurol Sci 2021; 42:3305-25. doi:10.1007/s10072.020.05003-2.

[40] Keller SS, Roberts N. Voxel-based morphometry of temporal lobe epilepsy: an introduction and review of the literature. Epilepsia 2008; 49:741-57. doi:10.1111/j.1528-1167.2007.01485.x.

[41] Moran NF, Lemieux L, Kitchen ND, Fish DR, Shorvon SD. Extrahippocampal temporal lobe atrophy in temporal lobe epilepsy and mesial temporal sclerosis. Brain 2001; 124(Pt 1):167-75. doi:10.1093/brain/124.1.167.

[42] Alhusaini S, Doherty CP, Palaniyappan L, et al. Asymmetric cortical surface area and morphology changes in mesial temporal lobe epilepsy with hippocampal sclerosis. Epilepsia 2012; 53:995-1003. doi:10.1111/j.1528-1167.2012.03457.x.

[43] Chowdhury FA, Silva R, Whatley B, Walker MC. Localisation in focal epilepsy: a practical guide. Pract Neurol 2021; 21:481-91. doi:10.1136/practneurol-2019-002341.

[44] Kowski AB, Voges J, Heinze HJ, Oltmanns F, Holtkamp M, Schmitt FC. Nucleus accumbens stimulation in partial epilepsy—a randomized controlled case series. Epilepsia 2015; 56:e78-82. doi:10.1111/epi.12999.

[45] Schmitt FC, Voges J, Heinze HJ, Zaehle T, Holtkamp M, Kowski AB. Safety and feasibility of nucleus accumbens stimulation in five patients with epilepsy. J Neurol 2014; 261:1477-84. doi:10.1007/s00415.014.7364-1.

[46] Kong XZ, Mathias SR, Guadalupe T, et al. Mapping cortical brain asymmetry in 17,141 healthy individuals worldwide via the ENIGMA Consortium. Proc Natl Acad Sci U S A 2018; 115:E5154-E63. doi:10.1073/pnas.171.841.8115.

[47] Cao Z, Ottino-Gonzalez J, Cupertino RB, et al. Mapping cortical and subcortical asymmetries in substance dependence: Findings from the ENIGMA Addiction Working Group. Addict Biol 2021; 26:e13010. doi:10.1111/adb.13010.

[48] Kong XZ, Postema MC, Guadalupe T, et al. Mapping brain asymmetry in health and disease through the ENIGMA consortium. Hum Brain Mapp 2022; 43:167-81. doi:10.1002/hbm.25033.

[49] Zhang Y, Dou W, Zuo Z, et al. Brain volume and perfusion asymmetry in temporal lobe epilepsy with and without hippocampal sclerosis. Neurol Res 2021; 43:299-306. doi:10.1080/01616.412.2020.1853988.

[50] Zhao X, Yang R, Wang K, et al. Connectivity-based parcellation of the nucleus accumbens into core and shell portions for stereotactic target localization and alterations in each NAc subdivision in mTLE patients. Hum Brain Mapp 2018; 39:1232-45. doi:10.1002/hbm.23912.

[51] Yang R, Zhao X, Liu J, et al. Functional connectivity changes of nucleus Accumbens Shell portion in left mesial temporal lobe epilepsy patients. Brain Imaging and Behavior 2020; 14:2659-67. doi:10.1007/s11682.019.00217-1.

MARMARA
MEDICAL JOURNAL

Original Article

https://dergipark.org.tr/tr/pub/marumj

The effect of the mean platelet volume on short-term prognosis in acute ischemic stroke patients who underwent intravenous thrombolytic therapy

Cisil Irem OZGENC BICER[1], Isıl KALYONCU ASLAN[2], Eren GOZKE[2]

[1] Department of Neurology, School of Medicine, Marmara University, Istanbul, Turkey
[2] Department of Neurology, Fatih Sultan Mehmet Research and Training Hospital, Istanbul, Turkey

Corresponding Author: Cisil Irem OZGENC BICER
E-mail: cisiliremozgenc@gmail.com

Submitted: 18.12.2023 **Accepted:** 27.12.2023

ABSTRACT

Objective: To evaluate the effect of the mean platelet volume (MPV), on the short-term prognosis and bleeding complications of acute ischemic stroke patients who underwent intravenous tissue plasminogen activator (IV-tPA) treatment.

Patients and Methods: Between 01.01.2018 and 01.06.2021, 314 ischemic stroke patients who applied to our clinic with acute neurological deficit were included in the study retrospectively. Alteplase was administered as IV-tPA treatment for 1 hour. MPV value was measured before the treatment and was evaluated as the main parameter. The patients were examined under 4 groups (≤8.8fL, >8.8 – ≤9.9, >9.9-≤10.8, >10.8fL) according to their MPV values, and age, gender, comorbidities, and treatment initiation parameters were standardized by statistical methods. It was compared whether there was a significant difference between the MPV groups in terms of short-term prognosis according to the admission National Institutes of Health Stroke Scale (NIHSS) scores and discharge NIHSS scores and also bleeding complications.

Results: A total of 314 patients, 145 women with a mean age of 76.7±13.0, and 169 men with a mean age of 66.3±13.1, were included in the study. 31 patients (9.9%) died before discharge. The mean MPV value was 9.64±1.15fL and the mean NIHSS score was 9.1±4.9 at admission, and the mean NIHSS score was 4.3±4.7 at discharge. When the NIHSS difference between admission and discharge was compared in the 4 groups, it was found that the prognosis was better in Group 3 with MPV >9.9-≤10.8 compared to Groups 1 and 4. (p=0.002; p<0.01). Despite this, it was seen that low or high MPV values could not be considered as a prognostic factor alone in patients who received IV-tPA treatment, since, there was no significant difference between the 3rd group and the 2nd group in terms of NIHSS decrease and the 4th group had a worse prognosis than the 3rd group.

There was no statistical significance between MPV groups in terms of hemorrhage complications (p value for intracerebral, gastrointestinal, urogenital hemorrhage complications were 0.540, 0.980, 0.783, respectively).

Conclusion: In our study, it was revealed that MPV value, is not an independent risk factor in patients with acute ischemic stroke receiving IV-tPA treatment and cannot be used as a prognostic marker.

Keywords: Stroke, Prognosis, MPV, IV-tPA

1.INTRODUCTION

Stroke ranks third among the causes of loss of function worldwide, according to Disability Adjusted Life Years (DALY) measurements [1,2]. Nowadays, it is aimed to reduce the mortality and morbidity of stroke patients. Improvement in the prognosis of stroke is increased with intravenous tissue plasminogen activator (IV – tPA) therapy and mechanical thrombectomy (MT) treatments. The mechanism of thrombus formation and risk factors in ischemic stroke are a matter of interest for researchers both for primary prevention and for treatment planning. Due to the easy accessibility of blood parameters, many publications investigating the relationship with stroke draw attention. It is thought that hyperactive platelets play an important role in thrombus formation and the Mean Platelet Volume (MPV) value is associated with platelet activation [3]. The MPV is an indicator of the size of the platelets, and "increase in MPV value" means an increase in platelet diameters. The reference value is 7.4-12 fl (femtoliter:µm3) on average, and it can be checked during complete blood count without additional cost. It has been shown in various publications that as MPV increases, platelet activation increases (due to aggregation, thromboxane A2, platelet factor 4 and β-thromboglobulin release) [4,5]. The MPV value was found to be higher in all stroke types compared to the healthy population [6]. The elevated MPV may predict the disabling of the fatal ischemic stroke in the patients treated with tPA [7]. Additionally; the value of MPV in predicting the risk of the secondary hemorrhage in stroke patients receiving the reperfusion therapy remains unclear [8]. The aim of this study

How to cite this article: Bicer Ozgenc IC, Aslan Kalyoncu I, Gozke E. The effect of the mean platelet volume on short-term prognosis in acute ischemic stroke patients who underwent intravenous thrombolytic therapy. Marmara Med J 2024: 37(2):152-156. doi: 10.5472/marumj.1485342

ISSN: 1309-9469

http://doi.org/10.5472/marumj.1485342
Marmara Med J 2024;37(2): 152-156

was to evaluate the effect of MPV on the short-term prognosis and bleeding complications of acute ischemic stroke patients who underwent IV-tPA treatment.

2. PATIENTS and METHODS

We conducted a single-center, retrospective analysis of the patients who applied to Health and Sciences University Fatih Sultan Mehmet Training and Research Hospital emergency between 01.01.2018 and 01.06.2021 with acute stroke presentation. The patients who were in the first 4.5 hours of the onset of their complaints and got reperfusion therapy were informed about all risks and possible complications of the study, including death before treatment. MPV value, found in the routine hemogram taken before the reperfusion treatment was evaluated as the main parameter. Alteplase was used as a thrombolytic agent. The total dose recommended in stroke guidelines was 0.9 mg/kg for the treatment of alteplase. 10% of the calculated total dose was administered as a bolus and the remaining dose was administered as a 1-hour infusion. The max dosage was 90 mg in total. The National Institutes of Health Stroke Scale (NIHSS) was used for all patients included in the study before treatment (initial NIHSS) and at discharge inorder to evaluate their response to the treatment. Age, gender, comorbidities (diabetes, hypertension, atrial fibrillation), IV-tPA onset time were standardized by statistical methods, and it was evaluated whether the MPV value, which was measured at the time of admission, was effective on the NIHSS change and on the major bleeding complications that developed within the first 24 hours after IV – tPA treatment. Patients were divided into 4 groups according to the MPV cut-off values in the study of Debiec et al., in which they investigated the effect of MPV on prognosis [3]. In the 1st group MPV≤8.8fL (N:82), 2nd group >8.8 – ≤9.9 fL (N:123), 3rd group >9.9-≤10.8 fL (N:61), and 4th group >10.8 fL (N:48) was planned. It was evaluated whether there was a statistically significant difference between the groups in terms of age, gender, tPA onset time, admission NIHSS, discharge NIHSS, admission and discharge NIHSS difference, comorbidities, antiaggregant/anticoagulant use, bleeding complications and death rates during hospitalization.

ROC analysis was performed to predict the cut-off point of the MPV value for any bleeding complications. Patients under 18 years of age, patients who do not get anticoagulants but whose IV-tPA treatment was interrupted due to high INR, patients who underwent mechanical thrombectomy after thrombolytic therapy or known hematological pathology – malignancies, patients whose treatment could not be completed due to any allergic reaction, patients whose treatment could not be completed due to acute hemorrhagic complications while IV-tPA was continued were not included in the study.

Ethics committee approval was received from Health Sciences University Fatih Sultan Mehmet Training and Research Hospital Clinical Research Ethics Committee on 27.05.2021.

Statistical Analysis

Number Cruncher Statistical System (NCSS) 2007 (Kaysville, Utah, USA) program was used for statistical analysis. While evaluating the study data, the distribution of the data was evaluated with the Shapiro-Wilk Test, as well as the descriptive statistical methods (Mean, Standard Deviation, Median, Frequency, Ratio, Minimum, Maximum). Kruskall-Wallis test for comparison of quantitative data of three or more groups; Mann-Whitney U Test was used for comparison of two groups. Chi-square analysis was used to determine the relationship between qualitative data. Spearman's correlation analysis was used to determine the relationship between quantitative data. Significance was evaluated at $p<0.01$ and $p<0.05$ levels.

3. RESULTS

The study included 314 patients, 169 men with a mean age of 66.3± 13.1 years and 145 women with a mean age of 76.7± 12.9 years. It was found statistically significant that the mean age of the male group was lower than that of the females ($p=0.001$; $p<0.05$). It was found that 9.9% (n=31) of 314 patients included in the study died in the hospital. Of the patients who died, 32.3% (n:10) were male and 67.7% (n:21) were female. The mean MPV and platelet in the cohort were 9.64 ±1.15 fL and 269.7 ± 73.7 x 10^3/μL respectively. Age, gender, tPA onset time, medical history (diabetes, hypertension, atrial fibrillation), antiplatelet / anticoagulant use according to MPV groups were evaluated. (Table I).

According to the MPV groups; age, tPA onset time, gender and comorbidities did not show any statistically significant differences. Although there was no difference in terms of antiplatelet use ($p>0.05$); it was found statistically significant that the anticoagulant use in the 1st group was lower than in the 4th group ($p=0.001$; $p<0.01$) (Table I).

Admission NIHSS, discharge NIHSS, admission and discharge NIHSS difference, intracerebral hemorrhage, gastrointestinal system hemorrhage, urogenital hemorrhage, other bleeding complications and their relationship with MPV groups were evaluated in Table II.

No statistically significant difference was observed between MPV groups in terms of bleeding complications and death rates. However; it was statistically significant that the initial-discharge difference of NIHSS in the 1st group is lower than that of groups 2 and 3 and ($p=0.001$; $p<0.01$) that the initial-discharge difference of NIHSS in the 3rd group is higher than that of group 1 and group 4 ($p=0.001$; $p<0.01$). No statistical significance was observed between groups 2 and 3 ($p>0.05$).

ROC analysis was performed to predict the cut-off point of the MPV value for any bleeding complications. When the MPV cut-off taken as 8.85, the sensitivity was 76%; the specificity was 69.1%. It was found statistically significant that all patients with other bleeding complications (epistaxis, gingival, hemoptysis otorrhagia, and subcutaneous hematoma) were observed in the second group which MPV higher than 8.85 fL ($p=0.034$, $p>0.05$). However, no statistical significance was observed in terms of intracranial, gastrointestinal and urogenital bleeding complications ($p>0.05$) (Table III).

http://doi.org/10.5472/marumj.1485342
Marmara Med J 2024;37(2): 152-156

Table I. *Comparison of prognostic factors according to MPV groups*

MPV (fL)	Group 1 8.8 (82)	Group 2 8.8< 9.9 (123)	Group 3 9.9< 10.8 (61)	Group 4 >10.8 (48)	P*	Post Hoc**
Age	70.8 (14.8)	70.5 (12.3)	72.4 (15.5)	71.6 (14.9)	0.490	
Gender (Female)	38 (26.2%)	58 (40%)	28 (19.3%)	21 (14.5%)	0.983	
Atrial Fibrillation	15 (19.5%)	31 (40.3%)	13 (16.9%)	18 (23.4%)	0.091	
Hypertension	58 (25.7%)	89 (39.4%)	41 (18.1%)	38 (16.8%)	0.575	
Antiaggregant Use	33 (26%)	52 (40.9%)	26 (20.5%)	16 (12.6%)	0.729	
Anticoagulant Use	1 (6.3%)	7(43.8%)	2(12.5%)	6 (37.5%)	0.037*	1 vs 4
IV-tPA Onset Time (Minute)	185.0 (57.7)	180.2 (52.9)	176.7 (54.3)	193.0 (54.1)	0.394	

*Values are mean ± SD for quantitative variables and % for qualitative variables. MPV: mean platelet volume; fL: femtolitre; IV-tPA: intravenous tissue plasminogen activator *p <0.05, **Post Hoc: statistically significant results*

Table II. *NIHSS changes and bleeding complications according to MPV groups*

MPV (fL)	Group 1 8.8 (82)	Group 2 8.8< 9.9 (123)	Group 3 9.9< 10.8 (61)	Group 4 >10.8 (48)	P*	Post Hoc**
Initial NIHSS	8.5 (4.7)	9.0 (4.9)	10.0 (4.9)	9.1 (5.1)	0.243	
Discharge NIHSS	5.2 (5.3)	4.05 (4.8)	3.1 (3.2)	4.8 (4.8)	0.084	
Initial- Discharge NIHSS	2.7 (5.0)	4.5 (4.8)	5.9 (4.6)	3.8 (5.2)	0.002**	1vs 2.3 3vs 1.4
Intracranial Hemorrhage	9 (19.1%)	21 (44.7%)	8 (17%)	9 (19.1%)	0.540	
Urogenital Hemorrhage	3 (42.9%)	2 (28.6%)	1 (14.3%)	1 (%14,3)	0,783	
GIS Hemorrhage	2 (25%)	3 (37.5%)	2 (25%)	1 (12.5%)	0.980	
Other bleeding Complications	0 (0%)	6 (54.5%)	3 (27.3%)	2 (18.2%)	0.252	
Death	6 (19.4%)	12(38.7%)	9 (29%)	4 (12.9%)	0.876	

*MPV: mean platelet volume; fL: femtolitre; NIHSS : National Institute of Health Stroke Scale; GIS; gastrointestinal system, *p <0.05, **Post Hoc: statistically significant results*

Table III. *ROC analysis for bleeding complications*

MPV (fL)	<8.85 (82)	8.85> (232)	P*
Age	70.8 (14.8)	71.2 (14.8)	0.946
Gender (Female)	38 (26.2%)	107 (73.8%)	0.973
IV-tPA Onset Time (Minute)	185.0 (57.7)	181.9 (53.6)	0.716
Initial NIHSS	8.5 (4.7)	9.3 (4.9)	0.112
Discharge NIHSS	5.2 (5.3)	3.9 (4.5)	0.055
Initial- Discharge NIHSS	2.7(5.0)	4.7 (4.9)	0.941
Atrial Fibrillation	15 (19.5%)	62 (80.5%)	0.127
Hypertension	58 (25.7%)	168 (74.3%)	0.771
Diabetes Mellitus	25 (23.1%)	83 (76.9%)	0.386
Antiaggregant Use	33 (26.0%)	94 (74.0%)	0.965
Anticoagulant Use	1 (6.3%)	15 (93.8%)	0.079
Intracranial Hemorrhage	9 (19.1%)	38 (80.9%)	0.238
Urogenital Hemorrhage	3 (42.9%)	4 (57.1%)	0.308
Gastrointestinal Hemorrhage	2 (25.0%)	6 (75.0%)	0.942
Other Bleeding Complications	0 (0%)	11 (100%)	0.034*

MPV:Mean platelet volume; fL: Femtolitre; NIHSS: National Institute of Health Stroke Scale; IV-tPA: intravenous tissue plasminogen acti

http://doi.org/10.5472/marumj.1485342
Marmara Med J 2024;37(2): 152-156

4. DISCUSSION

Stroke is considered as one of the leading causes of morbidity and mortality all over the world. Considering that one quarter of all strokes are predicted to recur, modifiable risk factors such as DM, hypertension, dyslipidemia, obesity, smoking, and AF fibrillation must be controlled [9]. Although, studies on risk factors are still on the agenda, publications investigating stroke pathogenesis and prognosis of patients are increasing with new developing treatment methods.

The contribution of platelets to the pathogenesis of thrombus formation is undeniable [10]. Aggregation has a positive association with indicators of platelet activity, including Tx A2, PF 4 and β-TG release. Larger platelets are more reactive, produce more prothrombotic factors, and can aggregate more easily [11,12]. In this study, it was hypothesized that the prognosis of the patient group with an acute ischemic stroke and receiving iv tPA treatment and having a higher MPV value may have a worse prognosis; However, in a retrospective evaluation of 314 patients, it was found that MPV value alone could not be a prognostic factor.

Debiec et al., in their study, it was observed that patients with MPV above 10.8 fL had higher discharge NIHSS values and a worse prognosis [13]. In our study, in which the same MPV groups were used, no statistical significance was observed in terms of death, arrival NIHSS, discharge NIHSS or bleeding complications in all 4 MPV groups. However, when the groups were evaluated according to the decrease in NIHSS (arrival-discharge), it was observed that the NIHSS decrease, that is, the prognosis, in the 3rd group (MPV>9.9 and ≤10.8) was statistically better than the 1st and 4th groups. However, since there was no significant difference between the 3rd group and the 2nd group in terms of NIHSS decrease and the prognosis of the 4th group was worse than the 3rd group, it was observed that low or high MPV values could not be considered a prognostic factor alone in patients receiving iv-tPA treatment.

Arevalo-Lorido et al., in their study on 379 patients who were followed up for ischemic stroke but did not receive iv tPA treatment, it was found that at the end of first year higher MPV values (>11.5fL) were related with worse prognosis [13]. In our study, since the majority of the patients did not continue their follow-up, 3-month-6-month and 1-year MRS scores could not be evaluated, and no comment could be made regarding the effect of MPV on long-term prognosis.

In the PROGRESS study, which included 3134 people with a history of cerebrovascular disease, it was stated that high MPV was associated with an increased risk of stroke, and even every 1 fL increase in MPV value could cause an 11% increase in stroke risk [14]. In studies comparing ischemic stroke patients with control groups, it was observed that the MPV values of the stroke groups were higher than the healthy population [15,16]. In the study administered by Ntaios et al. on 623 patients, it was shown that MPV did not statistically affect stroke severity and prognosis, as in our study, in both 137 patients receiving iv tPA treatment and 486 patients who were not candidates for iv-tPA [17].

In our study, in addition to evaluating the effect of MPV on the short-term prognosis of patients, its relationship with intracranial, urogenital, GI and other bleeding complications after IV-tPA was also evaluated. When the patients were examined in 4 groups according to MPV values, no significant difference was found regarding bleeding complications. However, in ROC analysis it was found statistically significant that all other bleeding complications were in the higher MPV group (>8.85 fL). Nevertheless; it would not be totally correct to determine a clear MPV cut-off point since the number of patients with this complication was only 11.

Hemorrhage complications of iv-tPA other than intracerebral, GIS, and urogenital system are written on a case-by-case basis, but no data were found in the literature regarding other bleeding complications seen in patients receiving tPA in which the effect of MPV on prognosis was investigated. Khandelwal et al., They published the massive epistaxis, seen in 2 patients who were Covid-19 + and received IV-tPA as a case report and explained the epistaxis as the potentiation of coagulopathy due to Covid-19 infection by tPA, but they did not share any data about MPV in their study [18].

Conclusion

In this study, where it is hypothesized that short-term prognosis will worsen as MPV value increases, no statistically significant relationship can be found between increasing MPV values and prognosis. There is no difference in bleeding complications and death rates between MPV groups.

The increasing prevalence of IV-tPA treatment will allow studies to be conducted with a larger patient population. Studies that will contribute to the literature will increase day by day by diversifying prognostic evaluations, enabling long-term follow-up, and increasing the patient population.

Compliance with Ethical Standards

Ethical approval: The study protocol was approved by Fatih Sultan Mehmet Training and Research Hospital Ethics Committee (approval number: 2021/56). Informed consent was obtained from all patients.

Financial support: The authors have no relevant financial information to disclose.

Conflict of interest: The authors have no potential conflicts to declare.

Authors' contributions: CIOB: Literature search, EG, CIOB,: Study design, CIOB, IKA: Data collection, EK, IKA: Supervision and quality control, EG: Statistical advice, EG: Statistical data analysis, CIOB: Data interpretation, IKA, EG, CIOB: Drafting the manuscript. All authors read and approved the final version of the article.

REFERENCES

[1] Sacco RL, Kasner SE, Broderick JP, et al. An updated definition of stroke for the 21st Century. Stroke 2013; 44: 2064-89. doi: 10.1161/str.0b013e318296aeca

[2] Lozano R, Naghavi M, Foreman K, et al. Global and regional mortality from 235 causes of death for 20 Age groups in 1990 and 2010: A systematic analysis for the global burden of disease study 2010. The Lancet 2012; 380: 2095-128. doi: 10.1016/s0140-6736(12)61728-0

[3] Dębiec A, Pogoda-Wesołowska A, Piasecki P, et al. Mean platelet volume as a potential marker of large vessel occlusion and predictor of outcome in acute ischemic stroke patients treated with reperfusion therapy. Life 2021; 11:469. doi:10.3390/life11060469

[4] Virani SS, Alonso A, Benjamin EJ, et al. Heart disease and stroke statistics-2020 update: A report from the American Heart Association. Circulation 2020; 141. doi:10.1161/cir.000.000.0000000757.

[5] Loo B van, Martin JF. 6 megakaryocytes and platelets in vascular disease. Baillieres Clin Haematol 1997; 10: 109-23. doi: 10.1016/s0950-3536(97)80053-4

[6] Muscari A, Puddu GM, Cenni A, et al. Mean platelet volume (MPV) increase during acute non-lacunar ischemic strokes. Thromb Res 2009; 123: 587-91. doi: 10.1016/j.thromres.2008.03.025

[7] Staszewski J, Pogoda A, Data K, et al. The mean platelet volume on admission predicts unfavorable stroke outcomes in patients treated with IV thrombolysis. Clin Interv Aging 2019; Volume 14: 493-503. doi: 10.2147/cia.s195451

[8] Oji S, Tomohisa D, Hara W, et al. Mean platelet volume is associated with early neurological deterioration in patients with branch atheromatous disease: Involvement of platelet activation. J Stroke Cerebrovasc Dis 2018; 27: 1624-31. doi: 10.1016/j.jstrokecerebrovasdis.2018.01.012

[9] Ross R. Atherosclerosis-an inflammatory disease. N Engl J Med 1999; 340: 115-26. doi: 10.1056/nejm199.901.143400207

[10] Baidildinova G, Nagy M, Jurk K, et al. Soluble platelet release factors as biomarkers for cardiovascular disease. Front Cardiovasc Med 2021; 8. doi:10.3389/fcvm.2021.684920.

[11] Bath PM, Butterworth RJ. Platelet size. Blood Coagul Fibrinolysis1996;7:157-61.doi:10.1097/00001.721.199603000-00011

[12] Arévalo-Lorido JC, Carretero-Gómez J, Álvarez-Oliva A, et al. Mean platelet volume in acute phase of ischemic stroke, as predictor of mortality and functional outcome after 1 year. J Stroke Cerebrovasc Dis 2013; 22:297303. doi: 10.1016/j.jstrokecerebrovasdis.2011.09.009

[13] Bath P, Algert C, Chapman N, et al. Association of mean platelet volume with risk of stroke among 3134 individuals with history of cerebrovascular disease. Stroke 2004; 35: 622-6. doi: 10.1161/01.str.000.011.6105.26237.ec

[14] Van Gijn J. The progress trial: Preventing strokes by lowering blood pressure in patients with cerebral ischemia. Stroke 2002; 33: 319-20. doi: 10.1161/str.33.1.319

[15] D'erasmo E, Alıbertı G, Celı Fs, et al. Platelet count, mean platelet volume and their relation to prognosis in cerebral infarction. J Intern Med 1990; 227: 11-4. doi: 10.1111/j.1365-2796.1990.tb00111.x

[16] Kosalram J. A study on mean platelet volume in acute ischemic stroke. J Med Sci Clin Res 2017; 5. doi:10.18535/jmscr/v5i10.141.

[17] Ntaios G, Gurer O, Faouzi M, et al. Mean platelet volume in the early phase of acute ischemic stroke is not associated with severity or functional outcome. Cerebrovasc Dis 2010; 29: 484-9. doi: 10.1159/000297964

[18] Khandelwal P, Martínez-Pías E, Bach I, et al. Severe epistaxis after tissue plasminogen activator administration for acute ischemic stroke in SARS-COV-2 infection. Brain Circ 2021; 7: 135. doi: 10.4103/bc.bc_17_21

MARMARA
MEDICAL JOURNAL

Original Article

https://dergipark.org.tr/tr/pub/marumj

Developing a wearable device for upper extremity tremors

Sercan Dogukan YILDIZ[1], Gazi AKGUN[2], Dilek GUNAL[3], Erkan KAPLANOGLU[4], M. Caner AKUNER[2], Umit S. SEHIRLI[5]

[1] Department of Anatomy, Faculty of Dentistry, Istanbul Kent University, Beyoğlu, Istanbul, Turkey
[2] Control and Automation Systems Division, Department of Mecatronics Engineering, Faculty of Technology, Marmara University, Maltepe, Istanbul, Turkey
[3] Department of Neurology, School of Medicine, Marmara University, Pendik, Istanbul, Turkey
[4] Department of Computer Science and Engineering, University of Tennessee, Chattanooga, USA
[5] Department of Anatomy, School of Medicine, Marmara University, Maltepe, Istanbul, Turkey

Corresponding Author: Sercan Doğukan YILDIZ
E-mail: sercandogukanyildiz@gmail.com

Submitted: 23.11.2023 **Accepted:** 26.12.2023

ABSTRACT

Objective: This project aims to develop a wearable device to suppress both the essential and resting tremor and investigate its effectiveness.

Materials and Methods: This study details the development and assessment of a wearable device for upper extremity tremors. The wearable device underwent a comprehensive design and a prototype was produced with a 3D-printer. To refine the functionality of the prototype, a motor that mimics tremor was attached to a 3D-printed prototype. Then, the printed prototype was applied to the hand model, and tested its effectiveness for tremor suppressing. The wearable device was further investigated on patients with essential tremor and Parkinson`s disease seeking treatment at Neurology Clinics. We recorded the tremor data and processed and visualized the recorded data by using the MatLab (version R2021a, MathWorks Inc., USA) software.

Results: The wearable device effectively decreased the tremors both during the simulation phase and the patient testing phase. The data from the wearable device revealed a notable decrease in the amplitude of the tremor. This decrease signifies an achievement of tremor suppression.

Conclusion: The prototype of the wearable device signifies a remarkable efficacy in tremor supression. It holds promise for being a potential solution to alleviate the tremor symptoms of essential tremor and Parkinson`s disease patients.

Keywords: Wearable device, Essential Tremor, Parkinson`s Disease

1. INTRODUCTION

Tremors, most commonly seen among adults, are characterized by involuntary rhytmic and oscillatory movements of the body parts [1,2]. It commonly contracts agonist and antogonist muscles repeatedly. Tremors are predominantly central types, encompassing cortico-lenticular-thalamic-cortical and cortico-cerebellar pathways.

Essential tremor (ET) is a chronic and progressive disorder and its primary clinical feature is kinetic tremor with the frequency ranging between 4-10 Hertz (Hz) [3,4]. According to the International Parkinson and Movement Disorder Society, ET is defined as a bilateral upper extremity action tremor, which is potentially accompanied by such as head tremor, voice tremor, or lower extremity tremors without co-occuring dystonia, ataxia, or Parkinson's disease (PD) symptoms and persists for at least 3 years [5, 6].

The term of ET was first used by Pietro Burresi in 1874 [7]. In a global context, ET is a movement disorder associated with physical and psychological disabilities with a prevalence of 0.4% to 3.9% in the general population [8]. Notably, in the United States of America (USA), seven million patients are estimated to suffer from ET, representing approximately 2.2% of the population [9].

Although, ET is generally considered to be bening, it negatively impacts the overall quality of patients' lives [10, 11]. Patients with tremors generally feel social embarrasment and avoid drinking, eating or writing in public [12, 13].

How to cite this article: Yildiz D S, Akgun G, Gunal D, Kaplanoglu E, Akuner CM, Sehirli SU. Developing a wearable device for upper extremity tremors. Marmara Med J 2024: 37(2):157-165. doi: 10.5472/marumj.1483038

ISSN: 1309-9469

http://doi.org/10.5472/marumj.1483038
Marmara Med J 2024;37(2): 157-165

Parkinson's disease is the second most prevalent neurodegenerative disorder after Alzheimer's disease. Its prevalence increases with age, affecting around 1% of individuals aged 65 and above and approximately 4% of individuals over 80 years old [14]. PD is a chronic neurodegenerative disorder characterized by the degeneration of dopaminergic neurons in the substantia nigra pars compacta. This progressive disease results in motor and cognitive impairments, with bradykinesia, resting tremor, rigidity, and postural instability being its key clinical features. The tremor observed in PD is termed as resting tremor and typically presents itself asymmetrically. Pronation and supination movements are affected more common than flexion and extension movements [2].

Approximately 80% of ET disease cases are attributed to the familial ET (FET) gene, which is identified on chromosome 3q13 [15]. Another gene associated with ET is the ET maps (ETM) gene, and it is located on chromosome 2p22-p25 [16]. Chromosome 6p23 was reported to be associated with ET [17]. Mutations in fused in sarcoma (FUS), an RNA-binding protein, have been detected in ET patients, and similar pathogenic mutations have also been observed in patients with fronto-temporal dementia (FTD) and amyotrophic lateral sclerosis (ALS) [18]. The leucine-rich repeat and Ig domain containing 1 (LINGO1) gene has also been implicated in the pathophysiology of ET [19]. The condition of neurotransmitter deficiency has not been identified in ET patients. Despite these genetic insights, the precise mechanism behind tremor manifestation and the source and mechanism of pathological oscillations remain elusive.

In the treatment of ET, medications developed for other disorders are heavily relied on as there is no curative treatment for ET [20]. However, the existing medications have proven effective in symptomatic management of ET [18]. In cases where medical intervention fails or side effects become intolerable, surgical intervention such as neuromodulations, deep brain stimulation (DBS) and radiofrequency thalamotomy, gamma-knife radiothalamotomy, magnetic resonance-guided focused ultrasound (MRgFUS) may be considered [21]. It is worth noting that unilateral MRgFUS thalamotomy can result in side effects such as paresthesia and balance disturbances while bilateral thalamotomy may lead to cognitive impairments, postural disturbances, balance issues, and speech impairments [22].

Wearable devices designed to address tremors can be broadly categorized into two main groups: active and passive. Passive devices offer resistance to tremors without incorporating moving parts. Active devices, on the other hand, can detect tremors in real-time and respond based on the body's feedback. Active devices use actuators to counteract tremors and employ mechanisms like pneumatic systems, electric motors, and hydraulic systems to dampen tremors effectively [23]. This project aims to develop an active and passive force-controlled wearable device to suppress tremor in both ET and PD and to investigate the effectiveness of the wearable device.

2. MATERIALS and METHODS

A force-controlled wearable device to address upper extremity tremors was designed at Marmara University School of Medicine and Mecatronics Engineering. The design phase was executed using SolidWorks software (version 2020 SP2.0, Dassault Systèmes Inc., USA). The physical realization of the device was executed through 3D printing technology. Specifically, we employed Ender 5 Plus 3D printer and chose PLA filament as the construction material.

The device's key feature is its full mobility, eliminating the need to attach it to a table or chair, and its capacity to be affixed on the upper extremity. The device is powered by a unit with rechargeable batteries located on the upper extremity, and its design does not impede patients' daily activities. It does not restrict the flexion, extension, ulnar and radial deviation (abduction and adduction) of the hand. Patients can also comfortably perform fine motor movements such as flexion, extension, abduction, and adduction of their fingers and hand. It allows for a full range of hand movements, enabling tasks such as writing, buttoning, holding a cup, and using utensils like forks, spoons, and knives with ease.

To mimic tremor phenomena in a controlled laboratory environment, a 3D-printed hand model was crafted. In the anatomical alignment, we affixed two motors, each of which was equipped with an unbalanced load, to the hand model. One motor was placed on lateral side of the first metacarpophalangeal joint. The other motor was affixed between the third and fourth metacarpophalangeal joints. These motors were engineered to generate tremors in three orthogonal axes, encompassing flexion-extention (X – axis), abduction-adduction (Y-axis) and supination-pronation (Z-axis). The orchestration of motor functions were facilitated through an ardinuo interface, which was controlled by MatLab (version R2021a, MathWorks Inc., USA) software. This precision allowed us to produce artificial tremors. We employed a strategically positioned accelerometer, which was located on proximal of palmar surface of the hand (Figure 1), upon activation of motors, the accelerometer recorded the movement patterns for one minute. This experimental setup enabled us to accurately capture and analyze tremor data.

For testing our prototype of the wearable device on computer, a hand was designed by SolidWorks software (version 2020 SP2.0, Dassault Systèmes Inc., USA) and then simulated hand which had a real hand`s features was transferred to the MatLab (version R2021a, MathWorks Inc., USA) software.

Our prototype of the wearable device was securely affixed to the simulated hand and a 5 Hz tremor was generated. In the subsequent step, the prototype was turned on, and data were recorded both before and after its activation. The wearable device was assembled by integrating electronic and mechanical components, and it was affixed to the hand model to perform artificial tremors. Data were obtained from the tremor model when the wearable device was both activated and de-activated.

In this study, the wearable device was applied to patients diagnosed with ET and PD. The patients were selected from individuals seeking treatment at Marmara University School

http://doi.org/10.5472/marumj.1483038
Marmara Med J 2024;37(2): 157-165

of Medicine Department of Neurology. Four ET patients (three females and one male) and four PD patients (two females and two males) were included. All of these four patients had been suffering from their diseases for at least 5 years. None of them had undergone DBS before. The mean age of the patients was 64.4 ± 4.98 years.

All patients were right-handed, and we collected the data through the right-hand trials. All the patients were informed about the clinical study. We kindly asked the patients to flex their arms (keeping them paralel to the ground), extend their forearms, and pronate their hands for minimum 30 seconds. Movements of the hands were recorded by an accelerometer affixed to the wearable device, both when activated and deactiviated. Data were logged at a rate of four times per second and subsequently processed and visualized using MatLab (version R2021a, MathWorks Inc., USA) software.

Statistical Analysis

For statistical analysis SAS (SAS Institute Inc., USA) software was used. Analyses were presented using means.

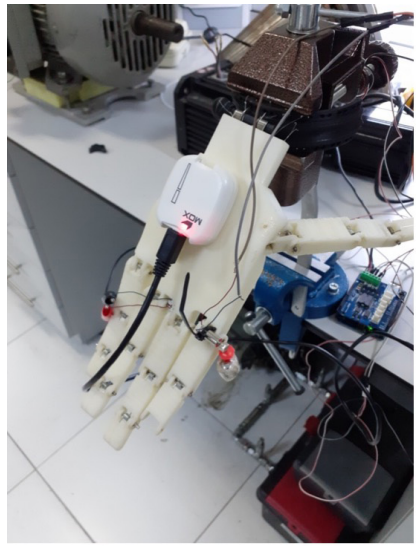

Figure 1. *Tremor in laboratory and measurement by an accelerometer.*

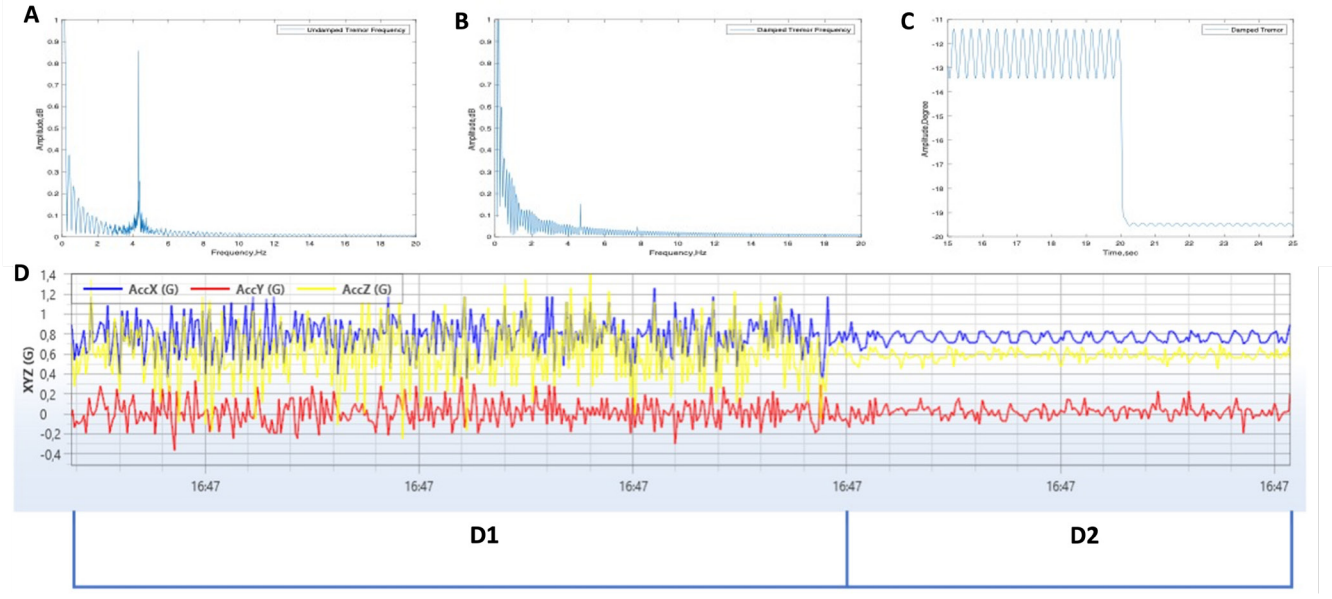

Figure 2 A: *Frequency of tremor which is generated on computer. B: Damped tremor (the wearable device is on). C: Amplitude of damped tremor. D: Generated tremor by using motors that contain unbalanced load, D1: the wearable device is off, D2: the wearable device is on.*

http://doi.org/10.5472/marumj.1483038
Marmara Med J 2024;37(2): 157-165

3. RESULTS

Accelerometric data analysis showed that the frequency of computer-generated tremors were approximately 5 Hz. When the wearable device was turned on in the simulation, a discernible suppression effect was observed. The amplitude of tremor decreased while the frequency of tremor remained unchanged (Figures 2A, 2B, 2C).

We affixed the wearable device on 3D-printed hand model. Subsequently, the motors equipped with unbalanced loads were activated to induce tremors. The frequency and amplitude of tremors were recorded by an accelerometer, which was attached to the wearable device (Figure 2D).

The wearable device was administered to a total of eight patients, comprising four ET patients and four PD patients.

ET patients

In the case of ET patient 1, ET patient 2, ET patient 3, the wearable device was activated on two separate occasions, in the case of ET patient 4 the wearable device was activated on three separate occasions. During each active phase, it effectively suppressed the tremor (Figure 3). During the experimental investigation of effiency, the patients maintained the specified hand position as described above.

Supression rate calculations of ET patients

Following two device activations, suppression rates were computed for each phase within the range of 4-6 Hz. Suppression rates were calculated for each axis, with mean suppressions ranging between 4-6 Hz (Table I).

PD patients

The experiment was conducted with four PD patients. The force-controlled wearable device was activated twice for all patients. Throughout the efficiency investigation experiment, all four patients maintained their hand position as described in the methods section.

For the PD patient 1, PD patient 2, PD patient 3 and PD patient 4 the wearable device effectively suppressed tremors in both active phases (Figure 4).

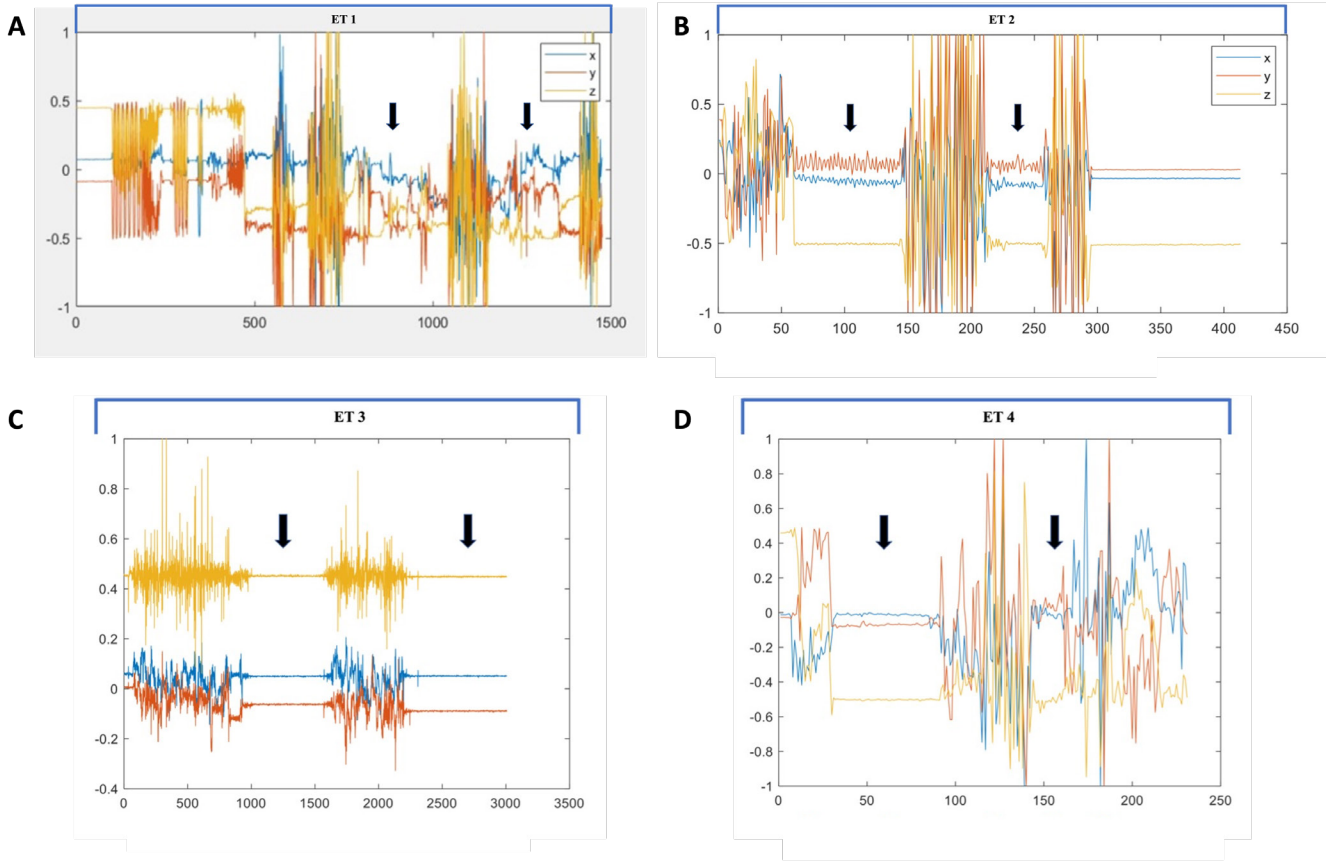

Figure 3 A: *Graphic for first ET patient, ET1: ET patient 1. B: Graphic for second ET patient, ET2: ET patient 2. C: Graphic for third ET patient, ET3: ET patient 3. D: Graphic for fourth ET patient, ET4: ET patient 4. Arrows: phases of wearable device were turned on.*

http://doi.org/10.5472/marumj.1483038
Marmara Med J 2024;37(2): 157-165

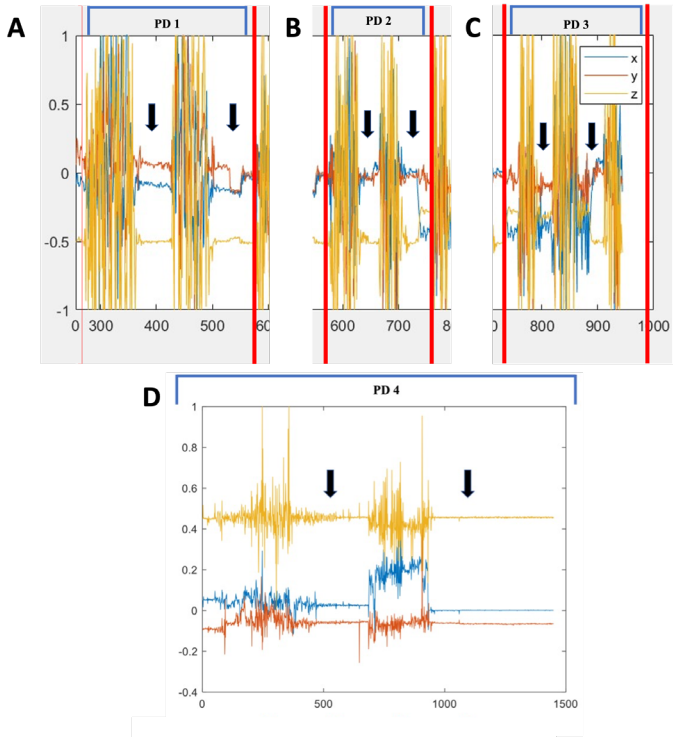

Figure 4 A: *Graphic for PD patient 1, PD 1: PD patient 1. B: Graphic for PD patient 2, PD 2: PD patient 2. C: Graphic for PD patient 3, PD 3: PD patient 3. D: Graphic for PD patient 4, PD 4: PD patient 4. Arrows: phases of wearable device were turned on.*

Table I. *Data of ET patients. Means of suppression rates of X, Y and Z axes and means of suppression rates of the phases*

	Mean suppression rate (%) X axis	Mean suppression rate (%) Y axis	Mean suppression rate (%) Z axis	Mean suppression rate (%) of X, Y and Z	Mean suppression rate (%) of phases
ET Patient 1 Phase 1	99.0818	84.2615	81.5181	88.2871	89.9182
ET Patient 1 Phase 2	89.2636	90.5513	94.8326	91.5492	
ET Patient 2 Phase 1	88.6713	86.1441	97.8149	90.8768	88.2673
ET Patient 2 Phase 2	77.7305	93.2357	86.0073	85.6578	
ET Patient 3 Phase 1	88.7549	87.6694	97.1523	91.1922	89.6474
ET Patient 3 Phase 2	81.5548	90.9011	91.8516	88.1025	
ET Patient 4 Phase 1	79.7907	56.2578	97.1351	77.7279	73.8278
ET Patient 4 Phase 2	96.713	93.6223	93.8368	94.724	
ET Patient 4 Phase 3	57.2295	69.3926	20.4729	49.0316	

http://doi.org/10.5472/marumj.1483038
Marmara Med J 2024;37(2): 157-165

Suppression rate calculations of PD patients

Suppression rates were individually calculated for each axis, focusing on the 4-6 Hz range for all four patients (Table II).

Table II. *Data of PD patients. Means of suppression rates of X, Y and Z axes and means of suppression rates of the phases.*

	Mean suppression rate (%) X axis	Mean suppression rate (%) Y axis	Mean suppression rate (%) Z axis	Mean suppression rate (%) of X, Y and Z	Mean suppression rate (%) of phases
PD patient 1 Phase 1	80.9480	68.1980	63.3810	70.8420	77.2840
PD patient 1 Phase 2	63.8290	94.6480	92.6990	83.7250	
PD patient 2 Phase 1	90.4640	65.4750	75.5420	77.1600	76.5240
PD patient 2 Phase 2	65.0940	89.3210	73.0480	75.8880	
PD patient 3 Phase 1	67.9560	77.7160	88.6520	78.1080	79.4360
PD patient 3 Phase 2	70.6670	87.7790	83.8460	80.7640	
PD patient 4 Phase 1	84.3940	52.7754	78.2841	71.8178	83.4433
PD patient 4 Phase 2	96.895	92.4836	95.8277	95.0688	

4. DISCUSSION

Essential tremor reportedly affects 0.9% of the world population, amounting to at least seventy-two million individuals [24]. However, this number may actually be higher because there may be un-reported individuals who have limited access to medical treatment or may not deem treatment as neccessary. PD, on the other hand, has an impact over six million [25]. According to the United Nations in 2022, the global population reached eight billions, and the aging population is on the rise, with an estimated one billion people aged over sixty-five by 2030 [26]. Age is one of the main factors in the development of tremors [27]. A retrospective study spanning forty-five years found that the incidence of ET increased with age, with rates of 58.6 per 100.000 for those aged 50-59, 76.6 per 100.000 for those aged 70-70, and 84.3 per 100.000 for those aged over 80 [28].

The wearable device demonstrated successful results in both computer simulation and laboratory tests. Clinical study results further confirmed its efficiency. This study included both ET and PD patients due to the observed link between ET and PD conditions. A previous study conducted with 247 ET patients reported that 11 of 247 participants had mild PD symptoms [29]. Another study conducted with 678 ET patients reported that approximately 6.1% were also diagnosed with the PD disease [30]. Additionally, 24 participants of 130 ET patients had PD clinical criteria [31]. It was reported that childhood ET may evolve to severe PD in adult life [32].

The studies reporting the prevalence of ET widely focused on the impact of gender. Numerous studies demonstrated no significant difference based on gender, yet gender based differences were observed in some studies [24]. A study conducted in the province of Edirne, Turkey, showed higher prevalence of ET among women [33]. On the contrary, another study conducted in Şile district of Istanbul, Turkey, reported a higher prevalence of ET among men [34]. However, no statistically significant difference was reported in both of these studies.

The patients in our study were randomly selected, and all were over 50 years old right-handed female and male individuals. While, ET is typically asymmetric, we were unable to employ electomyographic measurement to determine dominant side of tremor [35]. However, patients in our study stated that the tremor afflicts their lives when the tremor is experienced on the hand used more frequently in their daily activities. It underscores the importance of addressing tremor in the hand dominantly used by patients, not just any hand.

http://doi.org/10.5472/marumj.1483038
Marmara Med J 2024;37(2): 157-165

The wearable device was constructed using PLA filament due to its compatibility with 3D printers and several advantageous properties, such as high load-bearing capacity, impact resistance, low odor during printing, high printing speed, and recyclability. The device's weight is crucial both for daily use and tremor suppression. Research involving 50 patients has demonstrated that the addition of weights ranging from 480 g to 600 g reduced action tremor in a significant percentage (58%) of participants. It also contributed to improved performance in daily household and workplace in the 36% of those participants [36]. Applying weights ranging from 600 g to 2160 g to the wrist also reduced the magnitude of tremor in individuals with ET [37]. The wearable device in this study weighed 491 g, located on the dorsum of the hand and contribute to hand stabilization.

While many wearable device prototypes exist in the literature, majority of these active wearable prototypes have not advanced to clinical trials due to the concerns related to ergonomics, weight, size, and aesthetics for patient use [38]. The studies with these wearable devices conducted laboratory tests based on the data obtained from previous laboratory studies rather than implementing clinical trials. These laboratory trials demonstrated over 90% tremor supression rate [39, 40].

The studies involving a prototype testing with clinical trials demonstrated tremor suppression. One study involving with a PD patient achieved an 85% tremor suppression using weight and spring systems for energy transfer in passive devices [41]. In 2020, a study conducted with one PD patient reported a prototype reduced tremor by 74% to 82% [42]. Another study using a pneumatic actuator in a single ET patient reduced tremor magnitude by 70% [43]. In a pilot study using non-invasive handheld active tremor-reducing device, an average tremor supression of 73% was reported [44]. Another pilot study involving 10 PD patients showed no significant benefit from a gyroscope-spoon system for resting tremor [45].

In our study, the wearable device achieved an average tremor supression rate of 86.3792% for ET patients and 77.748% for PD patients. This result indicates a high level of patient satisfaction. Notably, the prototype has been developed, the mentioned active and passive power-controlled wearable device falls into both the active and passive device categories. Its inclusion in the passive device group is due to the fact that the device's own weight creates a damping effect on the tremor. The reason for its inclusion in the active device group is that it generates counteracting forces based on the magnitude and frequency of the tremor.

Conclusion

In summary, our comprehensive study encompassed simulation, laboratory testing, and clinical research. The wearable device not only demonstrated efficacy in simulation and laboratory settings but also achieved a high success rate in tremor supression among patients during clinical trials. A patent application has already been filed for the first prototype, with plans to extend patent protection to subsequent prototypes. The efficacy of this wearable device is promising for diminishing the impacts of upper extremity tremors of ET and PD patients.

Acknowledgement

This study was written based on the doctoral dissertation study conducted and written by Sercan Dogukan Yildiz, under the supervision of Prof. Dr. Umit S. Sehirli, and Prof. Dr. M. Caner Akuner.

Compliance with the Ethical Standards

Ethical approval: The study protocol was approved by the Institutional Review Board and the Ethics Committee of Marmara University School of Medicine (Protocol number: 09.2020.420).

Conflict of interest: The authors have no conflicts of interest to declare.

Funding sources: This study was financially supported by a grant of Marmara University (project number 10448 and project code TDK-2022-10448)

Authors' contributions: SDY, USS: Designed the study, SDY and GA: Performed the laboratory work and analysed the data, SDY and DG: Obtained data from patients and analysed the data, SDY, GA, MCA and EK: Designed the active and passive force controlled wearable device. SDY, GA: performed the statistical analysis. SDY, GA and USS: wrote the manuscript. All authors approved the final manuscript.

REFERENCES

[1] Lenka A, Jankovic J. Tremor syndromes: An updated review. Front Neurol 2021; 12: 684835. doi: 10.3389/fneur.2021.684835

[2] Louis ED. Diagnosis and management of tremor. Continuum 2016; 22: 1143-58. doi: 10.1212/CON.000.000.0000000346

[3] Louis ED. Essential tremor: a nuanced approach to the clinical features. Pract Neurol 2019; 19: 389-98. doi: 10.1136/practneurol-2018-002183

[4] Chen JJ, Swope DM. Essential tremor: diagnosis and treatment. Pharmacotherapy 2003; 23: 1105-22. doi: 10.1592/phco.23.10.1105.32750

[5] Bhatia KP, Bain P, Bajaj N, et al. Consensus Statement on the classification of tremors. from the task force on tremor of the International Parkinson and Movement Disorder Society. Mov Disord 2018; 33: 75-87. doi: 10.1002/mds.27121

[6] Saifee TA. Tremor. Br Med Bull 2019; 130: 51-63. doi: 10.1093/bmb/ldz017

[7] Louis ED, Broussolle E, Goetz CG, Krack P, Kaufmann P, Mazzoni P. Historical underpinnings of the term essential tremor in the late 19th century. Neurology 2008; 71: 856-9. doi: 10.1212/01.wnl.000.032.5564.38165.d1

[8] Zesiewicz TA, Kuo SH. Essential tremor. BMJ Clin Evid 2015; 12: 1206-1247.

[9] Louis ED, Ottman R. How many people in the USA have essential tremor? Deriving a population estimate based on epidemiological data. Tremor Other Hyperkinet Mov (N Y) 2014; 4: 259-9. doi: 10.7916/D8TT4P4B

[10] Lorenz D, Schwieger D, Moises H, Deuschl G. Quality of life and personality in essential tremor patients. Mov Disord 2006; 21: 1114-8. doi: 10.1002/mds.20884

[11] Louis ED. Etiology of essential tremor: Should we be searching for environmental causes? Mov Disord 2001; 16: 822-9. doi: 10.1002/mds.1183

[12] George MS, Lydiard RB. Social phobia secondary to physical disability. A review of benign essential tremor (BET) and stuttering. Psychosomatics 1994; 35: 520-3. doi: 10.1016/s0033-3182(94)71720-5

[13] Traub RE, Gerbin M, Mullaney MM, Louis ED. Development of an essential tremor embarrassment assessment. Parkinsonism Relat Disord 2010; 16: 661-665. doi: 10.1016/j.parkreldis.2010.08.017

[14] Lonneke ML, Breteler MM. Epidemiology of Parkinson's disease. Lancet Neurol 2006; 5: 525-35. doi: 10.1016/S1474-4422(06)70471-9

[15] Gulcher JR, Jónsson P, Kong A, et al. Mapping of a familial essential tremor gene to chromosome 3q13. Nat Genet 1998; 6: 150-1. doi: 10.1038/ng0997-84

[16] Higgins JJ, Pho LT, Nee LE. A gene (ETM) for essential tremor maps to chromosome 2p22-p25. Mov Disord 1997; 12: 859-64. doi: 10.1002/mds.870120605

[17] Shatunov A, Sambuughin N, Jankovic J, et al. Genomewide scans in North American families reveal genetic linkage of essential tremor to a region on chromosome 6p23. Brain 2006; 129: 2318-31. doi: 10.1093/brain/awl120

[18] Rajput AH, Rajput A. Medical treatment of essential tremor. J Cent Nerv Syst Dis 2014; 6: 29-39. doi: 10.4137/JCNSD.S13570

[19] Stefansson H, Steinberg S, Petursson H, et al. Variant in the sequence of the LINGO1 gene confers risk of essential tremor. Nat Genet 2009; 41: 277-9. doi: 10.1038/ng.299

[20] Deuschl G, Raethjen J, Hellriegel H, Rodger E. Treatment of patients with essential tremor. Lancet Neurol 2011; 10: 148-61. doi: 10.1016/S1474-4422(10)70322-7

[21] Sharma S, Pandey S. Treatment of essential tremor: current status. Postgrad Med J 2020; 96: 84-93. doi: 10.1136/postgradmedj-2019-136647

[22] Mohammed N, Patra D, Nanda A. A meta-analysis of outcomes and complications of magnetic resonance-guided focused ultrasound in the treatment of essential tremor. Neurosurg Focus 2018; 44: E4. doi: 10.3171/2017.11.FOCUS17628

[23] Fromme NP, Camenzind M, Riener R, Rossi MR. Need for mechanically and ergonomically enhanced tremor-suppression orthoses for the upper limb: a systematic review. J Neuroeng Rehabil 2019; 16: 93. doi: https://doi.org/10.1186/s12984.019.0543-7

[24] Louis ED, Ferreira JJ. How common is the most common adult movement disorder? Update on the worldwide prevalence of essential tremor. Mov Disord 2010; 25: 534-41. doi: 10.1002/mds.22838

[25] Verhoeff MC, Koutris M, Vries R, Berendse HW, Dijk KD, Lobbezoo F. Salivation in Parkinson's disease: A scoping review. Gerodontology 2023; 40: 26-38. doi: 10.1111/ger.12628

[26] Chen LK. Urbanization and population aging: Converging trends of demographic transitions in modern world. Arch Gerontol Geriatr 2022; 101: 104709. doi: 10.1016/j.archger.2022.104709

[27] Louis ED, Ottman R, Hauser W A. How common is the most common adult movement disorder? Estimates of the prevalence of essential tremor throughout the world. Mov Disord 1998; 13: 5-10. doi: 10.1002/mds.870130105

[28] Rajput AH, Offord KP, Beard CM, Kurland LT. Essential tremor in Rochester, Minnesota: a 45-year study. J Neurol Neurosurg Psychiatry 1984; 47: 466-70. doi: 10.1136/jnnp.47.5.466

[29] Cleeves L, Findley LJ, Koller W. Lack of association between essential tremor and Parkinson's disease. Ann Neurol 1988; 24: 23-26. doi: 10.1002/ana.410240106

[30] Koller WC, Busenbark K, Miner K. The relationship of essential tremor to other movement disorders: report on 678 patients. Ann Neurol 1994; 35: 717-23. doi: https://doi.org/10.1002/ana.410350613

[31] Geraghty JJ, Jankovic J, Zetusky WJ. Association between Essential Tremor and Parkinsons-Disease. Ann Neurol 1985; 17: 329-33. doi: 10.1002/ana.410170404

[32] Shahed J, Jankovic J. Exploring the relationship between essential tremor and Parkinson's disease. Parkinsonism Relat Disord 2007; 13: 67-76. doi: 10.1016/j.parkreldis.2006.05.033

[33] Guler S, Caylan A, Turan FN, Dağdeviren N. The prevalence of essential tremor in Edirne and its counties accompanied comorbid conditions. Neurological Research 2019; 41: 847-56. doi: https://doi.org/10.1080/01616.412.2019.1628409

[34] Sur H, İlhan S, Erdoğan H, Öztürk E, Taşdemir M, Börü TU. Prevalence of essential tremor: a door-to-door survey in Sile, Istanbul, Turkey. Parkinsonism Relat Disord 2009; 15: 101-4. doi: 10.1016/j.parkreldis.2008.03.009

[35] Louis ED, Wendt KJ, Pullman SL. Is essential tremor symmetric? Observational data from a community-based study of essential tremor. Arch Neurol 1998; 55: 1553-9. doi: 10.1001/archneur.55.12.1553

[36] Hewer RL, Cooper R, Morgan MH. An investigation into the value of treating intention tremor by weighting the affected limb. Brain 1972; 95: 579-90. doi: 10.1093/brain/95.3.579

[37] Heroux ME, Pari G, Norman KE. The effect of inertial loading on wrist postural tremor in essential tremor. Clin Neurophysiol 2009; 120: 1020-9. doi: 10.1016/j.clinph.2009.03.012

[38] Bhidayasiri R, Maytharakcheep S, Phumphid S, Maetzler W. Improving functional disability in patients with tremor: A clinical perspective of the efficacies, considerations, and challenges of assistive technology. J Neurol Sci 2022; 435: 120197. doi: 10.1016/j.jns.2022.120197

[39] Herrnstadt G, Menon C. Voluntary-driven elbow orthosis with speed-controlled tremor suppression. Front Bioeng and Biotechnol 2016; 4: 29. doi: https://doi.org/10.3389/fbioe.2016.00029

[40] Taheri B, Case D, Richer E. Adaptive suppression of severe pathological tremor by Torque Estimation Method. Ieee-Asme

Transactions on Mechatronics 2015; 20: 717-27. doi: 10.1109/TMECH.2014.231.7948

[41] Rudraraju S, Nguyen T. Wearable tremor reduction device (TRD) for human hands and arms. Design of Medical Devices Conference 2018; doi: 10.1115/DMD2018-6918

[42] Fromme NP, Camenzind M, Riener R, Rossi MR. Design of a lightweight passive orthosis for tremor suppression. Journal of NeuroEngineering and Rehabilitation 2020; 17: 47. doi: https://doi.org/10.1186/s12984.020.00673-7

[43] Skaramagkas V, Andrikopoulos G, Manesis S. An Experimental Investigation of Essential Hand Tremor Suppression via a Soft Exoskeletal Glove. European Control Conference 2020; 1: 889-94. doi: 10.23919/ECC51009.2020.914.3932

[44] Pathak A, Redmond AJ, Allen M, Chou KL. A noninvasive handheld assistive device to accommodate essential tremor: a pilot study. Mov Disord 2014; 29: 838-42. doi: 10.1002/mds.25796

[45] Ryden LE, Matar E, Szeto JYY, Hammond DA, Clouston P, Lewis SJG. Shaken not Stirred: A pilot study testing a gyroscopic spoon stabilization device in Parkinson's disease and tremor. Ann Indian Acad Neurol 2020; 23: 409-11. doi: 10.4103/aian.AIAN_251_19

MARMARA
MEDICAL JOURNAL

Original Article

https://dergipark.org.tr/tr/pub/marumj

Effect of methylglyoxal on Parkinson's disease pathophysiology in the rotenone model

Yekta CULPAN[1], Lara OZDEN[2], Yakup GOZDERESI[2], Beril KOCAK[2], Zeynep Hazal BALTACI[2], Ayberk DENIZLI[2], Betul KARADEMIR YILMAZ[3], Rezzan GULHAN[1]

[1] Department of Medical Pharmacology, School of Medicine, Marmara University, Istanbul, Turkey
[2] School of Medicine, Marmara University, Istanbul, Turkey
[3] Department of Medical Biochemistry, School of Medicine, Marmara University, Istanbul, Turkey

Corresponding Author: Yekta CULPAN
E-mail: yculpan@yahoo.com.tr

Submitted: 22.12.2023 **Accepted:** 05.01.2024

ABSTRACT

Objective: Type 2 diabetes mellitus patients have been reported to have a higher incidence of Parkinson's disease. This study aimed to explore the effect of advanced glycation end products precursor methylglyoxal (MGO) on the pathophysiology of Parkinson's disease in a rotenone model.

Materials and Methods: Adult female Wistar rats (n=42) were divided into four groups. Rotenone toxicity was assessed by daily weight measurements and mortality rates. Effect of MGO on blood glucose was evaluated. Locomotor activity, rearing, and rotarod tests were performed to evaluate motor functions, and for neurodegeneration, tyrosine hydroxylase immunoreactivity in the striatum and substantia nigra regions was assessed.

Results: The mortality rate was 9% in the rotenone-applied rats. The mean weight, locomotor activity, rearing activity, and longest time spent on a rotarod were lower in the MGO+Rotenone group than in the Control group. Tyrosine hydroxylase immunoreactivity in the striatum rostral to the anterior commissure in the MGO+Rotenone group was lower than that in the Control and MGO groups. The number of tyrosine hydroxylase positive cells in the substantia nigra pars compacta was comparable among the groups.

Conclusion: When nigrostriatal degeneration was triggered, MGO was found to worsen motor dysfunction and increase damage to dopaminergic neuron projections.

Keywords: Parkinson's disease, Type 2 diabetes mellitus, Methylglyoxal, Rotenone, Tyrosine hydroxylase, Locomotor activity

1. INTRODUCTION

Parkinson's disease (PD) is the second most common neurodegenerative disorder after Alzheimer's disease. The prevalence of PD is reported to be 1-2‰ in the general population and >1% in the population over 65 years of age [1, 2]. As the incidence of the disease increases with age, PD is becoming an even more important health problem in our aging world.

Parkinson's disease is characterized by the loss of dopaminergic neurons, particularly in the substantia nigra pars compacta (SNpc). Loss of dopaminergic neurons causes a marked reduction in dopamine in the nigrostriatal dopaminergic terminals from the SNpc to the striatum and is the main cause of the classical motor symptoms of PD, such as bradykinesia, tremor, postural instability, and rigidity [3].

Although, the molecular mechanisms have not been fully elucidated, the pathogenesis of PD is generally thought to be associated with oxidative stress, mitochondrial disorders, endoplasmic reticulum stress (ERS), genetic factors, excitotoxicity, impaired vesicular transport, protein processing disorders, and loss of synapses in dopaminergic neurons [4, 5]. Misfolding, aggregation, and toxicity of the alpha-synuclein protein encoded by the alpha-synuclein gene (SNCA) is one of the most important points in the pathophysiology of PD [6]. Precipitated alpha-synucleins contribute to the increase in misfolded proteins, ERS, and thus to the development of PD by disrupting protein homeostasis [7].

Among the risk factors for PD are advanced age, genetic factors, exposure to pesticides and heavy metals, traumatic brain injury, excessive consumption of dairy products, and type 2 diabetes mellitus (T2DM) [8, 9].

The association between PD and T2DM has started to receive attention as a result of the high incidence of PD in T2DM patients

How to cite this article: Culpan Y, Ozden L, Gozderesi Y, et al. Effect of methylglyoxal on Parkinson's disease pathophysiology in the rotenone model. Marmara Med J 2024: 37(2):166-177. doi: 10.5472/marumj.1480086

ISSN: 1309-9469

http://doi.org/10.5472/marumj.1480086
Marmara Med J 2024;37(2): 166-177

in recent studies [10]. In the meantime, studies have shown that PD treatment is less effective and that PD progression is more severe in patients with T2DM [11].

Type 2 diabetes mellitus is characterized by progressive loss of insulin secretion from pancreatic beta cells, relative insulin deficiency, and hyperglycemia in the background of insulin resistance [12]. Recent studies indicate that β-cell dysfunction and insulin resistance, which are the two most important parameters of T2DM, may be caused by oxidative stress [13]. The association of T2DM with oxidative stress is partly related to the overproduction of reactive oxygen species (ROS). Advanced glycation end products (AGEs) have drawn attention among the sources of ROS identified in diabetic conditions. AGEs are harmful compounds that occur more often, especially under hyperglycemic conditions, and are thought to be involved in the pathology of T2DM and the development of complications [14]. Methylglyoxal (MGO) is a highly reactive AGE precursor that occurs during the glycation process and is involved in the pathology of diabetes [15]. The amount of MGO in the serum of T2DM patients was higher than that of healthy individuals [16].

The molecular cause of this remarkable association between T2DM and PD is currently being investigated. MGO may play a role in this relationship. One of the target proteins of MGO is the alpha-synuclein protein involved in PD pathology [17]. Furthermore, MGO is structurally similar to 3,4-dihydroxyphenylacetaldehyde, which has been shown to increase the risk of developing PD [18, 19]. Finally, MGO induces ERS, and ERS is one of the common and early findings in PD [7].

In our study, we aimed to investigate the effect of long-term MGO administration on the pathophysiology of PD in a rotenone model in rats. For this purpose, the effect of MGO both alone and in the presence of a predisposing condition to PD was investigated.

2. MATERIALS and METHODS

Animals

Forty-two adult female Wistar albino rats (2-3 months old, 203-274 g weight) were used in the experiments. Animals were housed two animals per plexiglass cage under a 12-hour light/dark cycle at 22±2°C and had free access to standard rat chow and tap water. All rats were purchased from Istanbul University Aziz Sancar Institute of Experimental Medicine and the experiments were started after a one-week adaptation period.

All experimental procedures were approved by the Marmara University Ethical Committee for Experimental Animals (96.2021mar).

Experimental design

First, the rats were divided into MGO or control (water) administration groups. Then, the groups were further divided into rotenone or its vehicle (2% dimethyl sulfoxide, 98% Miglyol 812 N) subgroups. Consequently, a total of four groups were formed: Control (water+vehicle of rotenone, n=10), MGO (MGO+vehicle of rotenone, n=10), Rotenone (water+rotenone, n=11), and MGO+Rotenone (n=11). MGO and water were administered orally, rotenone and its vehicle were administered subcutaneously.

Rats were treated with MGO (100 mg/kg/day) or water for 8 weeks (55 days, per oral). Before the rotenone administration, two weeks of MGO were administrated to mimic the AGE effect of T2DM. The rotenone (1.5 mg/kg/day) or its vehicle was started at day-16 and applied for 40 days while MGO or water was administrated concurrently. Behavioral experiments were carried out on day 56, the day after the last treatment. Then, all rats were sacrificed on day 56 under diethyl ether (Merck, Darmstadt, Germany, 100921) anesthesia, and their brains were removed for immunohistochemistry (Figure 1).

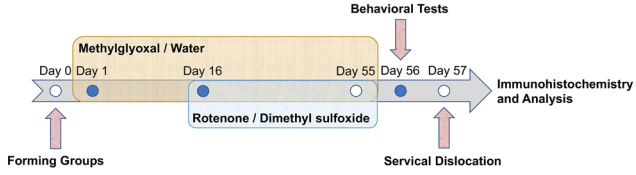

Figure 1. *Timeline of the experimental design. (Blue dots represent days of blood glucose measurement)*

Drugs

Methylglyoxal (Sigma-Aldrich, St. Louis, Missouri, United States of America, M0252) was supplied as a 40% solution in water. To be able to apply 100 mg/kg/day MGO to animals orally, a volume of 213 µL/kg of MGO solution was administered by an automatic pipette (Socorex Acura Manuel, Ecublens, Switzerland, 825). Water (213 µL/kg) administration was similar to MGO administration.

Rotenone (Sigma-Aldrich, St. Louis, Missouri, United States of America, R8875) was prepared daily as a 50x (75 mg/mL) solution in 100% dimethyl sulfoxide (DMSO) (Supelco, St. Louis, Missouri, United States of America, 1.02952). Then, it was diluted with the medium-chain triglyceride Miglyol 812 N (IOI oleochemical, Pulau Pinang, Malaysia) to obtain a rotenone concentration of 1.5 mg/mL (98% Miglyol 812 N, 2% DMSO). The solutions were protected from light. The possibility of precipitation was eliminated by vortexing before each application, and 1.5 mg/kg/day (1 ml/kg) rotenone was administered subcutaneously [20].

A vehicle solution of rotenone was prepared with DMSO and Miglyol 812 N. DMSO was diluted in Miglyol 812 N to a 2% concentration (98% Miglyol 812 N, 2% DMSO). Then, the solution was applied as 1 ml/kg subcutaneously.

Animals were weighed every morning during the experiment, and solutions were applied according to their daily weight. To prevent rotenone-related deaths, the injections were skipped in

http://doi.org/10.5472/marumj.1480086
Marmara Med J 2024;37(2): 166-177

the animals that lost more than 15% of their initial weight until they recovered their weight back.

Behavioral tests and blood glucose measurement

Behavioral experiments were carried out between 9:00 a.m. and 12:00 p.m. The experiments were started after the animals were acclimated to the room for 30 minutes.

Locomotor activity

Locomotor activity test allows a comprehensive study of locomotor and behavioral activity levels in experimental animal models of PD [21]. The test was performed after an acclimation period to the locomotor activity cage. Animals were kept in the room for thirty minutes before the behavioral tests began. The test was performed under moderate illumination and the researcher observed the experiment away from the locomotor activity cage. The rats were placed in a 40x40x40 cm locomotor activity cage (Commat, ACT 508, Ankara, Türkiye), and all movements were recorded for 5 minutes. Before the experiment with the next animal, the locomotor activity cage was cleaned with 70% ethanol (Sigma-Aldrich, St. Louis, Missouri, United States of America, V001229), followed by distilled water, and allowed to dry. Data (distance traveled, % of ambulatory and stereotypical movement time, % of resting time, vertical movement time) were collected with the activity measurement program (Activity metering software, version 2.1, Commat, Ankara, Türkiye) and saved as Microsoft Office Excel (Microsoft Corporation, Redmond, WA, USA) output.

Rearing activity

Rats were placed in a clear plexiglass cylinder (height=30 cm, diameter=20 cm) and recorded for 2 minutes by a video camera. The number of contacts of the forelimbs to the cylinder wall was evaluated [22]. For the behavior to be considered rearing, the animal must raise its forelimb above shoulder level and touch one or both forelimbs against the cylinder wall. Before another rearing, the rat must pull its forelimbs off the cylinder wall and touch the table surface.

Rotarod test

The rotarod test is used to measure motor coordination in mice and rats and to detect motor impairment in experimental PD models[21]. Before the test, the rats were placed on the rod twice daily for three days to allow for acclimatization. The test was performed using a 5 cm diameter rotor (Northel, Bursa, Türkiye). On the experiment day, the rats were placed on the rotating bar, which was accelerating at a constant acceleration, reaching a speed of 40 rotations per minute after 300 seconds. The time spent on the rod was recorded. The test was repeated three times at intervals on the same day. The data were analyzed to determine the average time of the three tests and the longest time spent on the rod.

Blood glucose measurement

Blood glucose was measured between 12:00 – 12:30 p.m. on the 1st, 16th, and 56th days of the experimental protocol (Figure 1). Before the measurement, the tails of the rats were cleaned with 70% ethanol solution and allowed to dry. The lateral vein of the tail was punctured with the help of an insulin injector. The first drop of blood was wiped with cotton, and the second drop of blood was analyzed on a glucometer (Roche, Accu-Chek Performa Nano, Basel, Switzerland) with an appropriate strip (Roche, Accu-Chek Performa, Basel, Switzerland).

Immunohistochemistry

Tissue preparation

The brains were removed after cervical dislocation under diethyl ether anesthesia and placed in a 4% paraformaldehyde (AFG Bioscience, 668011, Illinois, United States of America) solution prepared with 0.1 M phosphate-buffered saline (PBS) (Sigma-Aldrich, St. Louis, Missouri, United States of America, P4417) for immunohistochemistry analyses [23]. The brains were kept in 4% paraformaldehyde solution for 3 days. Then, they were placed into 15% and 30% sucrose (Sigma-Aldrich, St. Louis, Missouri, United States of America, S8501) solutions prepared with 0.1 M PBS, one day apart and were allowed to sink to the bottom in 30% PBS-sucrose solution at 4°C. Then, the brains were treated with methylbutane (Sigma-Aldrich, St. Louis, Missouri, United States of America, 277258), brought to – 30°C with the help of dry ice for 3 minutes, and raised to – 80°C until sectioning. Serial coronal sections (40 µm thick) were taken by a freezing microtome (Microm, Witney, United Kingdom, HM450) from the level of bregma 3.70 mm to the level of bregma – 6.72 mm according to the stereotaxic rat brain atlas [24]. Free floating sections were stored in antifreeze solution (phosphate solution containing 30% glycerol and 30% ethylene glycol) at 4°C.

Immunohistochemical labeling of tyrosine hydroxylase

Sections were rinsed with Tris-buffered saline (TBS) three times, then kept in Tris-EDTA solution at 80°C for 30 minutes and then at room temperature for 20 minutes for possible antigen retrieval treatment. Rinsed sections were kept in a mixture of 3% H_2O_2 and 10% methanol in TBS for 30 min to quench endogenous peroxidase activity and rinsed twice with TBS and once with TBS-Triton X (TBS-T). Nonspecific binding sites were blocked by incubation in TBS-T containing 5% (w/v) normal serum (Vector Laboratories, S2000, RRID: AB_2336617, California, United States of America). Sections were incubated with a tyrosine hydroxylase (TH) antibody (Merck, MAB5280, RRID: AB_2201526, 1:3000, Darmstadt, Germany) containing 1% (w/v) bovine serum albumin/TBS-T for a whole day at room temperature. The next day, the sections were rinsed with TBS-T three times and incubated with biotinylated secondary antibody (Vector Laboratories, BA-2001, RRID: AB_2336180, 1:200, California, United States of America) for 1 hour, rinsed with TBS-T, and incubated in avidin-biotin-peroxidase solution (Vectastain, PK-6100, RRID: AB_2336819, California, United

http://doi.org/10.5472/marumj.1480086
Marmara Med J 2024;37(2): 166-177

States of America) for 1 hour. Finally, the staining was visualized using 2% 3,3′-diaminobenzidine in TBS solution containing 0.01% H_2O_2.

Evaluation of tyrosine hydroxylase immunostaining

All sections were photographed by a microscope (Zeiss Axio Zoom. V16, Zeiss, Germany) connected to a camera system. The striatum region, which contains the dopaminergic fibers, was assessed for TH immunoreactivity positivity (TH+) using densitometric measurement. The evaluation of the SNpc region, where the dopaminergic cell bodies are located, was evaluated by counting TH+ cell bodies. Densitometric measurement and cell count were made using ImageJ software (V1.53, NIH, USA) and evaluated by using Microsoft Office Excel.

Striatum

The striatum is divided into 3 regions according to the rat brain atlas to analyze the immunoreactivity [24]. For ease of explanation, sections taken from the striatum in between AP: 2.28 mm — 0.00 mm from the bregma were labeled as rostral to the anterior commissure (RAC), from AP: 0.00 mm — – 0.48 mm level of the anterior commissure (LAC), and from AP: – 0.48 mm — 1.08 mm caudal to the anterior commissure (CAC). For the striatum region, a total of 7 photographs were evaluated from the RAC, LAC, and CAC regions at x20 magnification. Because the striatum has a patchy appearance, 6 areas with immunoreactivity and 3 areas without immunoreactivity (background regions) were selected in each photograph for immunoreactivity density assessment. To standardize the values, the average immunoreactive region value was subtracted from the average background region value and corrected for each animal by calculating the immunoreactivity of naive animals. Data are given as averages for the RAC, LAC, and CAC measurements.

SNpc

Sections between AP: – 4.80 mm — – 5.40 mm reference to bregma were named SNpc sections. For each brain, 5 photos per section from 3 sections containing the SNpc region were taken at x40 magnification. Cell bodies were marked and counted with the free-marking option using the ImageJ software program. Data are given as the average number of cells contained in each photograph.

Statistical Analysis

All statistical analyses and graphical representations were performed using GraphPad Prism v8 (GraphPad Prism version 8.0.0 for Mac, GraphPad Software, San Diego, California USA, www.graphpad.com) and Microsoft Office Excel. Continuous data are presented as the mean ± standard error. Frequency and percentage (%) were used to represent categorical variables. The experimental groups were compared with one-way ANOVA, and pairwise comparisons were performed using the post hoc Tukey test. Blood glucose measurements on the 1st, 16th, and 56th days were compared using analysis of variance for repeated measurements (repeated-measures ANOVA). The statistical significance level was accepted as $p<0.05$.

3. RESULTS

Administration of solutions and mortality

All animals in the control (n=10) and MGO+Rotenone (n=11) groups survived. One animal out of 10 from the MGO group died on the 51st day of the experiment, while two animals out of 11 from the Rotenone group died on the 31st and 47th days of the experiment. In our study, mortality in animals treated with rotenone was 9% (2/22).

To prevent rotenone-related deaths, the rotenone injections were skipped in the animals that lost more than 15% of their initial weight until they recovered their weight back while MGO/water administration was continued as long as the animal survived. The rotenone group received rotenone for 35±2 days, and the MGO+Rotenone group received rotenone for 30±3 days.

Weight change

The average daily weights of the groups recorded throughout the experiment are shown in Figure 2. The mean weights of the groups on day 0, day 16 (the beginning of rotenone/vehicle application), and day 55 (the last day of the experiment) were compared both within and between groups. There was a significant weight gain in the control group ($p<0.001$). While there was no significant difference between weights at baseline (238±14 g) and on the 16th day (241±14 g) ($p=0.333$), weight on the 55th day (262±5 g) was significantly higher than that on days 0 and 16 ($p<0.001$, both). The mean weight of the MGO group increased on day 55, but there was no significant difference between the weight at baseline (236±7 g), day 16 (241±7 g), and day 55 (247±13 g) ($p=0.322$). The mean weight of the Rotenone group decreased on day 55 of the experiment, but there was no significant difference between the weight at baseline (234±17 g), on day 16 (237±15 g) and day 55 (226±32 g) ($p=0.194$). The mean weight of the MGO+Rotenone group decreased on day 55 of the experiment, but there was no significant difference between the weight at baseline (241±23 g), day 16 (244±19 g) and day 55 (217±42 g) ($p=0.082$).

When the weight was compared between the groups, there was no significant difference between the weight of the groups at baseline and the 16th day ($p=0.737$; $p=0.822$, respectively), while there was a significant difference between the weight on the 55th day ($p=0.022$). In pairwise comparisons, while there was a significant difference between the weight of the control group and the MGO+Rotenone group ($p=0.023$), there was no significant difference between the MGO group and the Rotenone group with each other and with the other groups ($p>0.05$).

Behavioral tests and blood glucose measurement

Behavioral experiments were performed in the Control group (n=10), the MGO group (n=9), the Rotenone group (n=9) and the MGO+Rotenone group (n=9). In addition to the 3 animals that died, 2 rats in the MGO+Rotenone group were not included in the locomotor activity tests due to their unfavorable general condition.

http://doi.org/10.5472/marumj.1480086
Marmara Med J 2024;37(2): 166-177

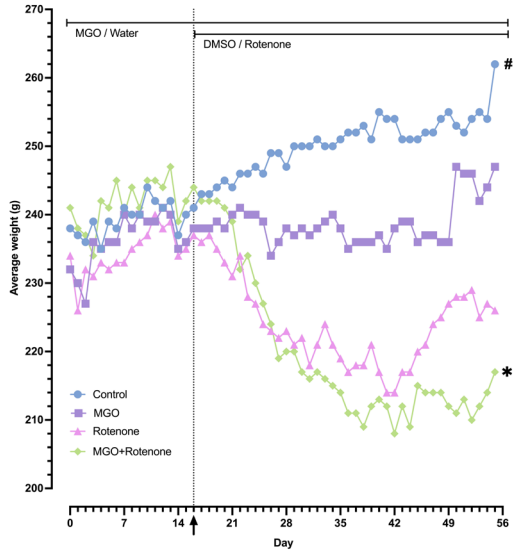

Figure 2. *The average daily weight of the groups recorded throughout the experiment. (The dotted line and arrow indicate the start day of rotenone or DMSO administration. * There was a significant difference between the average weights of the groups on the 55th day (p=0.022). In pairwise comparisons, the average weight of the MGO+Rotenone group was lower than that of the Control group on the 55th day (p=0.023). # There was a significant weight gain in the Control group on the 55th day (262±5 g) than that on days 0 and 16 (p<0.001, both))*

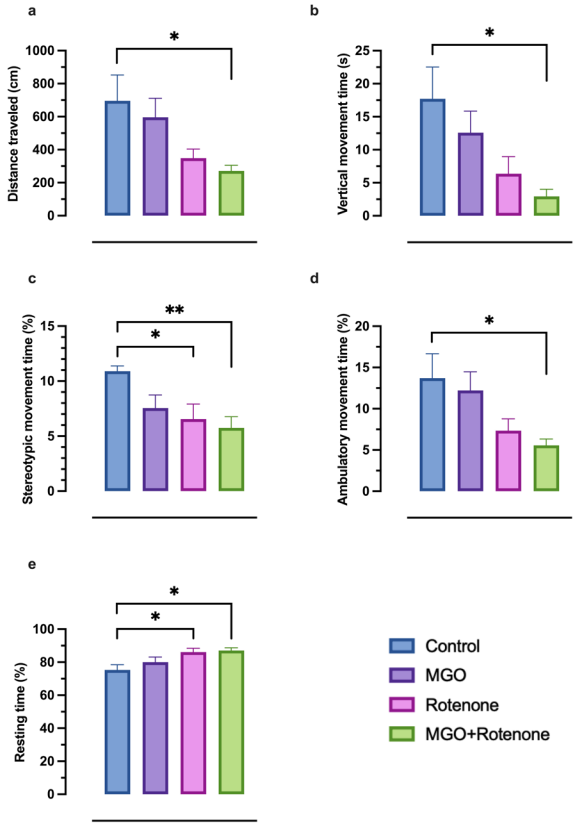

Figure 3. *Comparison of the locomotor activities of the groups. (a) Distance traveled (cm), (b) vertical movement time (s), (c) stereotypic movement time (%), (d) ambulatory movement time (%), (e) resting time (%). (Mean ± standard error of mean was given. * p<0.05, ** p<0.01, one-way ANOVA)*

http://doi.org/10.5472/marumj.1480086
Marmara Med J 2024;37(2): 166-177

Locomotor activity

The distance traveled was significantly different between groups (p=0.023). In pairwise comparisons, the distance traveled by the MGO+Rotenone group (272±33 cm) was significantly lower than that the distance traveled by the Control group (696±157 cm) (p=0.035). There was no significant difference according to the distance traveled between the MGO group (596±115 cm) and the Rotenone group (348±55 cm) and the other groups (p>0.05) (Figure 3a).

The vertical movement time was significantly different between groups (p=0.017). In pairwise comparisons, the vertical movement time of the MGO+Rotenone group (2936±1100 ms) was significantly lower than that of the Control group (17721±4808 ms) (p=0.017). There was no significant difference according to vertical movement time between the MGO group (12580±3265 ms) and the Rotenone group (6382±2583 ms) and the other groups (p>0.05) (Figure 3b).

The percentage of stereotypical movement time was significantly different between groups (p=0.006). In pairwise comparisons, the % of stereotypical movement time in the Control group (10.9%±0.5) was significantly higher than that in the MGO+Rotenone (5.8%±1.0) and Rotenone groups (6.6%±1.4) (p=0.008, p=0.024, respectively). There was no significant difference between the other groups (p>0.05) (Figure 3c).

The percentage of ambulatory movement time was significantly different between groups (p=0.028). In pairwise comparisons, the % ambulatory movement time in the Control group (13.7%±3) was significantly higher than that in the MGO+Rotenone group (5.6%±0.8) (p=0.043). There was no significant difference according to % of ambulatory movement time between the MGO group (12.2%±2.2) and the Rotenone group (7.3%±1.4) and with the other groups (p>0.05) (Figure 3d).

The percentage of resting time was significantly different between groups (p=0.012). In pairwise comparisons, the % of resting time in the MGO+Rotenone group (87.1%±1.7) and the Rotenone group (86.1%±2.3) was significantly higher than that in the Control group (75.3%±3.2) (p=0.018, p=0.035, respectively). There was no significant difference between the other groups (p>0.05) (Figure 3e).

Rearing activity

The rearing activity was significantly different between groups (p=0.002). In pairwise comparisons, the rearing activity of the Control group (10±2) was significantly higher than that of the MGO+Rotenone group (2±1) and the Rotenone group (3±1) (p=0.007, p=0.030, respectively). Additionally, the rearing activity of the MGO group (9 ± 1) was significantly higher than that of the MGO+Rotenone group (p=0.021). There was no significant difference in other pairwise comparisons (p>0.05) (Figure 4).

Rotarod Test

The average time spent on the rod in the three tests was 215±25 s in the Control group, 150±40 s in the MGO group, 155±38 s in the Rotenone group, and 94±31 s in the MGO+Rotenone group. Although, the average time spent on the rod in the three tests was shorter in the MGO+Rotenone group, there was no significant difference between the groups (p=0.098) (Figure 5a).

The longest time spent on the rod was significantly different between groups (p=0.015). In pairwise comparisons, the longest time spent on the rod in the Control group (263±19 s) was significantly longer than that in the MGO+Rotenone group (103±29 s) (p=0.008). There was no significant difference according to the longest time spent on the rod between the MGO group (181±43 s) and the Rotenone group (171±38 s) and with the other groups (p>0.05) (Figure 5b).

Blood glucose measurement

When the blood glucose levels measured on the 1st, 16th and 56th days were compared within the group and between the groups, no significant difference was found in any group (p>0.05).

Immunohistochemistry

The TH immunoreactivities of the striatum and SNpc regions in the coronal sections taken from the experimental groups at x2 magnification are shown in Figure 6a. Additionally, TH immunoreactivities at x20 magnification for the striatum and x40 for the SNpc are shown in Figure 6b.

TH immunoreactivity in the striatum

There was a significant difference in the percentages of RAC TH immunoreactivity of the groups (p=0.019). In pairwise comparisons, the percentage of RAC TH immunoreactivity in the Control group (58.8%±1.8) and MGO group (57.2%±1.5) was significantly higher than that in the MGO+Rotenone group (37.8%±7) (p=0.027, p=0.047, respectively). The percentage of RAC TH immunoreactivity in the Rotenone group (47.6%±6) was not significantly different from that in the other groups (p>0.05). The comparison of the percentages of RAC TH immunoreactivity of the groups is shown in Figure 7a.

When the percentage of LAC TH immunoreactivity of the groups was evaluated, the percentage of the Control group was 55.7%±1.7, 55.6%±1.6 in the MGO group, 48.4%±4.3 in the Rotenone group, and 49.7%±3.9 in the MGO+Rotenone group. There was no significant difference between the percentages of LAC immunoreactivity positivity of the groups (p=0.255). The comparison of the percentages of LAC immunoreactivity positivity of the groups is shown in Figure 7b.

When the percentages of CAC TH immunoreactivity of the groups were evaluated, the percentages of the Control group were 51.5%±2.1 and 49.9%±1.9 in the MGO group, 48.2%±2.6 in the Rotenone group, and 49.2%±1.6 in the MGO+Rotenone group. There was no significant difference between the percentages of groups' CAC immunoreactivity positivity (p=0.720). The comparison of the percentages of CAC immunoreactivity positivity of the groups is shown in Figure 7c.

TH-immunoreactivity in the SNpc

When the number of TH+ cells in the SNpc of the groups was evaluated, the number of cells in the Control group was determined to be 19±1, 18±1 in the MGO group, 17±1 in the Rotenone group and 15±2 in the MGO+Rotenone group. There was no significant difference between the numbers of TH+ cells in the SNpc of the groups (p=0.136). A comparison of the groups in terms of the number of TH+ cells in the SNpc is shown in Figure 7d.

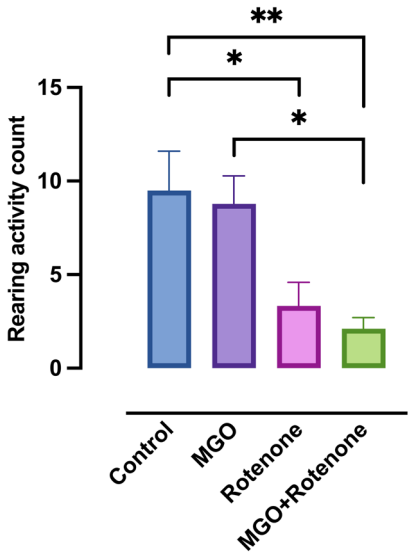

Figure 4. *Comparison of the rearing activity of the groups. (Mean ± standard error of mean was given. * p<0.05, ** p<0.01, one-way ANOVA)*

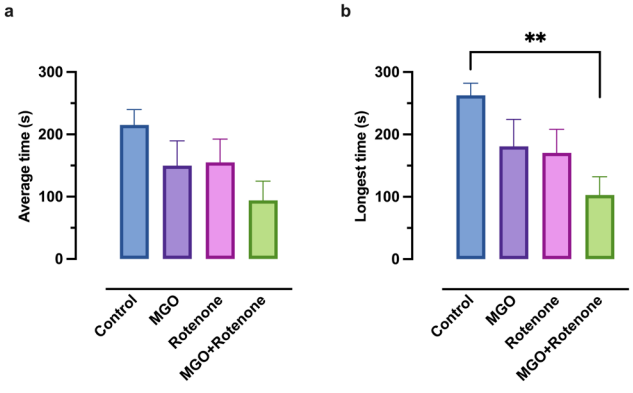

Figure 5. *Comparison of time spent on the rod of the groups in the rotarod test. (a) The average time spent on the rod, (b) the longest time spent on the rod. (Mean ± standard error of mean was given. ** p<0.01, one-way ANOVA)*

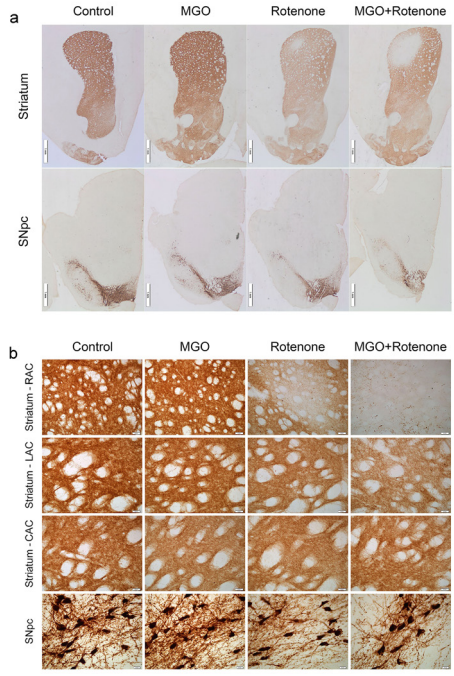

Figure 6. *TH immunoreactivity in the striatum and SNpc in coronal section samples of the groups. (a) Coronal sections at x2 magnification (chart scale= 1 mm), (b) coronal sections at x20 magnification for the striatum (chart scale= 50 µm) and x40 magnification for the SNpc (chart scale= 20 µm).*

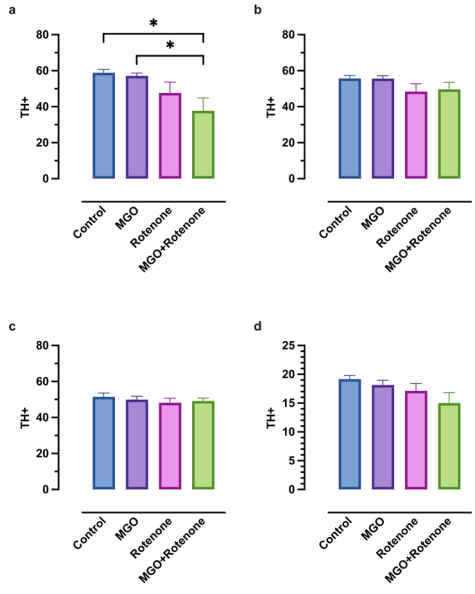

Figure 7. *Comparison of the tyrosine hydroxylase positivity of the groups. (a) Rostral to the anterior commissure, (b) level of the anterior commissure, (c) caudal to the anterior commissure, (d) substantia nigra pars compacta. (Mean ± standard error of mean was given. * p<0.05, one-way ANOVA)*

http://doi.org/10.5472/marumj.1480086
Marmara Med J 2024;37(2): 166-177

4. DISCUSSION

In this study, the effect of the advanced glycation end product precursor MGO on the development of PD pathophysiology was investigated. MGO application in the rotenone-induced PD model aggravated motor disorders and increased striatal dopaminergic damage without any statistically significant change in the number of dopaminergic cells in the SNpc. It also noticeably amplified the weight loss in animal however, no significant effect was observed on blood sugar. The findings of our study indicate that advanced glycation end product precursor MGO may play a role in increased PD pathophysiology in patients with T2DM.

Previous studies reported that rotenone administration, used in modeling PD, causes a decrease in axonal dopamine in the dorsal striatum, and chronic rotenone administration reduces dopamine concentrations in the anterior striatum [25, 26]. In our study, the MGO+Rotenone group had TH+ in the RAC striatum region that was significantly lower than that of the other groups, but there was no significant difference between the groups in the LAC and CAC striatum regions. In other words, the administration of MGO in conjunction with rotenone exacerbated dopaminergic loss in the striatum, but this loss was limited to the dorsolateral region of the anterior striatum.

Degeneration of dopaminergic neurons in the SNpc is thought to be a possible cause of dysfunction in the dorsal striatum, which is the projection target [27, 28]. The dorsal striatum is responsible for action selection and movement control, so dysfunction of this region also contributes to the common symptoms of Parkinson's disease [29, 30]. According to our findings, the deterioration in motor activity observed in the MGO+Rotenone group may be due to the dopaminergic loss observed in the RAC striatum.

In a study conducted on Thy1-aSyn mice, intracerebroventricular administration of MGO did not show any significant difference in TH immunoreactivity in the SNpc between the MGO-treated and nontreated groups [31]. On the other hand, in another study in which MGO injection was applied to the SNpc and striatum in Thy1-aSyn mice, a statistically significant decrease in TH+ neurons was reported in the experimental group compared to the control group [17]. In our study, the number of TH-immunoreactive cells in the SNpc decreased in the MGO+Rotenone group compared to the other groups, but there was no statistically significant difference between the groups. Consistent with our results, a study that established a PD model in mice by intranasal rotenone administration showed significant motor loss, but no dopaminergic loss was observed in the striatum and SNpc [23]. Although, striatal dopaminergic degeneration was observed in our study, the reason why there was no difference in TH immunoreactivity between groups in the SNpc may be that not enough time had passed for the neuron bodies in the SNpc to degenerate. Another possible reason may be that due to the weight loss in the MGO + Rotenone group, they received fewer Rotenone/DMSO injections compared to the other groups for ethical reasons.

In PD, the decrease in dopamine levels in the striatum leads to a decrease in voluntary motor movement control, bradykinesia and akinesia, which are the classic symptoms of PD [32]. Damage to the nigrostriatal circuit reduces locomotor activity in experimental animal models of PD [33]. In our study, the distance traveled, stereotypic movement and resting time obtained from the locomotor activity test were evaluated together in this context. The distance traveled and stereotypic movement time were significantly lower, and the percentage of resting time was higher in the MGO + Rotenone group than in the Control group, which is a clear indication of a significant decrease in locomotor movement. Although, the stereotypical movement time was lower and the resting time was higher in the Rotenone group than in the Control group, this difference was higher in the MGO+Rotenone group. Similar to our findings, animal studies have shown that locomotor activity decreases in PD groups compared to Control groups [33, 34]. In a study conducted in healthy animals to evaluate the effect of MGO on behavioral parameters, MGO was infused into the cerebral lateral ventricle in a volume of 5 µL at a concentration of 3 µM/µL. In the open field test performed at the 12th hour after MGO injection, a statistically significant decrease in locomotor activity was reported in the experimental group compared to the control group [35]. A single dose of 50 mg/kg/day MGO did not alter locomotor activity in a study looking at the impact of intraperitoneal MGO injection on motor activity in mice, but doses of 80 and 200 mg/kg/day caused a significant reduction in locomotor activity [36]. The reason for the loss of motor activity may be that MGO-derived free radicals and toxins react with dopamine in the brain and reduce the effect of dopamine [37]. MGO has also been reported to act as a partial agonist of $GABA_A$ receptors, and acutely high levels of MGO induce locomotor depression [38].

Another parameter obtained from the locomotor activity test is the ambulatory movement time. It has been shown that a decrease in locomotor activity, including ambulatory movement, occurred in the PD model created by applying 2 mg/kg rotenone subcutaneously to Sprague Dawley rats for 35 days, and this decrease could be partially prevented with antioxidant treatment [39]. In our study, the ambulatory movement time in the MGO+Rotenone group was significantly lower than that in the Control group. This finding indicates that MGO, which causes oxidative stress, increases motor impairment in the rotenone model of PD.

One of the parameters measured by the locomotor activity test is the number and duration of vertical movements. Another test method used to evaluate vertical movement is the rearing test. In animal models of PD, a decrease in the number of vertical movements, vertical movement time, and number of rearings is expected [21]. In a previous study, while no difference was observed between the experimental and control groups in vertical movements in rats receiving 2, 2.5 or 3.5 mg/kg rotenone intravenously for 21 days, a significant decrease in the number of rearings was reported in the experimental group compared to the control group [22]. It has also been shown that rearing behavior is reduced in rotenone models performed

http://doi.org/10.5472/marumj.1480086
Marmara Med J 2024;37(2): 166-177

with different doses and application routes [20, 40]. Our results obtained from the MGO+Rotenone group suggest that MGO decreases the number of rearings and the number and duration of vertical movements that develop due to PD.

The time spent on the rotarod device is shortened in rats and mice with PD [20, 40]. In a study in which the rotarod test was performed to evaluate motor coordination, 1.5 mg/kg rotenone was administered subcutaneously every other day for 11 days, and the time the rotenone group remained on the rod was found to be lower than that of the control group [41]. In the present study, the MGO+Rotenone group had a shorter average time spent on the rod, but this difference was not statistically significant. The high intragroup variation and the limited number of subjects to overcome this variation prevented statistical significance from being reached. When evaluated according to the longest time spent on the rod, the MGO+Rotenone group was able to stay on the rod for a shorter time than the Control group. In a study conducted on Thy1-aSyn mice, intracerebroventricular MGO was administered to the mice, and it was shown that the experimental group was able to stand on the rod less than the control group [31]. Our results demonstrate that MGO contributes to the decline in motor coordination, and they are consistent with findings from the literature.

One of the disadvantages of the PD rotenone model is the high mortality rate with systemic administration [42]. In our study, the mortality rate in animals administered rotenone was 9% (2/22). In the study conducted by Zhang et al., rotenone was administered subcutaneously to rats at a dose of 1.5, 2 or 2.5 mg/kg/day for 5 weeks, and mortality rates were reported as 0%, 6.7% and 46.7%, respectively [20]. In the study conducted by Fleming et al., the mortality rates of rotenone administered subcutaneously at doses of 2, 2.5, 3.5, or 5 mg/kg/day were 33% (4/12), 64% (7/11), 91% (10/11), and 100% (3/3), respectively [22]. In another study conducted in 2017, the mortality rate was reported as 28.5% (12/42) in rats administered 1.5 mg/kg/day rotenone intraperitoneally for 45 days [43]. There could be a number of reasons for the reported variations in death rates, including different animal strains, sexes, and housing circumstances. In our study, animals that lost more than 15% of their basal weight were not given the injection on that particular day to decrease mortality related to rotenone. For the same reason, Miglyol 812 N, which contains medium-chain fatty acids, was used to dilute rotenone, and the amount of DMSO in the application solution was kept at 2%. Additional losses were prevented by applying rotenone subcutaneously at a dosage of 1.5 mg/kg/day. The 9% mortality rate in our study shows that the methods we used in the rotenone model were successful in reducing deaths.

It has been reported that chronic systemic administration of rotenone causes weight loss in animals, and this is related to the systemic toxicity of rotenone as well as weight loss due to PD symptoms [44, 45]. In our study, the average weight of the MGO+Rotenone group was found to be significantly lower than that of the Control group at the end of the experiment. In a study published by Sharma et al., 2 mg/kg/day rotenone was administered subcutaneously to rats for 35 days. In weekly weight monitoring, no weight loss was observed in the first 2 weeks, but gradually increasing weight loss was reported in the 3rd, 4th, and 5th weeks [46]. In another study, 3 mg/kg/day rotenone infusions were given subcutaneously for 28 days. The rotenone groups showed a time-dependent decrease in body weight compared to rats administered vehicle or saline. In the study, regular weight loss was observed in the rotenone group, especially in the first 2 weeks [47]. In our study, low-dose rotenone application was preferred, and weight loss was minimized by skipping the dose in animals with a weight loss of more than 15% compared to their basal weight.

MGO binds to insulin by targeting arginine residues located in the insulin B chain and N-terminus. MGO-modified insulin chain B is heavier than free insulin, resulting in less glucose uptake and utilization [48]. In a study conducted with continuous infusion of MGO at a dose of 60 mg/kg/day for 28 days, a significant increase in fasting blood glucose along with a decrease in fasting plasma insulin levels was reported [49]. While some research indicates that hyperglycemia triggers the production of MGO and that MGO aids in the development of hyperglycemia, other works do not track these effects. Despite impaired glucose tolerance, no significant change in fasting blood glucose was observed in mice administered a low dose (1% v/v) of MGO in drinking water for 2 months with fetal exposure [50]. In a study in which MGO was given to Wistar albino rats at a dose of 50-75 mg/kg/day for 14 weeks, no significant difference was observed in terms of fasting blood glucose between the control group and the group receiving MGO [51]. The lack of apparent difference in blood glucose levels between the groups in our study that received and did not receive MGO may be because the dose of MGO used was insufficient to induce beta cell dysfunction and insulin resistance. Another important point to note is that fasting blood glucose was not measured in our study, and spot blood glucose was measured at 12:30 pm while they had access to feed and water in their cages.

On the other hand, there are limitations in this study. To cope with the problems of weight loss and mortality caused by choosing the rotenone model, rotenone was not administered to rats that lost 15% of their basal weight. One result of this is that the MGO+Rotenone administered group received fewer rotenone injections than the Rotenone group. This may have limited the progression of motor impairment and nigrostriatal degeneration in the MGO+Rotenone group. It is possible that this prevented the difference between the two groups from becoming more evident. Another limitation of the study is that a-synuclein accumulation is not measured in the brain, and blood levels of orally administered MGO could not be measured.

Conclusion

In this study, which examined a possible mechanism of the T2DM-PD relationship through MGO, an advanced glycation end-product precursor, it was determined that the use of MGO together with rotenone exacerbated the motor symptoms of PD and increased the neurodegeneration seen in the disease. To the best of our knowledge, this study is the first to investigate

http://doi.org/10.5472/marumj.1480086
Marmara Med J 2024;37(2): 166-177

the potential effect of long-term MGO administration on PD pathophysiology using the rotenone model of PD. Therefore, we believe that our study will contribute to filling the gap of T2DM-PD relationship in the literature. Although, our study showed the possible contribution of methylglyoxal to the pathophysiology of PD, the mechanism of this effect needs to be investigated in terms of biochemical processes.

Compliance with Ethical Standards

Ethical approval: Approval of the study for all experimental procedures was obtained from The Marmara University Ethical Committee for Experimental Animals (96.2021mar) and performed in line with guidelines.

Financial support: This work was supported by the Marmara University Scientific Research Committee with the thesis project number TTU-2022-10441.

Conflict of interest: The authors have no relevant financial or nonfinancial interests to disclose.

Authors' contributions: All authors contributed to the study's conception and design. YC and RG: Material preparation, data collection, and analysis, YC: Writing the first draft of the manuscript. All authors commented on the first draft of the manuscript. All authors read and approved the final manuscript.

REFERENCES

[1] von Campenhausen S, Bornschein B, Wick R et al. Prevalence and incidence of Parkinson's disease in Europe. Eur Neuropsychopharmacol 2005; 15: 473-90. doi: 10.1016/j.euroneuro.2005.04.007.

[2] Aarsland D, Batzu L, Halliday G M et al. Parkinson disease-associated cognitive impairment. Nat Rev Dis Primers 2021; 7: 47. doi: 10.1038/s41572.021.00280-3.

[3] Dauer W and Przedborski S. Parkinson's disease: mechanisms and models. Neuron 2003; 39: 889-909.

[4] Exner N, Lutz A K, Haass C, Winklhofer K F. Mitochondrial dysfunction in Parkinson's disease: molecular mechanisms and pathophysiological consequences. Embo J 2012; 31: 3038-62. doi: 10.1038/emboj.2012.170.

[5] Ebrahimi-Fakhari D, Wahlster L, and McLean P J. Protein degradation pathways in Parkinson's disease: curse or blessin. Acta Neuropathol 2012; 124: 153-72. doi: 10.1007/s00401.012.1004-6.

[6] Stefanis L. α-Synuclein in Parkinson's disease. Cold Spring Harb Perspect Med 2012; 2: a009399. doi: 10.1101/cshperspect.a009399.

[7] Hetz C, Saxena S. ER stress and the unfolded protein response in neurodegeneration. Nat Rev Neurol 2017; 13: 477-91. doi: 10.1038/nrneurol.2017.99.

[8] Ascherio A, Schwarzschild M A. The epidemiology of Parkinson's disease: risk factors and prevention. Lancet Neurol 2016; 15: 1257-72. doi: 10.1016/s1474-4422(16)30230-7.

[9] De Pablo-Fernandez E, Goldacre R, Pakpoor J, Noyce A J, Warner T T. Association between diabetes and subsequent Parkinson disease: A record-linkage cohort study. Neurology 2018; 91: e139-e142. doi: 10.1212/wnl.000.000.0000005771.

[10] Cereda E, Barichella M, Pedrolli C, et al. Diabetes and risk of Parkinson's disease: a systematic review and meta-analysis. Diabetes Care 2011; 34: 2614-23. doi: 10.2337/dc11-1584.

[11] Sandyk R. The relationship between diabetes mellitus and Parkinson's disease Int J Neurosci 1993; 69: 125-30. doi: 10.3109/002.074.59309003322.

[12] Galicia-Garcia U, Benito-Vicente A, Jebari S, et al. Pathophysiology of Type 2 diabetes mellitus. Int J Mol Sci 2020; 21:6275. doi: 10.3390/ijms21176275.

[13] Henriksen E J, Diamond-Stanic M K, Marchionne E M. Oxidative stress and the etiology of insulin resistance and type 2 diabetes. Free Radic Biol Med 2011; 51: 993-9. doi: 10.1016/j.freeradbiomed.2010.12.005.

[14] Nowotny K, Jung T, Höhn A, Weber D, Grune T. Advanced glycation end products and oxidative stress in type 2 diabetes mellitus. Biomolecules 2015; 5: 194-222. doi: 10.3390/biom5010194.

[15] Dornadula S, Elango B, Balashanmugam P, Palanisamy R, Kunka Mohanram R. Pathophysiological insights of methylglyoxal induced type-2 diabetes. Chem Res Toxicol 2015; 28: 1666-74. doi: 10.1021/acs.chemrestox.5b00171.

[16] Lu J, Randell E, Han Y, Adeli K, Krahn J, Meng Q H. Increased plasma methylglyoxal level, inflammation, and vascular endothelial dysfunction in diabetic nephropathy. Clin Biochem 2011; 44: 307-11. doi: 10.1016/j.clinbiochem.2010.11.004.

[17] Vicente Miranda H, Szego É M, Oliveira L M A, et al. Glycation potentiates α-synuclein-associated neurodegeneration in synucleinopathies. Brain 2017; 140: 1399-419. doi: 10.1093/brain/awx056.

[18] Biosa A, Outeiro T F, Bubacco L, Bisaglia M. Diabetes mellitus as a risk factor for Parkinson's disease: a molecular point of view. Mol Neurobiol 2018; 55: 8754-63. doi: 10.1007/s12035.018.1025-9.

[19] Fitzmaurice A G, Rhodes S L, Lulla A, et al. Aldehyde dehydrogenase inhibition as a pathogenic mechanism in Parkinson disease. Proc Natl Acad Sci U S A 2013; 110: 636-41. doi: 10.1073/pnas.122.039.9110.

[20] Zhang Z N, Zhang J S, Xiang J, et al. Subcutaneous rotenone rat model of Parkinson's disease: Dose exploration study. Brain Res 2017; 1655: 104-13. doi: 10.1016/j.brainres.2016.11.020.

[21] Meredith G E, Kang U J. Behavioral models of Parkinson's disease in rodents: a new look at an old problem. Mov Disord 2006; 21: 1595-606. doi: 10.1002/mds.21010.

[22] Fleming S M, Zhu C, Fernagut P O, et al. Behavioral and immunohistochemical effects of chronic intravenous and subcutaneous infusions of varying doses of rotenone. Exp Neurol 2004; 187: 418-29. doi: 10.1016/j.expneurol.2004.01.023.

[23] Sharma M, Kaur J, Rakshe S, Sharma N, Khunt D, Khairnar A. Intranasal exposure to low-dose rotenone Induced alpha-synuclein accumulation and Parkinson's like symptoms without loss of dopaminergic neurons. Neurotox Res 2022; 40: 215-29. doi: 10.1007/s12640.021.00436-9.

[24] Paxinos G, Watson C. The rat brain in stereotaxic coordinates. Hard cover 6th edition. Elsevier, 2006.

[25] Bao L, Avshalumov M V, Rice M E. Partial mitochondrial inhibition causes striatal dopamine release suppression and medium spiny neuron depolarization via H2O2 elevation, not ATP depletion. J Neurosci 2005; 25: 10029-40. doi: 10.1523/jneurosci.2652-05.2005.

[26] Alam M, Danysz W, Schmidt W J, Dekundy A. Effects of glutamate and alpha2-noradrenergic receptor antagonists on the development of neurotoxicity produced by chronic rotenone in rats. Toxicol Appl Pharmacol 2009; 240: 198-207. doi: 10.1016/j.taap.2009.07.010.

[27] Cenci M A, Francardo V, O'Sullivan S S, Lindgren H S. Rodent models of impulsive-compulsive behaviors in Parkinson's disease: How far have we reached? Neurobiol Dis 2015; 82: 561-73. doi: 10.1016/j.nbd.2015.08.026.

[28] Samii A, Nutt J G, Ransom B R. Parkinson's disease. Lancet 2004; 363: 1783-93. doi: 10.1016/s0140-6736(04)16305-8.

[29] Kravitz A V, Freeze B S, Parker P R, et al. Regulation of parkinsonian motor behaviours by optogenetic control of basal ganglia circuitry, Nature, 2010; 466: 622-6. doi: 10.1038/nature09159.

[30] Cataldi S, Stanley A T, Miniaci M C, Sulzer D. Interpreting the role of the striatum during multiple phases of motor learning. Febs j, 2022; 289: 2263-2281. doi: 10.1111/febs.15908.

[31] Chegão A, Guarda M, Alexandre B M et al. Glycation modulates glutamatergic signaling and exacerbates Parkinson's disease-like phenotypes, NPJ Parkinsons Dis 2022; 8: 51. doi: 10.1038/s41531.022.00314-x.

[32] Panigrahi B, Martin K A, Li Y, et al. Dopamine is required for the neural representation and control of movement vigor. Cell, 2015; 162: 1418-30. doi: 10.1016/j.cell.2015.08.014.

[33] Taylor T N, Greene J G, Miller G W. Behavioral phenotyping of mouse models of Parkinson's disease. Behav Brain Res 2010; 211: 1-10. doi: 10.1016/j.bbr.2010.03.004.

[34] Su R J, Zhen J L, Wang W, Zhang J L, Zheng Y, Wang X M. Time-course behavioral features are correlated with Parkinson's disease-associated pathology in a 6-hydroxydopamine hemiparkinsonian rat model. Mol Med Rep 2018; 17: 3356-63. doi: 10.3892/mmr.2017.8277.

[35] Lissner L J, Rodrigues L, Wartchow K M, et al. Short-term alterations in behavior and astroglial function after intracerebroventricular infusion of methylglyoxal in rats. Neurochem Res 2021; 46: 183-96. doi: 10.1007/s11064.020.03154-4.

[36] Szczepanik J C, de Almeida G R L, Cunha M P, Dafre A L. Repeated methylglyoxal treatment depletes dopamine in the prefrontal cortex, and causes memory impairment and depressive-like behavior in mice, Neurochem Res 2020; 45: 354-70. doi: 10.1007/s11064.019.02921-2.

[37] Hipkiss A R. On the relationship between energy metabolism, proteostasis, aging and Parkinson's disease: Possible causative role of methylglyoxal and alleviative potential of carnosine. Aging Dis 2017; 8: 334-45. doi: 10.14336/ad.2016.1030.

[38] Distler M G, Plant L D, Sokoloff G, et al. Glyoxalase 1 increases anxiety by reducing GABAA receptor agonist methylglyoxal. J Clin Invest 2012; 122: 2306-15. doi: 10.1172/jci61319.

[39] Nehru B, Verma R, Khanna P, Sharma S K. Behavioral alterations in rotenone model of Parkinson's disease: attenuation by co-treatment of centrophenoxine. Brain Res 2008; 1201: 122-7. doi: 10.1016/j.brainres.2008.01.074.

[40] Palle S, Neerati P. Improved neuroprotective effect of resveratrol nanoparticles as evinced by abrogation of rotenone-induced behavioral deficits and oxidative and mitochondrial dysfunctions in rat model of Parkinson's disease. Naunyn Schmiedebergs Arch Pharmacol 2018; 391: 445-53. doi: 10.1007/s00210.018.1474-8.

[41] Kandil E A, Abdelkader N F, El-Sayeh B M, Saleh S. Imipramine and amitriptyline ameliorate the rotenone model of Parkinson's disease in rats. Neuroscience. 2016; 332: 26-37. doi: 10.1016/j.neuroscience.2016.06.040.

[42] Greenamyre J T, Cannon J R, Drolet R, Mastroberardino P G. Lessons from the rotenone model of Parkinson's disease. Trends Pharmacol Sci 2010; 31: 141-2; author reply 142-3. doi: 10.1016/j.tips.2009.12.006.

[43] Khadrawy Y A, Salem A M, El-Shamy K A, Ahmed E K, Fadl N N, Hosny E N. Neuroprotective and therapeutic effect of caffeine on the rat model of Parkinson's disease induced by rotenone. J Diet Suppl 2017; 14: 553-72. doi: 10.1080/19390.211.2016.1275916.

[44] Greene J G, Noorian A R, Srinivasan S. Delayed gastric emptying and enteric nervous system dysfunction in the rotenone model of Parkinson's disease. Exp Neurol 2009; 218: 154-61. doi: 10.1016/j.expneurol.2009.04.023.

[45] Drolet R E, Cannon J R, Montero L, Greenamyre J T. Chronic rotenone exposure reproduces Parkinson's disease gastrointestinal neuropathology. Neurobiol Dis 2009; 36: 96-102. doi: 10.1016/j.nbd.2009.06.017.

[46] Sharma N, Khurana N, Muthuraman A, Utreja P. Pharmacological evaluation of vanillic acid in rotenone-induced Parkinson's disease rat model. Eur J Pharmacol 2021; 903: 174112. doi: 10.1016/j.ejphar.2021.174112.

[47] Ravenstijn P G, Merlini M, Hameetman M, et al. The exploration of rotenone as a toxin for inducing Parkinson's disease in rats, for application in BBB transport and PK-PD experiments. J Pharmacol Toxicol Methods 2008; 57: 114-30. doi: 10.1016/j.vascn.2007.10.003.

[48] Jia X, Olson D J, Ross A R, Wu L. Structural and functional changes in human insulin induced by methylglyoxal. Faseb J 2006; 20: 1555-7. doi: 10.1096/fj.05-5478fje.

[49] Dhar A, Dhar I, Jiang B, Desai K M, Wu L. Chronic methylglyoxal infusion by minipump causes pancreatic beta-cell dysfunction and induces type 2 diabetes in Sprague-Dawley rats. Diabetes 2011; 60: 899-908. doi: 10.2337/db10-0627.

[50] Ankrah N A, Appiah-Opong R. Toxicity of low levels of methylglyoxal: depletion of blood glutathione and adverse effect on glucose tolerance in mice. Toxicol Lett 1999; 109: 61-7. doi: 10.1016/s0378-4274(99)00114-9.

[51] Matafome P, Santos-Silva D, Crisóstomo J, et al. Methylglyoxal causes structural and functional alterations in adipose tissue independently of obesity. Arch Physiol Biochem 2012; 118: 58-68. doi: 10.3109/13813.455.2012.658065.

MARMARA
MEDICAL JOURNAL

Original Article

https://dergipark.org.tr/tr/pub/marumj

Evaluation of sarcopenia-associated survival in breast cancer with computed tomography-based pectoral muscle area measurements

Beyza Nur KUZAN[1], Nargiz MAJIDOVA[2], Can ILGIN[3], Hulya ARSLAN KAR[2,7], Meltem KURSUN[4], Salih OZGUVEN[5], Ibrahim Vedat BAYOGLU[2], Onur BUGDAYCI[4], Perran Fulden YUMUK[2,8], Handan KAYA[6]

[1] Department of Radiology, Kartal Dr. Lutfi Kırdar City Hospital, Istanbul, Turkey
[2] Division of Medical Oncology, Department of Internal Medicine, School of Medicine, Marmara University, Istanbul, Turkey
[3] Department of Radiation Oncology, Istanbul Training and Research Hospital, Istanbul, Turkey
[4] Department of Radiology, School of Medicine, Marmara University, Istanbul, Turkey
[5] Department of Nuclear Medicine, School of Medicine, Marmara University, Istanbul, Turkey
[6] Department of Pathology, School of Medicine, Marmara University, Istanbul, Turkey
[7] Division of Medical Oncology, Department of Internal Medicine, School of Medicine, Istanbul Medeniyet University, Istanbul, Turkey
[8] Division of Medical Oncology, Department of Internal Medicine, School of Medicine, Koç University, Istanbul, Turkey

Corresponding Author: Beyza Nur KUZAN
E-mail: drbeyzauzun@hotmail.com

Submitted: 11.08.2023 **Accepted:** 23.12.2023

ABSTRACT

Objective: Breast cancer is the most common and deadly female cancer. In breast cancer cases, survival is closely related to muscle mass, which is one of the components of body composition. Our aim was to investigate the usefulness of computed-tomography (CT)-based pectoral muscle measurements in detecting sarcopenia in patients with non-metastatic breast cancer and the relationship of these measurements with survival.

Patients and Methods: Our study included 62 adult female breast cancer cases diagnosed with breast cancer between January 2012 and January 2018 and without metastasis in positron emission tomography/CT (PET/CT) examination obtained for pre-treatment staging. To evaluate sarcopenia, skeletal muscle index (SMI) and pectoral muscle index (PMI) were calculated by measuring pectoral muscle area and skeletal muscle area at L3 vertebra level on PET/CT images.

Results: Deceased patients were significantly older (Median=73.90, IQR=27.04) than surviving patients (Median=54.60, IQR=13.37, p=0.025) and were diagnosed with cancer later in life (Median=63.92 IQR=30.16' vs. Median=47.51 IQR=15.0, p=0.030). When the threshold of 31 cm2/m2 was selected, there was a statistically significant difference in survival between sarcopenic and non-sarcopenic groups (p=0.031).

Conclusion: In conclusion, the presence of sarcopenia in female breast cancer cases is a parameter that affects survival and can be measured using radiological imaging methods. In addition to the measurements accepted in the literature regarding sarcopenia, pectoral muscle measurements can be chosen as an alternative method in the diagnosis of sarcopenia.

Keywords: Breast cancer, Computed tomography, Sarcopenia, Pectoral muscle

1. INTRODUCTION

Breast cancer is the leading cancer among women worldwide [1]. According to the 2020 Turkey Cancer Statistics, breast cancer has the highest incidence rate, with 23.9%, according to the number of new cases reported in women of all age groups in Turkey [2]. Risk factors for breast cancer include female sex, advanced age, family history of breast cancer, and certain genetic mutations [3]. Although, obesity may be a risk factor in specific groups, its direct association with breast cancer cases remains unclear [4].

Sarcopenia is defined as the loss of skeletal muscle mass [5]. Changes in skeletal muscle proteins with aging cause a loss of muscle mass and strength. Risk factors for sarcopenia include aging, decreased anabolic hormone activity, anorexia, and decreased physical activity [6]. Sarcopenia causes functional loss in healthy individuals and is associated with disability, injury, and death in individuals with non-malignant diseases [7]. In gastrointestinal and genitourinary cancers, overall survival is adversely affected in patients with sarcopenia [8]. Sarcopenia has also been reported to strong and independent predictive factor for poor survival in patients with breast cancer [9].

Sarcopenia is frequently evaluated using total skeletal muscle area measurements at the lumbar level [10,11] on computed

How to cite this article: Kuzan NB, Majidova N, Ilgın C, et al. Evaluation of sarcopenia-associated survival in breast cancer with computed tomography-based pectoral muscle area measurements. Marmara Med J 2024: 37(2):178-184. doi: 10.5472/marumj.1484705

ISSN: 1309-9469

http://doi.org/10.5472/marumj.1484705
Marmara Med J 2024;37(2): 178-184

tomography (CT) examinations, which provide information on muscle mass and density [12]. Pectoral muscle measurements can be a practical and helpful radiological parameter that can be performed simultaneously in cross-sectional imaging of the chest obtained during a cancer diagnosis. However, only a few studies of sarcopenia have used pectoral muscle measurements. [13,14].

The aim of this study was to investigate the usefulness of CT-based pectoral muscle measurements in detecting sarcopenia and the correlation of these measurements with survival in patients with non-metastatic breast cancer.

2. PATIENTS and METHODS

Patients

We included women aged 18 years and older diagnosed with breast cancer at our hospital from 1 January 2012 to 1 January 2018. An important inclusion criterion was a lack of evidence of metastasis on positron emission tomography/CT (PET-CT). We retrospectively evaluated chest and abdomen CT and PET-CT scans, which had been obtained for staging purposes prior to treatment or within six months after the initial diagnosis. We excluded patients with lobular-mixed type breast cancer (n = 4), which is much less common, for tumor type standardization and homogeneity; patients without imaging data before the operation or during chemotherapy/radiotherapy (n = 194); patients whose histopathologic subtype of cancer was not available (n = 3) and patients with metastasis at the time of admission (n = 24). Finally, 62 patients were considered for analysis. The study was approved by the Marmara University School of Medicine Clinical Research Ethics Committee (Protocol no: 09.2023.64, Date: 06.01.2023).

Demographic data such as sex, age, age at breast cancer diagnosis, height, weight, body mass index (BMI), and menopausal status were obtained from the patients' electronic medical records. In histopathologic analysis, estrogen receptor (ER)/progesterone receptor (PR) percentage, human epidermal growth factor 2 (HER2) presence, and Ki-67 indices were determined, and the patients were divided into three groups according to histopathologic subtypes: luminal A-B, HER2 enriched, and triple-negative breast cancer (TNBC) groups. Tumor grade and stage at diagnosis were determined according to the American Joint Committee on Cancer (AJCC) [1] Tumor-Node-Metastasis (TNM) staging system definitions [1]. The TNM stage, treatment protocols, dates, and methods (adjuvant chemotherapy, adjuvant radiotherapy, and operation history) were also noted. During the follow-up period, the patients' survival status, the relevant dates (date of progression/death), and their progression status were recorded.

Image analysis

Measurements were performed on non-contrast enhanced images. Images were acquired on a 128-slice CT machine with a slice thickness of 5 mm (Discovery ST PET/CT scanner; GE Healthcare, Milwaukee, WI). Images were evaluated by a single radiologist in the axial plane after reconstruction with 1-millimeter thin slices on the local Picture Archiving Communication Systems (PACS) software (Infinitt PACS, invented by Infinitt Co., Seoul, Korea). Thresholding between – 29 and +150 Hounsfield Unit (HU) was performed to isolate skeletal muscle groups from surrounding tissue [15]. The total area and average density of both pectoral muscles were measured at the T4 vertebral level (Figure 1). In the abdominal sections, the total skeletal muscle area (mm^2) and density were measured at the L3 vertebral level. All measurements were performed using the free-hand technique.

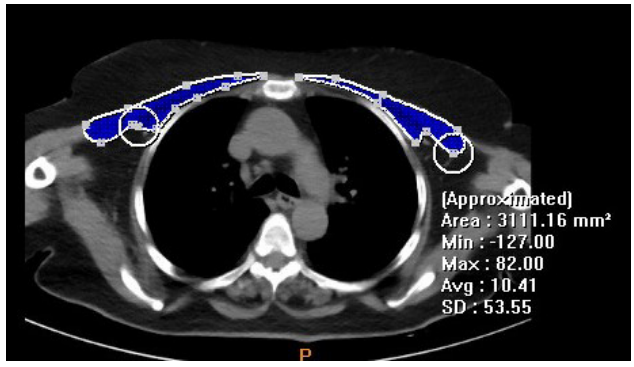

Figure 1. *Bilateral pectoral muscle area and density measurement is shown.*

Data analysis

The participants' BMI was calculated by dividing the body weight (kg) by the square of the height (m^2), and obesity was defined as a BMI of ≥30 kg/m^2 [16]. To calculate the pectoral muscle index (PMI), the total muscle area measured at the T4 vertebral level was converted from square millimeter (mm^2) to square centimeter (cm^2) and divided by the square of the height in meters (cm^2/m^2). To calculate the skeletal muscle index (SMI), the total muscle area obtained at the L3 vertebral level was converted from mm^2 to cm^2 and divided by the square of height in meters (cm^2/m^2). Because the threshold value for the presence of sarcopenia in CT measurements has not been reported for a Turkish population, we used the SMI of <38.5 cm^2/m^2, as recommended by the European Working Group on Sarcopenia in Older People (EWGSOP) for sarcopenia in women [7]. We also considered the value of ≤31 cm^2/m^2 used by Lee et al., for the presence of sarcopenia in Korean participants as an alternative [16].

Statistical Analysis

The normality assumption for numerical variables was examined with a Q-Q plot, skewness-kurtosis, and Kolmogorov-Smirnov tests. The distribution of numerical variables among two independent groups was tested with the Mann-Whitney U test. The numerical variables were presented with median and IQR values. The categorical variables were analyzed with chi-square or Fisher's exact tests. The categorical variables were presented with counts and percentages. The survival analysis was visualized with Kaplan Meier curves, and the survival-time data were analyzed with equality of survivor function test

http://doi.org/10.5472/marumj.1484705
Marmara Med J 2024;37(2): 178-184

and univariate Cox regression analysis. The hazard ratios were presented with 95% confidence intervals. A p-value less than 0.05 was considered significant. All statistical analyses were executed with Stata 15.1 software (StataCorp 4905 Lakeway Drive College Station, Texas 77845 USA).

2. RESULTS

Out of 62 breast cancer patients without metastasis during admission, seven (11.29 %) died during follow-up. Deceased patients were significantly older (Median=73.90, IQR=27.04) than the surviving patients (Median=54.60, IQR=13.37, p=0.025). Similarly, deceased patients were diagnosed with cancer later in their lives (Median=63.92 IQR=30.16 vs. Median=47.51 IQR=15.0, p=0.030). Also, there was no significant difference between the two groups regarding BMI (p=0.079) and tumor size (p=0.902). The median follow-up duration for surviving group was 76.4 (IQR=39.0) and for the mortality group the median value was 38.07 (IQR=24.67), and there was a statistical significance between these two groups for follow-up durations (p<0.001). For all participants, the median follow-up duration was 73.9 (IQR=41.27).

In both deceased and surviving groups, most patients had grade II tumors (100.0% and 60.0%, respectively) with luminal subtypes (85.71% and 83.33%, respectively) at the time of diagnosis and the distributions showed no significant difference (p=1.00 and p=1.00, respectively). While most of the patients in the deceased group were either in the T1 or T2 category (42.86% and 42.86%) at the time of diagnosis, most of the patients in surviving group were in the T2 category (66.04%). However, no statistically significant difference was found. On the other hand, deceased patients were nearly twice as likely to have advanced disease (T3 or T4) (14.29% vs 7.55%, p=0.544) than surviving patients. Although, deceased patients tended to be in the N0 (42.86%) or N3 (42.86%) category at the time of diagnosis, most of the surviving patients were in the N1 category at the time of diagnosis (50.94%) (p=0.001). Nevertheless, the surviving patients had a higher percentage of lymph node positivity (n=46, 86.79%) compared to the deceased group (n=4, 57.14%) (p=0.083). The percentage of patients undergoing surgery and receiving adjuvant radiotherapy was higher in the surviving patient group (n=53, 96.36% and n=51 92.73%, respectively) compared to the deceased group (n=6, 85.71% and n=6, 85.71%). However, the difference was statistically non-significant (p=0.462). The percentage of patients receiving adjuvant chemotherapy was higher in the deceased group compared to surviving group, without statistical significance (p=0.696).

There was no statistically significant difference between right, left or total pectoral muscle areas between the deceased and surviving patient groups (p=0.345, p=0.991, and p=0.41 respectively). Similarly, no significant differences were found regarding right, left, and total pectoral muscle average densities (p=0.345, p=0.714, and p=0.312, respectively). In addition, there was no statistically significant difference regarding total muscle area, density, and SMI at the L3 vertebral level (p=0.588, p=0.863, and p=0.844, respectively).The median PMI for surviving group was 945.12 (IQR=297.71) and greater than mortality group (Median=798.72, IQR=439.45), however there was no significant difference among the groups (p=0.648) (Table I).

Table I. *Sociodemographic and clinical characteristics of patients*

Characteristics		Statistics	Survival (n=55, 88.71%)	Mortality (n=7, 11.29%)	P value
Age (year)		Median (IQR)	54.6 (14.37)	73.901 (27.04)	**0.025***
Age at diagnosis (year)		Median (IQR)	47.51 (15.0)	63.92 (30.16)	**0.030***
BMI		Median (IQR)	27.05 (4.804)	24.671 (3.186)	0.079
Tumor size		Median (IQR)	2.25 (1.5)	2.05 (1.3)	0.902
Follow-up duration (month)		Median (IQR)	76.4 (39.0)	38.07 (24.67)	**<0.001***
Tumor grade	1	Count (%)	3 (6.38%)	0 (0%)	1.00
	2	Count (%)	22 (46.81%)	3 (60.0%)	
	3	Count (%)	22 (46.81%)	2 (40.0%)	
Molecular Subtype	Luminal	Count (%)	45 (83.33%)	6 (85.71%)	1.00
	Her2+	Count (%)	2 (3.70%)	0 (0.0%)	
	TNBC	Count (%)	7 (12.96%)	1 (14.29%)	
T Stage	1	Count (%)	14 (26.42%)	3 (42.86%)	0.104
	2	Count (%)	35 (66.04%)	4 (42.86%)	
	3	Count (%)	4 (7.55%)	0 (0.0%)	
	4	Count (%)	0 (0.0%)	1 (14.29%)	
N stage	0	Count (%)	7 (13.21%)	3 (42.86%)	**0.001***
	1	Count (%)	27 (50.94%)	0 (0.0%)	
	2	Count (%)	16 (30.19%)	1 (14.29%9	
	3	Count (%)	3 (5.66%)	3 (42.86%)	
Operation		Count (%)	53 (96.36%)	6 (85.71%)	0.306
Adjuvant radiotherapy		Count (%)	51 (92.73%)	6 (85.71%)	0.462
Adjuvant chemotherapy		Count (%)	25(45.45%)	4(57.14%)	0.696
Right pectoralis muscle area		Median (IQR)	1167.3 (365.25)	1107.21 (459.68)	0.345
Left pectoralis muscle area		Median (IQR)	1146.31 (415.81)	1009.94 (597.85)	0.991
Total pectoralis muscle area		Median (IQR)	2357.48 (669.47)	2096.17 (940.32)	0.411
Right pectoralis muscle density		Median (IQR)	16.86 (20)	4.62 (44.6)	0.345
Left pectoralis muscle density		Median (IQR)	-1.1 (6.37)	-1.8 (8.52)	0.714
Total pectoralis muscle density		Median (IQR)	16.47 (15.96)	8.78 (29.84)	0.312
L3 total muscle area		Median (IQR)	10437.48 (2443.31)	9913.43 (3285.17)	0.588
L3 density		Median (IQR)	17.555 (19.77)	15.32 (20.22)	0.863
Skeletal muscle index (SMI)		Median (IQR)	41.95 (10.65)	42.91 (16.97)	0.844
Pectoral muscle index (PMI)		Median (IQR)	945.12 (297.71)	798.72 (439.45)	0.648

** A p-value of 0.05 or lower is considered statistically significant.*

http://doi.org/10.5472/marumj.1484705
Marmara Med J 2024;37(2): 178-184

According to the Cox regression analysis, age was a significant risk factor for mortality; each additional year increasing mortality with an HR of 1.087 (95% CI 1.017-1.162, p=0.015). Similar to patient age, the age at the time of diagnosis significantly affected mortality (HR=1.084, 95% CI 1.016-1.157 and p=0.014). However, BMI (HR=0.853 with 95% CI 0.691-1.052 and p=0.138) and tumour size (HR=1.0113, 95% CI=0.425-2.404 and p=0.980) did not affect mortality risk. Right pectoral muscle area (HR=0.999, 95% CI=0.996-1.002 and p=0.389), left pectoral muscle area (HR= 0.9995, 95%CI 0.997-1.002 and p= 0.736) and total pectoral muscle area (HR=0.9995, 95% CI =0.998-1.001 and p= 0.483) did not significantly affect mortality. Similarly, the average right pectoral muscle density (HR=0.984, 95% CI = 0.946-1.023 and p=0.413), left average pectoral muscle density (HR=1.049, 95% CI=0.907-1.212 and p=0.522) and average total pectoral muscle density (HR=0.986, 95%CI=0.946-1.028 and p=0.506) did not affect mortality. In addition, L3 total muscle area (HR=0.9997, 95% CI= 0.9991-1.0002 and p=0.221), L3 total muscle density (HR=0.994, 95% CI = 0.946-1.044 and p=0.812) and SMI (HR=0.993, 95%CI 0.906-1.089 and p=0.881) did not have a significant effect on mortality. Having a history of surgery (HR=4.807 95% CI= 0.569-40.592 and p=0.149), adjuvant radiotherapy (HR=1.887, 95% CI = 0.227-15.687 and p=0.557) or chemotherapy (HR=0.659, 95%CI= 0.148-2.946 and p= 0.585) had a non-significant effect on mortality.

We stratified patients according to the presence of sarcopenia regarding previous literature by using the thresholds of 38.5 cm^2/m^2 and 31 cm^2/m^2 [7,8,17]. According to the threshold of 38.5 cm^2/m^2, there was no statistically significant difference between the sarcopenic and non-sarcopenic groups in terms of survival functions equality (p=0.909). The Cox regression model using this stratification was not significant (HR=1.101, 95% CI =0.214 – 5.675 and p=0.909). However, there was a statistically significant survival difference between the sarcopenic and non-sarcopenic groups if the 31 cm^2/m^2 threshold was selected (p=0.031) (Figure 2, 3). Nevertheless, the higher risk of mortality of the sarcopenic group compared to the non-sarcopenic group as revealed by the Cox regression model was statistically not significant (HR= 7.389, 95% CI= 0.879-62.124 and p=0.066) (Table II).

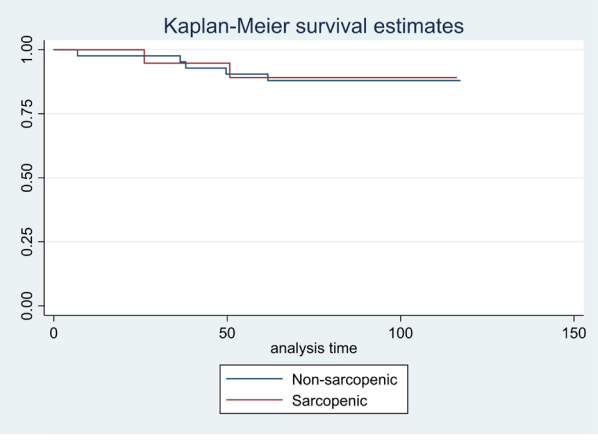

Figure 2. *Kaplan-Meier survival curves for sarcopenic and non-sarcopenic patients according to the threshold of 38.5 cm2/m2*

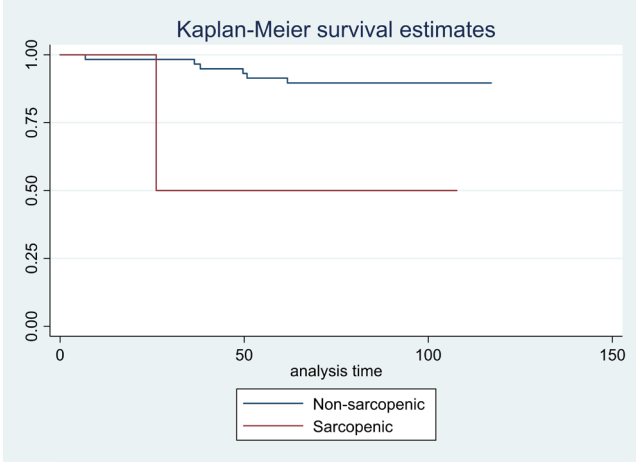

Figure 3. *Kaplan-Meier survival curves for sarcopenic and non-sarcopenic patients according to the threshold of 31 cm2/m2*

Table II. *Univariate Cox regression models for prediction of mortality*

Characteristics	Hazard Ratio with 95% Confidence Interval	P Value
Age	1.087 (1.017-1.162)	**0.015***
Age at diagnosis	1.084 (1.016-1.157)	**0.014***
BMI	0.853 (0.691-1.052	0.138
Tumor size	1.011 (0.425-2.404)	0.980
Right pectoralis muscle area	0.999 (0.996-1.002)	0.389
Left pectoralis muscle area	0.9995 (0.997-1.002)	0.736
Total pectoralis muscle area	0.9995 (0.998-1.001)	0.483
Right pectoral muscle density	0.984 (0.946-1.023)	0.413
Left pectoral muscle density	1.049 (0.907-1.212)	0.522
Total pectoral muscle density	0.986 (0.946-1.028)	0.506
L3 vertebral level total muscle area	0.9997 (0.9991-1.0002)	0.221
L3 vertebral level total muscle density	0.994 (0.946-1.044)	0.812
Skeletal muscle index (SMI)	0.993 (0.906-1.089)	0.881
Pectoral muscle index (PMI)	0.9991 (0.9956-1.0026)	0.604
History of surgery	4.807 (0.569-40.592)	0.149
Adjuvant radiotherapy	1.887 (0.227-15.687)	0.557
Adjuvant chemotherapy	0.659 (0.148-2.946)	0.585
Presence of sarcopenia (Threshold= 38.5 cm^2/m^2)	1.101 (0.214 – 5.675)	0.909
Presence of sarcopenia (Threshold= 31.0 cm^2/m^2)	7.389 (0.879-62.124)	0.066

** A p-value of 0.05 or lower is considered statistically significant.*

3. DISCUSSION

In the present study, we investigated the effect of sarcopenia assessed using pectoral muscle measurements on the survival of patients with non-metastatic breast cancer. Our data indicated that patient age and age at cancer diagnosis were the two prominent risk factors for mortality. Regarding the sarcopenia–survival relationship, no significant difference was found when the SMI threshold of <38.5 cm^2/m^2 was used, but the sarcopenic

http://doi.org/10.5472/marumj.1484705
Marmara Med J 2024;37(2): 178-184

group had a significantly increased mortality risk when the SMI threshold of ≤31 cm^2/m^2 was selected (p = 0.031).

Pectoral muscle measurements have been used to assess sarcopenia and found to be more practical and straightforward compared to the standard way of measuring sarcopenia from the whole muscle area at the abdominal level [9,13]. Go et al., compared pectoral muscle and total skeletal muscle areas at the L3 vertebral level in lymphoma patients and reported that pectoral muscle measurements could also be used to define sarcopenia [17]. They also report that combining pectoral muscle area measurements with L3 vertebral level total muscle area may provide more information to predict a patient's prognosis [17]. Kinsey et al., emphasized the relationship between poor overall survival and low pectoral muscle area in a study involving pectoral muscle measurements on chest CT examinations in patients with small-cell lung cancer. This enabled sarcopenia assessments without the need for additional imaging [18]. In our study, no statistically significant correlation was found between pectoral muscle measurements and survival, which may be due to the small sample size and the younger mean age of the patients compared to the literature [17, 18]. The prediction of sarcopenia based on pectoral muscle measurements in female breast cancer patients and its effect on survival need to be clarified in studies conducted in larger patient groups and among different age groups.

The literature has reported that sarcopenia increases the risk of death in lung, stomach, and colorectal cancer cases [19]. In addition, sarcopenia in cancer patients has been associated with increased chemotherapy toxicity and postoperative complications during treatment [20]. Different results have been reported in the literature regarding the relationship between sarcopenia and breast cancer. Unrelated results may be attributed to the different cancer types and stages of the cases and the different thresholds accepted for sarcopenia during imaging [21]. In a meta-analysis investigating sarcopenia and the causes of mortality in female breast cancer patients, it was recommended that all breast cancer cases be screened for sarcopenia, an important prognostic marker [22].

Among the contrasting results reported in the literature, Del Fabbro et al., investigated sarcopenia, BMI, and survival processes in breast cancer cases and found longer survival rates in sarcopenic cases. They attributed this unexpected result to the fact that chemotherapy toxicity was well tolerated and that the study specifically focused on cases of earlier-stage breast cancer [23]. Our study examined the association between sarcopenia and survival in non-metastatic breast cancer cases by measuring the pectoral muscles. However, we found no significant relationship between sarcopenia and survival based on SMI values calculated from measurements at the L3 vertebral level. This lack of significance at specific threshold values may also be attributed to the inclusion of early-stage cancer cases and a relatively younger female population compared to previous studies in the literature. Additionally, thresholds for sarcopenia differ between populations [16].

The pectoral muscle has also been studied in non-oncological scenarios and can be used to predict prolonged hospitalization and death [24,25]. Recently, during the COVID-19 pandemic, a relationship between pectoral muscle density and disease severity and mortality was reported [26]. In another study, a decrease in pectoral muscle area and density was associated with 30-day mortality in cases of acute pulmonary embolism [27]. Pectoral muscle measurements can also be performed simultaneously in breast MR images obtained in breast cancer cases and have been reported to correlate with CT measurements [9].

Our study identified the patient's current age and their age at breast cancer diagnosis as independent risk factors contributing to an increased mortality risk. The large-scale Health, Eating, Activity, and Lifestyle (HEAL) study conducted by Villasenor et al., also supported the notion that age at diagnosis is a significant risk factor for poor prognosis [28]. Another study revealed that an early age at breast cancer diagnosis, specifically cases diagnosed younger than 35 years, was linked to a poorer prognosis, potentially attributable to cancer type and aggressiveness. Conversely, cases diagnosed older than 65 years, had higher mortality rates, likely due to increased comorbidity and treatment noncompliance [29]. It is important to note that the age at breast cancer diagnosis can vary based on racial, genetic, and environmental risk factors, which may introduce heterogeneity to the results [3].

Studies examining the impact of body mass index (BMI) on survival in cancer cases have yielded varying results, which can be attributed to the specific type of cancer under investigation [30]. Increased BMI is generally considered a risk factor in liver, colon, gallbladder, kidney, endometrium, and ovarian cancers [31]. However, in the case of female breast cancer, the relationship is more complex and influenced by menopausal status [32]. While, obesity during the premenopausal period may exhibit a protective effect in female breast cancer cases, a paradoxical association arises in the postmenopausal period when accompanied by sarcopenia, which poses a mortality risk factor [33,34]. In our study, there was no difference in BMI between the groups, and BMI was not a risk factor for mortality. In evaluating survival in obese oncology patients, the possibility of discordant and unexpected results should be considered by bearing in mind the increased cardiovascular risk, comorbidities, and chemoradiotherapy toxicities seen with an increased BMI [32].

The limitations of our study include its retrospective nature and the small number of patients involved. Another area for improvement was the absence of nationally standardized cut-off values based on radiologic measurements for diagnosing sarcopenia. Large prospective studies involving different age groups in female breast cancer cases are needed to understand the relationship between sarcopenia and breast cancer.

In conclusion, sarcopenia is a prognostically important parameter in female breast cancer cases and can be determined using radiologic imaging methods. In addition to the measurements accepted in the literature, measurements of the pectoral muscle can be used as an alternative method for diagnosing sarcopenia.

http://doi.org/10.5472/marumj.1484705
Marmara Med J 2024;37(2): 178-184

Compliance with Ethical Standards

Ethical approval: The study was approved by the Marmara University School of Medicine Clinical Research Ethics Committee (Protocol no: 09.2023.64, Date: 06.01.2023).

Financial support: The authors have no relevant financial information to disclose.

Conflict of interest: The authors have no conflict of interest to declare.

Authors' contributions: BNK: Project development, Data analysis, Manuscript writing, NM: Data collection, Data management, Conceived and designed the analysis, CI:Performed the analysis, Manuscript editing, HAK and MK: Conceived and designed the analysis, SO and IVB: Data collection, OB: Manuscript editing, Organising and supervising, PFY and HK: Organising and supervising. The manuscript has been read and approved by all authors.

REFERENCES

[1] Sung H, Ferlay J, Siegel RL, et al. Global cancer statistics 2020: GLOBOCAN estimates of incidence and mortality worldwide for 36 cancers in 185 countries. *CA*. CA Cancer J Clin 2021;71:209-49. doi:10.3322/caac.21660

[2] Globocan. Cancer today. International Agency for research. Published 2020. Accessed July 8, 2023. https://gco.iarc.fr/today/fact-sheets-populations

[3] Momenimovahed Z, Salehiniya H. Epidemiological characteristics of and risk factors for breast cancer in the world. Breast Cancer Res Treat 2019;11:151-64. doi:10.2147/BCTT.S176070

[4] Lauby-Secretan B, Scoccianti C, Loomis D, Grosse Y, Bianchini F, Straif K. Body fatness and cancer — Viewpoint of the IARC working Group. N Engl J Med 2016;375:794-8. doi:10.1056/NEJMsr1606602

[5] Muscaritoli M, Anker SD, Argilés J, et al. Consensus definition of sarcopenia, cachexia and pre-cachexia: Joint document elaborated by Special Interest Groups (SIG) " cachexia-anorexia in chronic wasting diseases" and " nutrition in geriatrics." . Clinical Nutr 2010;29:154-9. doi:10.1016/j.clnu.2009.12.004

[6] Morley JE, Baumgartner RN, Roubenoff R, Mayer J, Nair KS. Sarcopenia. J Lab Clin Med 2001;137:231-43. doi:10.1067/mlc.2001.113504

[7] Cruz-Jentoft AJ, Baeyens JP, Bauer JM, et al. Sarcopenia: European consensus on definition and diagnosis: Report of the European Working Group on Sarcopenia in Older People. Age Ageing 2010;39:412-23. doi:10.1093/ageing/afq034

[8] Prado CM, Lieffers JR, McCargar LJ, et al. Prevalence and clinical implications of sarcopenic obesity in patients with solid tumours of the respiratory and gastrointestinal tracts: a population-based study. Lancet 2008;9:629-35. doi:10.1016/S1470-2045(08)70153-0

[9] Rossi F, Valdora F, Barabino E, Calabrese M, Tagliafico AS. Muscle mass estimation on breast magnetic resonance imaging in breast cancer patients: comparison between psoas muscle area on computer tomography and pectoralis muscle area on MRI. Eur Radiol 2019;29:494-500. doi:10.1007/s00330.018.5663-0

[10] Shen W, Punyanitya M, Wang ZM, et al. Total body skeletal muscle and adipose tissue volumes: Estimation from a single abdominal cross-sectional image. J Appl Physiol 2004;97:2333-8. doi:10.1152/japplphysiol.00744.2004

[11] Jones KI, Doleman B, Scott S, Lund JN, Williams JP. Simple psoas cross-sectional area measurement is a quick and easy method to assess sarcopenia and predicts major surgical complications. Colorectal Dis 2015;17:O20-O26. doi:10.1111/codi.12805

[12] Tosato M, Marzetti E, Cesari M, et al. Measurement of muscle mass in sarcopenia: from imaging to biochemical markers. Aging 2017;29:19-27. doi:10.1007/s40520.016.0717-0

[13] Sanders KJC, Degens JHRJ, Dingemans AMC, Schols AMWJ. Cross-sectional and longitudinal assessment of muscle from regular chest computed tomography scans: L1 and pectoralis muscle compared to L3 as reference in non-small cell lung cancer. Int Journal COPD 2019;14:781-9. doi:10.2147/COPD.S194003

[14] Hemke R, Buckless C, Torriani M. Quantitative imaging of body composition. Semin Radiol 2020;24:375-85. doi:10.1055/s-0040.170.8824

[15] Pi-Sunyer FX. Obesity: criteria and classification. Proc Nutr Soc 2000;59:505-9. doi:10.1017/s002.966.5100000732

[16] Lee JS, Kim YS, Kim EY, Jin W. Prognostic significance of CT-determined sarcopenia in patients with advanced gastric cancer. PLoS ONE 2018;13:e0202700. doi:10.1371/journal.pone.0202700

[17] Go SI, Park MJ, Song HN, et al. A comparison of pectoralis versus lumbar skeletal muscle indices for defining sarcopenia in diffuse large B-cell lymphoma – two are better than one. Oncotarget 2017;8:47007-19. doi:10.18632/oncotarget.16552

[18] Kinsey C M, San José Estépar R, van der Velden J, Cole BF, Christiani DC, Washko GR. Lower pectoralis muscle area is associated with a worse overall survival in non–small cell lung cancer. Cancer Epidemiol Biomarkers Prev 2017;26:38-43. doi: 10.1158/1055-9965.EPI-15-1067

[19] Prado CMM, Lieffers JR, McCargar LJ, et al. Prevalence and clinical implications of sarcopenic obesity in patients with solid tumours of the respiratory and gastrointestinal tracts: a population-based study. Lancet 2008;9:629-35. doi:10.1016/S1470-2045(08)70153-0

[20] Aleixo GFP, Williams GR, Nyrop KA, Muss HB, Shachar SS. Muscle composition and outcomes in patients with breast cancer: meta-analysis and systematic review. Breast Cancer Res Treat 2019;177:569-79. doi:10.1007/s10549.019.05352-3

[21] Rossi F, Valdora F, Bignotti B, Torri L, Succio G, Tagliafico AS. Evaluation of body Computed Tomography-determined sarcopenia in breast cancer patients and clinical outcomes: A systematic review. Cancer Treat Res 2019;21:100154. doi:10.1016/j.ctarc.2019.100154

[22] Zhang XM, Dou QL, Zeng Y, Yang Y, Cheng ASK, Zhang WW. Sarcopenia as a predictor of mortality in women with breast cancer: A meta-analysis and systematic review. BMC Cancer 2020;20:172. doi:10.1186/s12885.020.6645-6

[23] Del Fabbro E, Parsons H, Warneke CL, et al. The relationship between body composition and response to neoadjuvant chemotherapy in women with operable breast cancer. Oncologist 2012;17:1240-5. doi:10.1634/theoncologist.2012-0169

[24] McDonald MLN, Diaz AA, Ross JC, et al. Quantitative computed tomography measures of pectoralis muscle area and disease severity in chronic obstructive pulmonary disease. a cross-sectional study. Ann Thorac Surg 2014;11:326-34. doi:10.1513/AnnalsATS.201307-229OC

[25] Teigen LM, John R, Kuchnia AJ, et al. Preoperative pectoralis muscle quantity and attenuation by computed tomography are novel and powerful predictors of mortality after left ventricular assist device implantation. Circ Heart Fail 2017;10:e004069. doi:10.1161/CIRCHEARTFAILURE.117.004069

[26] Hocaoglu E, Ors S, Yildiz O, Inci E. Correlation of pectoralis muscle volume and density with severity of COVID-19 pneumonia in adults. Acad Radiol 2021;28:166-72. doi:10.1016/j.acra.2020.11.017

[27] Meyer HJ, Kardas H, Schramm D, et al. CT-defined pectoralis muscle mass and muscle density are associated with mortality in acute pulmonary embolism. A multicenter analysis. Clin Nutr 2023;42:1036-40. doi:10.1016/j.clnu.2023.04.022

[28] Villaseñor A, Ballard-Barbash R, Baumgartner K, et al. Prevalence and prognostic effect of sarcopenia in breast cancer survivors: the HEAL Study. J Cancer Survivorship 2012;6:398-406. doi:10.1007/s11764.012.0234-x

[29] Foukakis T, Bergh J. Prognostic and predictive factors in early, non-metastatic breast cancer. Dizon Ed UpToDate 2016.

[30] Calle EE, Thun MJ, Petrelli JM, Rodriguez C, Heath CW. Body-mass index and mortality in a prospective cohort of U.S. adults. N Engl J Med 1999;341:1097-105. doi:10.1056/NEJM199.910.073411501

[31] Obesity and overweight. Accessed July 8, 2023. https://www.who.int/news-room/fact-sheets/detail/obesity-and-overweight

[32] Flegal KM, Graubard BI, Williamson DF, Gail MH. Cause-specific excess deaths associated with underweight, overweight, and obesity. JAMA 2007;298:2028-37. doi:10.1001/jama.298.17.2028

[33] Van Den Brandt PA, Spiegelman D, Yaun SS, et al. Pooled analysis of prospective cohort studies on height, weight, and breast cancer risk. Am J Epidemiol 2000;152:514-27. doi:10.1093/aje/152.6.514

[34] White AJ, Nichols HB, Bradshaw PT, Sandler DP. Overall and central adiposity and breast cancer risk in the sister study. Cancer 2015;121:3700-8. doi:10.1002/cncr.29552

MARMARA
MEDICAL JOURNAL

Original Article

https://dergipark.org.tr/tr/pub/marumj

Bone mineral density in patients with Cushing's syndrome

Aysun SEKER [1], Dilek GOGAS YAVUZ[2]

[1] Department of Internal Medicine, School of Medicine, Marmara University, Istanbul, Turkey
[2] Divison of Endocrinology and Metabolism, Department of Internal Medicine, School of Medicine, Marmara University, Istanbul, Turkey

Corresponding Author: Aysun SEKER
E-mail: dr.aysunozdemir@hotmail.com

Submitted: 27.02.2023 **Accepted:** 25.10.2023

ABSTRACT

Objective: Cushing's syndrome is caused by the excessive secretion of cortisol or the intake of exogenous cortisol. Morbidity caused by osteoporosis is a major complication that cannot be ignored. We conducted a study to evaluate bone density and fracture risk factors in patients with Cushing's syndrome.

Patients and Methods: This retrospective case-control study involved 176 patients diagnosed with Cushing's syndrome [153 female and 34 male patients] and 84 controls [72 female and 12 male patients]. Patients admitted to the clinics within the last eight years were included in the analysis. We collected demographic, clinic laboratory data, and bone densitometry measurements from electronic patient files. The classification of patients into normal, osteopenia, or osteoporosis groups is determined by their Body Mineral Density measurements based on the World Health Organization criteria.

Results: Among the patients, 135 were diagnosed with Cushing's disease and 41 with adrenal adenomas. Patients with Cushing' syndrome showed a higher incidence of osteopenia (11.4%) and osteoporosis (2.8%) when compared to the control group. No osteoporosis cases were found in the control group, while nine cases of osteopenia were detected. Osteopenia was significantly more common in adrenal adenoma patients than in those with pituitary Cushing's disease. Osteopenia was present in 39.1% of adrenal Cushing's patients, with only 8.7% (n = 2) having osteoporosis. Osteopenia was observed in 11 patients (23.4%) with pituitary Cushing's disease, while only 4 patients (8.5%) had osteoporosis.

Conclusions: Osteopenia is more prevalent in patients with adrenal Cushing's syndrome.

Keywords: BMD, Bone, Cushing's syndrome, Low bone density, Osteopenia, Osteoporosis

1. INTRODUCTION

Cushing's syndrome (CS) is a pathological condition that is characterized by hypercortisolemia of various origins. Etiologic causes of the syndrome can vary from long-term glucocorticoid utilization (results with iatrogenic CS), corticotropin-releasing hormone (CRH), and adrenocorticotropic hormone (ACTH) secretion either from pituitary or non-pituitary sources (results with endogenic CS). Although, it is less common, excessive glucocorticoid secretion from the adrenal gland is also described in the disease pathophysiology [1].

Numerous complications and related treatments associated with hypercortisolism are well described. All discussion aside, today, early detection and intervention still weigh their importance in successfully managing long-term complications [2].

Osteopenia and osteoporosis are considered common comorbidities in Cushing's syndrome patients, with an estimated frequency between 60-80% and 30-65% of various Cushing's syndrome populations [3]. Skeletal complications manifesting with uncoupled suppressed bone formation and enhanced bone resorption contribute to distinct skeletal damage, accelerating the vertebral fracture risk. Bone mineral density (BMD) is a routine part of Cushing's patient evaluation. Vertebral fractures (VF) are frequently reported and may occur even in patients with mild reduction of BMD results [5,6].

Bone fractures caused by Cushing's syndrome are scarce, despite extensive literature [7-10]. These fractures most commonly occur in the thoracic and lumbar vertebrae, hip, ribs, and pelvis. Fracture development is not uncommon after spontaneous or low-energy trauma. Articles also mention that the risk of fracture increases two years prior to the diagnosis of Cushing's disease, and the risk can be normalized with appropriate treatment [11]. Routine thoracolumbar spinal radiographs in patients with Cushing's disease demonstrate that 76% of patients have vertebral fractures at any time of the disease, and 48% are reported as asymptomatic [8].

How to cite this article: Seker A, Yavuz Gogas D. Bone mineral density in patients with Cushing's syndrome. Marmara Med J 2024: 37(2):185-191. doi: 10.5472/marumj.1485351

ISSN: 1309-9469

http://doi.org/10.5472/marumj.1485351
Marmara Med J 2024;37(2): 185-191

In this study, we aimed to evaluate BMD measurements and bone metabolism markers in our group of patients diagnosed with Cushing's disease and cortisol-secreting adrenal adenoma.

2. PATIENTS and METHODS

Patients

The study protocol was approved by the Marmara University Medical School Ethics Committee (09.2017.118) and conducted following the International Conference on Harmonization Guidelines for Good Clinical Practice and the Declaration of Helsinki.

One hundred seventy-six patients diagnosed with Cushing's disease, admitted to the Marmara University Pendik Training and Research Hospital between January 2010 to February 2018 were included in this retrospective study. A control group (n = 84) was selected by matching sex and age distribution with no Cushing's disease diagnosis, sourced from available study datasets from the same healthcare facility.

The sample size was calculated as 260 subjects prior to the study implementation. The 2:1 ratio resulted in 176 and 84 sample sizes in the case and control groups.

Methods

Data included demographic data (age, sex), laboratory tests performed within the diagnosis and treatment timespan, including basal cortisol, 1 mg dexamethasone suppression test, 24-hour urine-free cortisol, adrenocorticotropic hormone (ACTH), thyroid-stimulating hormone, (TSH), thyroxine (T4), follicle-stimulating hormone (FSH), luteinizing hormone (LH), prolactin (PRL), calcium (Ca), phosphorus(P), parathormone (PTH), 25-OH Vitamin D, fasting blood sugar, hemoglobin A1C (HbA1C), triglyceride (TG), high-density lipoprotein (HDL), low-density lipoprotein (LDL) levels and radiological (adrenal and pituitary MRI findings, bone mineral densitometry) assessments.

Parameters and techniques used for each subject were confirmed solely. 24-hour urine-free cortisol, ACTH, TSH, T4, FSH, LH, PRL, and 25-OH vitamin D were studied by chemiluminescence immunoassay (CLIA). Ca was studied with Schwarzenbach by the o-cresolphthaleincomplexone. P level was studied by ammonium molybdate. HbA1C was studied by boranate affinity chromatography. Fasting blood sugar was studied by enzymatic UV test (hexokinase method).

Bone mineral density (BMD) was analyzed by dual-energy X-ray absorptiometry (DXA). Within DXA assessment, L1 – L4 was measured in anteroposterior projection (AP), additionally for right and left hip assessment Lunar DPX-L (GE-Lunar Corp., Madison, WI) was used. Coefficient of variation (CV) was set to 1.0%. According to World Health Organization criteria, osteopenia was defined as BMD values over 1.0 and less than 2.5 standard deviation from reference mean values. Osteoporosis was defined as 2.5 or more deviation from reference BMD values (T score less or equal to −2.5 SD).

Hypercortisolism was evaluated with 1 mg dexamethasone suppression test, 24-hour urine free cortisol and midnight cortisol levels. 2x2 mg dexamethasone suppression test and inferior petrosal sinus sampling were used to confirm both the diagnosis and detect the pathological location.

Statistical Analysis

IBM SPSS 23 software was used to analyze the collected data. Descriptive statistics were presented as mean and standard deviation for continuous variables. Categorical variables were interpreted as counts and percentages. Appropriate chi-square ($\chi 2$) test or Fisher's exact test were selected for categorical data analysis. Student's t-test used for parametric variables. Spearman rank correlation was utilized to reveal variable associations. The results were evaluated at a 95% confidence interval. Post hoc analysis based on contingency tables, using GPower (Version 3.1.9.7, HHU) found that the study power (1-β) was 0.986 (ω = 0.314, N = 176, df = 1). p

3. RESULTS

One hundred seventy-six patients with Cushing's syndrome were included in the study. Of the included subjects, 153 (86.9%) were female, and 23 (13.1%) were male. The mean age was calculated as 50.52 (± 0.97) in females, 51.65 (± 3.09) in males, and 50.66 (± 0.93) in the whole case group.

Table I. *Baseline characteristics of Cushing's patients*

	Total (n = 176)	Female (n = 153)	Male (n = 23)	p
Age	50.66 (± 0.93)	50.52 (± 0.97)	51.65 (± 3.09)	0.729
Age at diagnosis	44.96 (± 0.99)	44.74 (± 1.04)	46.43 (± 3.15)	0.563
Disease location				
Pituitary	76.3 % (n = 135)	77.4 % (n = 119)	68.2 % (n = 16)	0.266
Adrenal	23.1 % (n = 41)	21.9 % (n = 34)	68.2 % (n = 7)	
Pituitary Adenoma				
Macroadenoma	19.3 % (n = 26)	20.5 % (n = 24)	14.3 % (n = 2)	0.845
Microadenoma	62.2 % (n = 84)	60.3 % (n = 72)	71.4 % (n = 12)	
Comorbidities				
Diabetes Mellitus	47.2 % (n= 83)	47.7 % (n = 73)	43.5 % (n = 10)	0.440
Hypertension	57.9 % (n =102)	58.2 % (n = 89)	60.8 % (n = 14)	0.497
Hyperlipidemia	**59.1 % (n =104)**	**62.7 % (n = 96)**	**34.8 % (n = 8)**	**0.012**
Obesity	57.4 % (n =101)	56.9 % (n = 87)	60.9 % (n = 14)	0.449
Central Hypogonadism	13.7 % (n=24)	13.8 % (n = 21)	13.0 % (n = 3)	0.610
Physical Examination				
BMI	35.74 (± 0.99)	35.95 (± 1.09)	33.94 (± 1.10)	0.206
Systolic BP	136.47 (± 2.24)	136.30 (± 2.45)	138.0 (± 4.44)	0.746
Diastolic BP	86.27 (± 1.61)	86.21 (± 1.71)	86.83 (± 5.08)	0.911

BMI: Body Mass Index, BP: Blood Pressure

http://doi.org/10.5472/marumj.1485351
Marmara Med J 2024;37(2): 1-191

Considering the pathologic aspects, lesions in pituitary gland were detected in 135 patients (76.3%) whereas, 41 (23.1%) patients had adrenal adenoma. In Cushing's disease with pituitary pathophysiology, macroadenoma was detected in 20.5% (n = 15) of female and 14.3% (n = 1) of male patients, and again, microadenoma frequency was 60.3% (n = 44) and 71.4% (n = 5) respectively. Macroadenoma and microadenoma were observed in 20% (n = 16) and 61.3% (n = 49) of the pituitary Cushing's patients, respectively. Although, microadenoma was more common in each group, no statistical significance could be shown between the sexes. A significant difference was observed in age at diagnosis (Adrenal: 44.96 vs. Pituitary: 43.63; p = 0.015). Student's t-test results revealed that patients with pituitary pathophysiology were diagnosed earlier. Except for the age of diagnosis, no significant difference was found between the sex of the patients, bone densitometry measurements, and other biochemical results (Table I).

The most common comorbidities in Cushing's group were hyperlipidemia (59.1%), hypertension (57.9%), obesity (57.4%), and diabetes mellitus (47.0%). Central hypogonadism (13.7%) was noted as the least frequent comorbidity. Analysis of demographic data revealed that the mean BMI was 35.74 (±0.99), and systolic and diastolic blood pressure were 136.47 (±2.24) and 86.27 (±1.61), respectively (Table I).

Table II. *Biochemistry and bone metabolism results of Cushing's patients*

	Total (n = 176)	Female (n = 153)	Male (n = 23)	p
Biochemistry Results				
ACTH	52.67 (± 4.58)	54.61 (± 5.00)	37.82 (± 9.99)	0.144
24 H Free Urine Cortisol	373.49 (± 39.58)	381.40 (± 43.69)	310.80 (± 70.80)	0.631
1 mg Dx Cortisol	10.36 (± 0.72)	10.44 (± 0.76)	9.88 (± 2.12)	0.804
2 mg Dx Cortisol	9.71 (± 0.99)	10.11 (± 1.09)	6.75 (± 1.89)	0.141
8 mg Dx Cortisol	5.41 (± 0.78)	5.37 (± 0.85)	5.76 (± 2.01)	0.859
TSH	**1.54 (± 0.10)**	**1.62 (± 0.11)**	**1.00 (± 0.20)**	**0.010**
T4	1.59 (± 0.19)	1.62 (± 0.22)	1.32 (± 0.16)	0.266
FSH	**16.92 (± 2.03)**	**18.01 (± 2.26)**	**8.89 (± 2.51)**	**0.010**
LH	**10.53 (± 1.20)**	**11.29 (± 1.34)**	**5.15 (± 1.28)**	**0.002**
PRL	**22.10 (± 3.98)**	**18.75 (± 1.78)**	**43.80 (± 27.54)**	**0.032**
FBG	111.46 (± 3.21)	112.44 (± 3.54)	104.96 (± 6.97)	0.345
HbA1C	6.28 (± 0.12)	6.31 (± 0.13)	5.99 (± 0.23)	0.224
Bone Metabolism Results				
Ca	9.40 (± 0.05)	9.40 (± 0.05)	9.39 (± 0.13)	0.926
P	3.50 (± 0.05)	3.55 (± 0.05)	3.19 (± 0.14)	**0.010**
PTH	57.87 (± 3.66)	56.13 (± 3.22)	71.07 (± 20.13)	0.192
25 – OH D Vitamin	18.67 (± 0.97)	18.70 (± 1.06)	18.47 (± 2.31)	0.928

ACTH: Adrenocorticotropic hormone, H: Hour, Dx: Dexamethasone, TSH: Thyroid stimulating hormone, T: Thyroid Hormone, FSH: Follicle-stimulating hormone, LH: Luteinizing hormone, PRL: Prolactin, FBG: Fasting blood glucose, HbA1C: Hemoglobin A1C, Ca: Calcium, P: Phosphor, PTH: Parathormone

Table II shows the differences between sexes in the biochemistry test results in Cushing's patients. TSH (p = 0.01), FSH (p = 0.01), LH (p = 0.002), and PRL (p = 0.032) levels varied between sexes. Cortisol levels in 1, 2, and 8 mg dexamethasone suppression tests were similar in both sexes. In contrast to cortisol values, 24-hour urinary-free cortisol levels were higher in women with 381.40 ug/day (± 43.69; p = 0.631). However, no significant difference has been shown between male and female patients.

Both biochemical tests and bone densitometry measurements were examined to analyze bone metabolism (Table II). Serum levels of Ca, P, PTH, and 25-OH vitamin D are given by age group. A significant difference was found only between P levels in sex groups. P levels were 3.55 mg/dL (± 0.05) in females, 3.19 mg/dL (± 0.14) in males, and 3.50 mg/dL (± 0.05) in the whole case group. P levels in male patients were significantly lower (p = 0.01).

Table III. *Bone marker results and interpretations of case and control groups*

	Case Group		Control Group		p
	Female (n = 85)	Male (n = 13)	Female (n = 72)	Male (n = 12)	
Bone Densitometry Results					
Femur Neck BMD	0.847 (± 0.017)	0.892 (± 0.036)	0.983 (± 0.155)	0.982 (± 0.143)	0.972
Femur Neck T Score	-0.399 (± 0.138)	-1.100 (± 0.297)	0.266 (± 1.281)	-0.383 (± 1.066)	0.810
Femur Neck Z Score	-0.343 (± 0.121)	-0.430 (± 0.175)	0.262 (± 1.097)	-0.025 (± 1.039)	0.844
L1 – L4 BMD	1.062 (± 0.040)	1.197 (± 0.773)	1.131 (± 0.153)	1.146 (± 0.144)	0.154
L1 – L4 T Score	-0.720 (± 0.149)	0.380 (± 0.586)	-0.117 (± 1.243)	0.267 (± 1.174)	0.801
L1 – L4 Z Score	-0.511 (± 0.182)	0.413 (± 0.672)	-	-	0.610
Patients based on Bone Density					
Low Bone Density*	5.9% (n = 5)	0.0% (n = 0)	0.0% (n = 0)	0.0% (n = 0)	0.160
Osteopenia	**16.5% (n = 14)**	**46.1% (n = 6)**	**11.1% (n=8)**	**8.3% (n = 1)**	**<0.001**
Osteoporosis	7.1% (n = 6)	0.0% (n = 0)	0.0% (n = 0)	0.0% (n = 0)	0.979

**Assessed by Z score, BMD: Bone mineral density*

Bone mineral density tests were encountered only in 98 patients in case groups, thus, we ran the analysis, considering this limitation. Although, high standard error occurred in BMD analysis, L1-4 T score differed in sex groups, being higher in males (p = 0.801). No significant difference was found in the femoral neck measurements (Table III).

Osteoporosis was less common than osteopenia in both sex subgroups. While, 16.5% of female patients had osteopenia, only 7.1% (n = 6) had osteoporosis. Similarly, 46.1% of male patients had osteopenia, and no patients with osteoporosis were recorded. In addition, low bone density was only found

in women at the rate of 5.9%. The chi-square test was used for osteopenia, and no statistically significant difference was found between the sex groups. Also, bone densitometry data of the patients in the control group revealed no significant difference between sex subgroups (Table III).

Table IV. *Bone marker results and interpretations of Cushing's syndrome patients by pathology locations*

	Adrenal (n = 41)	Pituitary (n = 134)	p
Femur Neck BMD	0.851 (± 0.350)	0.853 (± 0.279)	0.972
Femur Neck T Score	-0.888 (± 0.279)	-0.888 (± 0.141)	0.810
Femur Neck Z Score	-0.388 (± 0.249)	-0.339 (± 0.121)	0.844
L1 – L4 BMD	0.988 (± 0.088)	1.107 (± 0.039)	0.154
L1 – L4 T Score	-0.668 (± 0.375)	-0.581 (± 0.155)	0.801
L1 – L4 Z Score	-0.558 (± 0.450)	-0.326 (± 0.205)	0.610
Low Bone Density	11.1 % (n = 2)	3.4 % (n = 3)	0.160
Osteopenia	**39.1 % (n = 9)**	**23.4 % (n = 11)**	**< 0.001**
Osteoporosis	8.7 % (n = 2)	8.5 % (n = 4)	0.979

BMD: Bone mineral density

We also investigated low bone density, osteopenia, and osteoporosis in terms of Cushing's localization. In a similar fashion, osteoporosis was less common than osteopenia in both pituitary and adrenal groups. Osteopenia was present in 39.1% of adrenal Cushing's patients, with only 8.7% (n = 2) having osteoporosis. Whereas 23.4% of pituitary Cushing's patients had osteopenia, osteoporosis was recorded in 8.5%. However, low bone density is observed in 11.1% and 3.4% in adrenal and pituitary Cushing's patients. There was a statistically significant difference between the adrenal and pituitary Cushing's patients regarding osteopenia ($p < 0.001$) (Table IV).

In general, bone density measurements were lower in the case group compared to the control group. Within line with the study findings, osteoporosis was less frequent than osteopenia in both groups. While osteopenia was observed in 11.4% to 10.7% of the patients in the case and control groups, respectively, 2.8% (n = 5) of the case group had osteoporosis, and none encountered it in control. Also, low bone density appears to be around 2.8% in the case group, with none reported in the control.

Table V: *Correlations between bone narrow density biochemistry markers*

	Femur Neck BMD	p	L1 – L4 BMD	p
24 H Free Urine Cortisol	0.02	0.458	– 0.08	0.305
Basal ACTH	– 0.25	0.059	**– 0.28**	**0.039**
BMI	**0.45**	**0.002**	**0.29**	**0.036**
1 mg DST	**– 0.25**	**0.017**	-0.12	0.252

H: Hour, ACTH: Adrenocorticotropic hormone, BMI: Body mass index, DST: Dexamethasone

Collected data were further analyzed to reveal possible correlations in Table V. The analysis observed correlation between 24-hour urine cortisol, 1 mg dexamethasone suppression test results, and BMI and BMD values. Femur neck BMD and BMI indicated a moderate-to-high correlation. Also, an increase in BMI was aligned with an increase in both the femur neck and L1 L4 BMD values. The correlation between the suppression test of 1 mg dexamethasone and the femoral neck BMD was statistically significant ($p = 0.017$).

The mean 24-hour urinary cortisol level was 373.49 (± 39.58) in the whole case group, 381.40 (± 43.69) in females, and 310.80 (± 70.80) in male patients. Mean ACTH levels were 52.67 (± 4.58) in all patients, 54.61 (± 5.00) in females, and 37.82 (± 9.99) in males.

4. DISCUSSION

This study was conducted on a large group of Cushing's syndrome patients admitted to a single health facility. The ratio of female patients had a higher frequency of 3–8:1 compared to males [11,12]. Our findings were similar to other published findings. The female/male patient ratio in the study population was 6:1. Published papers stated that the community-based incidence of Cushing's disease is 2-3, and the prevalence is believed to be around 40 in 1.000,000 individuals.

The number of Cushing's patients investigated in this study was 176. This number can be considered relatively high compared to other studies on Cushing's disease published in the last five years. In our patient group, the average age at diagnosis was 44. Although, there was no significant difference between the sexes, women were diagnosed 1.5 years earlier. We had an elderly patient group when compared to the patient groups of published articles (44 vs 30-40 years of age); this can be attributed to the fact that our study center is positioned as a third-level treatment facility in current healthcare access policies [13]. We can assume that the patients we have encountered in our study either had an earlier final or differential diagnosis in low-level healthcare facilities. Patients may have to endure a lengthy process to receive an accurate diagnosis because of the current referral system. The older age of the study population may cause a bias in terms of bone density and comorbidity.

Pituitary Cushing's disease was diagnosed in 76.3% of the study patients and adrenal Cushing's disease in 23.1%. Only one male patient was diagnosed with ectopic Cushing's disease and the age at diagnosis was 55. Although, pituitary Cushing's disease was more common in both sexes, male patients had lower frequency than female patients. Previous studies reported the rate of pituitary Cushing's disease around 60-80% and adrenal Cushing's disease between 15-35% [14 – 17]. In this respect, our study was compatible with the literature.

Microadenoma was observed in 61.3% of the patients, with a higher incidence in males (71.4%). Some studies showed that the ratio of microadenoma / macroadenoma was 65 – 90% [17,18].

In general, articles reported hypertension frequency in Cushing's disease within the range of 45-100%. Diabetes was 25-68.8%, obesity was 32.1-75% and dyslipidemia was 9.1-71.4% among Cushing's patients [19]. Also, male sex had a higher risk of hypertension and dyslipidemia [20]. Data of our study showed that hyperlipidemia (59.1%) was the most common comorbidity in study cases. Hyperlipidemia was observed twice as often in women than in men. Our findings partially supported the recent literature.

Fasting blood sugar (FBS), HbA1c, and cholesterol were also examined in context with the study. Mean FBS (111.46 ± 3.21),

http://doi.org/10.5472/marumj.1485351
Marmara Med J 2024;37(2): 1-191

mean HbA1C (6.28 ± 0.12), and mean total cholesterol (223.19 ± 4.06) levels were recorded for the case group. Measurements did not vary between the sexes. Liu's study with 73 Cushing's patients presented similar results, with no significant difference between males and females [21].

In our study, neither urinary cortisol nor ACTH levels differed between sexes. Contradictory data were published in 2014. A study on 67 Cushing's patients concluded that ACTH and urinary cortisol levels were higher in males [20].

Statistical analysis revealed a significant difference between the male and female case groups regarding L1-4 T scores. We concluded that the location of the mass in Cushing's disease patients and sex did not affect other measurements. The L1-4 BMD scores were the only measurement we found to be different between the case and control groups. The case group had lower scores in all parameters. The difference between the femur neck T score was especially higher than the other BMD scores. The femur neck T score average was – 0.836 (± 0.126) in the case group, while it was 0.172 (± 0.141) in the control.

A study by Apaydın et al., reported that femoral neck BMD (but not lumbar BMD) was independently associated with age, BMI, and PTH levels. Our findings regarding BMI association with BMD were compatible with the literature [22].

Mancini et al., in 2004, stated that osteoporosis caused by glucocorticoids might be reversible, but at least ten years of treatment was required for the normalization of BMD values [23]. Kawamata et al., observed an improvement in BMD values within three months after surgical intervention [24]. Di Somma and Colao suggested that alendronate treatment was more effective in improving BMD values than cortisol normalization [25].

We also investigated the bone densitometry measurements of the patients according to age. Although, patients with low bone density were more common in the our case group, the statistical inferences obtained were not considered strong enough to implement. Since, patients with low bone density and osteoporosis could not be detected in the control group, we hesitate to form a conclusion. Valassi et al., conducted a multicenter observational study in 620 Cushing's patients, which provides essential evidence regarding bone-related morbidities. In the study, osteopenic findings were detected in the spine at 40% and in the hips at 46% of the patients [26]. Our study results had a much lower rate (20.4%) of osteopenia. Another article published in 2010 reported that the prevalence of osteoporosis was between 30 and 67% in Cushing's patients [27]. Rates of osteoporosis / vertebral fracture varied between 24% and 68.8% in other studies in the literature [28]. In our patient group, osteopenia was observed more frequently in adrenal Cushing's patients than in pituitary Cushing's patients ($p = <0.001$).

A 2021 study conducted on 135 patients reported 75% vertebral fractures. In the same study, 40% of patients with vertebral fractures had normal bone mineral densitometry results [29]. Various studies reported that osteoporotic fracture prevalence was up to 50% and, in this setting, 15% of all patients with Cushing's syndrome also experienced non-traumatic peripheral fractures at the wrist, humerus, elbow, hip, patella, and ankle [11,30].

Miwa Kmura et al., in 2022, stressed that 24-hour urinary cortisol follow-up in patients with adrenal Cushing's disease had a significant and negative correlation with lumbar BMD [31]. Again in 2015, a study by Belaya et al., reported a significant association between plasma and urinary cortisol levels and osteoporosis and vertebral fracture [32]. In another study conducted in 2006 observed that more and more severe vertebral fractures were detected in cases with similar urinary cortisol excretion [33]. Our study also found the same interpretations in 24-hour urinary cortisol excretion and lumbar BMD ($p <0.05$).

Our study included 176 Cushing's patients who had been followed up in the Department of Endocrinology at Marmara University for the past 10 years. Compared to recent studies, our study had a high number of patients with Cushing's syndrome.

The age at diagnosis may be higher than what is described in the literature because our hospital is a third-level health center. The situation causes bias, particularly in regard to comorbidity and bone density. The patient and control groups both have missing data, which presents another challenge. Another limitation of this study is the low count of male patients and the presence of only one patient with ectopic Cushing's disease. The study's generalizability is limited by the retrospective nature of the study design.

Conclusion

In this study, our findings support the current literature that pituitary and adrenal Cushing's disease increases the risk of osteoporosis and osteopenia. Study analyses showed that osteopenia was more common in adrenal Cushing's patients than in pituitary Cushing's patients. Also, we encountered significant reverse correlations between femoral neck median BMD measurements, BMI, 24-hour urine cortisol level, and 1 mg dexamethasone suppression test. This correlation may be helpful in current clinical practice and in treating physicians to investigate possible fractures in relevant patients.

The study by design is limited to comprehensive interpretations. Writers suggest multicenter prospective studies with a larger sample size to gain strong evidence and better understand the disease.

Compliance with Ethical Standards

Ethical approval: The study was approved by the Marmara University, School of Medicine Clinical Research Ethics Committee (Reference no: 09.2017.118). The study was conducted in accordance with the World Medical Association Declaration of Helsinki and Good Clinical Practices Guidelines.

Funding: This study did not receive any specific grants from funding agencies in the public, commercial, or not-for-profit sector.

Conflict of interest: Both authors have no conflict of interest to declare.

Authors' contributions: AS and DGY: Made substantial contributions to the conception and design, and/or acquisition

of data, and/or analysis and interpretation of data, participated in drafting the article or revising it critically for important intellectual content, and gave final approval of the version to be submitted.

REFERENCES

[1] TEMD. Adrenal ve Gonadal Hastalıklar Kılavuzu. Ankara: Bayt Bilimsel Araştırmalar Basın Yayın Ltd. Şti, 2018: 17-37.

[2] Limumpornpetch P, Morgan AW, Tiganescu A, et al. The effect of endogenous cushing syndrome on all-cause and cause-specific mortality. J Clin Endocrinol Metab 2022; 107:2377-88. doi: 10.1210/clinem/dgac265.

[3] Fleseriu M, Auchus R, Bancos I, et al. Consensus on diagnosis and management of cushing's disease: a guideline update. Lancet Diabetes Endocrinol 2021; 9:847-75. doi: 10.1016/S2213-8587(21)00235-7.

[4] Schmid HA. Pasireotide (SOM230): development, mechanism of action and potential applications. Mol Cell Endocrinol 2008; 286:69-74. doi: 10.1016/j.mce.2007.09.006.

[5] Mazziotti, G, Giustina, A. Glucocorticoid-induced osteoporosis. Osteoporosis in men (Second Edition) 2010; 415 – 21. doi.org/10.1016/B978-0-12-374602-3.00034-1.

[6] Mancini T, Doga M, Mazziotti G, Giustina A. Cushing's syndrome and bone. Pituitary 2004; 7:249-52. doi: 10.1007/s11102.005.1051-2.

[7] Biller BM, Grossman AB, Stewart PM, et al. Treatment of adrenocorticotropin-dependent Cushing's syndrome: a consensus statement. J Clin Endocrinol Metab 2008; 93:2454-62. doi: 10.1210/jc.2007-2734.

[8] Newell-Price J, Trainer P, Perry L, Wass J, Grossman A, Besser M. A single sleeping midnight cortisol has 100% sensitivity for the diagnosis of cushing's syndrome. Clin Endocrinol (Oxf) 1995; 43:545-50. doi: 10.1111/j.1365-2265.1995.tb02918.x.

[9] Chandler WF, Schteingart DE, Lloyd RV, McKeever PE, Ibarra-Perez G. Surgical treatment of cushing's disease. J Neurosurg 1987; 66:204-12. doi: 10.3171/jns.1987.66.2.0204.

[10] Buliman A, Tataranu LG, Paun DL, Mirica A, Dumitrache C. Cushing's disease: a multidisciplinary overview of the clinical features, diagnosis, and treatment. J Med Life 2016; 9:12-8.

[11] Vestergaard P, Lindholm J, Jørgensen JO, et al. Increased risk of osteoporotic fractures in patients with cushing's syndrome. Eur J Endocrinol 2002; 146:51-6. doi: 10.1530/eje.0.1460051.

[12] Trementino L, Appolloni G, Ceccoli L, et al. Bone complications in patients with cushing's syndrome: looking for clinical, biochemical, and genetic determinants. Osteoporos Int 2014; 25:913-21. doi: 10.1007/s00198.013.2520-5.

[13] Warriner AH, Saag KG. Glucocorticoid-related bone changes from endogenous or exogenous glucocorticoids. Curr Opin Endocrinol Diabetes Obes 2013; 20:510-6. doi: 10.1097/01.med.000.043.6249.84273.7b.

[14] Lekamwasam S, Adachi JD, Agnusdei D, et al. A framework for the development of guidelines for the management of glucocorticoid-induced osteoporosis. Osteoporos Int 2012; 23:2257-76. doi: 10.1007/s00198.012.1958-1.

[15] Lacroix A, Feelders RA, Stratakis CA, Nieman LK. Cushing's syndrome. Lancet 2015; 386(9996):913-27. doi: 10.1016/S0140-6736(14)61375-1.

[16] Valassi E, Santos A, Yaneva M, et al. The european registry on cushing's syndrome: 2-year experience. Baseline demographic and clinical characteristics. Eur J Endocrinol 2011; 165:383-92. doi: 10.1530/EJE-11-0272.

[17] Füto L, Toke J, Patócs A, et al. Skeletal differences in bone mineral area and content before and after cure of endogenous cushing's syndrome. Osteoporos Int 2008; 19:941-9. doi: 10.1007/s00198.007.0514-x.

[18] Pivonello R, De Leo M, Vitale P, et al. Pathophysiology of diabetes mellitus in cushing's syndrome. Neuroendocrinology 2010; 92 Suppl 1:77-81. doi: 10.1159/000314319.

[19] Zografos GN, Perysinakis I, Vassilatou E. Subclinical Cushing's syndrome: current concepts and trends. Hormones (Athens) 2014; 13:323-37. doi: 10.14310/horm.2002.1506.

[20] Zilio M, Barbot M, Ceccato F, et al. Diagnosis and complications of Cushing's disease: gender-related differences. Clin Endocrinol (Oxf) 2014; 80:403-10. doi: 10.1111/cen.12299.

[21] Liu X, Zhu X, Zeng M, et al. Gender-specific differences in clinical profile and biochemical parameters in patients with cushing's disease: a single center experience. Int J Endocrinol 2015; 2015:949620. doi: 10.1155/2015/949620.

[22] Melmed S, Williams RH. Pituitary. In: Melmed S, Polonsky KS, Larsen RP, Kronenberg MH, eds. Williams Textbook of Endocrinology. Chapter 8. 12th Edition. Philadelphia: Elsevier, 2011: 12.

[23] Hur KY, Kim JH, Kim BJ, et al. Clinical guidelines for the diagnosis and treatment of cushing's disease in korea. Endocrinol Metab (Seoul) 2015; 27:30:7-18. doi: 10.3803/EnM.2015.30.1.7.

[24] Arnaldi G, Angeli A, Atkinson AB, et al. Diagnosis and complications of cushing's syndrome: a consensus statement. J Clin Endocrinol Metab 2003; 88:5593-602. doi: 10.1210/jc.2003-030871.

[25] Nieman LK, Biller BM, Findling JW, et al. The diagnosis of cushing's syndrome: an endocrine society clinical practice guideline. J Clin Endocrinol Metab 2008; 93:1526-40. doi: 10.1210/jc.2008-0125.

[26] Heyn J, Geiger C, Hinske CL, et al. Medical suppression of hypercortisolemia in cushing's syndrome with particular consideration of etomidate. Pituitary 2012; 15:117-25. doi: 10.1007/s11102.011.0314-3.

[27] Kaltsas G, Makras P. Skeletal diseases in cushing's syndrome: osteoporosis versus arthropathy. Neuroendocrinology 2010; 92 Suppl 1:60-4. doi: 10.1159/000314298.

[28] Hamrahian AH, Yuen KC, Hoffman AR, et al. AACE/ACE disease state clinical review: medical management of cushing disease. Endocr Pract 2014; 20:746-57. doi: 10.4158/EP14147.RA.

[29] Dillard TH, Gultekin SH, Delashaw JB Jr, et al. Temozolomide for corticotroph pituitary adenomas refractory to

standard therapy. Pituitary 2011; 14:80-91. doi: 10.1007/s11102.010.0264-1.

[30] Colao A, Petersenn S, Newell-Price J, et al. A 12-month phase 3 study of pasireotide in cushing's disease. N Engl J Med 2012 8; 366:914-24. doi: 10.1056/NEJMoa1105743.

[31] Elamin MB, Murad MH, Mullan R, et al. Accuracy of diagnostic tests for cushing's syndrome: a systematic review and metaanalyses. J Clin Endocrinol Metab 2008; 93:1553-62. doi: 10.1210/jc.2008-0139.

[32] Carroll TB, Aron DC, Findling JW, Tyrrell B. Chapter 9. Glucocorticoids and adrenal androgens. Chapter 9. In: Gardner DG, Shoback D. eds. Greenspan's Basic and Clinical Endocrinology. The McGraw-Hill Companies: 2011.

[33] Starke RM, Reames DL, Chen CJ, Laws ER, Jane JA Jr. Endoscopic transsphenoidal surgery for cushing disease: techniques, outcomes, and predictors of remission. Neurosurgery 2013; 72:240-7. doi: 10.1227/NEU.0b013e31827b966a.

MARMARA
MEDICAL JOURNAL

Original Article

https://dergipark.org.tr/tr/pub/marumj

Assessment of macular microcirculation in patients with multiple sclerosis by swept-source optical coherence tomography angiography

Serhat EKER[1], Yalcin KARAKUCUK[2], Haluk GUMUS[3]

[1] Ophthalmology Clinic, Isparta Yalvac State Hospital, Isparta, Turkey
[2] Private Practice, Ophthalmology, Istanbul, Turkey
[3] Department of Neurology, Faculty of Medicine, Selcuk University, Konya, Turkey

Corresponding Author: Serhat EKER
E-mail: drserhateker@gmail.com

Submitted: 22.07.2023 **Accepted:** 19.12.2023

ABSTRACT

Objective: To investigate the changes in the retinal microcirculation in multiple sclerosis (MS) patients by swept-source optical coherence tomography angiography (SS-OCTA).

Patients and Methods: Thirty-seven patients with relapsing-remitting MS and 40 healthy volunteers were included into this cross-sectional study. Clinical history, Expanded Disability Status Scale and duration of MS were collected. SS-OCTA by deep range imaging (DRI) OCT measurements were performed on all subjects. Macular perfusion parameters including superficial and deep foveal avascular zones (FAZs, FAZd, respectively) (%), vascular densities of superficial capillary plexus (SCP) (%), deep capillary plexus (DCP) (%) and choriocapillaris (CC) (%) were compared with healthy subjects.

Results: Vascular densities of SCP, DCP and CC were found to be statistically lower in the study group compared to the control group ($p = 0.02$, $p = 0.03$, $p = 0.03$, respectively). FAZs and FAZd, areas were significantly higher in the study group ($p = 0.02$, $p = 0.02$, respectively). Central macular thickness and subfoveal choroidal thickness were significantly lower than in the control group ($p = 0.015$, $p = 0.047$, respectively).

Conclusion: Evaluation of retinal blood flow in patients with MS is useful both for understanding the physiopathology of the disease and in the clinical follow-up.

Keywords: Multiple sclerosis, Retinal vasculature, Vascular density, Macular perfusion, Swept-source optical coherence tomography angiography

1. INTRODUCTION

Multiple sclerosis (MS) is a chronic and demyelinating disease in the central nervous system (CNS), associated with autoimmune mechanisms [1]. The primary cause of MS is unclear, but immunologic, environmental, infectious and genetic factors may contribute to the development of MS [2]. Cell-mediated and humoral immune systems agents attack CNS myelin or oligodendrocytes, causing neurodegeneration and neurological disability. Approximately, 2.5 million people worldwide are affected, most of them between the ages of 20-40 [3].

Multiple sclerosis especially affects the periventricular area, pons and spinal cord on the CNS [4]. Weakness in the extremities, sensory symptoms, ataxia, cognitive complaints and visual disturbance may occur as a result of axonal damage. Ophthalmological signs are impaired visual acuity, visual field defect, internuclear ophthalmoplegia or a relative afferent pupillary defect in MS. Ocular related symptoms such as optic neuropathy, retinal vasculitis and intermediate uveitis may occur in the course of MS [5].

The McDonald criteria with information from magnetic resonance imaging (MRI), examination of the cerebrospinal fluid, potential evoked visual tests, optical coherence tomography (OCT) and cognitive tests are used for the diagnosis of MS [6]. Disease-modifying therapies (DMTs) such as interferon beta-1a, interferon beta-1b, teriflunomide, daclizumab, natalizumab, fingolimod, etc. may be used after acute attacks [7].

Vascular structures may be affected in MS pathophysiology [8]. Cerebral hypoperfusion was reported in MS patients [9,10]. Recently, some studies showed retinal vascular density (VD) reduction in MS [11-13]. However, there is still a need for further investigation regarding vascular changes in MS.

Retinal micro vascularization can be evaluated quantitatively with developing technology. Swept-source optical coherence

How to cite this article: Eker S, Karakucuk Y, Gumus H. Assessment of macular microcirculation in patients with multiple sclerosis by swept-source optical coherence tomography angiography. Marmara Med J 2024: 37(2):192-197. doi: 10.5472/marumj.1487767

ISSN: 1309-9469

http://doi.org/10.5472/marumj.1487767
Marmara Med J 2024;37(2): 192-197

tomography angiography (SS-OCTA) devices can provide detailed imaging of the retinal vascular network by sequential optical coherence scans of a particular retinal region, based on the motion contrast of erythrocytes in vascular structures and processing [14]. It evaluates retinal micro vascularization non-invasively, without the necessity for intravenous contrast material which can cause adverse reactions [15]. There are a few studies comparing the microvascular findings of MS patients with the healthy group using swept-source deep range imaging (DRI) OCT Triton device in the literature [16,17]. The aim of this study is to measure macular perfusion in patients with MS using OCTA and to compare our results with the existing literature.

2. PATIENTS and METHODS

Study participants

This retrospective and cross-sectional study was performed on MS patients who had referred to the Selcuk University Faculty of Medicine, Department of Ophthalmology from January 2020 to March 2020. The research protocols were applied in accordance with the principles of the Declaration of Helsinki and was approved by Selcuk University's Institutional Review Board and Ethics Committee (Protocol No: 2020/177). All participants gave written informed consent.

Clinical data

Patients with relapsing-remitting MS applying to the Faculty of Medicine, Department of Neurology, Selcuk University, were advised routine eye examinations according to the 2010 McDonald criteria [6]. Those aged 18-65 and with an Extended Disability Status Scale score below 6 (mobile without support) were enrolled into the study. Detailed ophthalmological examination was performed including auto refractometer (Tonoref III, Nidec Co. Ltd, Aichi, Japan) measurement, best corrected visual acuity (BCVA) as measured on the standard Snellen chart, intraocular pressure (IOP) (mmHg) measured by Goldmann applanation tonometry, slit lamp and fundus examination using a +90 D lens after pharmacological dilatation with 1% tropicamide for each patient. After physical examination, OCTA was performed in participants with full vision and no pathological findings were determined in the examination. The exclusion criteria were having an additional systemic disease other than MS, BCVA under 20/50, high refractive correction (higher than +3 or – 3 dioptre spherical equivalent), low quality images in OCTA, any ophthalmological pathology (Glaucoma, diabetic retinopathy, hypertensive retinopathy, retinal vascular diseases, uveitis, amblyopia etc.), history of intraocular surgery and history of optic neuritis in the 6 months prior to enrolment in the study. After the evaluation of the including and excluding criteria, 37 MS patients were included in this study. The control group consisted of 40 age and sex matched healthy individuals. The right eye of each individual was assessed.

Optical coherence tomography angiography technique

We obtained OCTA images with the SS DRI OCT Triton (Topcon Corp, Tokyo, Japan) device. The participants were then asked to rest for ten minutes. All parameters were measured by one experienced operator (S.E.) using SS-OCTA which operates a 1.050 nm wavelength light source and 100,000 A Scan/s [18]. We used OCTA function to obtain 6 × 6 mm cubes focused on the fovea (Figure 1). The OCTA software (IMAGEnet 6 V.1.14.8538) system did the macular segmentation which consists of four 'en face' OCT slabs: (1) superficial vascular complex (SVC) is defined as from 2.6 µm below the internal limiting membrane (ILM) to the 15.6 µm below the inner plexiform layer (IPL); (2) deep vascular complex (DVC) is defined as from IPL offset of 15.6 µm to the IPL offset of 70.2 µm and (3) choriocapillaris vascular complex (CC) is identified as from BM to 10.4 µm under the Bruch's membrane (BM) [19].

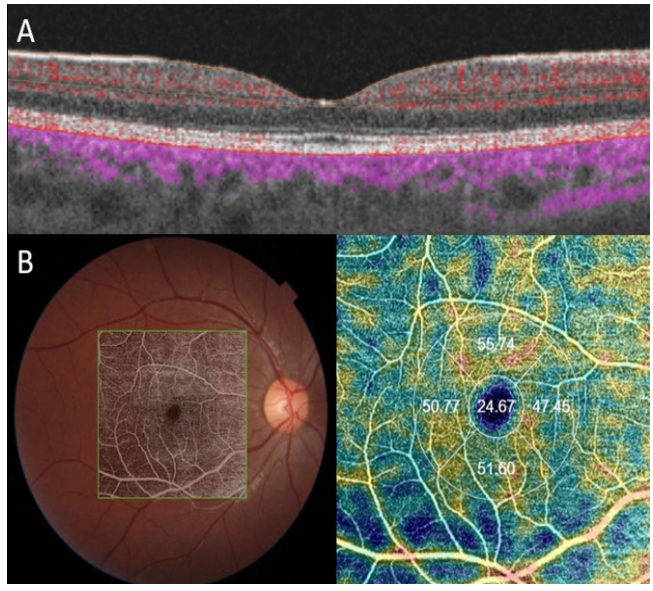

Figure 1. *Image of optical coherence tomography angiography measurement in 6x6mm area with grid centered in macula. Superficial vascular plexus density is shown with color lines (A). On density map with grid divided in five areas; central, nasal, interior, temporal and superior with number of percentages of vessel density are demonstrated (B).*

GNU Image Manipulation Program (GIMP) 2.8.14 was used to analyse quantitatively the VD of the SVC, DVC and CC as VDs, VDd and VDc, respectively. Superficial foveal avascular zone (FAZs) and deep foveal avascular zone (FAZd) were measured separately. VD was measured as the percentage of the vascularized tissue in the grid centred in macula. The subfoveal choroidal thickness (SFCT) and central macular thickness (CMT, respectively) analyses were performed for the eyes of all subjects in 9 regions of the macula. Macula sections were identified objectively with radii of 0.5 mm (center 1 mm), 0.5 to 1.5 mm (inner ring), and 1.5 to 3.0 mm (outer ring). CMT and SFCT values were obtained from central 1 mm measurements. Only the right eye of each subject enrolled in the study, was included in the analysis. All measurements were performed at the same time interval of the day. Two experienced observers examined two consecutive scans of a subject to detect interobserver reproducibility at different

http://doi.org/10.5472/marumj.1487767
Marmara Med J 2024;37(2): 192-197

times. The mean value of two independent measurements was used for each OCTA parameter. Patients with any pathologic condition detected in structural OCT scans, or if the Image Quality Index (IQI) was under 70, were excluded to avoid inaccuracy in the measurements due to image artifact [15].

Statistical Analysis

Data on demographic features, VDs of three vascular plexus, FAZs, FAZd, CMT, SFCT and disease duration were collected as mean ± standard deviation (SD). Normality for each variable for groups was measured using the Kolmogorov–Smirnov test. Categorical data were compared between groups using Pearson's chi-square test; independent samples test was used for variables with normal distribution and the Mann-Whitney U test was used for variables with abnormal distribution for comparison of means between groups using Statistical Package for the Social Sciences (version 26.0; SPSS Inc., Chicago, IL). Spearman correlation coefficient was used for correlation between variables. P values of less than 0.05 were noted as statistically significant.

3. RESULTS

There were 37 MS patients with an average age of 36.2 ± 12.1 years. The healthy control group was comprised of 40 individuals with a mean age of 35.6 ± 14.6 years. The mean onset time of the disease in the study group was 22.4 ± 5.1 (months). The age and gender distribution of the participants in both groups did not show any significant difference significantly ($p > 0.05$; Table I). Demographic data of MS patients and healthy controls and OCTA parameters are demonstrated in Table I.

FAZs and FAZd values were increased significantly in MS patients compared to the control group (p=0.026; p=0.022, respectively). VDs central value was found to be significantly decreased (p=0.02) in the MS cases compared to the control group. In the case group, the VDs superior and VDs temporal values were significantly lower than in the control group ($p = 0.04$; $p = 0.01$, respectively). However, VDs inferior and VDs nasal value did not change significantly ($p>0.05$).

VDd central value was found to be significantly lower than in the control group ($p = 0.03$). In addition, VDd inferior and VDd nasal values were significantly lower in MS cases than in the control group ($p = 0.01$; $p = 0.02$), while VDd superior and VDd temporal values did not vary significantly ($p>0.05$).

In MS patients, VDc central, VDc superior, VDc temporal, VDc inferior and VDd nasal values were significantly lower than in the control group ($p<0.05$, each of them). CMT and SFCT values were significantly lower in the MS group ($p = 0.015$; $p = 0.047$, respectively). Also, CMT and SFCT values correlated with the duration of MS onset time ($r= -0.335$; $p = 0.043$ and $r= -0.452$; $p=0.005$).

Table I. *The demographic characteristics and OCTA parameters of patients with multiple sclerosis and healthy eyes (Control group).*

		MS group				Control group				p	
		Mean±ss /n-%			Median	Mean±ss /n-%			Median		
Age		36.2	±	12.1	31	35.6	±	14.6	28	0.609	m
Gender	Female	23		62.2%		24		60%		0.846	X^2
	Male	14		37.8%		16		40%			
FAZs		175	±	57.4	164.9	150.5	±	67.1	136.2	0.026	m
FAZd		258.2	±	59.7	244.7	240.1	±	124.2	200.9	0.022	m
VDs Central		20.4	±	4.4	21.5	24	±	7.3	22.8	0.02	m
VDs Superior		48.9	±	2.1	48.2	49.5	±	2.8	49.8	0.048	m
VDs Temporal		43.6	±	3.1	42.4	45.4	±	3.5	44.4	0.011	m
VDs Inferior		46.1	±	2.7	44.9	47.8	±	3.8	47.7	0.077	m
VDs Nasal		43.4	±	2.9	43.6	44.6	±	3.6	45.1	0.097	t
VDd Central		18.8	±	6.2	18.7	22.1	±	8	21	0.03	m
VDd Superior		50.6	±	1.8	50.8	50.9	±	3.3	50.9	0.526	m
VDd Temporal		45.5	±	2.7	44.7	46.7	±	3.7	46.5	0.131	m
VDd Inferior		47.2	±	2.8	47	49.1	±	3.6	48.9	0.016	m
VDd Nasal		44.8	±	3.4	45.6	46.8	±	4.1	47.5	0.02	t
VDc Central		22.2	±	4.5	19.9	31.2	±	15.2	23.9	0.034	m
VDc Superior		49	±	2	48.1	50.5	±	3.5	50.4	0.009	m
VDc Temporal		44.7	±	2.2	44.6	47.1	±	5.0	46.8	0.043	m
VDc Inferior		46.5	±	2.7	46.1	49.1	±	4.7	48.3	0.012	m
VDc Nasal		43	±	2.7	43.7	46.2	±	5.4	45.7	0.004	m
CMT		177.9	±	13.1	178	189.1	±	21.8	183	0.015	m
SFCT		250.5	±	43.5	256	298.6	±	87.7	277	0.047	m

m: Mann-Whitney U test / t: Independent Sample t Test / X^2: Chi-squared test. SD: standard deviation; FAZs: superficial foveal avascular zone; FAZd: deep foveal avascular zone; VDs: superficial vascular density; VDd: deep vascular density; VDcc: choriocapillaris vascular density; CMT: central macular thickness; SFCT:subfoveal choroidal thickness. Italicized bold values represent p<0.05.

http://doi.org/10.5472/marumj.1487767
Marmara Med J 2024;37(2): 192-197

4. DISCUSSION

The development of the retina and optic nerve from the diencephalon during the embryological development reveals the similarity of the retina to the cerebral cortex [20]. Thus, pathophysiological changes in the CNS may affect the optic nerve and retina. Retinal microcirculation and CNS vascular structures have similar features. Neuronal metabolic activity plays an essential role in the autoregulation mechanism of these vascular structures with high oxygen concentration [21]. MS, is characterized by autoimmune, demyelinating and chronic inflammatory processes, which can cause vascular dysfunction along with neuroaxonal degeneration. Endothelial dysfunction as a result of chronic inflammation is thought to cause impairment in the vascular system [22]. In the past, parameters that could be used in the diagnosis and follow-up of MS patients were evaluated with the OCT devices [23]. In recent years, it has been aimed to observe vascular change in MS patients with the OCTA device, which provides retinal microvasculature evaluation. Researchers had focused on parameters that could be used in the follow-up of MS patients [12,24-29]. The present study aims to examine the changes in macular perfusion based on the different results seen in the literature through OCTA.

The SVC and DVC creates a capillary free zone in the fovea which is associated with ischemia [30]. The current study showed statistically significant FAZs and FAZd enlargement in MS patients. However, Yilmaz et al., did not report any difference in FAZ metrics in the eyes of MS patients [11]. On the other hand, Ulusoy et al., found enlargement of the FAZ, correlated by the reduction in the SVC [26]. Similar to our work, Alzheimer's disease, which is a neurodegenerative disease such as MS, FAZ enlargement, was shown as a result of decreased blood flow [31]. Impaired vascular blood flow might induce FAZ enlargement because of decreased neuron metabolism. It was observed that the increase in the FAZs area was more significant than the FAZd. Because the retinal nerve fibre layer and ganglion cell layer are supplied by the SVC, it is expected to be more affected in MS patients.

VDs values of the central, temporal and superior sectors were statistically significantly lesser than the VD values of the controls. Farci et al., reported significant reduction in all sectors of the SVC [32]. In addition, Ulusoy et al., showed a statistically significant decrease in the superior and inferior sectors of the SVC [26]. In the current study, it was observed that the superior and temporal sectors of the SVC seemed to be primarily affected by MS. There was no significant difference in the inferior and nasal sectors of VDs in the eyes of MS patients than in those of the control group. This is because the mean follow-up period of MS patients included in the study was limited to a short period. If this period had been longer, we could have found a decrease in all sectors of the VDs.

The current study demonstrated a significant decrease in the VD values of the central, inferior and nasal sectors in the VDd, while we did not see any significant change in the superior and temporal sector density values. Similarly, Yilmaz et al. and Feucht et al., found a significant reduction in the VDd values [11,27]. However, Ulusoy et al., did not report any statistical difference, although they found a decrease in VDd [26]. In addition, Farci et al. and Murphy et al., did not detect a significant change in the DVC capillary flow density [28,32]. In another study, it was stated that VD of DVC in MS patients with optic neuritis history were significantly decreased than those in eyes of MS patients without optic neuritis [29]. Although, different results were seen in the literature, we thought that the cerebral impaired vascular architecture in MS patients could affect the VDd in addition to diminished SVC blood flow [33].

In terms of VDc, this study showed a significant decrease in all sectors of MS patients compared to the control group. Cennamo et al., observed that VDc values did not change significantly in the MS groups included [34]. However, Feucht et al., reported that increased VDc values are associated with ongoing inflammatory disease activity [27]. Contrary to Feucht's results, we did not see an increase in VDc. Cerebral hypoperfusion may play a role in the pathogenesis of MS lesions. The current study is the first to show a decrease in all sectors of VDc. Concerning CMT and SFCT values, we found a significant reduction in MS patients. The decrease in CMT was consistant with the results of Waxman et al. and Britze et al. [35,36]. Furthermore, it has been reported that thinning in choroidal thickness is associated with the duration of MS disease [37]. The current data has also supported that there is a relationship between CMT and SFCT with disease duration.

The present study had some important limitations. The small sample size and short follow-up time were the features most lacking. The study did not include the patients'medication data that could alter the results. Additionally, since, cerebral perfusion was not measured, its relationship with retinal microvasculature could not be examined. Future studies should focus on the correlation between cerebral and retinal vascular values to study new follow-up parameters for MS.

The following conclusions can be drawn from the present study: that VD of SVC, DVC and CC measured by SS DRI OCT Triton device are reduced in the eyes of MS patients. In addition, CMT and SFCT values decreased in MS disease and correlated with MS disease onset. OCTA parameters can be a useful additional retinal marker in MS. Further detailed research is needed to investigate the value of OCTA in MS patients and to correlate with ongoing disease activity and cerebral perfusion.

Compliance with Ethical Standards

Ethical approval: The research protocols were applied in accordance with the principles of the Declaration of Helsinki and was approved by Selcuk University's Institutional Review Board and Ethics Committee (Protocol No: 2020/177). All participants gave written informed consent.

Funding: This study did not receive any specific grants from funding agencies in the public, commercial, or not-for-profit sector.

Conflict of interest: Authors have no conflict of interest to declare.

Authors' contributions: SE and YK : Concept, design, data collection and analysis, YK and HG: Supervision, SE and YK: Literature search and writing, SE: Critical review. All authors critically revised the manuscript, approved the final version to be published, and agreed to be accountable for all aspects of the work.

REFERENCES

[1] Dobson R, Giovannoni G. Multiple sclerosis – a review. Eur J Neurol 2019; 26: 27-40. doi: 10.1111/ene.13819.

[2] Coles A. Multiple sclerosis. Pract Neurol 2009; 9: 118-126. doi: 10.1136/jnnp.2008.171132.

[3] Alshammari YHM, Aldoghmi AKB, Al Afif HSA, et al. Multiple sclerosis diagnosis and management: A simple literature review. Arch Pharma Pract 2019; 10: 33-7.

[4] Goldenberg MM. Multiple sclerosis review. P T 2012; 37: 175-84.

[5] Lublin FD, Reingold SC, Cohen JA, et al. Defining the clinical course of multiple sclerosis: the 2013 revisions. Neurology 2014; 15;83: 278-86. doi: 10.1212/WNL.000.000.0000000560.

[6] Thompson AJ, Banwell BL, Barkhof F, et al. Diagnosis of multiple sclerosis: 2017 revisions of the McDonald criteria. Lancet Neurol 2018; 17: 162-73. doi: 10.1016/S1474-4422(17)30470-2.

[7] Huang W-J, Chen W-W, Zhang X. Multiple sclerosis: Pathology, diagnosis and treatments. Exp Ther Med 2017; 13: 3163-6. doi: 10.3892/etm.2017.4410.

[8] Plumb J, McQuaid S, Mirakhur M, Kirk J. Abnormal endothelial tight junctions in active lesions and normal-appearing white matter in multiple sclerosis. Brain Pathol 2002; 12: 154-69. doi: 10.1111/j.1750-3639.2002.tb00430.x.

[9] Inglese M, Adhya S, Johnson G, et al. Perfusion magnetic resonance imaging correlates of neuropsychological impairment in multiple sclerosis. J Cereb Blood Flow Metab 2008; 28: 164-71. doi: 10.1038/sj.jcbfm.9600504.

[10] Holland CM, Charil A, Csapo I, et al. The relationship between normal cerebral perfusion patterns and white matter lesion distribution in 1,249 patients with multiple sclerosis. J Neuroimaging 2012; 22: 129-36. doi: 10.1111/j.1552-6569.2011.00585.x.

[11] Yilmaz H, Ersoy A, Icel E. Assessments of vessel density and foveal avascular zone metrics in multiple sclerosis: an optical coherence tomography angiography study. Eye (Lond) 2020; 34: 771-8. doi: 10.1038/s41433.019.0746-y.

[12] Lanzillo R, Cennamo G, Criscuolo C, et al. Optical coherence tomography angiography retinal vascular network assessment in multiple sclerosis. Mult Scler 2018; 24: 1706-14. doi: 10.1177/135.245.8517729463.

[13] Wang X, Jia Y, Spain R, et al. Optical coherence tomography angiography of optic nerve head and parafovea in multiple sclerosis. Br J Ophthalmol 2014; 98: 1368-73. doi: 10.1136/bjophthalmol-2013-304547.

[14] Turgut B. Optical coherence tomography angiography–a general view. Eur Ophthalmic Rev 2016; 10: 39-42.

[15] Wylegala A, Teper S, Dobrowolski D, Wylegala E. Optical coherence angiography: A review. Medicine (Baltimore) 2016; 95: e4907. doi: 10.1097/MD.000.000.0000004907.

[16] Cordon B, Vilades E, Orduna E, et al. Angiography with optical coherence tomography as a biomarker in multiple sclerosis. PLoS One 2020; 15: e0243236. doi: 10.1371/journal.pone.0243236.

[17] Lee GI, Park KA, Oh SY, Min JH, Kim BJ. Differential patterns of parafoveal and peripapillary vessel density in multiple sclerosis and neuromyelitis optica spectrum disorder. Mult Scler Relat Disord 2021; 49: 102780. doi: 10.1016/j.msard.2021.102780.

[18] Kashani AH, Chen C-L, Gahm JK, et al. Optical coherence tomography angiography: A comprehensive review of current methods and clinical applications. Prog Retin Eye Res 2017; 60: 66-100. doi: 10.1016/j.preteyeres.2017.07.002.

[19] Al-Sheikh M, Ghasemi Falavarjani K, Akil H, Sadda SR. Impact of image quality on OCT angiography based quantitative measurements. Int J Retina Vitreous 2017; 3: 13. doi: 10.1186/s40942.017.0068-9.

[20] Heavner W, Pevny L. Eye development and retinogenesis. Cold Spring Harb Perspect Biol 2012; 4: a008391. doi: 10.1101/cshperspect.a008391.

[21] Pellegrini M, Vagge A, Ferro Desideri L, et al. Optical coherence tomography angiography in neurodegenerative disorders. J Clin Med 2020; 9: 1706. doi: 10.3390/jcm9061706.

[22] D'Haeseleer M, Cambron M, Vanopdenbosch L, De Keyser J. Vascular aspects of multiple sclerosis. Lancet Neurol 2011; 10: 657-66. doi: 10.1016/S1474-4422(11)70105-3.

[23] Petzold A, Balcer LJ, Calabresi PA, et al. Retinal layer segmentation in multiple sclerosis: a systematic review and meta-analysis. Lancet Neurol 2017; 16: 797-812. doi: 10.1016/S1474-4422(17)30278-8.

[24] Spain RI, Liu L, Zhang X, et al. Optical coherence tomography angiography enhances the detection of optic nerve damage in multiple sclerosis. Br J Ophthalmol 2018; 102: 520-4. doi: 10.1136/bjophthalmol-2017-310477.

[25] Lanzillo R, Cennamo G, Moccia M, et al. Retinal vascular density in multiple sclerosis: a 1-year follow-up. Eur J Neurol 2019; 26: 198-201. doi: 10.1111/ene.13770.

[26] Ulusoy MO, Horasanlı B, Işık-Ulusoy S. Optical coherence tomography angiography findings of multiple sclerosis with or without optic neuritis. Neurol Res 2020; 42: 319-26. doi: 10.1080/01616.412.2020.1726585.

[27] Feucht N, Maier M, Lepennetier G, et al. Optical coherence tomography angiography indicates associations of the retinal vascular network and disease activity in multiple sclerosis. Mult Scler 2019; 25: 224-34. doi: 10.1177/135.245.8517750009.

[28] Murphy OC, Kwakyi O, Iftikhar M, et al. Alterations in the retinal vasculature occur in multiple sclerosis and exhibit novel correlations with disability and visual function measures. Mult Scler 2020; 26: 815-28. doi: 10.1177/135.245.8519845116.

[29] Jiang H, Gameiro GR, Liu Y, et al. Visual function and disability are associated with increased retinal volumetric vessel density

in patients with multiple sclerosis. Am J Ophthalmol 2020; 213: 34-45. doi: 10.1016/j.ajo.2019.12.021.

[30] Spaide RF, Klancnik JM Jr, Cooney MJ. Retinal vascular layers imaged by fluorescein angiography and optical coherence tomography angiography. JAMA Ophthalmol 2015; 133: 45-50. doi: 10.1001/jamaophthalmol.2014.3616.

[31] Bulut M, Kurtuluş F, Gözkaya O, et al. Evaluation of optical coherence tomography angiographic findings in Alzheimer's type dementia. Br J Ophthalmol 2018; 102: 233-7. doi: 10.1136/bjophthalmol-2017-310476.

[32] Farci R, Carta A, Cocco E, Frau J, Fossarello M, Diaz G. Optical coherence tomography angiography in multiple sclerosis: A cross-sectional study. PLoS One 2020; 23;15: e0236090. doi: 10.1371/journal.pone.0236090.

[33] D'haeseleer M, Hostenbach S, Peeters I, et al. Cerebral hypoperfusion: a new pathophysiologic concept in multiple sclerosis? J Cereb Blood Flow Metab 2015; 35: 1406-10. doi: 10.1038/jcbfm.2015.131.

[34] Cennamo G, Carotenuto A, Montorio D, et al. Peripapillary vessel density as early biomarker in multiple sclerosis. Front Neurol. 2020; 17;11: 542. doi: 10.3389/fneur.2020.00542.

[35] Waxman SG, Black JA. Retinal involvement in multiple sclerosis. Neurology 2007;69:1562-3. doi: 10.1212/01.wnl.000.029.5993.08468.f3.

[36] Britze J, Frederiksen JL. Optical coherence tomography in multiple sclerosis. Eye (Lond) 2018; 32: 884-88. doi: 10.1038/s41433.017.0010-2.

[37] Esen E, Sizmaz S, Demir T, Demirkiran M, Unal I, Demircan N. Evaluation of choroidal vascular changes in patients with multiple sclerosis using enhanced depth imaging optical coherence tomography. Ophthalmologica 2016; 235: 65-71. doi: 10.1159/000441152.

MARMARA
MEDICAL JOURNAL

Original Article

https://dergipark.org.tr/tr/pub/marumj

The ameliorating effects of apigenin and chrysin alone and in combination on polycystic ovary syndrome induced by dehydroepiandrosterone in rats

Buket BERK[1], Nevin ILHAN[1], Solmaz SUSAM[2], Fatma TEDIK[1], Nalan KAYA TEKTEMUR[3]

[1] Department of Medical Biochemistry, Faculty of Medicine, Firat University, Elazig, Turkey
[2] Department of Medical Biochemistry, Faculty of Medicine, Adiyaman University, Adiyaman, Turkey
[3] Department of Histology and Embryology, Faculty of Medicine, Firat University, Elazig, Turkey

Corresponding Author: Buket BERK
E-mail: buketberk23@hotmail.com

Submitted: 31.05.2023 **Accepted:** 23.01.2024

ABSTRACT

Objective: Polycystic ovary syndrome (PCOS) is the most common endocrine disorder among women of reproductive age and is one of the main causes of ovulation infertility, affecting 5-10% of women. Inflammation, hormonal imbalances, and disruption of the oxidant-antioxidant balance are the main factors in the pathophysiology of PCOS. This study was designed to answer the question of whether apigenin and chrysin have therapeutic effects on the dehydroepiandrosterone (DHEA)-induced rat model of PCOS.

Materials and Methods: The experimental PCOS model was created by administering 6 mg/100g DHEA subcutaneously to 21-day-old female Wistar rats for 28 days, followed by treatment with natural agents 50 mg/kg apigenin and 50 mg/kg chrysin by oral gavage twice a week for one month. The predominant cell type was determined by microscopic analysis in vaginal smears daily from day 10 to day 28 of the experiment. In tissue supernatants, superoxide dismutase (SOD), catalase (CAT), glutathione peroxidase (GPx) activities, and malondialdehyde (MDA) levels were obtained by spectrophotometric method with appropriate manual methods; follicle-stimulating hormone (FSH), luteinizing hormone (LH), progesterone, interleukin (IL)-18, IL-1β, and IL-13 levels were determined by enzyme-linked immunosorbent assay (ELISA) method. In addition, histological sections obtained from ovarian tissue samples were stained with hematoxylin-eosin and examined under a light microscope.

Results: The results showed that treatment with apigenin and chrysin alone and in combination reduced MDA, LH, FSH, progesterone, IL-1β, IL-13, and IL-18 levels compared with PCOS rats. Furthermore, enzymatic activities of antioxidants including CAT, SOD, and GPx in the ovaries increased in therapeutic groups compared to the PCOS group.

Conclusion: In conclusion, this study demonstrates the potential therapeutic efficacy of apigenin and chrysin, either alone or in combination, in alleviating the hormonal imbalances, inflammation, and oxidative stress in DHEA-induced PCOS rats. Apigenin, in particular, emerges as a promising agent for PCOS treatment, showing superiority over chrysin and combination treatments in ameliorating cystic follicles and improving various parameters associated with PCOS pathophysiology. These findings suggest that apigenin holds promise as a novel therapeutic agent for PCOS and warrants further investigation in clinical settings.

Keywords: Polycystic ovary syndrome, Dehydroepiandrosterone, Apigenin, Chrysin

1. INTRODUCTION

Polycystic ovary syndrome (PCOS) is a gynecological and endocrine disease that negatively affects fertility and paves the way for the formation of many different diseases [1]. Individuals suffering from PCOS may experience menstrual irregularities, infertility, skin problems such as acne, hirsutism, and an increase in the number of small cysts in the ovaries [2]. If PCOS is left untreated for a long time, it can lead to many important metabolic abnormalities such as dyslipidemia, insulin resistance, type 2 diabetes mellitus, fatty liver, hypertension, infertility, depression, etc [3]. Although, the exact cause of PCOS is not known, it is suggested that genetic and environmental factors are effective in its emergence [4]. In addition, obesity is among the factors that paves the way for the formation of this disease. Excess weight and as a result insulin resistance cause hyperinsulinemia, which increases the synthesis of androgen hormones in the body. As a result, the balance of sex hormones in the body is disturbed, and ovulation disorders and the problems of inability to ovulate, called anovulation, occurs. Cyst formation in the ovaries is

How to cite this article: Berk B, Ilhan N, Susam S, Tedik F, Tekdemur Kaya N. The ameliorating effects of apigenin and chrysin alone and in combination on polycystic ovary syndrome induced by dehydroepiandrosterone in rats. Marmara Med J 2024: 37(2):198-207. doi: 10.5472/marumj.1479311

ISSN: 1309-9469

http://doi.org/10.5472/marumj.1479311
Marmara Med J 2024;37(2): 198-207

observed with the disruption of the ovulation pattern, and this situation progresses and leads to the emergence of PCOS [5].

An experimentally generated rodent model of PCOS helps us understand mechanisms and focus on clinical therapies for PCOS. In order to develop an experimental PCOS model in animals, the dehydroepiandrosterone (DHEA) application was first tried in the 1960s. In the study conducted by Roy et al., cystic degeneration and anovulation were observed in the ovaries after DHEA administration in guinea pigs with normal menstrual cycles [6]. In general, after DHEA treatment, female rats/mice form follicular cysts and become anovulatory like the human PCOS feature [7]. Hence, DHEA has been commonly preferred to cause PCOS-like phenotypes [8].

Although, there are options such as birth control pills, lifestyle changes, weight control, and surgery in the treatment of PCOS [9], there is a need for natural products that do not have side effects, are at a low cost, and that we can easily access and consume in daily life [10]. Traditional herbal compounds have been widely used to cure gynecological disorders [11]. Apigenin is a flavonoid and is found in many vegetables and fruits like parsley, celery and chamomile tea being the most common sources. It is known that apigenin exhibits antioxidant, anti-inflammatory, anti-tumor, anti-allergic, neuro-protective, anti-microbial properties and has therapeutic properties against many diseases [8]. Chrysin, another natural agent, is found in the foods we consume, such as parsley, thyme, bell pepper, celery, honey, and propolis. This natural agent is known to exhibit antioxidant, anti-inflammatory, anti-diabetic, anti-bacterial, and anti-tumor properties. The mechanisms most affected by chrysin are oxidative stress, inflammatory responses, autophagy, and apoptosis [12,13].

In this study, it was aimed to investigate the potential therapeutic effects of apigenin and chrysin alone and in combination in rats with PCOS induced by DHEA, and to reveal the level changes in selected hormones and inflammatory and oxidative stress pathway parameters in the pathophysiology and treatment of PCOS.

2. MATERIALS and METHODS

Animals and Ethics Statement

Female Wistar Albino rats of 21 days were kept in groups with free access to food and water and a controlled temperature of 22±2°C and in a reversed 12h light-dark cycle. Animals were allowed to acclimatize for one week before treatment. This study was carried out in accordance with the local ethics committee of Firat University, which approved the experimental procedure and protocols (approval number: 16/04/2020-389393).

Experimental Protocol and in Vivo Treatment

A total of 48 rats were randomly assigned to five groups that included the SHAM group (n=8) and PCOS group (n=10), PCOS+AGN group (n=10), PCOS+CH group (n=10) and PCOS+AGN+CH group (n=10). The doses and frequency of administration of the agents administered were summarized below:

SHAM Group (n=8): 0.02ml 95% ethanol + 0.18ml corn oil (0.2mL total) sc administered for 28 days, followed by 0.5ml dimethyl sulfoxide (DMSO) two times a week administered by oral gavage for one month.

PCOS Group (n=10): DHEA (6mg/100g body weight dose dissolved in 0.02ml 95% ethanol and mixed with 0.18ml corn oil) was administered sc for 28 days, followed by 0.5ml DMSO given twice a week by oral gavage for one month [14].

PCOS+AGN Group (n=10): DHEA (6mg/100g body weight) was administered sc for 28 days by dissolving in 0.02ml of 95% ethanol and mixing with 0.18ml of corn oil, then for 1-month AGN at a dosage of 50mg/kg twice a week was dissolved in 0.5ml DMSO and administered by oral gavage [15].

PCOS+CH Group (n=10): DHEA (6mg/100g body weight) was administered sc for 28 days by dissolving in 0.02ml 95% ethanol and mixing with 0.18ml corn oil, then for 1-month CH was dissolved in 0.5ml DMSO at a dosage of 50mg/kg twice a week and administered by oral gavage [16].

PCOS+AGN+CH Group (n=10): After DHEA is administered sc for 28 days, apigenin and chrysin were administered at the dose and application frequency mentioned above, 2 times a week for 1 month.

Biochemical Methods

Tissue and Supernatant Collection

At the end of the experiment, blood and tissue collection was performed during the diestrus stage of the estrous cycle and between 8 and 9 AM in the morning. Following the sacrification of animals, both ovaries of rats were quickly removed and cleaned. Then ovarian samples were homogenized, centrifuged at 4000 rpm for 10 minutes at +4^{0}C, and their supernatants were separated. Depending on the parameters to be studied, supernatant samples were divided into portions, put in eppendorf tubes and stored at – 80°C until the day of analysis.

Determination of Tissue Protein Levels

Protein levels in the supernatants were determined according to the Lowry method The basic principle of the Lowry method is based on the formation of a blue color by the Folin-Phenol reagent of proteins in alkaline medium [17].

Evaluation of Selected Hormones and Inflammation Markers by Using ELISA

Supernatant FSH (Catalog no: 201-11-0183), LH (Catalog no: 201-11-0180), progesterone (Catalog no: 201-11-0742), IL-18 (Catalog no: 201-11-0118), IL-1β (Catalog no: SG-20260), and IL-13 (Catalog no: 201-11-0113) levels were measured by enzyme-linked immunosorbent assay (ELISA) method in accordance with the manufacturer's instructions. FSH, LH, progesterone, IL-18, and IL-13 ELISA kits were obtained from Sunred Biological Technology Company, Shanghai, China. The IL-1β ELISA kit was obtained from SinoGeneClon Biotech, Hangzhou, China.

http://doi.org/10.5472/marumj.1479311
Marmara Med J 2024;37(2): 198-207

Determination of Tissue MDA Level

Tissue Malondialdehyde (MDA) levels and the end product of lipid peroxidation were measured spectrophotometrically as described by Ohkawa et al. [18]. Determination of lipid peroxidation is based on the spectrophotometric measurement at 532 nm of the pink complex formed as a result of incubation of tissue homogenate with 0.8% thiobarbituric acid (TBA) in a boiling water bath for 1 hour under aerobic conditions, where the pH is 3.5. 1,1,3,3 tetraethoxypropane was used as standard in the measurements.

Determination of Tissue SOD Activity

Tissue superoxide dismutase (SOD) activities were determined by the method of Sun et al., based on the inhibition of nitroblue tetrazolium [19]. In the assay, the xanthine-xanthine oxidase system was used as a superoxide generator. The absorbance of the reduction product (formazane) was measured at 560 nm. SOD activity was measured by the degree of inhibition of this reaction.

Determination of Tissue CAT Activity

Tissue Catalase (CAT) activity was determined using the UV spectrophotometric method which was developed by Aebi [20]. The principle of the test is based on the determination of the rate constant (s-1, k), or H_2O_2 decomposition rate, at 240 nm.

Determination of Tissue GPx Activity

Tissue glutathione peroxidase (GPx) activity levels were measured using the method of Paglia and Valentina in which GPx activity was coupled with the oxidation of nicotinamide adenine NADPH by glutathione reductase [21]. The oxidation of NADPH was followed spectrophotometrically at 340 nm.

Estrous Cyclicity and Vaginal Smear Test

Normal regular cyclic rats showed proestrus, estrus, metestrus, and diestrus stages for 4-5 days, whereas, acyclic rats showed the estrous cycle arrested in any one of the stages for 4 consecutive days. Hence, irregular estrous cycles and persistent vaginal cornification were used to indicate the successful formation of the PCOS model in all study groups [22].

To confirm whether the PCOS pattern was established, a cervical screening test (smear) was performed from day 10 to day 28 of the experiment, and the predominant cell type was microscopically analyzed in vaginal smears obtained daily. For this, approximately 0.2 ml of saline was drawn into the pasteur pipette, the animal to be smeared was held tightly with the abdomen facing upwards, the pipette tip was inserted into the vagina and the saline was sprayed inside. Afterward, the liquid sprayed into the vagina without removing the tip of the pipette was drawn back into the pipette and placed on the previously prepared clean slide. The liquid taken was examined under a light microscope without the need for staining, and finally, the cycle periods were determined depending on the presence and proportion of epithelial, cornified, and leukocyte cells.

Histopathological Analysis

After decapitation, the removed ovarian tissues were quickly placed in a 10% formaldehyde solution. After approximately 48 hours of fixation, the tissues that were washed under running tap water and passed through routine histological follow-up series were embedded in paraffin (Sigma-Aldrich Paraplast Embedding Media, U.S.A). Sections of 5 µm thickness were taken from the prepared paraffin blocks using a microtome. Hematoxylin-Eosin (H&E) staining was applied to the prepared preparations. Ovarian follicle count (primordial, primary, secondary follicles, and Graff follicles) was evaluated by Souza et al.'s (1986) method [23]. The classification of follicles was done as follows:

Primordial follicle: The oocyte is partially or completely surrounded by squamous granulosa cells.

Primary follicle: The oocyte is surrounded by one or more rows of cuboidal cells between squamous granulosa cells.

Secondary follicle: The oocyte contains two layers of granulosa cells or at least one layer of granulosa cells and at least one layer of granulosa cells in the second layer. Antral spaces begin to form between the granulosa cells.

Graff's follicle: The oocyte is surrounded by more than two layers of granulosa cells and the antrum has formed.

The Leica DM500 imaging system (DFC295; Leica, Wetzlar, Germany) was used to evaluate and photograph H&E staining on ovarian sections.

Statistical Analysis

To determine the method to be used in the analysis phase, the Shapiro-Wilk test was applied to determine whether the variable of interest in the data set comes from a normal distribution. In the general comparison of continuous measurements of more than two groups, One-Way Analysis of Variance was used if the assumptions were satisfied. Data are indicated as Mean ± SD. If the p-value is below 0.05, it means that there is a significant difference as a result of the comparison.

3. RESULTS

Weight and Growth Rates of Rats in the Study Groups

The weights of the rats in the study groups were regularly weighed and recorded on a weekly basis from the beginning to the end of the experiment. According to the data obtained, the initial weights of the rats in the experimental groups were close to each other and there was no statistical difference between them ($p>0.05$). When the weight of the rats before sacrification was evaluated at the end of the experiment, a statistically significant increase was found in the PCOS-induced groups compared to the SHAM group ($p<0.001$; only for the PCOS-formed group; $p<0.05$ in all groups in which the treatment protocol was applied) (Figure 1).

The growth rates of the experimental animals were calculated based on the following formula:

http://doi.org/10.5472/marumj.1479311
Marmara Med J 2024;37(2): 198-207

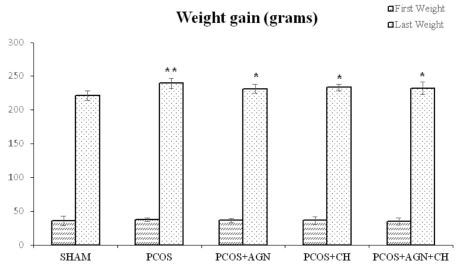

Figure 1. *Weight gains of rats in the study groups*
*A value of *p< 0.05, **p<0.001, was considered as significant versus the SHAM group.*

Growth Rate = (Final Weight-Initial Weight) / Total Experiment Time

The growth rates in the study groups are presented in Table I. According to the findings, the growth rates of the PCOS-induced groups were higher than the SHAM group. However, the growth rate increased the most only in the PCOS group (p<0.001 compared to the SHAM group). The growth rates of the PCOS+AGN and PCOS+AGN+CH treatment groups were statistically significant when compared to the SHAM group (p<0.05; for both groups).

Table I. *Growth rates in study groups*

Growth Rate	SHAM	PCOS	PCOS+AGN	PCOS+CH	PCOS+AGN+CH
	3.19±0.13	3.48±0.11**	3.36±0.96	3.39±0.71*	3.40±0.22*

*A value of *p < 0.05, **p < 0.01, was considered as significant versus the SHAM group. PCOS: Polycystic ovarian syndrome, AGN: apigenin, CH: Chrysin*

Ovarian Tissue Weights of Study Groups

When the values obtained from the measurement of the ovarian weights of the study groups were examined, it was observed that the mean ovarian weights of the rats belonging to the PCOS group were higher than those of the SHAM group, which was statistically significant only in the PCOS group (p<0.05). When the mean ovarian weights were analyzed among the groups with PCOS, it was found that the mean ovarian weight was statistically lower in the PCOS+AGN treatment group compared to the PCOS group (p<0.05) (Figure 2).

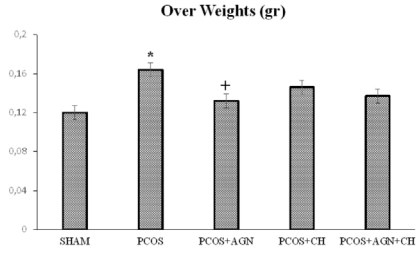

Figure 2. *A value of *p < 0.05 was considered as significant versus the SHAM group.*
A value of $^{+}p < 0.05$, was considered as significant versus the PCOS group.

Effect of Apigenin and Chrysin on Hormonal Levels

Follicle-stimulating hormone levels were higher in the supernatant samples compared to the SHAM group, which was statistically significant in the PCOS group (p<0.05; compared to the SHAM group). A decrease in supernatant FSH levels was observed in the treated groups compared to the PCOS group, but it was not statistically significant (p>0.05). Supernatant LH levels were statistically higher in the PCOS group compared to the SHAM group (p<0.05), and a statistical decrease was observed in the PCOS+AGN+CH group, which was one of the treatment agent-administered groups, compared to the PCOS group. (p<0.05). The supernatant LH/FSH ratio was increased in the PCOS-induced group compared to the SHAM group, but this increase was not statistically significant (p>0.05). A non-statistical decrease in the supernatant LH/FSH ratio was observed in the PCOS+AGN group, which is one of the treated groups, compared to the PCOS group (p>0.05). Supernatant progesterone levels were statistically lower in all PCOS-induced groups than in the SHAM group (p<0.001; for all PCOS-induced groups). On the other hand, there was a statistically insignificant decrease in progesterone levels in all groups in which the treatment agent was applied, compared to the PCOS group (p>0.05; in all treatment groups compared to PCOS group) (Table II).

Effect of Treatment Agents on Inflammation Parameters

Supernatant IL-18, IL-1β and IL-13 levels were found to be statistically higher in the PCOS group compared to the SHAM group (p<0.001; for all parameters). A statistically significant decrease was observed in the supernatant IL-18 levels in the treated groups compared to the PCOS group (p<0.05; in all treatment groups). A statistically significant decrease was observed in IL-1β levels in the PCOS+CH and PCOS+AGN+CH groups compared to the PCOS group (p<0.05). Finally, a decrease in supernatant IL-13 levels was noted in all groups treated with the treatment agent compared to the PCOS group, but this decrease was not statistically significant (Table III).

Effect of Treatment Agents on Supernatant Oxidative Stress Parameters

A statistical decrease in SOD and CAT activities and a statistical increase in MDA levels were observed in the PCOS group compared to the control group. A decrease in GPx activity was also observed compared to the control group, but this decrease was not statistically significant. When the treatment agent applied groups were compared with the PCOS group, a statistical increase in SOD activity was observed in the AGN and AGN+CH treatment groups. CAT and GPx activities were also increased in the treated groups compared to the PCOS group, but this increase was not statistically significant (p>0.05) (Table IV). Although, there was a decrease in MDA levels in all treatment groups compared to the PCOS group, this decrease was statistically significant only in the CH group.

http://doi.org/10.5472/marumj.1479311
Marmara Med J 2024;37(2): 198-207

Table II. *Effect of Apigenin and Chrysin on FSH, LH levels in DHEA-induced PCOS rats*

Factors/Groups	SHAM	PCOS	PCOS+AGN	PCOS+CH	PCOS+AGN+CH
FSH (mIU/mg protein)	31.75±2.55	39.54±5.79*	37.25±6.36	36.72±5.41	37.19±4.31
LH (mIU/mg protein)	34.30±3.03	45.91±8.30**	40.76±4.82	41.48±4.98	42.74±4.01*
LH/FSH	1.08±0.89	1.17±2.41	1.11±0.21	1.14±0.13	1.15±0.11
PROG (ng/mg protein)	112.81±15.24	79.87±16.25**	86.47±13.96**	82.48±10.27**	82.52±11.14**

*A value of *p < 0.05, **p < 0.01 was considered as significant versus the sham group. PCOS: Polycystic ovary syndrome, AGN: apigenin, CH: Chrysin, FSH: Follicle-stimulating hormone, LH: Luteinizing hormone, PROG: progesterone*

Table III. *Effect of Treatment Agents on Inflammation Parameters*

Factors/Groups	SHAM	PCOS	PCOS+AGN	PCOS+CH	PCOS+AGN+CH
IL-18 (ng/protein)	138.11±21.22	230.99±28.34**	187.83±23.47*+	193.91±34.88*+	194.54±15.28*+
IL-1β (ng/protein)	184.46±29.22	287.62±75.41**	242.27±20.76	232.45±29.77+	228.71±24.97+
IL-13 (ng/protein)	213.53±24.42	294.21±29.40**	275.02±27.35**	283.75±27.38**	278.11±31.93**

*A value of *p < 0.05, **p < 0.01 was considered as significant versus the SHAM group. PCOS: Polycystic ovary syndrome, AGN: apigenin, CH: Chrysin*

Table IV. *Effect of Treatment Agents on Supernatant Oxidative Stress Parameters*

Factors/Groups	SHAM	PCOS	PCOS+AGN	PCOS+CH	PCOS+AGN+CH
SOD activity	93.55±6.50	71.65±7.80**	84.83±9.57+	82.00±12.12	91.07±12.03++
CAT activity	6.69±1.16	4.96±1.07*	5.82±1.21	5.18±1.36	5.33±0.73
GPx activity	5179.23±364.92	4822.02±682.64	5124.46±488.66	5303.70±655.25	5070.61±559.81
MDA level	13.96±2.51	19.68±3.02**	16.94±1.86	17.60±2.40*	16.62±2.57

*A value of *p < 0.05, **p < 0.01 was considered as significant versus the SHAM group. A value of +p < 0.05, ++p < 0.001 was considered as significant versus the PCOS group. PCOS: Polycystic ovary syndrome, AGN: apigenin, CH: Chrysin. SOD: Superoxide dismutase, CAT: Catalase, GPx: Glutathione peroxidase, MDA: Malondialdehyde*

Histological Results

Vaginal Smear Reviews

Vaginal smear findings support the successful formation of PCOS with DHEA. When the rats in the SHAM group were examined, a regular estrous cycle was observed. In the rats in the PCOS group, the estrous cycle was found to be impaired, irregular and prolonged. It was observed that the irregular cycle started to improve in the groups that were treated with the treatment agent after PCOS occurred. Vaginal smear samples of the groups are as in Figure 3.

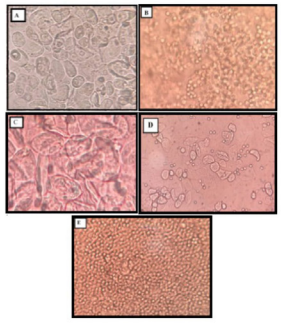

Figure 3. *Vaginal smear samples of SHAM and PCOS groups. A: Proestrous, B: Diestrous, C: Oestrous, D: Metestrous (belonging to the SHAM group), E: Diestrous (belonging to the PCOS group)*

Ovarian Follicle Count and Histological Appearance of Ovarian Tissues

When the rat ovary sections were evaluated under the light microscope, there were many corpus luteum and ovarian follicles at different stages of development (primordial, primary, secondary and Graff) in the ovarian cortex in the preparations belonging to the SHAM group. Granulosa cells and theca structures were histologically normal.Corpus luteum structures were normal and well-defined.

Similar to the SHAM group, multiple corpus luteum and follicles at different developmental stages were observed in the ovarian sections of the PCOS group. However, when the two groups were compared, it was found that the number of secondary follicles increased significantly in this group ($p<0.05$). It was also observed in this group that the number of primordial and primary follicles decreased and the number of cystic follicles increased compared to the SHAM group, but these changes were statistically insignificant ($p>0.05$). Again, in the PCOS group, excessive dilatation of the vessels in the cortical stroma was noted (Figure 4). In the PCOS+AGN, PCOS+CH and PCOS+AGN+CH groups, the secondary follicle counts were decreased compared to the PCOS group, and the Graff follicle counts were decreased compared to the SHAM group. It was determined that vascular dilatation observed in the PCOS group decreased in all treatment groups. However, vascular congestion was remarkable in the PCOS+AGN group. The follicle and corpus luteum count results of all groups are presented in Table V.

http://doi.org/10.5472/marumj.1479311
Marmara Med J 2024;37(2): 198-207

Table V. *Ovarian follicle count*

Groups	Primordial Follicle	Primary Follicle	Secondary Follicle	Graff Follicle	Corpus Luteum	Cystic Follicle
SHAM	9.50±0.64	8.25±2.05	17.75±1.47	1.50±0.95	13.75±2.86	0.25±0.25
PCOS	7.00±2.12	4.25±1.25	31.50±4.66[a]	1.25±0.25	14.00±0.91	2.00±0.70
PCOS+AGN	2.25±0.85	4.25±1.49	14.25±3.94[b]	0.00±0.00[a]	10.00±2.34	1.50±0.86
PCOS+CH	4.25±2.32	4.25±2.32	19.50±2.32	0.00±0.00[a]	13.50±1.89	1.00±0.40
PCOS+AGN+CH	8.25±2.65	3.75±0.62	10.00±1.63[b]	0.50±0.28[a]	8.50±0.93	0.50±0.28

a: Compared to the SHAM group, b: Compared to the PCOS group p<0.05 *PCOS: Polycystic ovary syndrome, AGN: Apigenin, CH: Chrysin.*

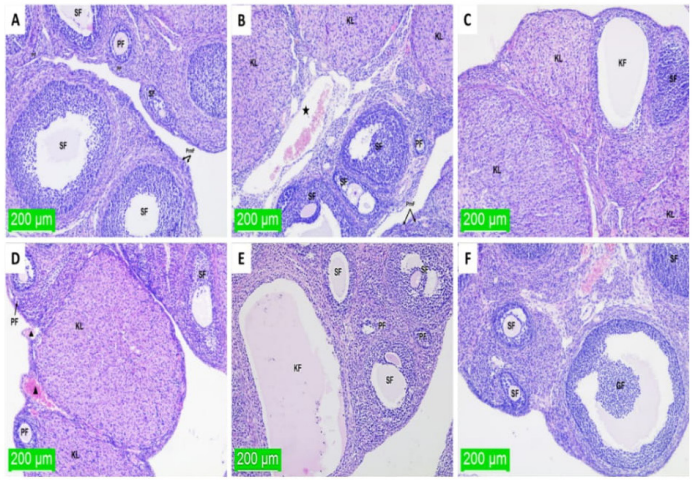

Figure 4. *Histological appearance of ovarian tissues. A: Sham group, B-C: PCOS group, D: PCOS+AGN group, E: PCOS+CH group, F: PCOS+AGN+CH group. KL: Corpus luteum; SF: Secondary follicle; PF: Primary follicle; PrmF: Primordial follicle; GF: Graff's follicle; CF: Cystic follicle. Star: Vascular dilatation; Triangle: Congestion. x100, H&E.*

4. DISCUSSION

Polycystic ovary syndrome is a very common endocrine disorder in women of reproductive age, which is characterized by enlargement of the ovaries and the formation of many small cysts, which paves the way for a number of hormonal problems in the individual, and whose exact cause is still unknown [24]. To understand the etiopathology of PCOS, the present study employed a DHEA-treated rat model, which exhibits metabolic signs similar to the human PCOS condition. To our knowledge, this is the first study using the PCOS rat model to investigate the effects of the combination of apigenin and chrysin on the estrous cycle, weight gain, and endocrine parameters such as testosterone and fasting insulin level. Combination therapies have proven to be an invaluable strategy in medical treatment ever since the inception of medicine [25]. In contemporary times, the utilization of appropriate drug combinations not only enhances therapeutic effectiveness in contrast to single-drug administration but also facilitates the attainment of positive outcomes with reduced doses of individual components. This, in turn, mitigates the occurrence of side effects, minimizes the development of drug resistance, and can also offer selective synergy against a specific target [26].

An irregular estrous cycle is used as an indicator of the successful establishment of PCOS in animal models [27] Hence, to verify PCOS in our study, the estrous cycle was noted from day 1 to 28, as well as changes in ovulation phases. The group of PCOS exhibited estrous cycle irregularity mostly at the stage of the diestrus phase, which is an indication of anovulation.

Women with PCOS have the problem of gaining weight together with hormonal imbalances. Namely, PCOS makes it difficult to use the insulin hormone and can lead to the development of insulin resistance. Increased insulin levels also increase the production of androgens, which lead to pilosity, acne, menstrual irregularity and weight gain [28]. In a study, it was reported that the body and ovarian weights of rats in the PCOS group were significantly higher than the control group [29]. In our study, it was also found that the body and ovarian weights of rats in the PCOS group increased statistically compared to the SHAM group, in line with the aforementioned study.

Follicle-stimulating hormone (FSH) is necessary for pubertal development and the function of women's ovaries and men's testes. This hormone stimulates the growth of ovarian follicles in the ovary before the release of an egg from one follicle at ovulation in women. It also increases estradiol production from the ovaries [30]. The normal level of serum FSH gradually increases from the beginning of the menstrual cycle to the middle of the cycle and decreases gradually to the basal value after ovulation [31]. LH a gonadotropin in glycoprotein structure, is responsible for inducing ovulation, preparation for fertilized oocyte uterine implantation, and the ovarian production of progesterone through stimulation of theca cells and luteinized granulosa cells [32]. Both FSH and LH play important functions in ovulation, and PCOS patients commonly show a two to three-fold increased LH/FSH ratio, which is sufficient to disrupt ovulation [33]. In a study it was reported LH, LH/FSH ratio in the PCOS model group significantly increased, in contrast, the level of FSH decreased [34]. In a letrozole-induced PCOS study, it was found that the PCOS-induced group had raised levels of LH, while the PCOS-induced group had lower levels of progesterone, estrogen, and FSH [35]. In our study, LH and FSH levels were higher in the PCOS group compared to the SHAM group, and a decrease was detected in the treatment agent-administered groups compared to the PCOS group. Progesterone is a 21-carbon steroid hormone of ovarian origin and is also secreted by the action of LH secreted from the anterior lobe of the pituitary [36]. Women with PCOS need high progesterone levels to reduce GnRH secretion because FSH synthesis is insufficient and LH synthesis is high. However, since low secretion of FSH will cause anovulation, progesterone levels may remain low [37]. It was reported in a study that in PCOS, progesterone levels were significantly lower than in the control group [38]. It was also reported that progesterone levels decreased in the PCOS model created with intramuscular estradiol valerate injection compared to the control group [39].

In our study, the supernatant progesterone levels were also statistically lower in all PCOS-induced groups compared to the control group. Apigenin treatment increased supernatant progesterone levels more than chrysin and AGN+CH treatment.

Inflammation is thought to be an important contributor to the pathogenesis of PCOS. That is, inflammation is likely to trigger events that lead to increased ovarian androgen production and reproductive dysfunction in PCOS patients [40]. Studies have reported that serum and follicular fluid IL-1β levels are elevated in women with PCOS [41,42]. It has been reported that ovarian tissue IL-1β levels in the PCOS model created with DHEA increased in the model group compared to the control group [43]. In our study, IL-1β levels were higher in the PCOS group compared to the SHAM group, and there was a decrease in the treatment agent-administered groups compared to the PCOS group. IL-18, a proinflammatory cytokine belonging to the IL-1 superfamily [44], is enhanced in PCOS patients [45]. In a study, IL-18 level was detected significantly higher in all the PCOS groups compared to the control group [46]. In our study, IL-18 levels were higher in the PCOS-induced groups than in the SHAM group. Moreover, previous studies showed that agents such as baicalin [47], and resveratrol [48] which have anti-inflammatory effects can improve the low-grade inflammation state by decreasing the levels of proinflammatory cytokines such as IL-18, including the PCOS rats. Also, in our study, a statistically significant decrease was observed in the supernatant IL-18 levels in the all-treatment groups compared to the PCOS group. Interleukin-13, a cytokine, increases the production of adhesion molecules on the endothelium and downregulates prostaglandin and E2 production [49]. In a study, it was reported that IL-12 and IL-13 levels in the follicular fluid were higher in a subgroup of patients with PCOS compared to women with normal ovulation [49]. It has been reported that serum IL-13 levels are higher in women with PCOS during pregnancy compared to the control group [50]. In our study, the selected cytokines levels were higher compared to the SHAM group. Moreover, apigenin and chrysin showed an anti-inflammation effect by decreasing of the inflammatory cytokine levels.

Oxidative stress is another factor that contributes to the pathological process of PCOS, which affects reproduction. Improving antioxidant activities, including SOD, GPx, CAT, and GSH, may be beneficial for inhibition and modulation of oxidative stress in PCOS [51]. Haslan et al., in their study of rat polycystic ovary induced by letrozole, stated that the oxidant-antioxidant balance was impaired in the PCOS group, while Ficus deltoidea improved the deteriorated balance [52]. In another PCOS study, it was reported that the activities of antioxidants such as SOD, GPx, CAT, and GSH were decreased in rats with PCOS, while they increased significantly with luteolin [51]. In our study, it was determined that MDA levels were higher and selected antioxidant enzyme activities were lower in PCOS-induced rats compared to the SHAM group, as in the studies mentioned above, which indicates an oxidant-antioxidant imbalance. Moreover, it was observed that the therapeutic agents applied decreased the MDA levels, and increased the antioxidant enzyme activities, restoring the deteriorated oxidant-antioxidant balance.

The effects of apigenin and chrysin on ovarian tissue and molecular changes in rats with PCOS induced by DHEA were examined. In a similar study, the effect of applying different amounts of apigenin on the changes in polycystic ovaries was investigated [53]. This study stated that apigenin prevented primordial follicles from turning into primary follicles. They also concluded that apigenin reduces various complications caused by PCOS and had protective effects on cystic follicles formed in the ovaries. In another study, it was observed that apigenin helped increase primary follicle, Graff follicle, and corpus luteum and decrease cystic follicles. It was stated that apigenin also played an important role in follicle development and the initiation of ovulation [54]. In our study, it was observed that apigenin, as an antioxidant and anti-angiogenic agent, reduced and improved the cystic follicles in the ovaries resulting from PCOS.

In conclusion, this study scientifically reveals the beneficial effects of apigenin and chrysin on the parameters involved in the inflammation and oxidative stress mechanisms in the pathophysiology of PCOS. Similar studies using different

http://doi.org/10.5472/marumj.1479311
Marmara Med J 2024;37(2): 198-207

treatment methods, emphasize that apigenin alone is more effective than chrysin or in combination with other treatment agents, and could be used for PCOS as an alternative therapeutic agent.

Compliance with Ethical Standards

Ethics Approval: This study was approved by the Ethics Committee of Firat University (approval number: 16/04/2020-389393).

Financial Support: This study was funded by the Firat University Scientific Research Projects Unit.

Disclosure Statement: The authors declare no conflict of interest.

Authors' Contributions: NI and SS: Data collection, data analysis, and manuscript writing, BB, FT and NKT: Data collection and data analysis, BB, FT, NI and SS: Protocol development. All authors read and approved the final version of the manuscript.

REFERENCES

[1] Yu J, Ding C, Hua Z, Jiang X, Wang C. Protective effects of berberine in a rat model of polycystic ovary syndrome mediated via the PI3K/AKT pathway. Journal of Obstetrics and Gynaecology Research 2021;47:1789-803. doi:10.1111/jog.14730.

[2] Kim JJ. Update on polycystic ovary syndrome. Clin Exp Reprod Med 2021;48:194-7. doi:10.5653/cerm.2020.04329.

[3] Azziz R. Polycystic ovary syndrome. Obstet Gynecol 2018;132:321-36. doi: 10.1097/AOG.000.000.0000002698.

[4] Fan Q, He J-F, Wang Q-R, et al. Functional polymorphism in the 5'-UTR of CR2 is associated with susceptibility to nasopharyngeal carcinoma. Oncol Rep 2013;30:11-6. doi: 10.3892/or.2013.2421.

[5] Xu Y, Qiao J. Association of insulin resistance and elevated androgen levels with polycystic ovarian syndrome (PCOS): A review of literature. J Healthc Eng 2022;2022 :2022:9240569. doi: 10.1155/2022/9240569.

[6] Roy S, Mahesh VB, Greenblatt RB. Effect of dehydroepiandrosterone and Δ4-androstenedione on the reproductive organs of female rats: production of cystic changes in the ovary. Nature 1962;196(4849):42-3. doi: 10.1038/196042a0.

[7] Ryu Y, Kim SW, Kim YY, Ku S-Y. Animal models for human polycystic ovary syndrome (PCOS) focused on the use of indirect hormonal perturbations: a review of the literature. Int J Cell Sci Mol Biol 2019;20:2720. doi: 10.3390/ijms20112720.

[8] Susam S, Çıkım G. A review on the potential pharmacological effects of apigenin. Archives Medical Review Journal 2023;32:113-9. doi:10.17827/aktd.1267942.

[9] Oguz SH, Yildiz BO. An update on contraception in polycystic ovary syndrome. Endocrinol Metab (Seoul) 2021;36:296-311. doi: 10.3803/EnM.2021.958.

[10] Iervolino M, Lepore E, Forte G, Laganà AS, Buzzaccarini G, Unfer V. Natural molecules in the management of polycystic ovary syndrome (PCOS): an analytical review. Nutrients 2021;13:1677. doi: 10.3390/nu13051677.

[11] Balamurugan S, Vijayakumar S, Prabhu S, Yabesh JM. Traditional plants used for the treatment of gynaecological disorders in Vedaranyam taluk, South India-An ethnomedicinal survey. Int J Tradit Complement Med Res 2018;8:308-23. doi: 10.1016/j.jtcme.2017.06.009.

[12] Naz S, Imran M, Rauf A, Orhan IE, Shariati MA, Shahbaz M, et al. Chrysin: Pharmacological and therapeutic properties. Life Sci 2019;235:116797. doi: 10.1016/j.lfs.2019.116797.

[13] Stompor-Gorący M, Bajek-Bil A, Machaczka M. Chrysin: Perspectives on contemporary status and future possibilities as pro-health agent. Nutrients 2021;13:2038. doi: 10.3390/nu13062038.

[14] Motta A B. Dehydroepiandrosterone to induce murine models for the study of polycystic ovary syndrome. J Steroid Biochem Mol Biol 2010;119:105-11. doi: 10.1016/j.jsbmb.2010.02.015.

[15] Adel A, Mansour A, Mohammad A, et al. Potential antioxidant activity of apigenin in the obviating stress-mediated depressive symptoms of experimental mice. Molecules 2022;27:9055. doi:10.3390/molecules27249055.

[16] Pai S A, Martis E A, Munshi R P, Gursahani M S, Mestry S N, Juvekar A R. Chrysin mitigated obesity by regulating energy intake and expenditure in rats. Int J Tradit Complement Med Res 2019:10: 577-85. doi: 10.1016/j.jtcme.2019.09.002.

[17] Classics Lowry O, Rosebrough N, Farr A, Randall R. Protein measurement with the Folin phenol reagent. J Biol Chem 1951;193:265-75. doi: 10.1016/S0021-9258(19)52451-6.

[18] Ohkawa H, Ohishi N, Yagi K. Assay for lipid peroxides in animal tissues by thiobarbituric acid reaction. Anal Biochem 1979;95:351-8. doi: 10.1016/0003-2697(79)90738-3.

[19] Sun Y, Oberley LW, Li Y. A simple method for clinical assay of superoxide dismutase. Clin Chem 1988;34:497-500. doi:10.1093/clinchem/34.3.497.

[20] Aebi H. Catalase methods of enzymatic analysis. In: Hu B, editor.New York: Academic Press Inc, 1974:673-77. doi: 10.1016/S0076-6879(84)05016-3.

[21] Paglia DE, Valentine WN. Studies on the quantitative and qualitative characterization of erythrocyte glutathione peroxidase. JLM 1967;70:158-69. doi: 002.221.4367900765.

[22] Zhuang Z, Pan X, Zhao K, et al. The effect of Interleukin-6 (IL-6), Interleukin-11 (IL-11), signal transducer and activator of transcription 3 (STAT3), and AKT signaling on adipocyte proliferation in a rat model of polycystic ovary syndrome. Med Sci Monit 2019;25:7218. doi: 10.12659/MSM.916385.

[23] Souza AZd, Fonseca A, Izzo V, Clauzet R, Salvatore C. Ovarian histology and function after total abdominal hysterectomy. Obstet Gynecol 1986;68:847-9.

[24] Ndefo UA, Eaton A, Green MR. Polycystic ovary syndrome: a review of treatment options with a focus on pharmacological approaches. Pharmacy and Therapeutics 2013;38:336.

[25] Yuan R, Lin Y. Traditional Chinese medicine.Pharmacology and Therapeutics 2000;86:191-8. doi: 10.1016/s0163-7258(00)00039-5.

[26] Podolsky S H, Greene J A. 2011. Combination drugs—hype, harm, and hope. NEJM AI 2011;365:488-91. doi: 10.1056/NEJMp1106161.

[27] Nallathambi A, Bhargavan R. Regulation of estrous cycle by Cynodon dactylon in letrozole induced polycystic ovarian syndrome in Wistars albino rats. Anat Cell Biol 2019;52:511-7. doi: 10.5115/acb.19.114.

[28] Baptiste CG, Battista M-C, Trottier A, Baillargeon J-P. Insulin and hyperandrogenism in women with polycystic ovary syndrome. J Steroid Biochem Molec Biol 2010;122:42-52. doi: 10.1016/j.jsbmb.2009.12.010.

[29] Furat Rencber S, Kurnaz Ozbek S, Eraldemır C, et al. Effect of resveratrol and metformin on ovarian reserve and ultrastructure in PCOS: an experimental study. J Ovarian Res 2018;11:1-16. doi: 10.1186/s13048.018.0427-7.

[30] Orlowski M, Sarao MS. Physiology, follicle stimulating hormone. Follicle StatPearls Publishing, NCBI Bookshelf: 2018.

[31] Reed BG, Carr BR, Feingold KR. The normal menstrual cycle and the control of ovulation. Endotext [Internet]. South Dartmouth (MA): MDText.com, Inc.; 2000

[32] Holesh JE, Bass AN, Lord M. Physiology, ovulation. In: StatPearls [Internet]. Treasure Island (FL): StatPearls Publishing; 2024 Jan 2023 May 1. 2017.

[33] Lee YH, Yang H, Lee SR, Kwon SW, Hong E-J, Lee HW. Welsh onion root (Allium fistulosum) restores ovarian functions from letrozole induced-polycystic ovary syndrome. Nutrients 2018;10:1430. doi: 10.3390/nu10101430.

[34] Zheng S, Chen Y, Ma M, Li M. Mechanism of quercetin on the improvement of ovulation disorder and regulation of ovarian CNP/NPR2 in PCOS model rats. J.Formosan Med.Assoc 2022;121:1081-92. doi: 10.1016/j.jfma.2021.08.015.

[35] Shrivastava VK. Turmeric extract alleviates endocrine-metabolic disturbances in letrozole-induced PCOS by increasing adiponectin circulation: A comparison with Metformin. Metabolism Open 2022;13:100160. doi: 10.1016/j.metop.2021.100160.

[36] Mihanfar A, Nouri M, Roshangar L, Khadem-Ansari MH. Therapeutic potential of quercetin in an animal model of PCOS: Possible involvement of AMPK/SIRT-1 axis. Eur J Med Chem Rep 2021;900:174062. doi: 10.1016/j.ejphar.2021.174062.

[37] Cable J, Grider M. Physiology, progesterone. In: StatPearls. StatPearls Publishing Copyright© 2022, StatPearls Publishing LLC Treasure Island: 2022.

[38] Szeliga A, Rudnicka E, Maciejewska-Jeske M, et al. Neuroendocrine determinants of polycystic ovary syndrome. Int J Environ Health Res 2022;19:3089. doi: 10.3390/ijerph19053089.

[39] Adelakun SA, Ukwenya VO, Peter AB, Siyanbade AJ, Akinwumiju CO. Therapeutic effects of aqueous extract of bioactive active component of Ageratum conyzoides on the ovarian-uterine and hypophysis-gonadal axis in rat with polycystic ovary syndrome: Histomorphometric evaluation and biochemical assessment. Metabolism Open 2022;15:100201. doi: 10.1016/j.metop.2022.100201.

[40] Khazaei F, Ghanbari E, Khazaei M. Improved hormonal and oxidative changes by Royal Jelly in the rat model of PCOS: An experimental study. Int J Reprod Biomed 2021;19:515. doi: 10.18502/ijrm.v19i6.9373.

[41] Li Y, Zheng Q, Sun D, et al. Dehydroepiandrosterone stimulates inflammation and impairs ovarian functions of polycystic ovary syndrome. J Cell Physiol 2019;234:7435-47. doi: 10.1002/jcp.27501.

[42] Amato G, Conte M, Mazziotti G, et al. Serum and follicular fluid cytokines in polycystic ovary syndrome during stimulated cycles. Obstet Gynecol 2003;101:1177-82. doi: 10.1016/s0029-7844(03)00233-3.

[43] Ebejer K, Calleja-Agius J. The role of cytokines in polycystic ovarian syndrome. Gynecology Endocrinolology 2013;29:536-40. doi: 10.3109/09513.590.2012.760195.

[44] Dinarello CA, Novick D, Kim S, Kaplanski G. Interleukin-18 and IL-18 binding protein. Front Immunol 2013;4:289. doi: 10.3389/fimmu.2013.00289.

[45] Yang Y, Qiao J, Li R, Li M-Z. Is interleukin-18 associated with polycystic ovary syndrome. Reprod Biol Endocrinol 2011;9:1-5. doi: 10.1186/1477-7827-9-7.

[46] Wu G, Hu X, Ding J, Yang J. The effect of glutamine on Dehydroepiandrosterone-induced polycystic ovary syndrome rats. J Ovarian Res 2020;13:1-7. doi: 10.1186/s13048.020.00650-7.

[47] Wang W, Zheng J, Cui N, et al. Baicalin ameliorates polycystic ovary syndrome through AMP-activated protein kinase. J Ovarian Res 2019;12:1-12. doi: 10.1186/s13048.019.0585-2.

[48] Brenjian S, Moini A, Yamini N, et al. Resveratrol treatment in patients with polycystic ovary syndrome decreased pro-inflammatory and endoplasmic reticulum stress markers. Am J Reprod Immunol 2020;83:e13186. doi: 10.1111/aji.13186.

[49] Gallinelli A, Ciaccio I, Giannella L, Salvatori M, Marsella T, Volpe A. Correlations between concentrations of interleukin-12 and interleukin-13 and lymphocyte subsets in the follicular fluid of women with and without polycystic ovary syndrome. Fertil Steril 2003;79:1365-72. doi: 10.1016/s0015-0282(03)00344-3.

[50] Stokkeland LMT, Giskeødegård GF, Ryssdal M, et al. Changes in serum cytokines throughout pregnancy in women with polycystic ovary syndrome. The J Clin Endocrinol Metab 2022;107:39-52. doi: 10.1210/clinem/dgab684.

[51] Huang Y, Zhang X. Luteolin alleviates polycystic ovary syndrome in rats by resolving insulin resistance and oxidative stress. Am J Physiol Endocrinol Metab 2021;320:E1085-E92. doi: 10.1152/ajpendo.00034.2021.

[52] Haslan MA, Samsulrizal N, Hashim N, Zin NSNM, Shirazi FH, Goh YM. Ficus deltoidea ameliorates biochemical, hormonal, and histomorphometric changes in letrozole-induced polycystic ovarian syndrome rats. BMC Complement Med Ther 2021;21:1-13. doi: 10.1186/s12906.021.03452-6.

[53] Koohestani Y, Abdi A, Salehiyeh S, Pourmirzaei F, Çiftci M, Emir Çoban O. Protective effect of apigenin on ovarian follicles in polycystic ovary syndrome-induced rats. Med Lab J 2022; 16:2. doi: 10.29252/mlj.16.2.7.

[54] Darabi P, Khazali H, Mehrabani Natanzi M. Therapeutic potentials of the natural plant flavonoid apigenin in polycystic ovary syndrome in rat model: via modulation of pro-inflammatory cytokines and antioxidant activity, Gynecology Endocrinology 2020; 36: 582-7. doi: 10.1080/09513.590.2019.1706084.

MARMARA
MEDICAL JOURNAL

Original Article

https://dergipark.org.tr/tr/pub/marumj

The relationship between gastrointestinal complaints and the use of pancreatin-derivated medications after cholecystectomy

Sefa ERGUN[1], Betul GUZELYUZ[2], Batuhan TOZAKOGLU[1], Osman SIMSEK[1], Salih PEKMEZCI[1]

[1] Department of General Surgery, Cerrahpasa Faculty of Medicine, Istanbul University, Cerrahpasa, Istanbul, Turkey
[2] General Surgery Clinic, Afsin State Hospital, Kahramanmaras, Turkey

Corresponding Author: Betul GUZELYUZ
E-mail: b.gzlyz1994@gmail.com

Submitted: 03.08.2023 **Accepted:** 10.02.2024

ABSTRACT

Objective: The aim of this study was to investigate the relationship between pancreatin-derived medications and the treatability of gastrointestinal complaints after cholecystectomy.

Patients and Methods: The relationship between postoperative symptomatic status and the use of proton pump inhibitors (PPIs) and pancreatin-derivated medications in patients admitted to our hepatobiliary surgery service who underwent cholecystectomy was retrospectively analyzed. IBM SPSS Statistics 23 (IBM SPSS,Turkey) was used for statistical analysis. Descriptive statistical methods (mean, standard deviation, median, frequency, ratio, minimum, maximum) were used to evaluate the study data. Pearson Chi-Square Test and Fisher's Exact test were used to compare qualitative data. Significance was evaluated at the $p<0.05$ level.

Results: Proton pump inhibitors and pancreatin-derivatives were prescribed to all patients in the postoperative period. Although, the rate of postoperative asymptomatic course was higher in all patients, the rate of postoperative symptoms was found to be higher in patients who received PPI and pancreatin therapy ($p=0.001$, $p=0.022$; $p<0.01$).

Conclusions: Although, the high rate of asymptomatic postoperative course in all patients indicates that cholecystectomy alone is curative, some symptoms may persist in the postoperative period and it was found to be more frequent in patients who used PPI and pancreatin-derived medications in the postoperative period.

Keywords: Cholecystectomy, Pancreatin-derivatives, Proton Pump Inhibitors, Dyspepsia

1. INTRODUCTION

Dyspepsia is a combination of symptoms including subjective complaints such as upper abdominal or retrosternal pain, bloating that does not resolve with defecation, early satiety, feeling of fullness and nausea, with a wide range of differential diagnoses and can be explained by multiple pathophsiologic mechanisms [1,2]. It has been reported that some patients presenting with dyspeptic complaints are diagnosed with gastritis or peptic ulcer, while many do not know the exact diagnosis [3]. In addition, it has also been reported that helicobacter pylori eradication treatment causes a significant decrease in dyspepsia complaints [4]. The main factors causing dyspepsia are gastritis, gastroesophageal reflux disease and peptic ulcer, as well as drugs and gastric malignancies [5]. Pancreatobiliary pathologies ranging from asymptomatic gallstones to malignancies are known to be among the causes of dyspepsia. Gallstones are usually clinically asymptomatic and incidentally detected. Cholecystectomy is the primary treatment method for symptomatic or complicated gallstones, and is used prophylactically in the presence of porcelain sacs, gallbladder polyps larger than 1 cm in diameter, sickle cell anemia and hereditary spherocytosis, even if asymptomatic [6,7]. However, major biliary pathologies may produce a clinical picture with pancreatic enzyme deficiency and many may be associated with gastrointestinal symptoms. Treatment of patients with pancreatic enzyme deficiency is a difficult clinical picture, especially in patients with chronic alcoholic pancreatitis or cystic fibrosis and after pancreatectomy [8].

Pancreatic enzyme deficiency is considered in patients with symptoms such as steatorrhea, diarrhea and weight loss, and this condition is shown by various diagnostic methods. In addition, findings such as pancreatic ductal dilatation or stones by various imaging or endoscopic methods and the presence of other symptoms support pancreatic enzyme deficiency and pancreatic enzyme replacement constitutes the basic treatment strategy

How to cite this article: Ergun S, Guzelyuz B, Tozakoglu B, Simsek O, Pekmezci S. The relationship between gastrointestinal complaints and the use of pancreatin-derivated medications after cholecystectomy. Marmara Med J 2024: 37(2):208-213. doi: 10.5472/marumj.1481286

ISSN: 1309-9469

http://doi.org/10.5472/marumj.1481286
Marmara Med J 2024;37(2): 208-213

in such cases [9]. Digestion of fats is the determining factor in pancreatic enzyme deficiency, and some systemic diseases such as denaturation of lipase by gastric acid, inappropriate timing of enzymes, concomitant small intestinal mucosal diseases, rapid intestinal transit, and some systemic diseases such as diabetes and some genetic diseases such as cystic fibrosis also affect the activity of pancreatic enzymes [10]. Furthermore, it has been shown that pancreatic exocrine insufficiency may ocur after gastrectomy in some patient subgroups [11].

Pancreatic enzyme replacement therapy has been found safe and effective in many complicated causes of pancreatic exocrine insufficiency, including chronic pancreatitis, cystic fibrosis and pancreatic cancer [12]. However, uncomplicated gallstones may also be accompanied by dyspeptic complaints and pancreatic enzyme replacement has been tried for treatment. In this study, we aimed to investigate the relationship between pancreatin-derived medications and the treatability of gastrointestinal complaints after cholecystectomy.

2. PATIENTS and METHODS

The data of patients admitted to the Istanbul University Cerrahpasa Medical Faculty, Hepatobiliary Surgery Service who underwent laparoscopic cholecystectomy were reviewed retrospectively. Preoperative examinations and evaluations as well as data recorded in patient files and hospital databases were analyzed, and age, gender, pre-cholecystectomy abdominal imaging results and clinics, preoperative complicated cholelithiasis status, preoperative pain and dyspepsia symptoms were recorded for each patient. The presence of complicated cholelithiasis was determined according to the preoperative history of cholangitis, choledocholithiasis, biliary pancreatitis, endoscopic retrograde cholangiopancreatography, and the presence of cholecystitis, cholecystostomy, and peropal conversion to open surgery. These findings were obtained by reviewing patient anamnesis and clinical course notes, radiological imaging and operative notes, and postoperative pathology reports in hospital databases. All patients were given perioperative antibiotic prophylaxis, and in the postoperative period, proton pump inhibitor (PPI) was prescribed once daily in the morning before meals and pancreatin derivetives were prescribed three times daily between meals. Pancreatin, a crude mixture, is derived from pig or ox pancreas and contains at least 2 United States Pharmacopeia (USP) units of lipase and 25 USP units of amylase and protease activity per milligram. The pancreatin product prescribed to the patients was 170 mg (5500 Amylase, 6500 Lipase, 400 Protease F.I.P units) (porcine origin). The symptomatic status of the patients after discharge and the use of the prescribed medications were learned by telephone. Preoperative symptoms and complaints, early postoperative symptoms at 1st month, and late postoperative symptoms at 3rd month were questioned separately. Gastritis history was recorded according to the presence of complaints and gastroscopy results. Patients without dyspeptic complaints and without gastroscopy were considered to have no history of gastritis.

Patients undergoing laparoscopic cholecystectomy who had no evidence of other organic, systemic, metabolic diseases to explain dyspeptic symptoms were included into the study; some systemic, gastrointestinal, and genetic diseases such as cystic fibrosis accompanied by pancreatic enzyme deficiency, patients who underwent major pancreatobiliary surgery, open cholecystectomies, patients who developed complications such as bilioma, biliary tract injury, etc. requiring rehospitalization after cholecystectomy, patients with pregnancy or breastfeeding status, and patients whose data could not be reached or who refused to participate were excluded. In addition, inability to provide standardization in detailing the cost for patients not using PPI and pancreatin derivatives, disregarding the treatment, considering medical treatment unnecessary/surgical sufficient, ideological and religious reasons, etc. were not examined and were excluded from the discussion for objectivity.

The study was reviewed by the Clinical Research Ethics Committee of Istanbul University Cerrahpasa Medical Faculty on 07.09.2021, and was approved with the number E-83045809-604.01.02-178270.

Statistical Analysis

IBM SPSS Statistics 23 (IBM SPSS, Turkey) program was used for statistical analysis while evaluating the findings obtained in the study. Descriptive statistical methods (mean, standard deviation, median, frequency, ratio, minimum, maximum) were used to evaluate the study data. Pearson Chi-Square Test and Fisher's Exact test were used to compare qualitative data. Significance was evaluated at the $p<0.05$ level.

3. RESULTS

In this study, a total of 290 patients, 61.4% (n=178) female and 38.6% (n=112) male, who underwent cholecystectomy were retrospectively analyzed. The ages of the patients ranged between 22-88 years with a mean age of 54.45±13.79 years. Preoperatively, 25.2% (n=73) had complicated cholelithiasis, 31.4% (n=91) had gastritis, 74.5% (n=216) had pain and 48.3% (n=140) had dyspeptic complaints. The mean length of hospitalization was 1.44 days. All patients received perioperative antibiotic prophylaxis and PPI and pancreatin derivatives were prescribed to all patients after discharge. In the postoperative period, 33.8% (n=98) of the patients used PPIs, 48.6% (n=141) used pancreatin derivatives, and 21.4% (n=62) used both PPIs and pancreatin. In the early postoperative period, 90.7% (n=263) of the patients were asymptomatic, 5.5% (n=16) had pain and 3.8% (n=11) had dyspeptic complaints. In the advanced postoperative period, 89.3% (n=259) of the patients were asymptomatic, 4.5% (n=13) had pain and 6.2% (n=18) had dyspeptic complaints (Table I).

There was no significant difference in the distribution of symptoms in the early postoperative period and in the advanced postoperative period according to age, gender, and the presence of complicated cholelithiasis in the preoperative period ($p>0.05$). There was also no significant difference in the distribution of symptoms according to the patients' history of gastritis ($p>0.05$). However, in the advanced postoperative period, the

rate of dyspeptic complaints was higher than pain complaints in patients with a history of gastritis (p=0.015; p<0.05) (Table II).

In the evaluation of postoperative symptoms, the rate of postoperative asymptomatic progression was higher in all groups compared to PPI use alone, however, both pain and dyspepsia rates were higher in PPI use alone (p=0.002, p=0.001; p<0.01) (Table III).

Table I. *Distribution of descriptive characteristics*

		n	%
Age (year)	Min-Max Mean±Sd	(Median); 22-88 (55)	54.45±13.79
	< 40 years	42	14.5
	≥ 40 years	248	85.5
Gender	Female	178	61.4
	Male	112	38.6
Having Preoperative Complicated Cholelithiasis	None	217	74.8
	Yes	73	25.2
Preoperative gastritis history	None	199	68.6
	Yes	91	31.4
Postoperative PPI use only	None	192	66.2
	Yes	98	33.8
Postoperative use of Pancreatin	None	149	51.4
	Yes	141	48.6
Postoperative use of PPI+Pancreatin	None	228	78.6
	Yes	62	21.4
Preoperative period symptoms	Pain	216	74.5
	Dyspepsia	140	48.3
Early postoperative period symptoms	Asymptomatic	263	90.7
	Pain	16	5.5
	Dyspepsia	11	3.8
Advanced postoperative period symptoms	Asymptomatic	259	89.3
	Pain	13	4.5
	Dyspepsia	18	6.2

(More than one symptom may occur together in each case.)
(PPI: Proton Pump Inhibitor)

Table II. *Evaluation of symptoms in early postoperative and postoperative advanced periods according to the presence of preoperative gastritis history*

		Preoperative Gastritis History		
		None (n=199)	Yes (n=91)	P
		n (%)	n (%)	
Early postoperative period symptoms	Asymptomatic	183 (92.0)	80 (87.9)	0.496
	Pain	10 (5.0)	6 (6.6)	
	Dyspepsia	6 (3.0)	5 (5.5)	
Advanced postoperative period symptoms	Asymptomatic	184 (92.5)	75 (82.4)	0.015*
	Pain	8 (4.0)	5 (5.5)	
	Dyspepsia	7 (3.5)	11 (12.1)	

Pearson Chi-Square Test *p<0.05

In the evaluation of postoperative symptoms, the rate of asymptomatic course was higher in all groups compared to postoperative pancreatin derivatives use alone; there was no significant difference in the distribution and rate of symptoms in the early postoperative period symptoms (p>0.05). However, in the advanced postoperative period, the rate of symptoms was higher in pancreatin users; among the symptoms, the incidence of dyspepsia was found to be higher (p=0.001; p<0.01) (Table IV).

Table III. *Evaluation of symptoms in the early postoperative and postoperative advanced periods based on PPI use only*

		PPI Use Only		
		None (n=192)	Yes (n=98)	P
		n (%)	n (%)	
Early postoperative period symptoms	Asymptomatic	182 (94.8)	81 (82.7)	0.002**
	Pain	7 (3.6)	9 (9.2)	
	Dyspepsia	3 (1.6)	8 (8.2)	
Advanced postoperative period symptoms	Asymptomatic	183 (95.3)	76 (77.6)	0.001**
	Pain	5 (2.6)	8 (8.2)	
	Dyspepsia	4 (2.1)	14 (14.3)	

Pearson Chi-Square Test **p<0.01

Table IV. *Evaluation of symptoms in early postoperative and postoperative advanced periods according to postoperative pancreatin derivative use*

		Use of Pancreatin Derivative Only		
		None (n=149)	Yes (n=141)	P
		n (%)	n (%)	
Early postoperative period symptoms	Asymptomatic	140 (94.0)	123 (87.2)	0.125
	Pain	6 (4.0)	10 (7.1)	
	Dyspepsia	3 (2.0)	8 (5.7)	
Advanced postoperative period symptoms	Asymptomatic	141 (94.6)	118 (83.7)	0.001**
	Pain	7 (4.7)	6 (4.3)	
	Dyspepsia	1 (0.7)	17 (12.1)	

Pearson Chi-Square Test **p<0.01

Table V. *Evaluation of symptoms in early postoperative and postoperative advanced periods according to postoperative PPI + pancreatin derivative concomitant use*

		Use of PPI + Pancreatin derivative		
		None (n=228)	Yes (n=62)	p
		n (%)	n (%)	
Early postoperative period symptoms	Asymptomatic	211 (92.5)	52 (83.9)	0.022*
	Pain	12 (5.3)	4 (6.5)	
	Dyspepsia	5 (2.2)	6 (9.7)	
Advanced postoperative period symptoms	Asymptomatic	213 (93.4)	46 (74.2)	0.001**
	Pain	10 (4.4)	3 (4.8)	
	Dyspepsia	5 (2.2)	13 (21.0)	

Fisher Freeman Halton Exact Test *p<0.05 **p<0.01

The rate of asymptomatic course was found to be higher; when the symptoms were analyzed, it was observed that the rate of being symptomatic increased in postoperative PPI and pancreatin combination use, and the rate of dyspepsia increased more than pain (p=0.022, p=0.001; p<0.05) (Table V). The distribution of symptoms in the postoperative period was similar according to age and gender, and according to the presence of a history of gastritis in postoperative PPI and pancreatin combination use (p>0.05).

When the distribution of postoperative symptoms in the combined use of PPI and pancreatin derivatives, it was observed that the rate of being asymptomatic was higher in all groups. However, the rate of symptomatic patients was higher in patients who used PPI+pancreatin combination; in patients who did not have preoperative complicated cholelithiasis, the pain seen in the early postoperative period decreased in the postoperative advanced period, and the rate of dyspepsia increased. In patients with preoperative complicated cholelithiasis, there was no change in the rate of pain in the postoperative period, while the rate of dyspepsia increased in the postoperative advanced period (p>0.05). In patients who did not use PPI + pancreatin combination postoperatively, both pain and dyspepsia rates decreased in the postoperative advanced period in patients without complicated cholelithiasis. However, in patients with complicated cholelithiasis, the postoperative advanced period pain rate did not change, whereas the dyspepsia rate increased (p=0.014; p<0.05) (Table VI).

Table VI. *Evaluation of symptoms in the early postoperative and postoperative advanced periods according to the presence of preoperative complicated cholelithiasis in the combination of postoperative PPI + pancreatin derivative*

Use of PPI + Pancreatin derivative	Period	Symptoms	Preoperative Complicated Cholelithiasis None (n=217) n (%)	Preoperative Complicated Cholelithiasis Yes (n=73) n (%)	p
Yes	Early post- operative period symptoms	Asymptomatic	38 (82.6)	14 (87.5)	1.000
		Pain	3 (6.5)	1 (6.3)	
		Dyspepsia	5 (10.9)	1 (6.3)	
	Advanced post-operative period symptoms	Asymptomatic	35 (76.1)	11 (68.8)	0.771
		Pain	2 (4.3)	1 (6.3)	
		Dyspepsia	9 (19.6)	4 (25.0)	
None	Early post-operative period symptoms	Asymptomatic	160 (93.6)	51 (89.5)	0.172
		Pain	9 (5.3)	3 (5.3)	
		Dyspepsia	2 (1.2)	3 (5.3)	
	Advanced post-operative period symptoms	Asymptomatic	163 (95.3)	50 (87.7)	0.014*
		Pain	7 (4.1)	3 (5.3)	
		Dyspepsia	1 (0.6)	4 (7.0)	

Fisher Freeman Halton Exact Test **p<0.05*

4. DISCUSSION

Gallstones are one of the most common gastrointestinal problems in the general population. In our study where 290 patients underwent cholecystectomy, 25.2% (n=73) had a history of complicated cholelithiasis and 31.4% (n=91) had a history of gastritis in the preoperative period; when the symptoms were examined, 74.5% (n = 216) had pain and 48.3% (n = 140) had dyspeptic complaints. Cholecystectomy is the main treatment for symptomatic or complicated gallstones. Studies have shown that although dyspeptic complaints are significantly reduced after cholecystectomy, dyspepsia and abdominal pain persist in some patients. There are also studies indicating that pathologies such as gastritis, duodenitis and ulcers may accompany patients with atypical gastrointestinal complaints and that persistent symptoms may be related to them [7]. In our study, the rate of asymptomatic course in the postoperative period was significantly higher in all patients, and this result is consist with the fact that cholecystectomy alone is curative in cholelithiasis. In our study, postoperative symptoms such as dyspepsia and abdominal pain were not releated to age, gender, and complexity of cholelithiasis; however, it was shown that postoperative dyspeptic symptoms were higher in patients with a history of gastritis.

Although, the evaluation of upper abdominal pain after cholecystectomy is subjective, its frequency has been reported in the literature between 10-33% and higher in women. Although, the causes have not been fully elucidated, periampullary pathologies and oddi sphincter dysfunction have been found to be the most common etiologies [13]. In our study, the frequency of pain after cholecystectomy was between 4.5-5.5%, and no difference was found according to age and gender.

The main causes of dyspepsia include peptic ulcer disease, gastroesophageal reflux disease, biliary pathologies, some drugs and gastric malignancies [14]. Studies have shown that

the most common findings in patients with dyspepsia are erosive esophagitis and peptic ulcer disease, and treatment has been reported to cause a significant reduction in dyspepsia complaints [14,15]. It is known that proton pump inhibitors alone or in combination have a place in the treatment of diseases such as gastritis and ulcers, and pancreatic enzymes are used in the treatment of digestive disorders in which fat digestion is the determinant [10]. In our study, only PPIs were used in 33.8% (n=98), only pancreatin derivatives in 48.6% (n=141) and both PPIs and pancreatin derivatives in 21.4% (n=62) of the patients in the postoperative period.

In our study, an increase was observed in postoperative symptoms with the use of PPI alone or pancreatin derivative alone. Similarly, the combination of PPI and pancreatin derivative caused an increase in postoperative symptoms and the rate of dyspepsia was higher. When the reasons for this are examined, it should be kept in mind that pancreatic enzyme replacement may not always provide the desired beneficial effect due to enzyme inactivation by gastric acid [16]. As a matter of fact, in our study, the distribution of symptoms was found to be similar in PPI and pancreatin use when evaluated according to the presence of history of gastritis; even in the presence of preoperative complicated cholelithiasis, which has been shown to be associated with postoperative symptomatic status, PPI and pancreatin derivated use did not decrease or even increased the symptoms.

Pancreatic enzyme replacement therapy (PERT) is a difficult clinical problem due to acid instability. To solve this problem, various preparations of porcine pancreatin or some fungal enzymes have been introduced to the market as enteric-coated tablets or microspheres, and sometimes combined therapies with H2 receptor antagonists are required [10]. Exocrine insufficiency occurs in more than 90% dysfunction of the pancreas and PERT is given to reduce malnutrition and morbidity to patients with insufficiency [17]. There are publications showing the benefits of routine PERT use after pancreatic resections [18]. In cases of pancreatic insufficiency after gastric surgery, PERT has been shown to improve malnutrition and improve quality of life [19].

Based on the data obtained in the study, postoperative PPIs and pancreatin derived medications had no positive effect on ongoing postoperative symptoms and even had a negative effect. Therefore, in the light of the available data, it can be concluded that such medications should be limited to major pancreatobiliary pathologies for which the indication is indisputable today. Prospective, randomized and large-scale studies are needed for more precise and effective results.

Compliance with Ethical Standards

Ethical Approval: The study was reviewed by the Clinical Research Ethics Committee of Istanbul University Cerrahpasa Medical Faculty on 07.09.2021, and was approved with the number E-83045809-604.01.02-178270.

Financial Support: This research did not receive any specific grant from funding agencies in the public, commercial, or not-for-profit sectors.

Conflict of Interest: The authors declare no competing interests.

Authors' Contibutions: SE: Providing study data, consultant, BG: Putting forward a hypothesis, researching the literature, writing the article, communicating, BT: Editing and analyzing study data, OS and SP: Providing study data. All authors read and approved the final version of the manuscript.

REFERENCES

[1] Talley NJ, Silverstein MD, Agréus L, Nyrén O, Sonnenberg A, Holtmann G. AGA technical review: evaluation of dyspepsia. American Gastroenterological Association. Gastroenterology 1998;114:582-95. doi: 10.1016/s0016-5085(98)70542-6.

[2] Medic B, Babic Z, Banic M, Ljubicic L. Modern approach to dyspepsia. Acta Clin Croat 2021;60:731-8. doi: 10.20471/acc.2021.60.04.21

[3] Çalışkan HM, Çelik B. Evaluation of management of patients who apply to emergency service with dyspeptic complaints. J Contemp Med 2021;11:640-6. doi:10.16899/jcm.913357

[4] Chey WD, Leontiadis GI, Howden CW, Moss SF. ACG clinical guideline: Treatment of Helicobacter pylori infection. Am J Gastroenterol 2017;112:212-39. doi: 10.1038/ajg.2016.563.

[5] Kavitt RT, Lipowska AM, Anyane-Yeboa A, Gralnek IM. Diagnosis and treatment of peptic ulcer disease. Am J Med 2019;132:447-56. doi: 10.1016/j.amjmed.2018.12.009

[6] Talley NJ, Vakil NB, Moayyedi P. American gastroenterological association technical review on the evaluation of dyspepsia. Gastroenterology 2005;129:1756-80. doi: 10.1053/j.gastro.2005.09.020.

[7] Kırık A, Yekdeş AC, Ergün U, Alp B, Ak MN, Doğru T, Investigation of cholecystectomy frequency and associated factors in asymptomatic gallstones. Ahi Evran Med J 2021;5:3-7 doi: 10.46332/aemj.776273

[8] Löser C, Fölsch UR, Clinical and pharmacological aspects of pancreatic enzyme substitution therapy. Leber Magen Darm 1991;21:56-65.

[9] Pongprasobchai S. Maldigestion from pancreatic exocrine insufficiency. J Gastroenterol Hepatol 2013;28(Suppl 4):99-102. doi: 10.1111/jgh.12406.

[10] Hammer HF. Pancreatic exocrine insufficiency: diagnostic evaluation and replacement therapy with pancreatic enzymes. Dig Dis 2010;28:339-43. doi: 10.1159/000319411.

[11] Huddy JR, Macharg FM, Lawn AM, Preston SR. Exocrine pancreatic insufficiency following esophagectomy. Dis Esophagus 2013;26:594-7. doi: 10.1111/dote.12004.

[12] Brennan GT, Saif MW, Pancreatic enzyme replacement therapy: A concise review. JOP 2019;20:121-5.

[13] Zhang J, Lu Q, Ren YF, et al. Factors relevant to persistent upper abdominal pain after cholecystectomy. HPB (Oxford) 2017;19:629-37. doi: 10.1016/j.hpb.2017.04.003.

[14] Ford AC, Marwaha A, Lim A, Moayyedi P. What is the prevalence of clinically significant endoscopic findings in subjects with dyspepsia? Systematic review and meta-analysis. Clin Gastroenterol Hepatol 2010;8:830-7. doi: 10.1016/j.cgh.2010.05.031.

[15] Moayyedi P, Lacy BE, Andrews CN, Enns RA, Howden CW, Vakil N. ACG and CAG clinical guideline: Management of dyspepsia. Am J Gastroenterol 2017;112:988-1013. doi: 10.1038/ajg.2017.154.

[16] Lankisch PG, Lembcke B, Göke B, Creutzfeldt W. Therapy of pancreatogenic steatorrhoea: does acid protection of pancreatic enzymes offer any advantage? Z Gastroenterol 1986;24:753-7.

[17] Sikkens EC, Cahen DL, Kuipers EJ, Bruno MJ. Pancreatic enzyme replacement therapy in chronic pancreatitis. Best Pract Res Clin Gastroenterol 2010;24:337-47. doi: 10.1016/j.bpg.2010.03.006.

[18] Phillips ME. Pancreatic exocrine insufficiency following pancreatic resection. Pancreatology 2015;15:449-55. doi: 10.1016/j.pan.2015.06.003

[19] Catarci M, Berlanda M, Grassi GB, Masedu F, Guadagni S. Pancreatic enzyme supplementation after gastrectomy for gastric cancer: a randomized controlled trial. Gastric Cancer 2018;21:542-51. doi: 10.1007/s10120.017.0757-y.

MARMARA
MEDICAL JOURNAL

Original Article

https://dergipark.org.tr/tr/pub/marumj

Comparison of Salter innominate osteotomy and Pemberton pericapsular osteotomy combined with open reduction through medial adductor approach on acetabular development in the treatment of developmental hip dysplasia

Bunyamin ARI[1], Hafiz AYDIN[2]

[1] Department of Orthopedics and Traumatology, Faculty of Medicine, Kutahya Health Sciences University, Kutahya, Turkey
[2] Department of Orthopaedics and Traumatology, School of Medicine, Karadeniz Technical University, Trabzon, Turkey

Corresponding Author: Bunyamin ARI
E-mail: drbunyaminari@hotmail.com

Submitted: 22.08.2023 **Accepted:** 12.01.2024

ABSTRACT

Objective: Combined with open reduction through medial adductor approach, Salter innominate osteotomy (SIO) and Pemberton pericapsular osteotomy (PPO) methods are common procedures for the repair of incomplete acetabulum structure in patients with developmental hip dysplasia (DHD). The aim of this study is to compare the outcomes of acetabulum development in patients treated using these two methods.

Patients and Methods: We retrospectively reviewed the medical records of 50 (65 hip joints) children who underwent SIO or PPO for DHD. Thirty-three patients underwent SIO and 32 patients underwent PPO as surgical treatment. The criteria of Tönnis, modified McKay, and Severin, and angles of acetabular index (AI) and acetabular center-edge (CE) angles of both groups were compared.

Results: There were significant differences between two groups in the time of operation, follow-up time after operation, preoperative and postoperative AI angles, and postoperative 1st year CE angles. AI was detected as lower in the PPO group at 1st month postoperatively. Whereas, mean AI was detected as higher in the preoperative PPO group. In addition, the acetabular CE angle was significantly lower in the PPO group at 1st year postoperatively. However, there was no significant difference between the groups in terms of the CE angle value measured at the final follow-up.

Conclusion: Salter innominate osteotomy and PPO methods used in the treatment of DHD have specific advantages and disadvantages. Preoperative and intraoperative evaluations of patients are very important in determining which procedure should be performed. When the choice is made properly, clinical and radiological results are both satisfactory.

Keywords: Developmental hip dysplasia, Pemberton pericapsular osteotomy, Salter innominate osteotomy

1. INTRODUCTION

The purpose of treatment for developmental hip dysplasia (DHD) is reduction and stabilization of the joint and establishment of the physiological development of the hip. Patients <24 months of age are routinely performed open reduction through medial approach, and surgical outcomes are satisfactory especially for patients <12 months [1]. This is a simple, less traumatic and safe procedure with minimal soft tissue dissection and blood loss, also it can be applied to both hips in the same session [2]. But, after 18 months of age, structural changes around the dislocated hip may prevent concentric reduction. In such hips, medial approach has two major disadvantages: i) capsulorrhaphy which is required to prevent recurrent luxation or subluxation cannot be performed, and ii) acetabular osteotomy is not an option [2].

Salter innominate osteotomy (SIO) and Pemberton pericapsular osteotomy (PPO) are common procedures that can be performed in addition to open reduction through medial adductor approach for the repair of dysplasic acetabulum in patients with DHD; especially >18 months of age [3,4]. SIO is a complete osteotomy that reorients the entire acetabulum to achieve the best possible femoral head-acetabulum accordance [3]. However, PPO is an incomplete osteotomy performed to change the shape of the acetabulum depending on the horizontal branch of the triradiate cartilage [5]. The objective of both methods are to improve the antero-lateral coverage of the femoral head [6,7].

Our hypothesis is; there are some differences between the two methods that should be considered by the surgeon, by evaluating each patient individually, to achieve similar clinical and radiological results. Based on this hypothesis; this study aims to compare the results of acetabulum development in patients who underwent SIO or PPO in addition to open reduction through medial adductor approach, for the treatment of DHD.

How to cite this article: Ari B, Aydin H. Comparison of Salter innominate osteotomy and Pemberton pericapsular osteotomy combined with open reduction through medial adductor approach on acetabular development in the treatment of developmental hip dysplasia. Marmara Med J 2024: 37(2):214-218. doi: 10.5472/marumj.1483336

ISSN: 1309-9469

http://doi.org/10.5472/marumj.1483336
Marmara Med J 2024;37(2): 214-218

2. PATIENTS and METHODS

Patients and ethical consideration

The data of patients who underwent DHD surgery in the Department of Orthopedics and Traumatology, Faculty of Medicine, Karadeniz Technical University, between 1980 and 2010 were collected retrospectively. Using the contact information in the files, the patients were invited to the clinic for a final follow-up, for which 52 patients applied. As a result, 65 hip joints of 52 patients were included in the study.

All procedures were based on the 1975 Declaration of Helsinki Human Declaration revised in 2000. The Experimental Committee was conducted in accordance with ethical standards and ethics committee approval was obtained by Karadeniz Technical University Faculty of Medicine Scientific Research Ethics Committee with the letter numbered 24237859-216 and dated 26/04/2016

Exclusion criteria

Patients who did not come to final controls, were not followed up regularly, had hip dislocation due to teratological, neurological and other pathological causes, required additional intervention for any reason, had missing data, were not included in the study.

The study was conducted with 65 hip joints of 50 patients, who met the inclusion criteria. Patients who did not meet the exclusion criteria and who volunteered to participate in the study and signed an informed consent form were included in the study. DHD was bilateral in 15 patients, on the left side in 39 patients and on the right side in 26 patients. In addition to open reduction through medial adductor approach; 33 patients had undergone SIO (Group 1), and 32 had undergone PPO (Group 2).

Surgical method and follow-up

Open reduction through medial approach was performed to the hip joint by a longitudinal incision between the adductor longus and gracilis muscles. The minor trochanter of femur was revealed through a blunt dissection, and iliopsoas tenotomy was performed. The hip joint capsule was opened longitudinally and inferomedially. Intensive care was given during the retraction to avoid damage to adjacent vessels in the operation area. The transverse acetabular ligament was divided into two and pulvinar was removed if hypertrophic. After the reduction of the femoral head to acetabulum, the stability of the hip was tested in various directions [2]. The hips requiring abduction and flexion for stability and/or having an acetabular angle above 35° on preoperative radiography, underwent osteotomy. Osteotomy was performed without capsulorhaphy as specified by the abovementioned criteria. A straight incision, starting just above the anterior-inferior iliac spina and ending in the major sciatic incisura, and a curved incision extending to the posterior wing of the triradiate cartilage were performed, for SIO and PPO; respectively [5]. After the osteotomy, the lower part of the osteotomy patient was moved downward, outward and forward. The triangular graft taken from the iliac crystal was placed on the osteotomy site. In all SIO cases, the graft was fixed with two K-wires, while most of the PPO cases did not require fixation. After osteotomy; hip stabilization was re-tested in the walking position. Hip spica plaster was applied to the hips in 20° of flexion, 30° of abduction and 10° of internal rotation for six weeks. After removal of the cast, the abduction splint was used continuously for three months.

Clinical and radiological evaluations

Pelvic anteroposterior X-ray graphies that were taken preoperatively, in the 1st year after the operation and in the last follow-ups were used. The position of the ossification center of femoral head was evaluated using Tönnis method on preoperative radiographies [8], acetabular center-edge and femoral neck angles were measured on all radiographies.

Acetebular index (AI) angle: Based on AP pelvis radiography, AI was determined as the angle between horizontal line (Hilgenreiner line) connecting two triradiate cartilages and the line connecting lowest side point of the ilium in the Y cartilage and the lateral edge of the sclerotic part of the acetabulum [9,10]. Pre-AI refers to preoperative acetebular index, and post1-AI refers to acetebular index measured one month after the operation.

Acetabular center-edge (CE) angle: CE was determined as the angle between vertical line (parallel to the midline of the trunk) passing through the center of the femoral head and, the line connecting the center of the femoral head and outermost point of the acetabulum [9,11]. The femoral head was fixated with the help of a template including central concentric circles [12]. CE-1 refers to CE angle in the postoperative 1st year and CE-last refers to the CE angle that was measured in last follow-up. McKay criteria, modified by Berkeley et al., were used for clinical evaluation [13] (Table I), and Severin criteria was used for radiological evaluation [14] (Table II).

Table I. *The modified McKay criteria [13]*

Class	Rating	Description
1	Excellent	Painless, stable hip; no limp; more than 15° internal rotation
2	Good	Painless, stable hip; slight limp or decreased motion; (–) Trendelenburg's sign
3	Fair	Minimum pain; moderate stiffness; (+) Trendelenburg's sign
4	Poor	Significant pain

Table II. *Severin's classification for radiological grading of hip dysplasia [14]*

Group	Criteria	Centre-edge angle (degrees)	Age Range
1	Normal hip	>15 >20	5 to 13 >14
2	Concentric reduction of the joint with deformity of the femoral neck, head or acetabulum	>15 >20	5 to 13 >14
3	Dysplasia but no subluxatio	<15 <20	5 to 13 >14
4	Articulation with false acetabulum		
5	Subluxation		
6	Redislocation		

http://doi.org/10.5472/marumj.1483336
Marmara Med J 2024;37(2): 214-218

Statistical Analysis

Shapiro-Wilk test was used to evaluate whether or not the groups had homogeneous distribution (were distributed normally). Since, the groups were not homogeneously distributed, Mann-Whitney U-test was used for binary comparisons. A p value of <0.05 was considered statistically significant.

3. RESULTS

The comparison of some descriptive and clinical outcomes of Group 1 and Group 2 are shown in Table III. There was a significant difference in age of operation (month) (p=0.010), follow-up period after the operation (month) (p<0.0001), pre-AI (p=0.002), post1-AI (p=0.001), and CE-1 (p<0.0001) values, between two groups. The operation age was higher in Group 1 (31.4±22.2 and 19.8±2.53 months; p=0.010). Postoperative follow-up period (278.5±107 and 143.1±34.6 month, p<0.0001), Post1-AI (22.88±4.65 and 19.22±3.33, p=0.001,), postoperative CE-1 were significantly higher in Group 1 (33.76±2.57 and 31.03±2.96; respectively, p 0.0001). The mean pre-AI was higher in Group 2 (39.73±6.40 and 44.38±5.12; respectively, p=0.002). However, there was no significant difference between the groups in terms of the CE-last values.

Table III. *Comparison of some descriptive and clinical results of SIO and PPO.*

	Group	Number	Mean	SD	Min.	Max.	p
Operation age (month)	Salter	33	31.42	22.22	12	96	0.010
	Pemberton	32	19.84	2.529	16	24	
Postoperative follow-up period (month)	Salter	33	278.48	106.98	132	408	<0.0001
	Pemberton	32	143.13	34.59	96	240	
Preoperative Tönnis grade (%)	Salter	33	2.73	0.801	2	4	NS.
	Pemberton	32	2.47	0.671	2	4	
McKay clinical evaluation score	Salter	33	1.09	0.292	1	2	NS.
	Pemberton	32	1.06	0.246	1	2	
SS	Salter	33	1.15	0.364	1	2	NS.
	Pemberton	32	1.09	0.296	1	2	
Pre-AI	Salter	33	39.73	6.400	29	55	0.002
	Pemberton	32	44.38	5.123	34	52	
Post1-AI	Salter	33	22.879	4.649	15	39	0.001
	Pemberton	32	19.219	3.329	15	26	
CE-1	Salter	33	33.76	2.574	29	38	<0.0001
	Pemberton	32	31.03	2.957	25	38	
CE-last	Salter	33	34.30	5.120	20	45	NS.
	Pemberton	32	35.59	3.564	28	43	
Percentage (%)	Salter	33	32.4633	11.812	14.29	56.67	NS.
	Pemberton	32	49.1399	12.656	20.41	75.56	

NS: *Not significant,* ***SD:*** *Standard deviation,* ***SIO:*** *Salter innominate osteotomy,* ***PPO:*** *Pemberton pericapsular osteotomy,* ***CE:*** *Acetabular center-edge (CE) angle* ***SS:*** *Severin radiological evaluation score,* ***p:*** p *value*

The results of clinical and radiological evaluations (Table IV) indicated that; in Group 1; 16 (48.5%) patients were Tönnis Grade 2, 10 (30.3%) were Tönnis Grade 3, and 7 (21.2%) were Tönnis Grade 4. Modified McKay was excellent in 30 (90.9%) hip joints and it was good in 3 (9.1%). Additionally; 28 (84.8%) patients were Severin Class 1 and 5 (15.2%) were Severin Class 2. In Group 2; 20 (62.5%) patients were Tönnis Grade 2, 9 (28.1%) were Tönnis Grade 3, and 3 (9.4%) were Tönnis Grade 4. Modified McKay was excellent in 30 (93.8%) hip joints and it was good in 2 (6.3%). Additionally, 29 (90.6%) patients were Severin Class 1 and 3 (9.4%) were Severin Class 2. No significant differences were found in any of these parameters, between two groups (p=0.968 and p=0.708; respectively).

Table IV. *Comparison of some clinical results of patients undergoing SIO and PPO.*

Clinical Parameters	Salter [n (%)]	Pemberton [n (%)]	Total [n (%)]	p
Tönnis Grade 2	16 (48.5%)	20 (62.5%)	36 (55.4%)	
Tönnis Grade 3	10 (30.3%)	9 (28.1%)	19 (29.2%)	
Tönnis Grade 4	7 (21.2%)	3 (9,4%)	10 (15.4%)	
Modified McKay Excellent	30 (90.9%)	30 (93.8%)	60 (92.3%)	NS.
Modified McKay Good	3 (9.1%)	2 (6,3%)	5 (7.7%)	
Severin Class 1	28 (84.8%)	29 (90.6%)	57 (87.7%)	
Severin Class 2	5 (15.2%)	3 (9,4%)	8 (12.3%)	

NS.: *Not significant,* ***SIO:*** *Salter innominate osteotomy,* ***PPO:*** *Pemberton pericapsular osteotomy,* ***p***: p *value*

During the follow-up period, no residual dysplasia was observed. Avascular necrosis occurred in 5 patients in the SIO group and 4 patients in the PPO group.

4. DISCUSSION

Salter innominate osteotomy and PPO was mainly developed for children aged 18 months to 6 years and PPO was mainly developed for children aged 18 months to 6 years [3,4,15]. Accordingly, these procedures were performed to the similar age group, in our study. However, Huang and Wang reported good results in patients, who were younger than 18 months but at walking age, using open reduction and Salter osteotomy [16]. The primary objectives of SIO and PPO adequately cover the femoral head, especially in the anterolateral plane, and provide stable reduction. SIO was shown to be more suitable for patients older than 18 months, whose AI is between 30-40° [3], on the other hand; PPO was shown to be more suitable for patients with anterolateral insufficiencies, patients aged between 2-4 years with AI above 40° or patients aged between 4-6 years with AI above 35°[5]. In our study, SIO patients were older than PPO patients; but the AI criteria were similar with these studies (between 30-40 in SIO and >40 in PPO). We think that AI is the first parameter for the choice of surgical procedure. AI and CE angles were used to evaluate the adequacy of femoral head cover, in a previous study; by using these angles, PPO was shown to provide better femoral head covering and a better anatomical position of the pelvis than SIO [15]. Ezirmik et al.,

http://doi.org/10.5472/marumj.1483336
Marmara Med J 2024;37(2): 214-218

compared the results of SIO and PPO surgeries, which they performed on each hip in the same session in children with bilateral DHD. They found that postoperative AI angle (15,16 and 12,11, respectively) was significantly lower and the mean angle of AI improvement was better in the PPO group (18.33 and 25.78, respectively, p<0.05) [6]. Studies have shown that the mean AI angle correction is between 10-23.5°with SIO and between 5-35° with PPO [17-19]. Ezirmik et al., found that the mean CE-last was significantly higher in the PPO group (37.15 and 43.11 in the SIO group and PPO group, respectively) [6]. In the present study, post1-AI was lower; but the mean pre-AI was higher in the PPO group, compared to SIO group. These findings are consistent with the literature. In this study, the CE-1 of the acetabulum was significantly lower in the PPO group. However, there was no significant difference between the groups in terms of the CE-last value. These results suggest that there is no difference between these two surgical methods in terms of this parameter.

Wang et al., compared long-term results of SIO and PPO (at least 10 years after surgery) in 42 patients with DHD, they evaluated pelvic height, increases in iliac crest and sacral inclination, besides Lumbar Cobb angle, Short Form-36 (SF-36) and Harris hip scores. They reported that while there was initially a higher increase in pelvic height in the children with Salter osteotomy (Salter 10.1%; Pemberton 4.3%, p<0.001), no significant difference was found between the two groups at the 10th year (Salter 4.4%; Pemberton 3.1%, p=0.249). Similarly, they found no significant difference between the two groups in terms of lumbar Cobb angle, SF-36 and Harris hip scores. Moreover, they reported no difference in functional outcomes or pelvic imbalance between Salter osteotomy and Pemberton acetabuloplasty in the treatment of children with DHD in the long-term [7].

In this study, 92.3% of our cases were evaluated as excellent and 7.7% as good according to the Modified McKay clinical criteria. The sequence and rates of SIO and PPO groups were also similar to those in the total group and there was no significant difference between the groups. Çıtlak et al., found these rates as 94.6% and 5.5%, respectively, consistent with our results [20].

According to Severin radiological classification, most of our cases (87.7%) were Severin 1, which was followed by Severin 2 (12.3%). The sequence was the same and the rates were similar in SIO and PPO groups. Çıtlak et al., found the rates of Severin 1 and 2 as, 74.6% and 11.8%; respectively [20]. These rates are lower than ours. In addition, they reported Severin 3 and 4 with a rate of 13.6%, but no Severin 3 and 4 were found in the present study.

Long-term follow-up of patients is required for accurate analysis of SIO and PPO surgical outcomes because many hips wear away over time. Severin 1+2 rate was 71% in the operated 93 hips that were followed up for approximately 10 years [21]. Other studies reported excellent and good results in 98% of hip joints that were followed for eight years after the surgery [22], 75% in those who were followed up for 10 years [1] and 79% in those that were followed up for 19.8 years [23].

Conclusion

SIO and PPO methods used in the treatment of DHD, have both advantages and disadvantages. Preoperative radiological and intraoperative evaluations are very important in determining which procedure should be performed. We believe that the present study will help surgeons determine the appropriate surgical procedure in patients with DHD.

Compliance with the Ethical Standards

Ethical approval: This study was approved by Karadeniz Technical University Faculty of Medicine Scientific Research Ethics Committee with the document numbered 24237859-216 and dated 26/04/2016

Financial support: The authors declare that this study did not receive any financial support.

Conflict of interest: The authors have no conflicts of interest to declare.

Authors' contibutions: BA: Conceptualization, data curation, formal analysis, investigation, methodology, validation, writing-original draft. HA: Funding acquisition, investigation, methodology, project administration, resources.

REFERENCES

[1] Garcia S , Demetri L , Starcevich A, Gatto A , Swarup I. Developmental Dysplasia of the Hip: Controversies in Management. Curr Rev Musculoskelet Med. 2022 ;15:272-82. doi: 10.1007/s12178.022.09761-8. Epub 2022 Apr 30.

[2] Baki C, Sener M, Aydin H, Yildiz M, Saruhan S. Single-stage open reduction through a medial approach and innominate osteotomy in developmental dysplasia of the hip. J Bone Joint Surg Br 2005;87-B:380-3. doi: 10.1302/0301-620x.87b3.14663

[3] Tukenmez M , Tezeren G Salter innominate osteotomy for treatment of developmental dysplasia of the hip. J Orthop Surg (Hong Kong) 2007 ;15:286-90. doi: 10.1177/230.949.900701500308.

[4] Waters P, Kurica K, Hall J, Micheli LJ. Salter innominate osteotomies in congenital dislocation of the hip. J Pediatr Orthop 1988;8:650-5. doi: 10.1097/01241.398.198811000-00004

[5] Aldhoon M , Almarzouq A , Aldeen ALRashdan D , Altarawneh , Otoum A , Ibrahim F. Salter innominate osteotomy for the management of developmental dysplasia of the hip in children: radiographic analysis. Indian J Orthop 2022;57:80-5. doi: 10.1007/s43465.022.00786-2.

[6] Ezirmik N, Yildiz K. A Biomechanical comparison between Salter Innominate Osteotomy and Pemberton Pericapsular Osteotomy. Eurasian J Med 2012;44:40-2. doi: 10.5152/eajm.2012.08 PMID: 25610203

[7] Wang CW, Wang TM, Wu KW, Huang SC, Kuo KN. The comparative, long-term effect of the Salter osteotomy and Pemberton acetabuloplasty on pelvic height, scoliosis and functional outcome. Bone Jt J 2016;98-B :1145-50. doi: 10.1302/0301-620X.98B8.37215

[8] Çekiç B , Toslak İ E, Sertkaya O, et al. Incidence and follow-up outcomes of developmental hip dysplasia of newborns in the Western Mediterranean Region. Turk J Pediatr 2015;57:353-8.

[9] İncesu M, Songür M, Sonar M, Sabri Uğur G. Evaluation of hip radiographs in children. Türk Ortop ve Travmatoloji Birliği Derneği Derg 2013;12:54-61. doi: 10.5606/totbid.dergisi.2013.07

[10] Ogata S, Moriya H, Tsuchiya K, Akita T, Kamegaya M, Someya M. Acetabular cover in congenital dislocation of the hip. J Bone Jt Surg – Ser B 1990;72:190-6. doi: 10.1302/0301-620X.72B2.2312554

[11] Ryo Mori R , Yasunaga Y, Yamasaki T, Hamanishi M, Shoji T, Ochi M. Ten-year results of transtrochanteric valgus osteotomy with or without the shelf procedure. Int Orthop 2013;37:599-604. doi: 10.1007/s00264.013.1810-z.

[12] Olivas A O R , Zamora E H , Maldonado E M. Legg-Calvé-Perthes disease overview Orphanet J Rare Dis 2022;17:125. doi: 10.1186/s13023.022.02275-z.

[13] Alfonso Vaquero-Picado , Gaspar González-Morán , Enrique Gil Garay , Luis Moraleda . Developmental dysplasia of the hip: update of management EFORT Open Rev 2019;4:548-56. doi: 10.1302/2058-5241.4.180019. eCollection 2019 Sep.

[14] Wang Y, Current concepts in developmental dysplasia of the hip and Total hip arthroplasty. Arthroplasty 2019;1:2. doi: 10.1186/s42836.019.0004-6.

[15] Bagatur AE, Zorer G, Sürel YB. Is sufficient femoral head coverage obtained after Pemberton's pericapsular osteotomy? Evaluation by three-dimensional computed tomographic reconstruction. Acta Orthop Traumatol Turc 2002;36:203-10.

[16] Huang S-C, Wang J-H. A Comparative study of nonoperative versus operative treatment of developmental dysplasia of the hip in patients of walking age. J Pediatr Orthop 1997;17:181-8. PMID: 9075093 doi: 10.1097/00004.694.199703000-00009

[17] Böhm P, Brzuske A. Salter Innominate Osteotomy for the treatment of developmental dysplasia of the hip in children. J Bone Jt Surgery-American Vol 2002;84:178-86.

[18] Karakurt L, Yilmaz E, Incesu M, Belhan O, Serin E. Early results of treatment for developmental dysplasia of the hip in children between the ages of one and four years. Acta Orthop Traumatol Turc 2004;38:8-15.

[19] Zamzam MM, Khosshal KI, Abak AA, et al. One-stage bilateral open reduction through a medial approach in developmental dysplasia of the hip. J Bone Joint Surg Br 2009;91-B :113-8. doi: 10.1302/0301-620X.91B1.21429

[20] Çıtlak A, Saruhan S, Baki C. Long-term outcome of medial open reduction in developmental dysplasia of hip. Arch Orthop Trauma Surg 2013;133:1203-9. doi: 10.1007/s00402.013.1793-7

[21] Morcuende JA, Meyer MD, Dolan LA, Weinstein SL. Long-term outcome after open reduction through an anteromedial approach for congenital dislocation of the hip. J Bone Jt Surg 1997;79:810-7. doi: 10.2106/00004.623.199706000-00002

[22] Tumer Y, Ward WT, Grudziak J. Medial Open reduction in the treatment of developmental dislocation of the hip. J Pediatr Orthop 1997;17:176-80. doi: 10.1097/00004.694.199703000-00008

[23] Ucar DH, Isiklar ZU, Stanitski CL, Kandemir U, Tumer Y. Open reduction through a medial approach in developmental dislocation of the hip. J Pediatr Orthop 2004;24:493-500. doi: 10.2106/00004.623.199309000-00008

MARMARA
MEDICAL JOURNAL

Original Article

https://dergipark.org.tr/tr/pub/marumj

Management of staple line leaks after laparoscopic sleeve gastrectomy: Single-center experience

Tevfik Kivilcim UPRAK, Mumin COSKUN, Mustafa Umit UGURLU, Omer GUNAL, Asim CINGI, Cumhur YEGEN

Department of General Surgery, School of Medicine, Marmara University, Istanbul, Turkey

Corresponding Author: Tevfik Kivilcim UPRAK
E-mail: uprak@gmail.com

Submitted: 14.08.2023 **Accepted:** 03.05.2024

ABSTRACT

Objective: In obesity surgery, laparoscopic sleeve gastrectomy (LSG) is a frequently applied method. However, there are certain complications. Leakage is one of the most serious complications after surgery, causing postoperative morbidity and sometimes mortality. There is no consensus about management of leaks after LSG. In our study, we aimed to present our experience on the management of LSG leaks.

Patients and Methods: Patients who underwent LSG between 2010-2017 in a tertiary university hospital were analyzed retrospectively. Demographic characteristics, endoscopic and surgical interventions, morbidity, and mortality rates of patients diagnosed with LSG leak were analyzed from prospectively recorded data.

Results: Leak was observed in 11 (2.15%) of a total of 510 LSG patients. Six (54%) patients were diagnosed as acute and 5 were early leaks. Stent was applied to most of the patients (72%) with or without surgical exploration. The average length of stay in hospital was 21 days. Mortality was observed in 2 patients.

Conclusions: Consequently, leakage after LSG is a complication that requires multimodal therapy. Surgical treatment combined with endoscopic intervention may increase success.

Keywords: Obesity, Morbid / surgery, Sleeve gastrectomy, Leakage management

1. INTRODUCTION

Obesity is a global epidemic with substantial health and economic burden. Based on the World Health Organization data, 650 million adults (13% of all adults) and more than 340 million children and adolescents are overweight or obese [1]. Laparoscopic sleeve gastrectomy (LSG) is one of most common surgical procedures performed frequently in recent years [2]. Regardless of its success for weight loss and improvements of comorbidities, LSG is associated with low but significant complication rates between 2 – 15% such as staple line leaks, bleeding, and stricture [3]. Leak, which is the most concerning complication after surgery, may result in morbidity, prolonged hospital stays, and even mortality. Leak rates can occur between 1-7% in different series, and the mortality rates can be up to 9% [3, 4].

Management modalities of staple line leaks after LSG consists of surgical methods such as early revision with reinforcement sutures, drainage (open or laparoscopic), conversion to gastric by-pass and endoscopic methods such as insertion of clips, stenting and fibrin glue application [5]. In the last decade, endoscopic interventions using the self-expanding metal stents (SEMS) had a significantly increasing role in the control of postoperative leakage [6, 7]. Although, the patient-based approach is appropriate, different centers have their own algorithms in the management of LSG leaks [8-10]. In this regard, there is no consensus on a comprehensive and validated management algorithm for suture line leaks after LSG. Herein, we aim to present our approach to patient management who have developed leakage after LSG.

2. PATIENTS and METHODS

Study design

A retrospective analysis of morbidly obese patients treated in a university hospital was performed. Patients who had the radiological and clinical diagnosis of leakage after LSG between 2010-2017 were included in the study. Demographic characteristics of patients, time of diagnosis for suture line leaks, radiological methods, endoscopic treatment and duration, operative approach, morbidity and mortality rates were analyzed from prospectively collected database. Exclusion

How to cite this article: Uprak KT, Coskun M, Ugurlu UM, Gunal O, Cingi A, Yegen C. Management of staple line leaks after laparoscopic sleeve gastrectomy: Single-center experience. Marmara Med J 2024: 37(2):219-223. doi: 10.5472/marumj.1484454

ISSN: 1309-9469

http://doi.org/10.5472/marumj.1484454
Marmara Med J 2024;37(2): 219-223

criteria included staple line leaks after bariatric surgeries other than LSG, loss of follow-up data and stenosis concomitant with staple line leak. Primary outcome was the clinical response to management of staple line leaks, secondary outcome included timing and clinical presentation of post-operative staple line leaks, length of hospital stays and adverse events after endoscopic or radiological intervention and overall surgical complications.

LSG technique and postoperative assessment

All patients were operated by two bariatric surgeons. Reinforcement of the staple line with suture was performed according to the surgeon's preference, 38 Fr bougie was used in all patients. All patients were tested for leak with upper gastrointestinal contrast diagnostic X-ray with diatrizoate meglumine and diatrizoate sodium solution (Gastrografin; Bayer, Leverkusen, Germany) on post-operative day (POD) 1. After a negative leak test, patients were allowed to start oral liquid feeding, and they were routinely discharged from the hospital on POD 3. Within a two-week period, patients followed a semi-solid diet, and a solid diet was allowed 15 days after the surgery.

Definition of post-operative leak and management strategies

Post-operative staple line leaks were classified regarding diagnosis time after the operation. Leaks detected within the postoperative 1st week were evaluated as acute leaks detected within post-operative 1-6 weeks were diagnosed as early and leaks detected later than post-operative 6 weeks were assessed as late leaks [11]. Radiological diagnosis of staple-line leak was defined as contrast extravasation into the abdominal cavity, abscess near the operation area or as free fluid in the abdominal cavity. Clinical diagnosis of staple-line leak was diagnosed as the presence of fever (over 37.5°C), tachycardia (over 100 beats/min), tachypnea (over 20 breathing/min), abdominal pain, distension, vomiting and abnormal drain content. For diagnosis and follow-up, computed tomography with peroral and intravenous contrast was performed on all patients with staple-line leaks. The management approach of staple-line leaks with surgery, endoscopy and/or interventional radiology was determined according to the patients' symptoms and hemodynamic status.

Hemodynamically unstable patients, characterized by unresponsive hypotension and tachycardia, with or without signs of peritonitis, underwent immediate surgical intervention. The majority of patients were managed with endoscopy (stent insertion, clip) and/or ultrasound-guided drain placement. All endoscopic and surgical procedures were performed by the bariatric surgery team. Surgical intervention consisted of intraabdominal irrigation and drain placement on leakage site. Visible and confirmable leakage sites were sutured with 2/0 silk suture.

This study was approved by the Ethics Committee of Marmara University School of Medicine Clinical Research Ethics Committee (Number: 08.10.2021.1087)

Statistical analysis

We performed statistical analysis using the Statistical Package for Social Sciences (Version 24 for Mac, IBM Corporation). Descriptive data for continuous variables were expressed as mean and standard deviation. Frequencies procedure was used on categorical variables.

3. RESULTS

Between 2010 and 2017, 510 LSGs were performed in our clinic. The staple-line leak was detected in 11 (2.15%) patients; 8 of the 11 patients were female, and the mean age of the patients was 36 (22-53) years. The mean pre-operative body mass index (BMI) of patients with staple-line leak was 46 kg/m^2 (range: 40-63). The median time to diagnosis of post-operative staple-line leak was 6.9 days (range: 1-17 days). Six (54%) patients had acute leak (<7 days); five patients had early leakage. None of the patients was diagnosed with late leakage. Ten patients had leak from cardia, 1 patient's leak site was cardia and antrum. The most frequent symptoms were fever and abdominal pain that was found in 7 (63%) patients. The characteristics of the patients and the treatments applied are shown in Table I.

Surgical intervention with/without endoscopic procedure

Five (45%) laparotomy and one (9%) laparoscopic exploration and drainage were performed. Endoscopic stent application was performed in 4 of these 6 patients in the same session. In 6 patients with surgical intervention and drainage, only in 2 patients, the leak site was repaired with reinforcement sutures.

Table I. *Patient characteristics and treatments applied*

Patients	Age	Sex	BMI	Days to diagnose	Stent	Stent revision	Clip	Operation	Length of stay in days	Radiologic Intervention
1	42	Female	44.0	9	-	N/A	-	+	mortality	-
2	40	Female	46.0	11	-	N/A	+	-	23	+
3	41	Male	45.3	2	+	+	-	-	47	+
4	53	Female	46.0	8	+	+	-	+	37	-
5	35	Female	46.4	4	+	-	-	-	20	-
6	36	Female	63.6	17	+	+	-	+	38	-
7	29	Female	52.0	1	+	-	-	+	5	-
8	51	Female	43.0	5	+	-	-	-	14	+
9	46	Female	40.0	3	+	-	-	+	mortality	-
10	26	Male	40	15	+	-	-	-	15	-
11	22	Male	50	1	-	N/A	-	+	14	-

http://doi.org/10.5472/marumj.1484454
Marmara Med J 2024;37(2): 219-223

Endoscopic procedure with/without radiologic drainage

Endoscopic stent was placed in 4 patients, whereas radiologic drainage was performed in 2 patients. In 1 case, intervention was completed with endoscopic clip application and drainage by interventional radiology. Patients' management scheme according to hemodynamic status and leakage time is shown in Figure 1 and Figure 2 respectively.

Evaluation of patients with stent

Eight (72%) patients underwent stenting using straight fully covered self-expandable metallic stents 20cm in length and 20mm in diameter which are not specifically designed for sleeve gastrectomy leaks (Micro-Tech, Nanjing Co., China). We changed these stents with fully covered metallic stents with 23 cm in length-24 Fr in diameter specifically designed for sleeve gastrectomy leaks (HANAROSTENT, M.I. I. Tech, Seoul, Korea) in 3 (24%) patients.

The median duration of stay time for stents was 34 days (range:14-77). All patients were assessed with contrast enhanced computed tomography before and after stent removal to determine whether the leak was under control. The mean length of hospital stay was 21 (5-47) days. Mortality was observed in 2 (0.3%) patients due to sepsis and multiorgan failure.

4. DISCUSSION

Laparoscopic sleeve gastrectomy is a technically feasible surgical treatment method for obesity and obesity-related morbidities with negligible long-term nutritional deficiencies [12]. Despite the appealing options of this surgery, post-operative complications following LSG, particularly staple-line leaks, remains a significant concern. The postoperative staple-line leaks are managed with multidisciplinary approach, however, there is still no consensus on comprehensive management algorithm [13, 14]. The majority of leaks are acute or early, rather than late. We preferred to use multiple treatment modalities in combination. The operative approach with or without stenting was the most selected method. Evaluation of leak control is performed using contrast-enhanced computed tomography before and after stent removal. Despite treatment efforts, the average hospital stay remains considerable at 21 days, and there is a low but notable mortality rate of 0.3%, primarily attributed to sepsis and multiorgan failure.

Csendes et al., evaluated 343 patients and reported a 4.7% leak rate, and they declared that most of the LSGs were performed by residents. Many of the acute leaks were managed by surgical intervention in contrast to early and late leakage. They refused to suture defects exceeding three days postoperatively due to edema and inflammation. They preferred drainage and nasojejunal feeding as adequate leakage control [3]. In our series, we could apply primary sutures only in 2 of 6 patients who underwent surgery. These patients were diagnosed as acute leakage. Due to the edema and inflammation of the leak site, suturing was hardly completed.

Studies showed that early surgical drainage was recommended in acute leaks, however, conservative treatment including adequate hydration, proton pump inhibitors, zero per os, nutritional support, percutaneous drainage of any collection, and broad-spectrum antibiotheraphy were suggested for the late leaks [5, 15]. In this study, 3 patients with early leak had hemodynamic instability and necessitated emergency exploration. Also, 3 patients with acute leak were treated with laparotomy and drainage with/without stent placement.

Abou et al., suggested endoscopic intervention for hemodynamically stable patients that do not recover using conservative treatment in 2 weeks [5]. In our series, endoscopic therapies without surgical drainage were performed in 5 patients. 3 of them were patients with an acute leak. In another study, all patients with leaks were treated only by endoscopic methods (washing, stenting, clip, and glue). The majority of the patients were referred to this clinic and half of them were classified as late leakage. They concluded that patients with the early leakage needed fewer endoscopic intervention than late leakage [16].

On the other hand, the usage of short-length stents was shown to be ineffective on management. Longer stents are recommended to cover all stomach and leak area [14,17]. In our cohort, 3 stents were replaced with specific longer stents due to refractory leakage and dislocation.

In a study including 19 patients (all patients underwent laparoscopic drainage), authors suggested using pigtail drain for fistulas smaller than 1cm and using the stent in case of fistula wider than 1cm [15]. However, we have no experience on the application of pigtail stent.

Southwell et al., treated 21 patients with LSG leak and only 1 patient required gastric-bypass surgery. 95% of patients were treated with endoscopic treatments. Stent migration rate was 48%. They recommended use of proximal uncovered, anti-migratory and wider stents [17]. Stent migration rate was even higher in our cohort (87%). A retrospective study showed that 37 patients with a stent replacement had 94.5% success healing rate. In this study author used endoscopic suturing for nearly half of the patients to prevent stent migration and the migration rate decreased from 41% to 15%. They concluded that specialized stents are needed for leak management after bariatric surgery [19]. In our study, we applied specified stents to three patients. However, they are not cost-effective.

Alazmi et al., retrospectively analyzed the effectiveness of stent application. Two staged method was used as metallic stent and plastic stent. All patients had surgical or radiological drainage. Among 17 patients, 10 patients with acute leaks were healed successfully. However, early and late leaks had lower healing rates [20]. El Hassan et al., concluded that treatment of patients with the operative approach without endoscopic stents was feasible after unsuccessful treatment and especially in chronic failure [21].

In our series, 2 patients were treated with stent application only, while 4 patients were treated with stents and surgical drainage.

Since, the number of patients is low, it is not appropriate to compare acute or early leaks.

Smaller sample size and retrospective nature are the limitations of this study. It is difficult to conduct randomized controlled studies to be carried out on this issue. There is no gold standard approach or guideline for LSG.

Conclusion

Leakage after LSG may result in morbidity and mortality. Leakage control through drainage with interventional radiology or minimally invasive procedures such as laparoscopic drainage with or without endoscopic stenting may reduce mortality and morbidity. Although, hemodynamic status is crucial, in case of acute leakage, rapid recovery is observed after immediate surgical intervention.

Compliance with Ethical Standards

Ethical approval: Ethical approval was obtained from Marmara University , School of Medicine Clinical Research Ethics Committee (approval no:: 08.10.2021.1087).

Funding: The authors declare that this study has received no financial support.

Conflict of interest: The authors declare that they have no conflict of interest.

Authors Contributions: TKU and CY: Concept and design, MC and TKU: Collecting data, AC,OG and MUU: Analysis and interpretation. All authors read and approved the final version of the manusctipt.

REFERENCES

[1] Levesque RJR. Obesity and overweight. In: Levesque RJR, ed. Encyclopedia of Adolescence. Springer, Charm 2018:2561-5. https://doi.org/10.1007/978-3-319-33228-4_447

[2] English WJ, DeMaria EJ, Brethauer SA, Mattar SG, Rosenthal RJ, Morton JM. American Society for Metabolic and Bariatric Surgery estimation of metabolic and bariatric procedures performed in the United States in 2016. SOARD 2018;14:259-63. doi:10.1016/j.soard.2017.12.013.

[3] Csendes A, Braghetto I, León P, Burgos AM. Management of leaks after laparoscopic sleeve gastrectomy in patients with obesity. J Gastrointest Surg 2010;14:1343-8. doi:10.1007/s11605.010.1249-0.

[4] De Aretxabala X, Leon J, Wiedmaier G, et al. Gastric leak after sleeve gastrectomy: Analysis of its management. Obes Surg 2011;21:1232-7. doi:10.1007/s11695.011.0382-5.

[5] Abou Rached A, Basile M, El Masri H. Gastric leaks post sleeve gastrectomy: Review of its prevention and management. World J Gastroenterol 2014;20:13904-10. doi:10.3748/wjg.v20.i38.13904.

[6] Eubanks S, Edwards CA, Fearing NM, et al. Use of endoscopic stents to treat anastomotic complications after bariatric surgery. J Am Coll Surg 2008;206:935-8. doi:10.1016/j.jamcollsurg.2008.02.016.

[7] Casella G, Soricelli E, Rizzello M, et al. Nonsurgical Treatment of staple line leaks after laparoscopic sleeve gastrectomy. Obes Surg 2009;19:821-6. doi:10.1007/s11695.009.9840-8.

[8] Musella M, Milone M, Bianco P, Maietta P, Galloro G. Acute Leaks Following laparoscopic sleeve gastrectomy: Early surgical repair according to a management algorithm. J Laparoendosc Adv Surg Tech 2016;26:85-91. doi:10.1089/lap.2015.0343.

[9] Nimeri A, Ibrahim M, Maasher A, Al Hadad M. Management algorithm for leaks following laparoscopic sleeve gastrectomy. Obes Surg 2016;26:21-5. doi:10.1007/s11695.015.1751-2.

[10] Noel P, Nedelcu M, Gagner M. Impact of the surgical experience on leak rate after laparoscopic sleeve gastrectomy. Obes Surg 2016;26:1782-7. doi:10.1007/s11695.015.2003-1.

[11] Rosenthal RJ, International Sleeve Gastrectomy Expert P, Diaz AA, Arvidsson D, Baker RS, Basso N et al. International Sleeve Gastrectomy Expert Panel Consensus Statement: best practice guidelines based on experience of and gt;12,000 cases. Surg Obes Relat Dis 2012;8:8-19. doi:10.1016/j.soard.2011.10.019.

[12] Salminen P, Grönroos S, Helmiö M, et al. Effect of laparoscopic sleeve gastrectomy vs roux-en-y gastric bypass on weight loss, comorbidities, and reflux at 10 years in adult patients with obesity: The SLEEVEPASS Randomized Clinical Trial. JAMA Surg 2022;157:656-66. doi:10.1001/jamasurg.2022.2229.

[13] Negm S, Mousa B, Shafiq A, et al. Endoscopic management of refractory leak and gastro-cutaneous fistula after laparoscopic sleeve gastrectomy: a randomized controlled trial. Surg Endoscop 2023;37:2173-81. doi:10.1007/s00464.022.09748-z.

[14] Nedelcu M, Manos T, Noel P, et al. Is the surgical drainage mandatory for leak after sleeve gastrectomy? J Clin Med 2023;12:1376. doi:10.3390/jcm12041376.

[15] Burgos AM, Braghetto I, Csendes A, et al. Gastric leak after laparoscopic-sleeve gastrectomy for obesity. Obes Surg 2009;19:1672-7. doi:10.1007/s11695.009.9884-9.

[16] Bège T, Emungania O, Vitton V, et al , undefined. An endoscopic strategy for management of anastomotic complications from bariatric surgery: a prospective study. Elsevier.

[17] Southwell T, Lim TH, Ogra R. Endoscopic therapy for treatment of staple line leaks post-laparoscopic sleeve gastrectomy (LSG): Experience from a large bariatric surgery centre in New Zealand. Obes Surg 2016;26:1155-62. doi:10.1007/s11695.015.1931-0.

[18] Nedelcu M, Manos T, Cotirlet A, Noel P, Gagner M. Outcome of leaks after sleeve gastrectomy based on a new algorithm adressing leak size and gastric stenosis. Obes Surg 2015;25:559-63. doi:10.1007/s11695.014.1561-y.

[19] Krishnan V, Hutchings K, Godwin A, Wong JT, Teixeira J. Long-term outcomes following endoscopic stenting in the management of leaks after foregut and bariatric surgery. Surg Endoscop 2019;0:0-. doi:10.1007/s00464.018.06632-7.

[20] Alazmi W, Al-Sabah S, Ali DA, Almazeedi S. Treating sleeve gastrectomy leak with endoscopic stenting: the kuwaiti experience and review of recent literature. Surg Endoscop 2014;28:3425-8. doi:10.1007/s00464.014.3616-5.

[21] El Hassan E, Mohamed A, Ibrahim M, Margarita M, Al Hadad M, Nimeri AA. Single-stage operative management of laparoscopic sleeve gastrectomy leaks without endoscopic stent placement. Obes Surg 2013;23:722-6. doi:10.1007/s11695.013.0906-2.

MARMARA
MEDICAL JOURNAL

Original Article

https://dergipark.org.tr/tr/pub/marumj

Complementary advantages of microsurgical treatment for vertebral artery dolicoarteriopathies: Mitigating symptoms of restless leg syndrome in refractory vertebrobasilar insufficiency

Efecan CEKIC[1], Iskender Samet DALTABAN[2], Mehmet Erkan USTUN[3]

[1] Department of Neurosurgery, Polatli Duatepe State Hospital, Ankara, Turkey
[2] Department of Neurosurgery, Trabzon Kanuni Training and Research Hospital, Trabzon, Turkey
[3] Department of Neurosurgery, Private Clinic, Ankara, Turkey

Corresponding Author: Efecan CEKIC
E-mail: drefecancekic@gmail.com

Submitted: 04.03.2024 **Accepted:** 26.04.2024

ABSTRACT

Objective: This retrospective study examines the impact of microsurgical treatment on vertebral artery (VA) dolicoarteriopathies and associated restless leg syndrome (RLS) in patients with refractory vertebrobasilar insufficiency (VBI).

Patients and Methods: We analyzed 78 patients with grade 2 and 3 kinks, and found out that the targeted microsurgical interventions, primarily designed to address VBI, improved secondary RLS symptoms in 12 patients. Procedures included arteriolysis and, depending on severity, grafting. Statistical analysis was conducted using Stata 16 (StataCorp LP, Texas, USA).

Results: In twelve patients aged 55 to 72 years with refractory VBI and drug-resistant RLS, micro-neurosurgical correction of V1 segment dolicoarteriopathy, abnormal elongation and kinks in the artery, demonstrated promising outcomes. Postoperatively, 83.33% (10 patients) reported complete resolution of RLS symptoms, and 16.66% (2 patients) experienced partial symptom relief ($p<0.05$). Overall, 86.8% of various VBI-related symptoms were significantly improved or resolved ($p<0.05$). The microsurgical technique, avoiding traditional flow-arresting procedures, proved to be highly effective in this preliminary study with no mortality and minimal temporary complications, underscoring its potential treatment avenue for such complex neurovascular conditions.

Conclusion: This study illuminates the relationship between VBI and RLS, proposing a potential vascular etiology for RLS, and highlights the need for a broader diagnostic approach for patients with refractory VBI.

Keywords: Vertebral artery dolicoarteriopathy, Microsurgical treatment, Restless leg syndrome, Vertebrobasilar insufficiency

1. INTRODUCTION

Vertebral artery (VA) dolicoarteriopathy, characterized by the pathological elongation, kinking, or coiling of the VA, has been increasingly recognized as a contributing factor to a spectrum of cerebrovascular pathologies [1,2]. Kinks are classified according to Metz et al., classification according to the severity of the angle [3]. (Grade 1:90-60 degrees (mild kinging), Grade 2: 60-30 (moderate kinging), Grade 3 < 30 degrees (severe kinging)). Especially, in grade 2 and 3 dolichoarteriopathies, there is a reduction in blood flow, which escalates the risk of ischemic events [4]. In simpler terms, a 'dolicoarteriopathy' is when a VA is abnormally long and twisted, which can sometimes squeeze or restrict blood flow to the brain, increasing the risk of stroke-like episodes and even imitating Parkinsonism-like symptoms [5]. These vascular aberrations can disrupt hemodynamic stability and play a role in vertebrobasilar insufficiency (VBI) pathophysiology, manifesting in a clinical spectrum that includes symptoms from cervicogenic dizziness to radiculopathy [6,7]. In cases of refractory VBI, when endovascular surgery is not feasible or appropriate, primary surgical interventions such as classical techniques, including bypass techniques, and new microsurgical interventions may be performed. These surgical procedures address the specific vascular anomalies in VBI, offering alternative avenues for restoring cerebral hemodynamics and alleviating the associated neurological symptoms [8-10].

Restless legs syndrome (RLS) or Willis–Ekbom disease is a prevalent sensorimotor disorder characterized by an irresistible urge to move the legs, especially during sleep or periods of inactivity, dramatically affecting the patients' quality of life [11]. Although, the etiology of RLS remains multifaceted, growing evidence suggests its connection with vascular pathologies

How to cite this article: Cekic E, Daltaban IS, Ustun ME. Complementary advantages of microsurgical treatment for vertebral artery dolicoarteriopathies: Mitigating symptoms of restless leg syndrome in refractory vertebrobasilar insufficiency. Marmara Med J 2024: 37(2):224-230. doi: 10.5472/marumj.1479815

ISSN: 1309-9469

http://doi.org/10.5472/marumj.1479815
Marmara Med J 2024;37(2): 224-230

extending from the cerebrovascular to cardiovascular domains [12]. Given the widespread occurrence of RLS, understanding its vascular implications is paramount, especially when considering ischemic conditions [13,14]. A recent research has particularly highlighted ischemic alterations in the brainstem, left amygdala, and globus pallidus, implicating these limbic, medial frontal region, and basal ganglia structures as critical components in the neurophysiological pathways of RLS [15]. Previous studies have underscored the association of RLS with an elevated risk of hypertension, heart disorders, iron deficiency, kidney diseases, and stroke [16,17]. Moreover, cerebral small vessel disease (SVD) has been implicated in RLS, with studies highlighting the prevalence of silent cerebral SVD in RLS patients without a history of stroke [18]. However, although these vascular correlations provide valuable insights, a gap exists in our understanding of etiology and potential therapeutic interventions that address the underlying vascular pathologies when we analyzed VA dolicoarteriopathy-related refractory VBI.

Clinical observations suggest a possible vascular etiology, particularly implicating anatomical abnormalities of the VA, such as dolicoarteriopathies, leading to VBI and RLS. This understanding is particularly crucial when considering VBI, which can affect brain regions critical for RLS [19]. Our retrospective study targets a specific patient group with medically resistant RLS co-occurrence with refractory VBI due to VA dolicoarteriopathies, which are deemed by endovascular interventionalists as unsuitable cases. Novel micro-neurosurgical approaches to the V1 segment of the VA, primarily to address VBI, also inadvertently resulted in the resolution of RLS symptoms. This unanticipated observation has prompted a more rigorous retrospective examination to elucidate the potential etiopathogenic relationship and therapeutic implications between these clinical manifestations and refractory VBI. Therefore, we aimed to evaluate the effect of microsurgical treatment on V1 segment dolicoarteriopathies and its concomitant impact on RLS in patients with refractory VBI.

2. PATIENTS and METHODS

Patient population and selection criteria

We retrospectively analyzed 78 patients who underwent surgical procedures primarily for refractory VBI due to dolicoarteriopathy (grade 2 and 3 kinks) of the V1 segment from 2016 to 2023. All surgeries were performed by the senior surgeon, with informed consent obtained from all participants. The local ethics committee approved the study, documented under approval number 2/12 dated 03.30.2022.

Patients included in this study were initially diagnosed with RLS at external centers utilizing a standardized questionnaire aligned with the 2003 International RLS Study Group criteria [20], subsequently verified by a neurologist. These individuals also presented with VBI symptoms and were undergoing medical management; however, they continued to experience persistent, life-impacting symptoms despite these maximum therapeutic interventions. Each patient underwent a thorough diagnostic process, including brain magnetic resonance imaging (MRI) and brain and cervical MR angiography starting from the aortic arch. Brain MRI is employed primarily to rule out additional intracranial pathologies, and MR angiography assesses the integrity of collateral circulation. Cervical MR angiography shows the lesion or anomaly in two VAs or one VA with hypofunction in the other VA that supports the diagnosis beside the clinic. Follow-up assessments were conducted within 3-6 months of recruitment. They had an average follow-up period of one year.

We meticulously recorded symptoms indicative of VBI, such as drop attacks, dysarthria, diplopia, dysphagia, dizziness, visual field defects, hemihypoesthesia, hemiparesis, ataxia, and dysmetria. To maintain the integrity of the study and ensure a clear association between the vascular pathologies and the symptoms observed, we implemented strict exclusion criteria. We excluded patients with endovascular candidates, medically responsive patients, and neurological disorders, including neuropathies or central nervous system conditions that could independently cause symptoms similar to RLS. This rigorous screening was vital to isolate the impact of refractory VBI and related vascular dolicoarteriopathy on the manifestation of medically resistant RLS symptoms in the patient group. The comparative analysis evaluated the preoperative conditions and postoperative surgical effectiveness for patients with the coexistence of RLS alongside VBI.

Surgical technique

After exposing the V1 segment of the VA, arteriolysis (removal or dissection of fibrous bands surrounding the artery to alleviate the stenosis and restore blood flowMetin girmek için buraya tıklayın veya dokunun.) was performed [21-23]. For significant kinks (grades 2 and 3) in the V1 segment, treatment varied with kink severity. Arteriolysis alone or with the traction of the subclavian artery (SCA) addressed moderate elongation, such as grade 2 kinks, as shown in Figure 1. In contrast, the severe elongation of the vessel involved grafting to reposition the VA, such as for grade 3 kinks, as demonstrated in Figure 2. Surgical precision was paramount to preserve vascular integrity.

Statistical analysis

Data analysis was conducted using Stata 16 (StataCorp LP, Texas, USA). Descriptive statistics were employed to summarize patient characteristics, preoperative symptoms, and postoperative 6. month follow-up symptom evaluation. The frequency and percentage of patients experiencing complete resolution or partial improvement of RLS symptoms following micro-neurosurgical intervention were calculated. A paired t-test was used to compare preoperative symptom severity and postoperative improvement in patients with refractory VBI. Symptom based assesment was performed using McNemar's test for related samples due to the binary nature of the outcome (improvement: yes/no). A p-value of less than 0.05 was considered indicative of statistical significance.

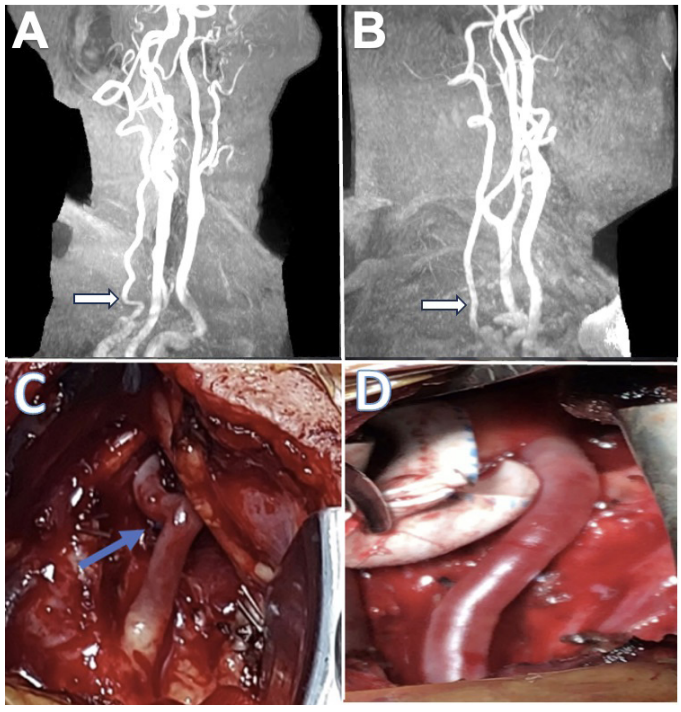

Figure 1. *A: Preoperative MR angiographic visualization of the grade 2 kink in the V1 segment (white arrow). B: Postoperative MR angiography image showing the vertebral artery after surgical correction of the grade 2 kink (white arrow). C: Perioperative microscopic image displaying the V1 segment of VA with grade 2 kinking (blue arrow) D: Perioperative microscopic view after the surgical correction.*

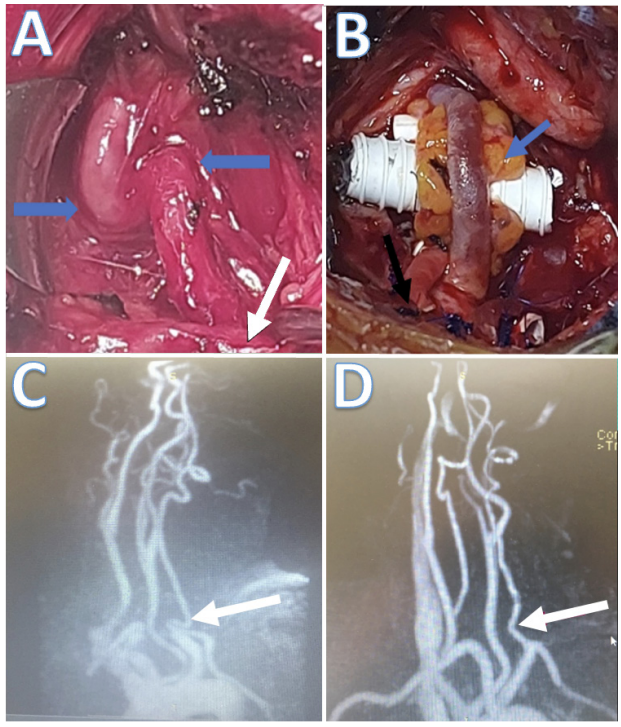

Figure 2. *A: Perioperative microscopic visualization of the grade 3 kink in the V1 segment (blue arrows) and subclavian artery (white arrow). B: Perioperative microscopic view after the surgical correction of grade 3 kink using vessel and adipose tissue grafts (blue arrow). C: Preoperative MR angiography image displaying the V1 segment of VA with grade 3 kinking (white arrow) D: Postoperative MR angiography image after the surgical correction (white arrow).*

http://doi.org/10.5472/marumj.1479815
Marmara Med J 2024;37(2): 224-230

Table I. *Clinical outcomes of micro-neurosurgical intervention in RLS for vertebral artery (V1 segment) dolicoarteriopathies*

Condition	Total Patients	Complete Resolution	Partial Improvement
Restless Leg Syndrome	12	10 (83.33%)	2 (16.66%)

Table II. *Preoperative symptoms and postoperative improvement rates of the refractory vertebrobasilar insufficiency symptoms*

Patient No.	Preoperative Symptoms	Postoperative Improvement
1	Dysmetria,Intentional Tremor,Ataxia,Dysphagia	Completely Resolved
2	Dysmetria,Intentional Tremor,Dizziness,Hemihipoestesia	Markedly Improved
3	Dysmetria,Intentional Tremor,Ataxia,Drop Attacks	Completely Resolved
4	Dysmetria,Intentional Tremor,Dizziness,Ataxia	Completely Resolved
5	Dysmetria,Intentional Tremor,Ataxia,Diplopia	Completely Resolved
6	Dysmetria,Intentional,Tremor,Dizziness,Ataxia, Drop Attacks	Completely Resolved
7	Dysmetria,Intentional Tremor,Dysphagia,Dysartria	Markedly Improved
8	Dysmetria,Intentional Tremor,Dizziness,Visual Field Defects	Completely Resolved
9	Dysmetria,IntentionalTremor,Ataxia,Dizziness,Diplopia	Completely Resolved
10	Dysmetria,Intentional Tremor,Dizziness,Ataxia	Completely Resolved
11	Dysmetria,Intentional Tremor,Dizziness,Ataxia	Completely Resolved
12	Dysmetria,Intentional Tremor,Dizziness,Ataxia	Completely Resolved

3. RESULTS

Our retrospective study evaluated the impact of micro-neurosurgical interventions on patients suffering primarily from refractor VBI due to V1 segment dolicoarteriopathy and its effect secondarily for medically resistant RLS symptoms. The patient cohort consisted of 12 individuals aged 55 to 72 years, with a mean age of 63. The group included a mixture of grade 2 and Grade 3 kinks (4 grade 2 kinks,8 grade 3 kinks) according to the Metz criteria in the V1 segment, indicative of varying degrees of severity in their condition. Following microsurgery, all the arterial kinks were rectified using new techniques that obviated the need for traditional flow-arresting procedures such as bypass.

Following the surgical procedures, a notable improvement in RLS symptoms was observed across the cohort. Specifically, 10 patients (83.33%) experienced complete resolution of RLS symptoms, evidencing the intervention's potential in treating the neurological manifestations associated with V1 segment dolicoarteriopathy. However, 2 patients (16.66%) showed partial improvement, indicating a reduction but not a complete cessation of symptoms ($p<0.05$), as shown in Table I.

Our study focused on 12 patients with refractory VBI, who presented with a spectrum of debilitating symptoms, including intentional tremors, drop attacks, dysarthria, diplopia, dysphagia, dizziness, visual field defects, hemihypoesthesia, ataxia, and dysmetria. Significant clinical improvement was observed following micro-neurosurgical interventions tailored to address VA dolicoarteriopathy, as demonstrated in Table II. The paired t-test revealed a significant reduction in symptom severity postoperatively ($p < 0.05$ for all compared symptoms). Table II summarizes the clinical outcomes of the patients' post-micro-neurosurgical intervention for refractory VBI, highlighting the overall success rate.

In assessing the overall symptomatic improvement postoperatively, our data indicates that approximately 86.8% of the observed symptoms across all patients were resolved entirely or markedly improved. This outcome suggests a high efficacy rate for the surgical technique implemented in our study, reinforcing its potential as a valuable treatment modality for patients with VBI who are unresponsive to medication. No operative mortality and low temporary morbidities such as ptosis, swallowing difficulties, hoarseness, and coughing were encountered.

The results suggest that in light of the clinical presentations observed, our proposed approach primarily addresses patients presenting with refractory VBI who also exhibit medically resistant RLS. In such cases where medical therapy has proven ineffective, and the patient's condition persists, it becomes imperative to consider the presence of VA anomalies, specifically dolicoarteriopathies in the cervical region.

4. DISCUSSION

In this retrospective study, we uncovered that micro-neurosurgery for VA dolicoarteriopathy resulted in complete resolution of RLS symptoms in 83.33% (10 out of 12) patients and partial improvement in 16.66% (2 out of 12) patients, with an overall symptomatic improvement rate of 86.8% for various refractory VBI-related symptoms. These findings underscore the potential of microsurgery as a pivotal treatment for VBI-related symptoms and emphasize the vascular relation of RLS. The findings align with emerging studies suggesting a vascular component to this traditional neurological syndrome.

http://doi.org/10.5472/marumj.1479815
Marmara Med J 2024;37(2): 224-230

The quantitative leap in symptom management observed postoperatively reinforces the argument for a vascular evaluation in RLS patients, especially those who do not respond to standard pharmacotherapy. Our data contributes to the evidence suggesting that micro-neurosurgical interventions may substantially improve the quality of life for these patients with complex neurovascular disorders, challenging the conventional pharmacological treatment alone.

Our retrospective analysis yielded a pivotal observation: patients undergoing micro-neurosurgical intervention for refractory VBI exhibited a notable resolution of RLS despite the absence of ischemic findings on MRI. This finding aligns with current literature, which often associates these symptoms with brain regions correlated with vertebrobasilar system feeding territory. The absence of overt ischemic changes on MRIs in our patients underscores the necessity of reevaluating the neurovascular interplay in RLS, advocating for a broader diagnostic lens encompassing structural and functional cerebral vascular integrity. When appropriate and feasible, endovascular therapy is often the first line of intervention. However, open surgical techniques, such as those employed in our patients, may be considered in scenarios where endovascular treatment is either ineffective or not feasible due to the surrounding fibrotic tissue and the significant angulation present, particularly in grade 2 and 3 kinks, which can compromise the success of endovascular interventions and may even pose additional risks. These new micro-neurosurgical methods offer an alternative for managing VA dolicoarteriopathies, potentially alleviating the complex symptoms associated with these vascular anomalies. Further research with larger sample sizes is warranted to confirm these findings and to refine surgical approaches for optimal patient outcomes.

The interrelation between RLS and vascular pathologies has become a focal point in recent neurological research. A series of studies have illuminated the prevalence of RLS following stroke, with an estimated occurrence in 10% of patients, underscoring the potential vulnerability of specific brain regions to ischemic events even though there are no MR image abnormalities [24,25]. The predictive quality of RLS for subcortical stroke has also been substantiated, with unilateral or asymmetrical RLS symptoms frequently preceding cerebrovascular incidents. This association advocates for a more vigilant approach to RLS as a possible early indicator of subcortical vascular complications. Moreover, the negative impact of RLS on post-stroke quality of life has been documented, raising the imperative for routine screening and potential treatment of RLS in the wake of cerebrovascular events to enhance patient recovery and well-being [26,27]. When RLS presents as an isolated condition, it is associated with various brain regions; however, when it precedes ischemic events and coexists with VBI, it suggests a more localized pathology. In such cases, the medial border zone, corresponding to the paracentral lobule where the anterior and posterior pericallosal arteries converge—essentially the interface between anterior and posterior circulation—may be the primary target area. This region, being part of the border zone territories, is known to be particularly vulnerable to ischemia, often being the first to be affected. This insight is crucial for the discussion section as it aligns the neurovascular implications of RLS with underlying ischemic conditions.

In light of the evidence in recent literature, RLS has been associated with alterations in several brain regions, including the anteromedial pons, body of the caudate nucleus, cingulate gyrus, medial frontal region, and paracentral lobule, limbic system, globus pallidus, and hippocampus [15,24,28]. These findings have elucidated a neural circuitry that could be vulnerable to vascular insufficiencies, especially in the vertebrobasilar feeding territory. In our current study, we observed that symptoms of RLS often presented in conjunction with symptoms indicative of VBI. Notably, these symptoms persisted despite resistance to medical therapy and the presence of dolicoarteriopathies, which were deemed unsuitable for endovascular treatment, thus necessitating surgical intervention.

The importance of a comprehensive vascular assessment, especially concerning the vertebrobasilar system, becomes apparent in patients presenting with RLS. Given the efficiency of current treatments, recognizing the vertebrobasilar system to RLS can significantly improve patient management. This approach may alleviate the refractory VBI and can benefit from the medically resistant RLS and address underlying vascular anomalies that could predispose individuals to more severe cerebrovascular events.

Our study's retrospective design and the limited number of participants may affect the breadth of our conclusions. The findings of our retrospective study should be considered in the context of its inherent limitations. Primarily, the relatively small sample size and the patients' specificity may limit our results' generalizability. Larger-scale, multicenter studies are necessary to corroborate our findings across diverse populations and clinical settings. Additionally, the observational nature of our study limits the ability to draw causal inferences between microsurgical interventions and improvement in RLS symptoms.

Furthermore, the average follow-up period of one year, while insightful, does not allow for the assessment of long-term outcomes and sustainability of symptom relief. Longer-term follow-up studies are essential to understand the durability of clinical improvements post-intervention.

Finally, while our study provides valuable insights into the clinical improvement of RLS symptoms following microsurgical intervention for VA dolicoarteriopathies, the underlying mechanisms remain fully elucidated. Establishing a clear mechanistic link between these interventions and improvements in RLS symptoms warrants further investigation. Future research should include more significant, prospective trials to confirm the efficacy of micro-neurosurgical interventions for refractory VBI and the secondary benefits of RLS. For future research, besides a questionnaire of RLS patients for VBI symptoms and obtaining brain and cervical MR angiography besides brain MR in these patients, it will be helpful to see the actual number of the patient population and the incidence of VBI and RLS to be seen together. In intravascular pathologies of the VA, endovascular management may be more appropriate, but as dense fibrosis

http://doi.org/10.5472/marumj.1479815
Marmara Med J 2024;37(2): 224-230

exists around the kinking side in dolicoarteriopathies, new techniques that do not interrupt the blood flow may be more beneficial. Endovascular surgery has primarily taken the place of traditional surgical approaches in the treatment of intravascular pathologies. It will be crucial to understand the long-term effects of surgery and its influence on neurovascular pathways. Additionally, there is a need for randomized controlled trials to solidify the relationship between surgical outcomes and symptom relief.

Exploring the role of such surgeries in the broader context of neurovascular and sensorimotor disorders will also be valuable. Further investigations should aim to harness advanced imaging techniques for a deeper insight into post-surgical neurophysiological changes. Our findings point towards a promising direction for enhancing the treatment of VBI-related disorders, which merits continued scientific inquiry.

Expanding upon the innovative methodologies exemplified by Cekic et al., who successfully harnessed deep learning to segment and classify brain tumors [29]. We envisage a future direction for our neurosurgical strategies. Deep learning algorithms possess the transformative potential to identify vascular anomalies within the intricate milieu of the neurovascular landscape. By incorporating AI-driven technology into neurosurgical operations, we could substantially refine the real-time identification and management of vascular anatomies. This approach could be especially beneficial in vertebrobasilar and carotid dolicoarteriopathies and tubular stenosis, where precision is paramount [30]. Future studies might explore the feasibility of employing such algorithms to distinguish between pathological and normal vascular tissues during surgery, thereby augmenting the surgeon's precision and expanding the horizons for the treatment of refractory VBI.

Conclusion

In conclusion, RLS, alongside refractory VBI, necessitates a thorough evaluation of the vertebrobasilar system, mainly via MR angiography, to assess for potential contributory factors such as V1 segment dolicoarteriopathies. When symptoms are refractory to medical treatment and endovascular interventions are not viable, implementing microsurgical techniques targeting VA dolicoarteriopathies primarily for refractor VBI has demonstrated promising outcomes secondarily for RLS. Our study supports the potential of such micro-neurosurgical interventions to effectively rectify these conditions, substantially improving patient symptoms and indicating a significant step forward in managing these complex cerebrovascular disorders.

Compliance with Ethical Standards

Ethical approval: The Clinical Studies Ethics Committee of Bilecik Seyh Edebali University approved the study protocol and amendments (2/12, 03.30.2022) accordingly, with the clinical approval of the hospital and the local health authorities. The study was performed in accordance with the ethical standards of principles of the Declaration of Helsinki and Good Clinical Practices. After detailed information was provided, informed consent was obtained from all subjects.

Financial support: The authors have no relevant financial information to disclose.

Conflict of interest: The authors reported no potential conflict of interest.

Authors' contributions: EC, ISD, and MEU: Conception and design, EC, and MEU: Data collection, EC, ISD, and MEU: Analyzed data, EC and MEU: Writing. All authors approved the final version of the article.

REFERENCES

[1] Ekşi MŞ, Toktaş ZO, Yılmaz B, et al. Vertebral artery loops in surgical perspective. Eur Spine J 2016;25:4171-80. doi: 10.1007/s00586.016.4691-1.

[2] Omotoso BR, Harrichandparsad R, Moodley IG, Satyapal KS, Lazarus L. An anatomical investigation of the proximal vertebral arteries (V1, V2) in a select South African population. Surg Radiol Anat 2021;43:929-41. doi: 10.1007/s00276.021.02712-x.

[3] Metz H, Bannister RG, Murray-Leslie RM, Bull JWD, Marshall J. Kinking of the internal carotid artery. The Lancet 1961;277:424-6. doi: 10.1016/S0140-6736(61)90004-6.

[4] Wang J, Lu J, Qi P, et al. Association between kinking of the cervical carotid or vertebral artery and ischemic stroke/tia. Front Neurol 2022;13. doi: 10.3389/fneur.2022.100.8328.

[5] Cekic E, Surme MB, Akbulut F, Ozturk R, Ustun ME. Secondary benefits of microsurgical intervention on the vertebral artery (V1 Segment) for refractory vertebrobasilar insufficiency: alleviation of Parkinsonism-like symptoms. World Neurosurg 2024. doi: 0.1016/j.wneu.2024.04.125.

[6] Yenigun A, Ustun ME, Tugrul S, Dogan R, Ozturan O. Classification of vertebral artery loop formation and association with cervicogenic dizziness. J Laryngol Otol 2016;130:1115-9. doi: 10.1017/S002.221.5116009117.

[7] Paksoy Y, Levendoglu FD, Ögün CÖ, Üstün ME, Ögün TC. Vertebral artery loop formation: a frequent cause of cervicobrachial pain. Spine (Phila Pa 1976) 2003;28:1183-8. doi: 10.1097/01.BRS.000.006.7275.08517.58.

[8] Rennert RC, Steinberg JA, Strickland BA, et al. Extracranial-to-intracranial bypass for refractory vertebrobasilar insufficiency. World Neurosurg 2019;126:552-9. doi: 10.1016/j.wneu.2019.03.184.

[9] Starke RM, Chwajol M, Lefton D, Sen C, Berenstein A, Langer DJ. Occipital artery-to-posterior inferior cerebellar artery bypass for treatment of bilateral vertebral artery occlusion. Neurosurgery 2009;64:E779-81. doi: 10.1227/01.NEU.000.033.9351.65061.D6.

[10] Lu X, Ma Y, Yang B, Gao P, Wang Y, Jiao L. Hybrid technique for the treatment of refractory vertebrobasilar insufficiencies. World Neurosurg 2017;107:1051.e13-1051.e17. doi: 10.1016/j.wneu.2017.08.081.

[11] Boulos MI, Wan A, Black SE, Lim AS, Swartz RH, Murray BJ. Restless legs syndrome after high-risk tia and minor stroke: association with reduced quality of life. Sleep Med 2017;37:135-40. doi: 10.1016/j.sleep.2017.05.020.

[12] Liu Z, Guan R, Pan L. Exploration of restless legs syndrome under the new concept: a review. Medicine 2022;101:e32324. doi: 10.1097/MD.000.000.0000032324.

[13] Wang X-X, Feng Y, Tan E-K, Ondo WG, Wu Y-C. Stroke-related restless legs syndrome: epidemiology, clinical characteristics, and pathophysiology. Sleep Med 2022;90:238-48. doi: 10.1016/j.sleep.2022.02.001.

[14] Kalampokini S, Poyiadjis S, Vavougios GD, et al. Restless legs syndrome due to brainstem stroke: a systematic review. Acta Neurol Scand 2022;146:440-7. doi: 10.1111/ane.13702.

[15] Mogavero MP, Mezzapesa DM, Savarese M, DelRosso LM, Lanza G, Ferri R. Morphological analysis of the brain subcortical gray structures in restless legs syndrome. Sleep Med 2021;88:74-80. doi: 10.1016/j.sleep.2021.10.025.

[16] Trenkwalder C, Allen R, Högl B, Paulus W, Winkelmann J. Restless legs syndrome associated with major diseases. Neurology 2016;86:1336-43. doi: 10.1212/WNL.000.000.0000002542.

[17] Ferini-Strambi L, Walters AS, Sica D. The relationship among restless legs syndrome (Willis–Ekbom Disease), hypertension, cardiovascular disease, and cerebrovascular disease. J Neurol 2014;261:1051-68. doi: 10.1007/s00415.013.7065-1.

[18] Ferri R, Cosentino FII, Moussouttas M, Lanuzza B, Aricò D, Bagai K, et al. Silent cerebral small vessel disease in restless legs syndrome. Sleep 2016;39:1371-7. doi: 10.5665/sleep.5966.

[19] Locke JA, Macnab A, Garg S, McKeown M, Stothers L. Characterizing the cortical pathways underlying visual trigger induced urinary urgency incontinence by functional MRI. Neurourol Urodyn 2022;41:48-53. doi: 10.1002/nau.24824.

[20] Allen RP, Picchietti DL, Garcia-Borreguero D, et al. Restless legs syndrome/Willis–Ekbom disease diagnostic criteria: updated international restless legs syndrome study group (IRLSSG) consensus criteria – history, rationale, description, and significance. Sleep Med 2014;15:860-73. doi: 10.1016/j.sleep.2014.03.025.

[21] Latz D, Grassmann J, Schiffner E, et al. Postoperative brachial artery entrapment associated with pediatric supracondylar fracture of the humerus: a case report. J Med Case Rep 2017;11:69. doi: 10.1186/s13256.017.1240-4.

[22] Sadri L, Myers RL, Paterson C, Lam Q-D, Pineda DM. Popliteal artery entrapment syndrome treated by a posterior approach in a 15-year-old athlete. J Vasc Surg Cases Innov and Tech 2022;8:248-50. doi: 10.1016/j.jvscit.2022.03.009.

[23] Teijink SBJ, Goeteyn J, Pesser N, van Nuenen BFL, Thompson RW, Teijink JAW. Surgical approaches for thoracic outlet decompression in the treatment of thoracic outlet syndrome. J Thorac Dis 2023;15:7088-99. doi: 10.21037/jtd-23-546.

[24] Ruppert E, Kilic-Huck U, Wolff V, et al. Brainstem stroke-related restless legs syndrome: frequency and anatomical considerations. Eur Neurol 2015;73:113-8. doi: 10.1159/000366416.

[25] Shiina T, Suzuki K, Okamura M, Matsubara T, Hirata K. Restless legs syndrome and its variants in acute ischemic stroke. Acta Neurol Scand 2019;139:260-8. doi: 10.1111/ane.13055.

[26] Gupta A, Shukla G, Mohammed A, Goyal V, Behari M. Restless legs syndrome, a predictor of subcortical stroke: a prospective study in 346 stroke patients. Sleep Med 2017;29:61-7. doi: 10.1016/j.sleep.2015.05.025.

[27] Boulos MI, Wan A, Black SE, Lim AS, Swartz RH, Murray BJ. Restless legs syndrome after high-risk tia and minor stroke: association with reduced quality of life. Sleep Med 2017;37:135-40. doi: 10.1016/j.sleep.2017.05.020.

[28] Kalampokini S, Poyiadjis S, Vavougios GD, et al. Restless legs syndrome due to brainstem stroke: a systematic review. Acta Neurol Scand 2022;146:440-7. doi: 10.1111/ane.13702.

[29] Cekic E, Pinar E, Pinar M, Dagcinar A. Deep learning-assisted segmentation and classification of brain tumor types on magnetic resonance and surgical microscope images. World Neurosurg 2023. doi: 10.1016/j.wneu.2023.11.073.

[30] Cekic E, Ustun ME. Adventitia layer-focused microsurgical flow reconstruction for long-segment tubular stenosis of the cervical segment (C1) internal carotid artery: clinical valuable experience in 20 cases. Brain Sci 2024;14:289. doi: 10.3390/brainsci14030289.

MARMARA
MEDICAL JOURNAL

Original Article

https://dergipark.org.tr/tr/pub/marumj

Prevalence of Turkish Ministry of Health e-Nabız application usage and the factors affecting its use

Ayse Nilufer OZAYDIN[1], Ibrahim NOKAY[2]

[1] Department of Public Health, School of Medicine, Marmara University, Istanbul, Turkey
[2] Information Technology and Systems Management, Gumuşhacikoy State Hospital, Amasya, Turkey

Corresponding Author: Ayse Nilufer OZAYDIN
E-mail: nozaydin@gmail.com

Submitted: 22.08.2022 **Accepted:** 26.02.2024

ABSTRACT

Objective: In this study, the frequency of using the e-Nabız application and the factors affecting its use were studied among adults living in a district of northern Turkey.

Materials and Methods: In this cross-sectional study, the sample (n:555, N:9264) was selected from those who applied, for any reason, to the only hospital in the district between March 1 and December 31, 2020. Data were collected by an online questionnaire (10 February–29 March 2021). Ethical permissions were obtained from the Ministry of Health, Republic of Turkey and the Marmara University, School of Medicine Clinical Researches Ethics Committee (05.02.2021/09.2021.70). All the participants gave informed consent.

Results: Among 458 participants, the response rate was 82.5% and 59.4% of the respondents were female. The median age was 44.0 years (44.7±13.7; range: 19–72). 57.4% of the females and 69.4% of the males had registered for the application (p: 0.006), and 56.6% of the females and 68.8% of the males had used e-Nabız (p: 0.011). The males, aged 26–45, with high school and above education levels, working in the public sector with a good monthly income, were the group with the highest usage of e-Nabız (respectively p: 0.001, p: 0.001, p: 0.001, and p: 0.001). Current health status did not affect the usage of e-Nabız (p:0.144).

Conclusion: We can promote environmentally friendly usage by enhancing health literacy through e-Nabız and securely storing personal health records. Therefore, educational sessions can be organized to inform citizens about the services provided by e-Nabız.

Keywords: Digital health applications, e-Health applications, Electronic medical records, Health information technologies

1. INTRODUCTION

An outbreak of an epidemic related to a new virus strain from the coronavirus family was reported in Wuhan, the capital of China's Hubei province, in December of 2019. On February 11, 2020, the World Health Organization (WHO) officially named this new coronavirus disease-19 (COVID-19) and expressed its concerns that the virus would spread worldwide. As a matter of fact, the COVID-19 infection spread rapidly worldwide, and WHO declared a "pandemic" on March 11, 2020 [1]. More than 767 million people have been infected with the disease, and almost 7 million people have died since the onset of the pandemic as of July 12, 2023 [2].

The COVID-19 pandemic presented challenges to people forced to change daily habits and take precautions in all areas. During this time, when we had to adapt old habits to different ways, the new possibilities offered by information technologies allowed us to digitize processes faster than ever before. All information processing was able to continue at the same speed without physical contact by using mobile phones, computers, and tablets. Some have argued that pandemic accelerated the digitalization process [3].

During the pandemic, healthcare resources were mobilized largely to focus on the treatment of patients infected by COVID-19. Hospital environments were considered unsafe for patients without COVID-19 due to the risks of nosocomial infections due to COVID-19 and they were avoided admission to hospitals for medical care except for emergency admissions. Hospitals in many countries responded to the health care needs of people with mild illnesses or diseases through telemedicine systems [4]. According to 45 responses from 24 countries, 68% of screening programs were suspended, 73% of magnetic resonance

How to cite this article: Ozaydin AN, Nokay I. Prevalence of Turkish Ministry of Health e-Nabız application usage and the factors affecting its use. Marmara Med J 2024: 37(2):231-237. doi: 10.5472/marumj.1493336

ISSN: 1309-9469

http://doi.org/10.5472/marumj.1493336
Marmara Med J 2024;37(2): 231-237

imaging procedures were postponed, and telemedicine was preferred at a rate of 71% depending on accessibility [5].

e-Nabız is a personal, digital, health record system that can manage all health information regardless of where your examinations, analyses, and treatments are performed and which provides patient and provider access to consolidated medical histories through a single source [6].

Turkish Ministry of Health has a telemedicine system named e-Nabız with 7/24 access to radiology images on the web, reports regarding these images, tele-consultation services between radiologists, evaluation of medical images, and reports in terms of quality, and sharing them with citizens via the e-Nabız application [7]. Mobile applications appear to accelerate the processes of benefiting from health services, such as making appointments, displaying test results, and choosing a physician, while differentiating business processes from physical boundaries [8]. Health administrators think that the inclusion of citizens in the provision of health services via the e-Nabız, will also increase health literacy and improve the sustainability of health services [9].

e-Nabız was launched on January 1, 2015 as a personal medical recording system managed directly by the citizens. With the e-Nabız, patients can enter their medical data such as blood pressure and glucose level, personal data such as heart rate and number of steps via smart devices (if any), and their health profiles, and they can view this information comparatively. Individuals can authorize physicians or health institution, at home or abroad to access their medical records, including diagnoses, prescriptions, medical images, etc. It is anticipated that when physicians can easily access their patients' health histories, the number of repeat examinations, diagnostic tests, or medical images may be reduced. Thus, individuals will be prevented from losing time for repeated services, and the economic interests of individuals and their health insurance will be protected [10-12].

This study aimed to investigate the prevalence of e-Nabız application use by adults living in a town (Gümüşhacıköy) in the north of Turkey during the pandemic, as well as the factors affecting their usage. Gümüşhacıköy was selected as a sample of northern Turkey.

The total population, which was 26,000 in 2008, continues to decline over the years. According to 2023 Turkish Statistical Institute data, the population of the town is 22,121 and 50.9% of this population are females [13,14].

2. MATERIALS and METHODS

This study was a cross-sectional study. The population of the study consisted of males and females, aged 18 and over, who applied at least once to the only state hospital of the town for any reason, between March 1 and December 31, 2020 (n=9264). The list of patients who applied was obtained from the Chief Physician's Office of Gümüşhacıköy State Hospital. The minimum sample size to represent the district was calculated as 370 people in OpenEPI, with a 95% confidence interval, and the sample size was expanded to 555 (370x1.5) assuming that the probability of not responding was 50%. The study sample was selected from the population by gender and age groups, stratified and a systematic sampling method was applied (Table I). Study permissions were obtained from the Republic of Turkish Ministry of Health, General Directorate of Health Services and from the State Hospital's Health Directorate. The study was approved by the Marmara University, School of Medicine Clinical Research Ethics Committee (protocol date and approval number: 05.02.2021/ 09.2021.70). Participants in the sample were reached online, informed consent was obtained, and data was collected via on online questionnaire between February 10, 2021 and March 29, 2021. During the data collection process, participants were reached by sending links via their hospital appointment or communication phone numbers. Illiterate or technologically inexperienced participants filled out the survey with the help of their caregivers. [12].

Table I. *Distribution of participants reached in the sample by strata*

Sex	Age Groups	Total Population		Sample Size(n)
		Size (n)	Distribution (%)	
Female	18-25	831	8.97	50
	26-35	1191	12.86	71
	36-45	1127	12.17	67
	46-55	1252	13.51	75
	56-65	1379	14.89	83
Male	18-25	375	4.05	22
	26-35	581	6.27	35
	36-45	643	6.94	39
	46-55	792	8.55	48
	56-65	1093	11.79	65
Total		9264	100.00	555

The online questionnaire consisted of two parts; where the first part included the socio-demographic characteristics of the participants (8 questions) and the second part included questions about awareness, use and satisfaction with the e-Nabız (15 questions) [12].

Statistical Analysis

The data of the study were analysed by the researcher using SPSS, through Kolmogorov-Smirnov test, Student's t test, Mann-Whitney U test and X^2 test. $p<0.05$ was accepted as the statistical significance level.

3. RESULTS

During the study, data were collected by reaching 458 out of 555 people (a response rate of 82.5%). Of the participants, 59.4% were female (n:272). The median age of participants was 44.0 years (range:19–72). The median age of the females was 42.0 (range:19–68, n:272), and the median age of the males was 48.0 years (range:19–72, n:186) (p= 0.002).

http://doi.org/10.5472/marumj.1493336
Marmara Med J 2024;37(2): 231-237

Table II. *Distribution of socio-demographic characteristics of participants by sex*

Socio-demographic characteristics	Sex				Total		
	Female		Male				p
	n	%	n	%	n	%	
Age groups (year)							
<25	29	10.7	12	6,5	41	9.0	
26-35	67	24.6	31	16.7	98	21.4	0.054*
36-45	58	21.3	39	21.0	97	21.2	
46-55	47	17.3	38	20.4	85	18.6	
55+	71	26.1	66	35.5	137	29.9	
Education							
Illiterate/Literate/ PrimarySchool	58	21.3	6	3.2	64	14.0	**0.001***
Secondary School	39	14.3	25	13.4	64	14.0	
High School	68	25.0	67	36.0	135	29.5	
University/ Postgraduate/PhD	107	39.3	88	47.3	195	42.6	
Marital status							
Married	201	73.9	153	82.3	354	77.3	
Single	54	19.9	31	16.7	85	18.6	**0.013***
Divorced/widowed	17	6.3	2	1.1	19	4.1	
Income							
Low	18	6.6	15	8.1	33	7.2	
Middle	155	57.0	101	54.3	256	55.9	0.775*
High	99	36.4	70	37.6	169	36.9	
Employment status							
Public sector	89	32.7	93	50.0	182	39.7	
Private sector	20	7.4	35	18.8	55	12.0	**0.001***
Retired	16	5.9	46	24.7	62	13.5	
Unemployed	9	3.3	6	3.2	15	3.3	

**Pearson Chi-Square Test*

Socio-demographic characteristics affecting e-Nabız registration

It was determined that 69.4% of the male participants were registered at the e-Nabız, which was higher than the registration rate of female participants (57.4%) (p:0.012). While, 83.7% of the participants in the 26-45 age group were registered with the e-Nabız, only 41.6% of those aged 55 and above were registered (p:0.001). University graduates in the study group were registered to the e-Nabız at the highest rate (81.5%), while only 20.3% of the illiterate/literate/primary school graduates were registered (p:0.001). It was determined that 74% of those with high income and 54.5% of those with low income were registered to the e-Nabız (p:0.001).

Public sector employees were registered at the e-Nabız (91.2%) at a much higher rate than the other employment groups (p:0.001). The 44.9% majority of the females declared that they were housewives, and only 33.6% of them were registered at the e-Nabız (p:0.0001) (Table III).

Table III. *Distribution of e-Nabız application registration by socio-demographic characteristics*

Being registered to e-Nabız	Total						
	Yes		No				P
	n	%	n	%	n	%	
Sex							
Female	156	57.4	116	42.6	272	100.0	**0.012***
Male	129	69.4	57	30.6	186	100.0	
Age Groups (year)							
<25	20	48.8	21	51.2	41	100.0	
26-35	82	83.7	16	16.3	98	100.0	
36-45	76	78.4	21	21.6	97	100.0	**0.001***
46-55	50	58.8	35	41.2	85	100.0	
55+	57	41.6	80	58.4	137	100.0	
Education							
Illiterate/Literate/ Primary School	13	20.3	51	79.7	64	100.0	
Secondary School	26	40.6	38	59.4	64	100.0	
High School	87	64.4	48	35.6	135	100.0	**0.001***
University/ Postgraduate/PhD	159	81.5	36	18.5	195	100.0	
Marital status							
Married	224	63.3	130	36.7	354	100.0	
Single	51	60.0	34	40.0	85	100.0	0.586*
Divorced/widowed	10	52.6	9	47.4	19	100.0	
Income							
Low	18	54.5	15	45.5	33	100.0	
Middle	142	55.5	114	44.5	256	100.0	**0.001***
High	125	74.0	44	26.0	169	100.0	
Employment status							
Publicsector	166	91.2	16	8.8	182	100.0	
Privatesector	27	49.1	28	50.9	55	100.0	
Retired	37	59.7	25	40.3	62	100.0	**0.001***
Unemployed	4	26.7	11	73.3	15	100.0	
Student	10	45.5	12	54.5	22	100.0	
Housewife	41	33.6	81	66.4	122	100.0	
Health status							
Healthy	82	59.4	56	40.6	138	100.0	
Occasional,non-serious health problem	108	68.4	50	31.6	158	100.0	0.141*
Chronic diseases	95	58.6	67	41.4	162	100.0	
Total	**285**	**62.2**	**173**	**37.8**	**458**	**100.0**	

**Pearson Chi-Square Test*

Prevalence of e-Nabız usage by participants

Among all participants, 61.6% declared that they have used the e-Nabız; 56.6% of the females and 68.8% of the males have used it (:0.008,Table IV, Figure 1). Of those who said they had used the e-Nabız, 80.5% stated that they could use it by themselves without assistance, and the results were similar for the females

http://doi.org/10.5472/marumj.1493336
Marmara Med J 2024;37(2): 231-237

and males (p:0.765). Also, 88.6% of those using the e-Nabız were using it via smart phones, and the results were similar for the males and females (p:1.000). However, half of the users (54.9%) stated that they rarely use it (p:0.934, Table IV).

Table IV. *Distribution of e-Nabız use by sex*

Sex	Female		Male		Total		p
	n	%	n	%	n	%	
e-Nabız system usage							
Never use	118	43,4	58	31,2	176	38,4	
Use	154	56,6	128	68.8	282	61.6	0.008*
Management of e-Nabız (n:282)							0.765*
Use by themself	125	81,2	102	79.7	227	80.5	
Use with support	29	18,8	26	20.3	55	19.5	
How e-Nabız is used (n:280)							1.000*
By computer	17	11,2	15	11.7	32	11.4	
By smartphone	135	88,8	113	88.3	248	88.6	
Frequency of e-Nabız Use (n:277)							
Rarely	83	55,3	69	54,3	152	54,9	0.934*
Once a month	39	26,0	35	27,6	74	26,7	
Once a week	16	10,7	15	11,8	31	11,2	
Every few days	12	8.0	8	6,33	20	7,2	
Total	**272**	**100.0**	**186**	**100.0**	**458**	**100.0**	

**Pearson Chi-Square Test*

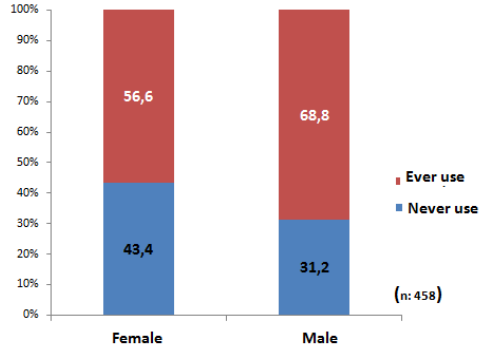

Figure 1. *Prevalence of e-Nabız use by sex*

Socio-Demographic characteristics affecting the use of the e-Nabız

Participants in the 26-45 age group used e-Nabız the most (82.7%), while only 41% of those aged 55 and above used it (p:0.001). The participants who graduated from university used e-Nabız more (81.5%), while only 18.8% of illiterate/literate/elementary school graduates used it (p:0.001). High-income participants (73.4%) used the e-Nabız more than the others (p:0.001). When employment status is considered, e-Nabız usage (90.1%) by public employees was found to be much higher than the others. The 44.9% majority of female participants declared that they were housewives, and only 33.6% of this group declared that they had used the e-Nabız (p:0.001). e-Nabız usage was found to be similar among marital status and health subgroups (p:0.386 and p:0.144 respectively, Table V).

Table V. *Distribution of e-Nabız usage by socio-demographic characteristics*

Use of The e-Nabız System	Yes		No		*p*
	n	%	n	%	
Age groups (Year)					
<25	20	48.8	21	51.2	
26-35	81	**82.7**	17	17.3	**0.001***
36-45	75	**77.3**	22	22.7	
46-55	50	58.8	35	41.2	
55+	56	40.9	81	59.1	
Education					
Illiterate/Literate/Primary School	12	18.8	52	81.3	
Secondary School	26	40.6	38	59.4	**0.001***
High School	85	63.0	50	37.0	
University/Postgraduate/ PhD	159	81.5	36	18.5	
Marital status					
Married	222	62.7	132	37.3	
Single	51	60.0	34	40.0	**0.386***
Divorced/widowed	9	47.4	10	52.6	
Income					
Low	17	51.5	16	48.5	
Middle	141	55.1	115	44.9	**0.001***
High	124	73.4	45	26.6	
Employment status					
Publicsector	164	90.1	18	9.9	
Privatesector	27	49.1	28	50.9	
Retired	36	58.1	26	419	**0.001***
Unemployed	4	26.7	11	73.3	
Student	10	45.5	12	54.5	
Housewife	41	33.6	81	66.4	
Health status					
Healthy	81	58.7	57	41.3	
Occasional,non-serious Health problem	107	67.7	51	32.3	**0.144***
Chronic diseases	94	58.0	68	42.0	
Total	**282**	**100.0**	**176**	**100.0**	

**Pearson Chi-Square Test*

http://doi.org/10.5472/marumj.1493336
Marmara Med J 2024;37(2): 231-237

Level of e-Nabız awareness

In this study, 81.7% of participants stated that they had heard about the e-Nabız. While, the majority of males stated that they had heard about the system, three out of every four females in the study stated that they had heard about it (p:0.001). Participants heard about e-Nabız mostly from public health service announcements on television and from social media (45.4%, 40%, p:0.002, p:0.014 respectively).

***TableVI**. Distribution of e-Nabız Awareness by Sex*

	Sex				Total		
	Female		Male				*p*
	n	%	n	%	n	%	
Heard of e-Nabız							
Yes	203	74.6	171	91.9	374	81.7	
No	69	25.4	15	8.1	84	18.3	**0.001***
Source of Information							
Social Media(Facebook,Twitter. etc.), Web							
Yes	96	35.3	87	46.8	183	40.0	**0.014***
No	176	64.7	99	53.2	275	60.0	
Public Spot							
Yes	107	39.3	101	54.3	208	45.4	**0.002***
No	165	60.7	85	45.7	240	54.6	
Newspaper							
Yes	20	7.4	19	10.2	39	8.5	0.364*
No	252	92.6	167	89.8	419	91.5	
Television, radio etc.							
Yes	68	25.0	58	31.2	126	27.5	0.177*
No	204	75.0	128	68.8	332	72.5	
Friends							
Yes	77	28.3	53	28.5	130	28.4	1.000*
No	195	71.7	133	71.5	328	71.6	
Family							
Yes	4	1.5	1	0.5	5	1.1	*
No	268	98.5	185	99.5	453	98.9	
Total	**272**	**100.0**	**186**	**100.0**	**458**	**100.0**	

**Pearson Chi-Square Test*

4. DISCUSSION

In this study, it was aimed to reveal the usage status and factors affecting the use of e-Nabız by adults living in a town in the northern Turkey during the pandemic period, when the importance and necessity of e-Nabız became more prominent. Data were successfully collected online from 458 individuals selected with a stratified sample, composed of 59.4% females and 40.6% males with a total response rate of 82.5%.

Although, the vast majority of participants (81.7%) were aware of e-Nabız, we found that a remarkable percentage of participants (18.3%) know nothing about e-Nabız. When the findings of the study were compared with the literature, it was observed that they were similar to other study findings [15-18]. In most studies, we see that almost all participants are aware of e-Nabız.

The educational level variable seems to be a determining factor in the awareness of digital health practices and that participants with higher educational levels have more knowledge about the e-Nabız than those with lower educational levels [16,19].

In our study, participants stated that they heard about the e-Nabız mostly from public service advertisements, followed by social media (40.0%), friends (27.4%), and information sources (27.5%) such as television and radio. In a master's thesis on e-Nabız and e-Health literacy, it was reported that nearly half of those who were aware of the e-Nabız application, heard about it from social media and the internet [16].

We found that the majority of participants (81.7%) did not reflect their knowledge about e-Nabız at a similar rate. Only slightly more than half (61.6%) of respondents use the e-Nabız system. Our study differs from other studies regarding the usage of e-Nabız system [12,17,20-22]. The reason for the difference may be due to the fact that the study was conducted in a region of northern Turkey and that e-Nabız was needed more in 2021 and during the pandemic period.

In our study, we found that 38.4% of participants never used e-Nabız, and that more than half (54.9%) of those who claimed to use it only used it rarely. In a study conducted by Demir with 422 university students, 88% had never used e-Nabız, and 5.7% used it rarely [12]. In the announcement of the e-Nabız application, the success rate was not achieved in terms of the application's content and usage frequency, but there was a small difference in usage. In Demir's study, participants may use e-Nabız less because they were relatively healthier and were in a younger age group.

In the current study, we found that the 26 – to 45-year-old group used the e-Nabız the most, and that those aged 55 and older used it less. As participants grew older, their independent usage rates decreased, and they needed more assistance from others. It was determined that older people tended to use information technology less than younger people, and there were differences between those born or raised with information technology tools compared to those who were not [23,25].

According to this study, males significantly indicated that they used e-Nabız more (males: 68%, females: 56%). This may be due to the high educational levels of male participants. In a study of 409 participants, 53.7% of the females and 38.3% of the males used e-Nabız [17]. The reason for this difference in our study was that the distribution of e-Nabız needs was not overlapping due to the level of education and chronic diseases.

In our study, we found that those with higher educational levels had more knowledge about e-Nabız and used it more. Our study supported literary data showing a positive relationship between education levels and e-Nabız usage [16,17,20]. This may be the reason why individuals with a higher level of education follow developments closely and gain new knowledge and skills as a result of their approaches to seeking information.

We found that almost all participants working in the public sector used e-Nabız, while others used much less. This can be explained by the fact that public sector employees are more trained and more familiar with using systems such as computers, smartphones, etc. due to their work. In the Kıraç and Yılmaz study, 38.1% did not work anywhere, 41.6% worked in the private sector, and 20.3% in the public sector [17].

In our study, those with higher incomes used e-Nabız more than others. Buying a computer or other device for access to the internet requires money, and it is difficult for low-income individuals who cannot own such devices to have the available technology and necessary skills [26, 27].

In our study, 49.3% of participants who used e-Nabız stated that they used it to make or cancel appointments in healthcare centers; 14.6% said that they used it to view their health history to evaluate and interpret services received from the health care organizations they visited; and a very few said that they were using it to record blood pressure, blood sugar levels, heart rate, and weight information by adding data or sharing health data with health professionals in other institutions. [12,15,17,18,20,22] The findings of our study were similar to other study findings in this regard.

Limitation

A limitation of our findings is that the study excludes sicker, less educated, poorer, more distant groups, etc., who did not apply to the hospital during the study duration. We suggest that our findings be evaluated in this context.

Conclusion

The majority of participants in this study were knowledgeable about the e-Nabız, which became more important during the pandemic period, but higher educated male public employees and those aged between 26 and 45 use the e-Nabız at a higher rate than other age and employment groups. People who use the e-Nabız mostly use it to access their health record and to make or cancel appointments. Training activities can be planned for other services offered by the e-Nabız explaining how citizens can benefit from the e-Nabız. Increasing health literacy, creating a useful medical record, and keeping the personal medical records of citizens in a safe environment by developing the e-Nabız can increase the use of this health application. In order to increase the use of e-Nabız and improve health literacy, e-Nabız training can be added to the training given to patients and their relatives in healthcare institutions. Further research is needed involving individuals with different socio-demographic characteristics.

Compliance with Ethical Standards

Ethical approval: This study was approved by the Marmara University Faculty of Medicine Clinical Research Ethics Committee (The protocol date and code: 05.02.2021/09.2021.70). The study adhered to the principles of the Helsinki Declaration.

Financial support: This study did not receive any specific grant from funding agencies in the public, commercial, or not for profit sectors.

Conflict of interest: The authors have stated explicitly that there are no conflicts of interest in connection with this article.

Authors contributions: IN: Contributed to the conception, design and acquisition of data or analysis and interpretation of data, ANO: Conducted analysis and interpretation of data. All authors approved the final manuscript.

REFERENCES

[1] Dickens BL, Koo JR, Wilder-Smith A, Cook AR. Institutional, not home-based, isolation could contain the COVID-19 outbreak. Lancet. 2020;395(10236):1541-2.

[2] WHO Coronavirus (COVID-19) Dashboard. https://covid19.who.int. (Accessed on 21 February 2020).

[3] Süleymanlı E. Pandemi Sonrası Süreçte Alışkanlıklarımız Değişecek Üsküdar Üniversitesi. e-koronafobi:2020. https://npistanbul.com/koronavirus/pandemi-sonrasi-surecte-aliskanliklarimiz-degisecek. (Accessed on 21 February 2020).

[4] Portnoy J, Waller M, Elliott T. Telemedicine in the Era of COVID-19. J Allergy Clin Immunol Pract. 2020;8(5):1489-91.

[5] Mathelin C, Ame S, Anyanwu S, et al. Breast cancer management during the COVID-19 pandemic: The Senologic International Society survey. Eur J Breast Health. 2021;17:188-196. doi: 10.4274/ejbh.galenos.2021.2021-1-4

[6] Turkish Ministry of Health Teleradiology System. https://teletip.saglik.gov.tr. (Accessed on 21 February 2020).

[7] Turkish Ministry of Health, Health Information System. e-Pulse User Guide. 2018. https://enabiz.gov.tr/document/KILAVUZ_.pdf. (Accessed on 21 February 2020).

[8] Ağaç F. Mobil Uygulamalar Sağlık Sistemini Kişiselleştiriyor, Bilişim Dergisi, 2015(174):42-51

[9] Ülgü MM, Gökçay Ö G. Sağlık Bakanlığında Büyük Veri Çalışmaları, Büyük Veri ve Açık Veri Analitiği: Yöntemler ve Uygulamalar. Ankara: Grafiker Yayınları, 2017:267-282.

[10] Turkish Ministry of Health, Personal Health Recort Platform: Information on e-Nabız. Ankara, 2015:8-55.

[11] Arslan ET, Demir H. University students' attitudes towards mobile health and personal health record management. 2017;9:17-36.

[12] Demir R. Medipol Üniversitesi Öğrencilerinin Sağlık Bilgi Sistemleri ve E-Nabız Sistemine İlişkin Farkındalık ve Kullanım Düzeylerinin Belirlenmesi. Yüksek Lisans Tezi Medipol Üniversitesi, Sağlık Bilimleri Entitüsü, Sağlık Yönetimi Anabilim Dalı, İstanbul 2017.

[13] T.C. Gümüşhacıköy Kaymakamlığı-Gümüşhacıköy İlçe Tanıtımı. http://www.gumushacikoy.gov.tr/ilce-tanitimi. (Accessed on 21 February 2020).

[14] 2020 Yılına Göre Gümüşhacıköy Nüfusu. https://www.nufusu.com/ilce/gumushacikoy_amasya-nufusu. (Accessed on 21 February 2020).

[15] Demir S. E-devlet kapsamında e-nabız uygulamasına dair farkındalığın incelenmesi: Atatürk Üniversitesi Sosyal Bilimler Enstitüsü Yönetim Bilişim Sistemleri Anabilim Dalı Yüksek Lisans Tezi, Erzurum; 2019.

[16] Akgün E. Necmettin Erbakan Üniversitesi Sağlık hizmetlerinde sayısal uçurumun e-nabız sistemi ve e-sağlık okuryazarlığı ile birlikte incelenmesi Yüksek Lisans Tezi Necmettin Erbakan Üniversitesi Sağlık Bilimleri Entitüsü, Sağlık Yönetimi Anabilim Dalı Konya; 2020.

[17] Kıraç R, Yılmaz, G. Yetişkinlerde e-Nabız sistemi farkındalığının belirlenmesine yönelik bir araştırma. 3. Uluslararası 13. Ulusal Sağlık ve Hastane İdaresi Kongresi 2019. p. 1658-668.

[18] Soysal A, Yalçın T. Bazı demografik değişkenlere göre e-nabız sisteminin kullanımı: öğrenciler üzerinde bir araştırma. Sağlık Akademisyenleri Dergisi. 2019;6(3):180-8.

[19] Kuh Z. Sağlık hizmetleri kullanımında dijital bölünme üzerine bir araştırma. : Süleyman Demirel Üniversitesi Sosyal Bilimler Enstitüsü, Sağlık Yönetimi Anabilim Dalı Yüksek Lisans Tezi Isparta; 2019.

[20] Yeşiltaş A. Factors affecting utilization of e-Pulse application. Health Care Academician Journal 2018;5:290-5. doi: 10.5455/sad.13-152.554.2718

[21] Ekiyor A, Çetin A. Awareness of the e-Pulse applıcatıon ın the scope of health care delıvery and socıal marketıng. Int J Healthc Manag 2017;3:88-103.

[22] Yorulmaz M, Odacı, Ş. Akkan M. Dijital sağlık ve e-nabız farkındalık düzeyi belirleme çalışması. Selçuk Üniversitesi Sosyal ve Teknik Araştırma Dergisi 2018(16):1-11.

[23] Tuffley D. Bridging the age based digital divide. Int J Digit Lit Digit Compet 2015;6:1-15. doi: doi:10.4018/IJDLDC.201.507.0101

[24] Ball C, Francis J, Huang KT, Kadylak T, Cotten SR, Rikard RV. The Physical-Digital Divide: Exploring the Social Gap Between Digital Natives and Physical Natives. J Appl Gerontol. 2019;38(8):1167-84.

[25] Choudrie J, Pheeraphuttranghkoon S, Davari S. The Digital Divide and Older Adult Population Adoption, Use and Diffusion of Mobile Phones: a Quantitative Study. Inf Syst Front. 2018(22):673-95.

[26] Lavery M, Abadi M, Bauer R, et al. Tackling Africa's digital divide. Nature Photonics. 2018;12(5):249-52.

[27] Araque C, Maiden RP, Bravo N, et al. Computer usage and access in low-income urban communities. Computers in Hurman Behavior. 2013;29:1393-401.

MARMARA
MEDICAL JOURNAL

Original Article

https://dergipark.org.tr/tr/pub/marumj

Apocynin exhibits an ameliorative effect on endothelial dysfunction/ atherosclerosis-related factors in high-fat diet-induced obesity in rats

Nurdan BULBUL AYCI[1], Busra ERTAS[2], Rumeysa KELES KAYA[3], Sevgi KOCYIGIT SEVINC[4], Gokce Gullu AMURAN[5], Feriha ERCAN[1], Goksel SENER[6], Oya ORUN[7], Mustafa AKKIPRIK[5], Sule CETINEL[1]

[1] Department of Histology and Embryology, Faculty of Medicine, Marmara University, Istanbul, Turkey.
[2] Department of Pharmacology, Faculty of Pharmacy, Marmara University, Istanbul, Turkey.
[3] Department of Medical Pharmacology, Hamidiye International School of Medicine, University of Health Sciences, Istanbul, Turkey.
[4] Department of Biophysics, Faculty of Medicine, Kutahya Health Sciences University, Kutahya, Turkey.
[5] Department of Medical Biology and Genetics, Faculty of Medicine, Marmara University, Istanbul, Turkey
[6] Department of Pharmacology, Faculty of Pharmacy, Fenerbahce University, Istanbul, Turkey.
[7] Department of Biophysics, Faculty of Medicine, Marmara University, Istanbul, Turkey

Corresponding Author: Nurdan BULBUL AYCI
E-mail: nrdnblbl@gmail.com

Submitted: 25.08.2023 **Accepted:** 17.11.2023

ABSTRACT

Objective: The aim of this study was to reveal the effect of apocynin (APO) on the factors involved in obesity-related endothelial dysfunction (ED) and atherosclerosis (AS).

Materials and Methods: Male Wistar albino rats were divided into control (CNT), high-fat diet (HFD) and HFD+APO groups. HFD and HFD+APO groups were fed HFD for sixteen weeks. APO (25 mg/kg) was administered to the HFD+APO group for the last four weeks. The effects of APO on: AS-related metabolic parameters (triglyceride, total cholesterol, high-density lipoprotein-cholesterol, insulin and leptin), oxidative stress (OS), [malondialdehyde, glutathione, nicotinamide adenine dinucleotide phosphate (NADPH)-oxidase-2, oxidised-low-density lipoprotein (ox-LDL) and 8-hydroxy-2-deoxyguanosine], low-density lipoprotein and ox-LDL uptake potential (activin receptor-like kinase-1 and lectin-like oxidized low-density lipoprotein receptor-1, respectively), tissue inflammation (myeloperoxidase, monocyte-chemoattractant-protein-1, tumor necrosis factor-alpha), ED (endothelial-nitric oxide synthase, inducible-nitric oxide synthase, nitric oxide), programmed cell death (terminal deoxynucleotidyl-transferase-dUTP-nick-end labeling, cleaved-poly-ADP-ribose-polymerase, gasdermin-D N-terminal fragment, caspase-1), smooth muscle cell transformation (alpha-smooth muscle actin), histology and ultrastructure of thoracic aorta were evaluated.

Results: In obesity, APO had an ameliorative effect on metabolic parameters, OS, inflammation, ED, programmed cell death and ox-LDL uptake potential, but not on foam cell formation and LDL uptake potential.

Conclusion: Apocynin may improve ED and AS in obesity by suppressing OS-linked factors involved in the early stage of AS.

Keywords: Apocynin, Atherosclerosis, Endothelial dysfunction, Oxidative stress, Obesity, High-fat diet

1. INTRODUCTION

Obesity is a disease characterized by a chronic low-grade inflammation causing a vicious cycle consisting of insulin resistance, oxidative stress (OS) and endothelial dysfunction (ED). It forms the basis of early and accelerated atherosclerosis (AS) [1]. The nicotinamide adenine dinucleotide phosphate (NADPH) oxidase (NOX) enzyme family is one of the most prominent producers of reactive oxygen species (ROS), which has been linked to atherogenesis [2]. NOX-2 in the endothelial cells (EC) is a major producer of ROS, giving rise to ED which predisposes cardiovascular complications in obesity [3].

ED, defined as the deterioration of endothelium-dependent vasodilatation due to decreased nitric oxide (NO) bioactivity in the vessel wall [4], has been associated with AS, hypercholesterolemia [5] and obesity [6]. Obesity is closely linked to ED via the presence of ROS in addition to reduced NO production [4] and/or NO bioavailability leading to impaired vasodilatation. The main cause of the onset of ED is the reduced NO bioavailability that may be a result (i.) of decreased endothelial NO synthase (e-NOS) protein expression [5,7] and (ii.) increased inducible NOS (i-NOS) activity.

How to cite this article: Aycı Bulbul N, Ertas B, Kaya Keles R, et al. Apocynin exhibits an ameliorative effect on endothelial dysfunction / atherosclerosis-related factors in high-fat diet-induced obesity in rats. Marmara Med J 2024: 37(2):238-247. doi: 10.5472/marumj.1479796

ISSN: 1309-9469

http://doi.org/10.5472/marumj.1479796
Marmara Med J 2024;37(2): 238-247

Because, decreased e-NOS expression results in decreased NO production and increased i-NOS activity reduces NO bioavailability by causing peroxynitrite formation from NO and e-NOS uncoupling that lead to the production of superoxide instead of NO [7]. It has been shown that a high-fat diet (HFD) increases i-NOS expression and decreases e-NOS expression in the aorta [8].

Atherosclerosis is the fundamental pathophysiological process underlying cardiovascular diseases. It begins with the retention of low-density lipoprotein cholesterol (LDL-c) in the subendothelial space, followed by oxidative modification of LDL to oxidized-LDL (ox-LDL) [9]. Activin receptor like-kinase-1 (ALK-1) is a receptor that functions in the uptake and transcytosis of LDL into the cell [10]. Ox-LDL plays a key role in AS, mostly through the scavenger receptor lectin-like oxidised low density lipoprotein receptor-1 (LOX-1), which enables its uptake into the cells [11]. It has been demonstrated that AS is associated with increased LOX-1 activity and gene knock-out of LOX-1 lead to a reduction in atherogenesis in LDL receptor deficient mice fed with a high-cholesterol diet [12].

Apocynin (APO) is an acetophenone that has an ameliorating effect on cardiovascular disorders. It acts as an inhibitor of NOX-2, in addition, as an antioxidant and scavenger of non-radical oxidant species [13]. Previous studies have reported that APO decreases blood pressure, increases e-NOS activity and resulting NO levels in the aorta by elevating e-NOS expression in spontaneously hypertensive rats [14]; decreases i-NOS expression in the aorta of diabetic rats [15] and descends the progression of AS in apoE-deficient mice [2].

Apocynin may ameliorate ED and AS in a wild – type obesity animal model through its anti-inflammatory and antioxidant effects. To address this issue, this study aimed to reveal the effect of APO on the factors involved in the development of ED and subsequent AS as a result of OS associated with HFD-induced obesity in wild – type rats. Meanwhile, this is the first study in the literature to address ALK-1 involvement regarding LDL uptake, and the effect of APO on pyroptosis in HFD-induced obesity-related ED/AS.

2. MATERIALS and METHODS

Animals and Experimental Design for an Obesity Model

Twenty-one adult male Wistar albino rats (aged two months, 250-300g) obtained from the Marmara University Experimental Animal Implementation and Research Center (DEHAMER), were used for this study. The animals were randomly assigned to three groups (7 animals per group). Standard control (CNT) group was fed with a standard laboratory chow (6% fat, 24% protein,70% carbohydrate) diet while HFD and HFD+APO groups were fed with HFD (45% saturated fat, 20% protein, 35% carbohydrate) for 16 weeks to obtain an obesity model. All animals were kept in 12/12 hours light/dark conditions. Access to water for the animals was ad libitum. Based on previous studies, solvent [16], APO administration method, dosage [16-18] and timing [19] were determined. APO (TRC, Toronto, Canada, 25 mg/kg dose dissolved in 8% dimethyl sulfoxide) and vehicle dimethyl sulfoxide were administered by orogastric gavage to the HFD+APO and HFD groups, respectively, five days a week for the last four weeks. Since, it has been shown in previous studies that the administration of APO (at the dose applied and above) alone to the standard control group does not have a significant effect on the tissues [16, 20, 21], we excluded the use of APO treated standard control group in this study to avoid unnecessary animal sacrifice. The rats were weighed once a week. The applied animal design was approved by the Marmara University Local Ethical Committee for Experimental Animals (07.05.2018-50.2018.mar). None of the rats died during the 6-week study. Finally, after 12 hours fasting by removal of chow, the rats were decapitated under light ether anaesthesia, then trunk blood and thoracic aorta tissue samples were collected. All the experiments and analyses were performed in blinded study groups by investigators.

Biochemical Analysis

The collected thoracic aorta tissue samples and serum were biochemically analysed by the ELISA method using commercial ELISA kits. The blood samples were centrifuged at 15000 rpm for 15-20 minutes. The aorta tissue samples were homogenized as 10% homogenates in phosphate buffered saline (PBS) solution (pH: 7.4). The homogenates were centrifuged at 15000 rpm for 15 minutes and supernatants were collected. Leptin (E-EL-M0039, Elabscience Biotechnology, Houston, USA), insulin, total cholesterol (TC), triglyceride (TG) and high-density lipoprotein cholesterol (HDL-c) (YLA0037RA, YLA0388RA, YLA0770RA and YLA0444RA, respectively, YL Biont, Shanghai, China) levels were measured in the serum. Malondialdehyde (MDA), glutathione (GSH) (MBS728071 and MBS265966, respectively, MyBioSource, San Diego, USA), tumor necrosis factor-alpha (TNF-α), monocyte-chemoattractant-protein-1 (MCP-1), ox-LDL (E0764RA, E0193RA and E0699RA, respectively, BTLab, Shanghai, China), NO (ADI-917-020, Enzo Life Sciences, Lausen, Switzerland), 8-hydroxy-2-deoxyguanosine (8-OHdG) levels and, myeloperoxidase (MPO) activity (SL2044Hu and SL1230Hu, respectively, Sunlong Biotech, Hangzhou, China) were measured in aorta tissue homogenates.

All procedures applied in the ELISA method were performed according to the manufacturer's instructions. Metabolic disorders caused by HFD were assessed by serum TG, TC, HDL-c, insulin and leptin levels. Lipid peroxidation and antioxidant capacity in the aorta were assessed by MDA and GSH levels, respectively. Inflammation was assessed by MPO activity, MCP-1 and TNF-α levels. Oxidative damage was assessed by ox-LDL and 8-OHdG (a marker for oxidative DNA damage) levels. Endothelial function was assessed by NO levels.

Histological Analysis

The aorta tissues were fixed in 10% formalin for 24 hours and routinely processed for light microscopic examination. Processed tissues were embedded and blocked in paraffin wax. Approximately, 4-µm thick paraffin sections were stained with haematoxylin-eosin (HE) and Verhoeff–Van Gieson stain. Stained aorta sections were observed under a light microscope

http://doi.org/10.5472/marumj.1479796
Marmara Med J 2024;37(2): 238-247

(Olympus BX51, Tokyo, Japan) and photographed. Medial elastic fiber degeneration (MEFD) and medial extracellular matrix accumulation (MEMA) were scored from 0 to 3 (0: none, 1: mild, 2: moderate and 3: severe). Smooth muscle cell nucleus (SMCN) number in the tunica media area was counted for each sample and expressed as SMCN / area (mm^2). Tunica intima + tunica media thickness (IMT) was measured in equally spaced 15 randomized parts of each specimen slide using Image J-Fiji 1.53c Software. Mean of measurements was evaluated as IMT value. Histopathological analyses were scored by two investigators blinded to the groups and the investigators' assessments concurred.

Immunohistochemical Analysis

Immunohistochemical staining was performed according to a previous protocol [16]. Assessed primary antibodies (all incubated at 4 °C) were: (i) NOX-2 as a marker of oxidative stress (1:200, bs-3889R, Bioss Antibodies, Woburn, Massachusetts, USA), (ii) e-NOS, (iii.) i-NOS as markers of ED (1:300 and 1:50, NB300-500 and NB300-605, Novus Biologicals, Centennial, USA), (iv) LOX-1 as a marker of ox-LDL uptake (1:200, BS-2044R, Bioss Antibodies) and (v) α-SMA as a marker of foam cell formation potential (1:2000, ab7817, Abcam, Cambridge, UK). Randomized five parts of each field were evaluated to calculate the density of immunoreactivity (ir), and density was expressed as the ratio of the DAB-stained area to the total related vessel wall area (%). To detect DNA strand breaks resulting in programmed cell death, terminal deoxynucleotidyl transferase-mediated dUTP nick-end labelling (TUNEL) method was performed using a commercial kit (EMD-Millipore, Darmstadt, Germany) according to the manufacturer's protocol. To evaluate TUNEL staining in tunica media, positive vascular smooth muscle cell (VSMC) nuclei were counted per 5 optical field (40× objective) at random locations in the vessel wall of the sections of each rat. TUNEL positive cell index was calculated by dividing the total number of TUNEL positive cell nuclei to the total cell nuclei number in the counted areas.

Transmission Electron Microscopy

Approximately 3 mm^3 pieces of aorta samples were fixed with 2.5% glutaraldehyde in PBS (pH 7.2, 0.1 M) for 12 hours at 4 °C. Then, the samples were post-fixed in 1% osmium tetroxide in PBS and dehydrated by passing through an ascending series of alcohols. Dehydrated samples were cleared in propylene oxide and embedded in Epon 812 (45359, Sigma–Aldrich Chemical, Schaffhausen, Switzerland).1-µm semi-thin sections were stained with toluidine blue. Ultrathin sections (60-80 nm-thick) were contrasted using uranyl acetate and lead citrate then were observed using a JEOL 120 EXII transmission electron microscope (Tokyo, Japan).

Western Blot Analyses

Tissue samples from the aorta were homogenized in 1x Radioimmunoprecipitation assay buffer (50 mM Tris–HCl, pH 8.0, 150 mM NaCl, 1% NP40, 0.5% Na-deoxycholate, 0.1% SDS) containing protease inhibitor cocktail (Complete, EDTA-free Protease Inhibitor Cocktail Tablets, Roche, Rotkreuz, Switzerland) using homogenizer. The tissue homogenates were centrifuged at 14,000 g for 15 min and the supernatant was collected. Total protein amounts were quantified using Take3™ Multi-Volume Plate (BioTek Instruments Inc., Vermont, USA). Proteins of 30 µg were separated by 10% SDS-PAGE electrophoresis and transferred to the nitrocellulose membranes. Membranes were incubated with primary and secondary antibodies. Primary antibodies used in this study were Beta-actin, i-NOS, e-NOS, cleaved-poly-ADP-ribose-polymerase (c-PARP) as a marker of apoptosis (1:500, 1:400, 1:500 and 1:500, NB600-501, NB300-605, NB300-500, and NBP2-27335; respectively, Novus Biologicals), caspase-1 and GSDMDC1 as markers of pyroptosis (1:200, sc-56036 and sc-393581; Santa Cruz Biotechnology, Dallas, USA) and ALK-1 as a marker of LDL uptake (1:200, sc-101556; Santa Cruz Biotechnology). All antibodies were HRP-conjugated. The bands were visualized using chemiluminescent HRP substrates (Western Bright ECL-Advansta, K-12045-050). Quantification was performed using Chemiluminescence Imaging System (Celvin S, BioStep, Burkhardtsdorf, Germany).

Ribonucleic Acid Isolation and Quantitative Real-Time Polymerase Chain Reaction Analysis

Ribonucleic acid (RNA) was isolated from fresh frozen tissues with PureLink™ RNA Mini Kit (12183018A, Thermo Fisher Scientific, Waltham, USA) according to the manufacturer's instructions. All RNA lysates were stored at – 80 °C until use. High-Capacity cDNA Reverse Transcription kit (4368814, Thermo Fisher Scientific) was used for cDNA synthesis in a reaction volume of 20 µL. Taqman expression assays (4453320, Thermo Fisher Scientific) were used for gene expression analysis. Quantitative real-time polymerase chain reaction (qRT-PCR) was performed in 20 µL of final reaction volume according to manufacturer's recommendations for cycling conditions. All reactions were performed in duplicate for reference housekeeping gene beta actin, oxidized low-density lipoprotein receptor1 (OLR1), activin receptor like kinase 1 (ACVRL1) and nitric oxide synthase 3 (NOS3) by using Light Cycler 480 instrument (Roche, Roche Diagnostics International AG, Rotkreuz, Switzerland). Relative expression was quantified by delta-delta Ct method after normalization of target gene expressions relative to the house keeping gene expression.

Statistical Analyses

Graph-Pad Prism 8.0.1 (GraphPad Software, San Diego, USA) program was used for statistical analysis. One-Way ANOVA method and post – hoc Tukey test for multiple comparisons were used for all statistical analyses. $P < 0.05$ was considered significant. All data are expressed as the mean ± standard error of the mean (SEM).

http://doi.org/10.5472/marumj.1479796
Marmara Med J 2024;37(2): 238-247

3. RESULTS

Body Weight Gain

At the end of the 16-week period, animals in the HFD group had increased (P < 0.0001) body weight gain compared to the CNT group. When the two groups fed a high-fat diet were compared within themselves, weight gain was less (P < 0.0001) in the APO-administered group (Figure 1a).

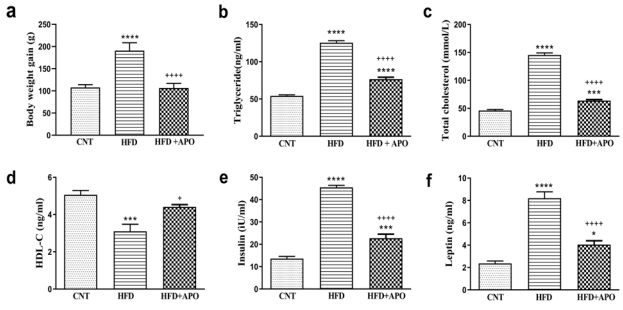

Figure 1. *The effect of HFD and APO on body weight gain and serum fasting metabolic parameters. *P < 0.05, ***P < 0.001 and ****P < 0.0001 vs CNT group, ⁺P < 0.05 and ⁺⁺⁺⁺P < 0.0001 vs HFD group. All data were expressed as mean ± SEM (n=7).*

Biochemical Serum Analysis

Serum TG and TC levels were increased significantly in the HFD (P < 0.0001 for both) and the HFD+APO (P < 0.0001 for TG and P < 0.001 for TC) groups while serum HDL-c levels were decreased significantly in the HFD group (P < 0.001) compared to the CNT group. APO decreased TG and TC levels but increased HDL-c levels significantly (P < 0.0001 for TG and TC, P < 0.05 for HDL-c) compared to the HFD group (Figure 1b-1d).

Serum insulin and leptin levels were increased significantly in the HFD (P < 0.0001 for both) and HFD+APO groups (P < 0.001 for insulin and P < 0.05 for leptin) compared to the control group. APO administration decreased both insulin and leptin levels significantly (P < 0.0001 for both) compared to the HFD group (Figure 1e and 1f).

Biochemical Tissue Analysis

In the HFD group, aortic MDA levels increased significantly compared to the CNT group (P < 0.001) while the APO had significantly decreased MDA levels compared to the HFD group (P < 0.0001, Figure 2a). In the HFD group, GSH levels decreased significantly compared to CNT group (P < 0.0001) while APO significantly increased GSH levels compared to the HFD group (P < 0.0001, Figure 2b). In the HFD group, MPO activity (P < 0.0001), MCP-1 (P < 0.01) and TNF-α (P < 0.01) levels increased significantly compared to the CNT group. APO significantly decreased MPO activity (P < 0.0001), MCP-1 (P < 0.05) and TNF-α (P < 0.01) levels compared to the HFD group (Figure 2c-2e). In the HFD group, ox-LDL (P < 0.001) and 8-OHdG (P < 0.05) levels increased significantly compared to the CNT group. APO significantly decreased 8-OHdG levels compared to the HFD group (P < 0.05, Figure 2g). In the HFD group, NO levels decreased significantly compared to the CNT group (P < 0.0001). In the HFD+APO group, NO levels increased significantly compared to the HFD group (P < 0.0001, Figure 2h).

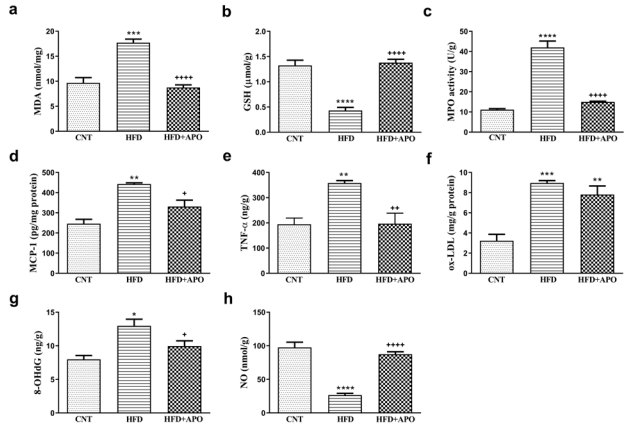

Figure 2. *The effect of HFD and APO on (a) MDA, (b) GSH, (c) MPO activity, (d) ox-LDL, (e) 8-OHdG, (f) MCP-1, (g) TNF-α and (h) NO levels in aorta tissue. *P < 0.05, **P < 0.01, ***P < 0.001 and ****P < 0.0001 vs CNT group, ⁺P < 0.05, ⁺⁺P < 0.01 and ⁺⁺⁺⁺P < 0.0001 vs HFD group. All data were expressed as mean ± SEM (n=7)*

Aorta Histology

Staining with HE demonstrated the structure of both the elastic lamina and the cellular density of tunica media. The CNT group had a smooth alignment of endothelium and elastic lamina (Figure 3a). The HFD group displayed prominent disintegration of elastic lamina (expressed as MEFD), accumulation of mucoid extracellular matrix (expressed as MEMA) and foam cells (Figure 3b). Treatment with APO ameliorated elastic lamina alignment and reduced MEMA (Figure 3c). Verhoeff–Van Gieson staining displayed the elastic lamina which was regularly structured in the CNT group (Figure 3d) and disintegrated in the HFD group (Figure 3e), but in the HFD+APO group the elastic lamina showed nearly regular morphology (Figure 3f). Toluidine blue stained sections displayed both elastic lamina and media structure; in the CNT group, elastic lamina aligned regularly (Figure 3g) whereas in the HFD group the medial layer showed disintegrated and expanded morphology besides in some regions the cellularity was reduced (Figure 3h). On the other hand, the HFD+APO group demonstrated regeneration in the elastic lamina and reduction of the space between the lamina besides the regular cellularity (Figure 3ı).

Medial elastic fiber disintegration and MEMA were increased in both the HFD (P < 0.0001 for both) and the HFD+APO (P < 0.01 and P < 0.0001, respectively) groups significantly , compared to the

http://doi.org/10.5472/marumj.1479796
Marmara Med J 2024;37(2): 238-247

CNT group. APO decreased MEFD ($P < 0.01$) and MEMA ($P < 0.001$) levels significantly compared to the HFD group (Figure 3j and 3k). The value of SMCN/Area (mm^2) indicating cellular loss, significantly decreased in the HFD group compared to the CNT group ($P < 0.01$). APO reversed this reduction close to CNT values ($P < 0.05$, Figure 3l). IMT increased in both HFD and HFD+APO groups, but it was not statistically significant (Figure 3m).

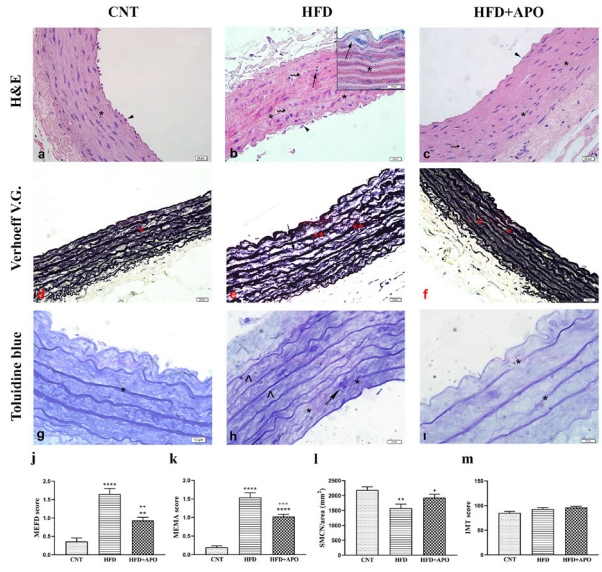

Figure 3. *Representative photomicrographs of HE (a-c), Verhoeff Van Gieson (d-f) and Toluidine blue (g-ı) – stained aorta tissue. ▶: endothelium; →: (b) foam cell formation, (e) impairment of elastic lamina, (h) twisted smooth muscle cell nucleus; broken arrows: mucoid extracellular matrix, ∗: elastic lamina; ∗∗: thickness in elastic lamina; Λ: reduction in cellularity of smooth muscle cells. Histopathological score for the (j) MEFD, (k) MEMA, (l) SMCN/area (mm2) and (m) IMT. **P < 0.01 and ****P < 0.0001 vs CNT group, $^{+}P < 0.05$ $^{++}P < 0.01$, $^{+++}P < 0.001$ and $^{++++}P < 0.0001$ vs HFD group. All data were expressed as mean ± SEM (n=7). Scale bar: a-f: 20 µm; g-ı: 10µm, insert: 10µm.*

Immunohistochemistry Assays

Compared to the CNT group, TUNEL positivity ($P < 0.0001$, Figure $4a_2$ and $4a_4$), i-NOS-ir levels ($P < 0.01$, Figure $4c_2$ and $4c_4$), LOX-1-ir levels ($P < 0.0001$, Figure $4e_2$ and $4e_4$) and NOX-2-ir levels ($P < 0.01$, Figure $4f_2$ and $4f_4$) were significantly higher while e-NOS-ir levels ($P < 0.001$, Figure $4b_2$ and $4b_4$) were significantly lower in the HFD group. APO treatment reversed these levels [($P < 0.001$ for TUNEL positivity, Figure $4a_3$ and $4a_4$), ($P < 0.01$ for i-NOS-ir, Figure $4c_3$ and $4c_4$), ($P < 0.0001$ for LOX-1-ir Figure $4e_3$ and $4e_4$), ($P < 0.01$ for NOX-2-ir, Figure $4f_3$ and $4f_4$) and ($P < 0.001$ for e-NOS-ir Figure $4b_3$ and $4b_4$)] compared to the HFD group. α-SMA-ir levels were decreased in the HFD group compared to the CNT group and increased in the HFD+APO group compared to the HFD group. But the differences among the groups were not statistically significant (Figure $4d_1$-$4d_4$).

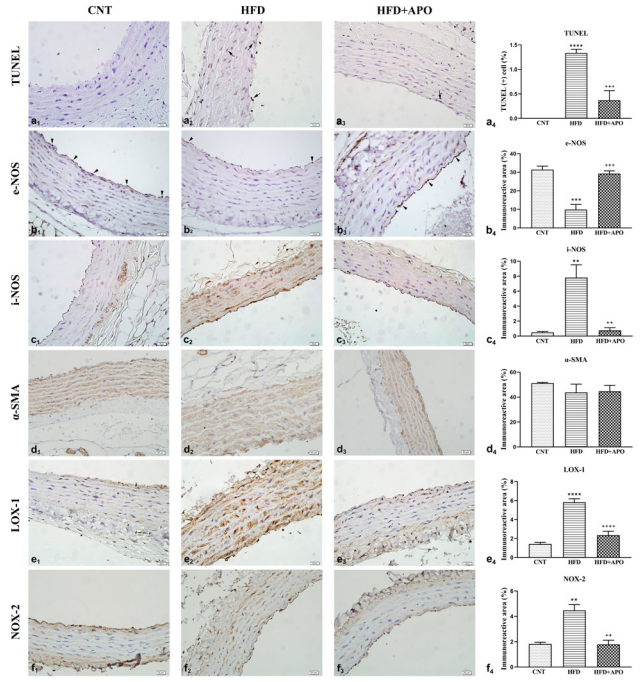

Figure 4. *Representative photomicrographs of immunohistochemically stained aorta tissue and corresponding graphs of immunoreactive area levels. **P < 0.01, ***P < 0.001 and ****P < 0.0001 vs CNT group, $^{++}P < 0.01$, $^{+++}P < 0.001$ and $^{++++}P < 0.0001$ vs HFD group. All data were expressed as mean ± SEM (n=7). Scale bar: 20 µm.*

Transmission Electron Microscopy

In CNT group, regularly arranged elastic lamina and in addition to local collagen fibers were observed (Figure 5a) while in HFD group, elastic lamina deteriorated and there was an increase in collagen between them (Figure 5b). In the HFD+APO group, improved appearance of elastic lamina and a decrease in collagen fiber density were observed (Figure 5c).

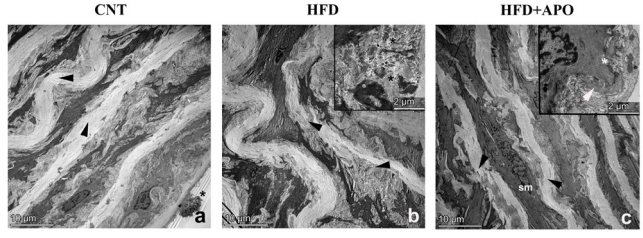

Figure 5. *Representative electron micrographs of aorta tissue. ▶: (a,c) Regular elastic lamina, (b) irregular elastic lamina; ∗ : (a) endothelial cell, (b-inset) increased and disorganized collagen fibers, (c) reduced density of collagen fibers, Sm: smooth muscle cell. Scale bar: 10 µm; insert: 2 µm*

Western Blot Analysis

The levels of c-PARP ($P < 0.01$), caspase-1 p10 ($P < 0.0001$) and GSDMD-N ($P < 0.01$) increased significantly in the HFD

http://doi.org/10.5472/marumj.1479796
Marmara Med J 2024;37(2): 238-247

group compared to the CNT group, while APO reversed these levels compared to the HFD group (P < 0.01, P < 0.0001 and P < 0.05, respectively, Figure 6a-6c). The level of e-NOS (P < 0.05) decreased while the level of i-NOS (P < 0.01) increased in the HFD group compared to the CNT group, and APO reversed both levels (P < 0.05, Figure 6d and 6e) compared to the HFD group. The level of ALK-1 increased in the HFD group compared to the CNT group and reversed in the HFD+APO group, but the difference between groups was not statistically significant (Figure 6f).

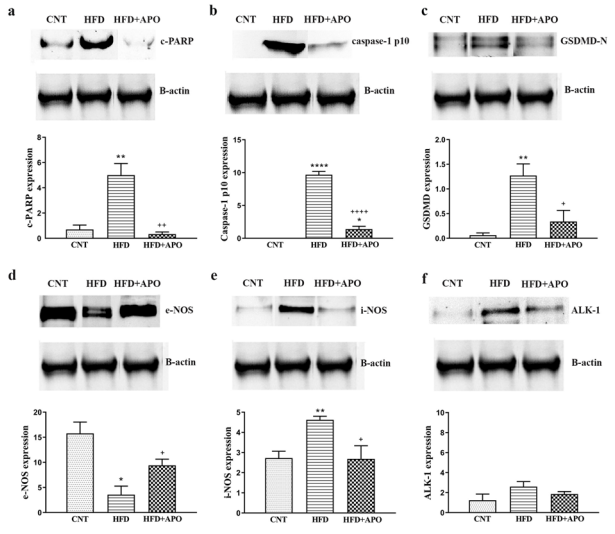

Figure 6. *Representative immunoblot images and the protein expression levels in aorta tissue. The expression levels of each band were determined using scanning densitometry and normalized to beta-actin. *P < 0.05, **P < 0.01 and ****P < 0.0001 vs CNT group, ⁺P < 0.05 ⁺⁺P < 0.01 and ⁺⁺⁺⁺P < 0.0001 vs HFD group. All data were expressed as mean ± SEM (n=7).*

qRT-PCR Analysis

The differences in mRNA expression levels of NOS-3 (e-NOS) and ACVRL1 (ALK-1) genes between groups were not statistically significant while only mRNA expression level of OLR1 (LOX-1) gene was statistically significant in the HFD+APO group compared to the HFD group (P < 0.05, Table I).

Table I. *Gene expression levels in aorta tissue.*

	CNT Group	HFD Group	HFD+APO Group
NOS3	0,9939 ± 0.3	1.197 ± 0.6	0.2593 ± 0.03
ACVRL1	1.584 ± 0.6	1.630 ± 0.4	2.388 ± 0.5
OLR1	1.772 ± 0.5	0.6144 ± 0.1	2.908 ± 0.7 *

*NOS3: Nitric oxide synthase 3, ACVRL1: Activin receptor-like kinase 1, OLR1: Oxidized low-density lipoprotein receptor 1, CNT: Standard control group, HFD: High-fat diet group, HFD+APO: High-fat diet+Apocynin group. *P < 0.05 vs HFD group. Results were expressed as fold change compared to control. All data were expressed as mean ± SEM (n=7).*

4. DISCUSSSION

Our study demonstrated that treatment of obese rats with APO for 4 weeks restored weight gain and parameters relevant to metabolic disturbance (TG, TC, HDL-c, insulin, leptin), OS (NOX-2, MDA, GSH, 8-OHdG), ED (NO, e-NOS, i-NOS), inflammation (MPO, MCP-1, TNF-α), programmed cell death (TUNEL, c-PARP, caspase-1, GSDMD-N), histologic damage and cellular ox-LDL uptake (LOX-1) which occurs in atherogenesis.

Apocynin is a natural inhibitor of the NOX-2 enzyme which is the main isoform of NOX family members up-regulated in obesity and HFD-induced vascular OS [3]. It limits the progression of AS in mice by NOX inhibition after the disease developed [22]. A previous study demonstrated a link between HFD-induced NOX-2 activity and weight gain, and administration of APO resulted in less weight gain [3]. Similar to these results, the weight gain levels in our study showed that APO significantly decreased the increased weight gain in the HFD group. Also, this decrease was paralleled by the significant decrease of NOX-2 expression, which implies oxidative stress, with APO administration in our study.

In obesity, hyperlipidaemia, a cardiovascular risk factor characterized by high TC, high TG and reduced HDL-c levels, is considered to be responsible for atherogenesis emergence [23]. In our obesity model, high fat consumption resulted in higher TC, higher TG and lower HDL-c levels in serum similar to previous studies [3, 4, 8] and APO reversed these levels similar to a previous study [24]. But our TC result did not support Gamez-Mendez's study, which showed that there was no significant difference via APO administration [4]. This difference may be caused by the use of different animal strains and dosage of APO from those used in our study.

Excess adiposity results in chronic hyperinsulinemia which occurs in atherogenesis by increasing growth and proliferation of VSMCs, monocyte/macrophage recruitment to endothelium, ROS production and inflammation, transport of LDL cholesterol into VSMCs and causing hypertension, especially ED [25]. In this study, as a result of HFD, hyperinsulinemia developed in HFD-fed rats in parallel with increased adiposity. APO reversed hyperinsulinemia similar to previous studies [3, 26]. These results indicate that APO may contribute to the suppression of ED/AS by reducing hyperinsulinemia in obesity.

In obesity, leptin is responsible for the relationship between ED and obesity, as it acts on the regulation of vascular tone / NO production and associated with proinflammatory mechanisms and ROS production leading to ED [4]. In addition, it stimulates ECs, leading to adhesion of monocytes and their migration from blood into tissue [27]. In the present study, we observed hyperleptinemia in HFD group and APO reversed this effect, similar to a previous report [4], indicating that APO may exhibit its ED-improving and AS-suppressive effects by reducing hyperleptinemia.

A high saturated fat diet over a long period of time functions as a stimulator of OS that is responsible for organ pathophysiology [28]. In our study, in addition to increased NOX-2 level, the other

http://doi.org/10.5472/marumj.1479796
Marmara Med J 2024;37(2): 238-247

OS markers: increased MDA, decreased GSH and increased 8-OHdG levels in the HFD group were significantly reversed by APO, indicating its suppressor effect on OS, similar to previous studies [16, 26, 29, 30].

In this study the results showed that (i.) MPO activity levels, (ii.) proinflammatory TNF-α, which participates in AS via stimulating superoxide production by NOX in ECs and VSMCs [31], and (iii.) MCP-1, which has a key role in monocyte/macrophage infiltration into vessel wall in the initial stage of AS [32], levels were increased along with ox-LDL levels in obese rats. But APO reversed TNF-α and MCP-1 levels as reported in previous studies [2, 33] and to our knowledge this is the first study demonstrating the impact of APO on ED/AS in HFD-induced obesity and MPO link. It is inferred from these results that APO has a limiting effect on AS by suppressing monocyte involvement and subsequent proinflammatory cytokine production, which contributes to the progression of AS.

Obesity leads to ED via increased ROS production by NOX-2 which causes a depletion on vasoprotective NO levels [3]. NO is the key regulator of vasodilatation. It has several antiatherogenic effects acting to inhibit platelet adhesion and aggregation, decrease leukocyte adhesion to endothelium and migration into vessel, VSMC proliferation [34, 35] and inhibit proinflammatory cytokine /chemokine expression [5]. Under physiological conditions, it is generated by e-NOS. But, in pathological circumstances such as OS and inflammation, it is generated by i-NOS in excessive amounts, disturbing endothelium-dependent vasodilatation. i-NOS decreases e-NOS activity by competing with it for its cofactor [34]. Continuous NO production by i-NOS may also impair signal cascades linking endothelial receptors to e-NOS activation [35]. ED can also be a result of decreased e-NOS expression and/or e-NOS activity [5]. As described in previous reports, ED is marked with NO decrement [4, 8], e-NOS expression reduction [36] and i-NOS expression induction [8] and can be reversed by perfusion of APO in obese subjects [37]. In our study, impaired endothelial function parameters were reversed by APO as in previous studies, demonstrating elevated NO levels [4, 14] and e-NOS expression [14] in addition to lowered i-NOS expression [15], indicating that APO in this study may supress ED.

Progression of atherogenesis occurs through the response of inflammatory cells to native and modified lipids accumulating in the subendothelial region [38]. In addition, ox-LDL formation by ROS has an atherogenic effect via inducing foam cell formation and accumulation of adhesion molecules, ox-LDL, neutrophils and monocytes in the vessel lumen that result in atherogenic plaque and cell death [39]. Besides, oxidation of LDL may be carried out by MPO in the endothelium [38]. So, resulting ox-LDL increases NOX activity and decreases e-NOS activity in the vessel [7]. LOX-1 which is a scavenger receptor present in ECs, VSMCs, platelets, macrophages and fibroblasts, participates in ED and AS via mediating ox-LDL uptake into the cells. Obesity induces LOX-1 expression. In the pathogenesis of AS, monocyte adhesion to activated ECs occurs. Monocytes in the subendothelial space transform into macrophages, internalize modified lipids such as ox-LDL and form foam cells. VSMCs migrate into the subendothelial space and proliferate there, then synthesize collagen. Foam cells, VSMCs and deposited collagen form atherosclerotic plaque. Ox-LDL binding to elevated LOX-1 results in several atherogenic and/or proinflammatory effects in the vessel wall that promote this pathogenesis. Namely, it increases (i.) LOX-1 expression and ox-LDL uptake by ECs and VSMCs, resulting foam cell formation, (ii.) proinflammatory cytokine expression such as TNF-α and MCP-1, hence monocyte attachment to ECs, (iii.) NOX-2 and NOX-4 expression, hence ROS production and OS, besides (iv.) collagen synthesis, (v.) apoptosis, (vi.) VSMC migration and proliferation. On the other hand, it decreases e-NOS activity/expression and endothelial NO level [40]. In our study it was observed an increase of oxidative and inflammatory parameters and changes in NO metabolism in the HFD group, however NOX-2 inhibitor apocynin treatment reversed all these parameters except ox-LDL to the control levels by regulating the oxidant/antioxidant balance.

Antioxidants have been reported to be inhibitors of LDL oxidation [39]. In this study, as an antioxidant agent, APO decreased the markedly alleviated LOX-1 protein expression levels. But, in contrast, gene expression levels were lower in the HFD group (statistically not significant) compared with the CNT group and were significantly higher in the HFD+APO group. This may because of that high LOX-1 protein expression levels in the HFD group, increased with alleviating OS, may induce a negative feedback mechanism on LOX-1 gene expression. Hence, it may result in a decrease in gene expression. But APO by means of its strong antioxidant effect may suppress OS and prevent related LOX-1 protein expression levels from reaching the similar levels as in the HFD group. Since LOX-1 protein level was low in the HFD+APO group, the negative feedback mechanism was not activated, and LOX-1 gene expression levels may have remained high for a longer period in the HFD+APO group.

The initiation of AS is believed to occur from retention and accumulation of cholesterol-rich particles, especially LDL-c, in the subendothelial space. ALK-1 can function as a binding protein for uptake and transcytosis of LDL-c throughout vascular endothelium [10, 41]. LDL-c is not degraded when taken into cells via ALK-1 [38]. It has been demonstrated that ALK-1 activity alleviated in atherosclerotic vessel, and it is thought to have a role in VSMC proliferation in AS [41]. For the first time, this study investigated the difference in ALK-1 expression in obesity to assess LDL uptake. ALK-1 protein and mRNA expression did not differ significantly between the groups. This result may be related to the fact that increased LDL concentration in athero-prone areas in the vessel wall is caused by increased LDL retention rather than increased uptake of LDL [38].

Foam cell formation is a hallmark of AS. It may be generated from both macrophages and VSMCs [42]. Over a high cholesterol loading, VSMCs undergo dedifferentiation and downregulate some genes that is specific for contractile phenotype including α-SMA to switch to secretory phenotype in atherosclerotic lesions [43]. In our study, HFD and APO did not affect the α-SMA protein expression significantly. We demonstrated the

http://doi.org/10.5472/marumj.1479796
Marmara Med J 2024;37(2): 238-247

presence of lipid loaden foam cell formation by VSMCs in media layer in HE stained sections. But it is concluded from α-SMA results that HFD consumption has not yet caused a phenotypic transition in VSMCs that will participate in plaque formation in the intima.

High levels of cholesterol, ox-LDL, TNF-α and ROS act as inducers of apoptosis and pyroptosis in many stages of AS. In the early stage of AS, apoptosis and pyroptosis in ECs lead to loss of endothelial function and integrity, resulting in increased permeability for lipid and monocyte which will form foam cells [44, 45]. In the progressing stages of AS, apoptosis and pyroptosis in EC, VSMCs and macrophages participate in destabilization of atheromatous plaque and thrombosis formation [44, 46]. As reported in previous studies [13, 47,48], in our study, we demonstrated the suppressor effect of APO on apoptosis marked with reduced c-PARP protein levels, which indicates apoptotic caspase-3 activity, in addition to TUNEL positivity, and on pyroptosis marked with reduced caspase-1 and GSDMD-N protein levels in addition to TUNEL positivity. Besides, TUNEL positivity was overt especially in ECs and VSMCs supporting a previous report for pyroptosis [49]. The simultaneous increase in TUNEL positivity of tunica media, ox-LDL and LOX-1 expression levels in our study supported the fact that high levels of ox-LDL cause an increment in apoptosis of VSMCs through LOX-1 [50].

Histopathologic and ultrastructural evaluations revealed a correlation with other results demonstrating metabolic disturbance and presence of factors leading to atherosclerosis. In the HFD group, we examined disintegration/disorganization in elastic lamina, VSMC nuclei loss, foam cell formation, expanded elastic lamella, twisted SMCN, mucoid extracellular matrix accumulation and increase/ disorganization of collagen fibers. APO administration significantly regressed these results, demonstrating a suppressor effect of APO on HFD-induced vessel pathology at an aorta tissue basis.

Conclusion

It is probable that APO demonstrates its improving effect on HFD-induced obesity linked ED/AS-related factors by acting on OS, programmed cell death, ox-LDL uptake and inflammation mechanisms.

Acknowledgement

We thank Marmara University Scientific Research Project Commission (SAG-C-DRP-080.519.0182) for financial support and Naziye OZKAN YENAL for her support in histologic staining techniques.

Compliance with the Ethical Standards

Ethics Committee approval: This study was approved by the Marmara University, Local Ethical Committee for Experimental Animals (Protocol Number: 50.2018.mar, Approval Date: 07.05.2018).

Conflicts of interest: Authors declare no conflict of interest.

Funding: This study was financially supported by Marmara University Scientific Research Project Commission (SAG-C-DRP-080.519.0182).

Authors' Contributions: NBA, FE, GS and SC: Contributed to the conception and design, NBA, BE, RKK, SKS, GGA, FE, GS, OO and SC: Performed the experiments, NBA, BE, RKK, SKS and GGA: Did data collection, NBA, BE, RKK, SKS, GGA, GS, OO, MA and SC: Analyzed data, NBA. and SC: Contributed to writing the article. All authors approved the final version of the article.

REFERENCES

[1] Pastore I, Bolla AM, Montefusco L, et al. The Impact of Diabetes Mellitus on Cardiovascular Risk Onset in Children and Adolescents. Int J Mol Sci 2020; 21:4928-45. doi: 10.3390/ijms21144928.

[2] Kinoshita H, Matsumura T, Ishii N, et al. Apocynin suppresses the progression of atherosclerosis in apoE-deficient mice by inactivation of macrophages. Biochem Biophys Res Commun. 2013; 431:124-30. doi: 10.1016/j.bbrc.2013.01.014.

[3] Du J, Fan LM, Mai A, Li JM. Crucial roles of Nox2-derived oxidative stress in deteriorating the function of insulin receptors and endothelium in dietary obesity of middle-aged mice. Br J Pharmacol 2013; 170:1064-77. doi: 10.1111/bph.12336.

[4] Gamez-Mendez AM, Vargas-Robles H, Ríos A, Escalante B. Oxidative Stress-Dependent Coronary Endothelial Dysfunction in Obese Mice. PLoS One 2015;10m: e0138609. doi: 10.1371/journal.pone.0138609.

[5] Incalza MA, D'Oria R, Natalicchio A, Perrini S, Laviola L, Giorgino F. Oxidative stress and reactive oxygen species in endothelial dysfunction associated with cardiovascular and metabolic diseases. Vascul Pharmacol 2018; 100:1-19. doi: 10.1016/j.vph.2017.05.005.

[6] Lozano I, Van der Werf R, Bietiger W, et al. High-fructose and high-fat diet-induced disorders in rats: impact on diabetes risk, hepatic and vascular complications. Nutr Metab (Lond) 2016; 13:15-28. doi: 10.1186/s12986.016.0074-1.

[7] Kattoor AJ, Pothineni NVK, Palagiri D, Mehta JL. Oxidative Stress in Atherosclerosis. Curr Atheroscler Rep 2017;19: 42-53. doi: 10.1007/s11883.017.0678-6.

[8] Yang S, Liu L, Meng L, Hu X. Capsaicin is beneficial to hyperlipidemia, oxidative stress, endothelial dysfunction, and atherosclerosis in Guinea pigs fed on a high-fat diet. Chem Biol Interact 2019; 297:1-7. doi: 10.1016/j.cbi.2018.10.006.

[9] Hartley A, Haskard D, Khamis R. Oxidized LDL and anti-oxidized LDL antibodies in atherosclerosis – Novel insights and future directions in diagnosis and therapy. Trends Cardiovasc Med 2019;29: 22-26. doi: 10.1016/j.tcm.2018.05.010.

[10] Tao B, Kraehling JR, Ghaffari S, et al. BMP-9 and LDL crosstalk regulates ALK-1 endocytosis and LDL transcytosis in endothelial cells. J Biol Chem 2020; 295:18179-18188. doi: 10.1074/jbc.RA120.015680.

[11] Lund AK, Lucero J, Harman M, et al. The oxidized low-density lipoprotein receptor mediates vascular effects of inhaled

vehicle emissions. Am J Respir Crit Care Med 2011; 184:82-91. doi: 10.1164/rccm.201.012.1967OC.

[12] Mehta JL, Sanada N, Hu CP, et al. Deletion of LOX-1 reduces atherogenesis in LDLR knockout mice fed high cholesterol diet. Circ Res. 2007; 100:1634-42. doi: 10.1161/CIRCRESAHA.107.149724.

[13] Savla SR, Laddha AP, Kulkarni YA. Pharmacology of apocynin: a natural acetophenone. Drug Metab Rev 2021; 53:542-562. doi: 10.1080/03602.532.2021.1895203.

[14] Perassa LA, Graton ME, Potje SR, et al. Apocynin reduces blood pressure and restores the proper function of vascular endothelium in SHR. Vascul Pharmacol 2016; 87:38-48. doi: 10.1016/j.vph.2016.06.005.

[15] Olukman M, Orhan CE, Celenk FG, Ulker S. Apocynin restores endothelial dysfunction in streptozotocin diabetic rats through regulation of nitric oxide synthase and NADPH oxidase expressions. J Diabetes Complications 2010; 24:415-23. doi: 10.1016/j.jdiacomp.2010.02.001.

[16] Köroğlu KM, Çevik Ö, Şener G, Ercan F. Apocynin alleviates cisplatin-induced testicular cytotoxicity by regulating oxidative stress and apoptosis in rats. Andrologia 2019;51: e13227. doi: 10.1111/and.13227.

[17] Castro MM, Rizzi E, Rodrigues GJ, et al. Antioxidant treatment reduces matrix metalloproteinase-2-induced vascular changes in renovascular hypertension. Free Radic Biol Med 2009; 46:1298-307. doi: 10.1016/j.freeradbiomed.2009.02.011.

[18] Fan R, Shan X, Qian H, et al. Protective effect of apocynin in an established alcoholic steatohepatitis rat model. Immunopharmacol Immunotoxicol 2012; 34:633-8. doi: 10.3109/08923.973.2011.648266.

[19] Wu M, Xing Q, Duan H, Qin G, Sang N. Suppression of NADPH oxidase 4 inhibits $PM_{2.5}$-induced cardiac fibrosis through ROS-P38 MAPK pathway. Sci Total Environ 2022; 837:155558. doi: 10.1016/j.scitotenv.2022.155558.

[20] Zhang R, Ran HH, Ma J, Bai YG, Lin LJ. NAD(P)H oxidase inhibiting with apocynin improved vascular reactivity in tail-suspended hindlimb unweighting rat. J Physiol Biochem. 2012; 68:99-105. doi: 10.1007/s13105.011.0123-1.

[21] Cheng X, Zheng X, Song Y, et al. Apocynin attenuates renal fibrosis via inhibition of NOXs-ROS-ERK-myofibroblast accumulation in UUO rats. Free Radic Res 2016; 50:840-52. doi: 10.1080/10715.762.2016.1181757.

[22] Kinkade K, Streeter J, Miller FJ. Inhibition of NADPH oxidase by apocynin attenuates progression of atherosclerosis. Int J Mol Sci 2013; 14:17017-28. doi: 10.3390/ijms140817017.

[23] Affane F, Louala S, El Imane Harrat N, et al. Hypolipidemic, antioxidant and antiatherogenic property of sardine by-products proteins in high-fat diet induced obese rats. Life Sci 2018; 199:16-22. doi: 10.1016/j.lfs.2018.03.001.

[24] Kuru Yaşar R, Kuru D, Şen A, Şener G, Ercan F, Yarat A. Effects of *Myrtus communis* L. Extract and Apocynin on Lens Oxidative Damage and Boron Levels in Rats with a High Fat-Diet. Turk J Ophthalmol 2021;51(6):344-350. doi: 10.4274/tjo.galenos.2021.27981.

[25] Love KM, Liu Z. DPP4 Activity, Hyperinsulinemia, and Atherosclerosis. J Clin Endocrinol Metab 2021; 106:1553-1565. doi: 10.1210/clinem/dgab078.

[26] Meng R, Zhu DL, Bi Y, Yang DH, Wang YP. Anti-oxidative effect of apocynin on insulin resistance in high-fat diet mice. Ann Clin Lab Sci 2011; 41:236-43.

[27] Yan M, Mehta JL, Hu C. LOX-1 and obesity. Cardiovasc Drugs Ther 2011; 25:469-76. doi: 10.1007/s10557.011.6335-3.

[28] Chung APYS, Gurtu S, Chakravarthi S, Moorthy M, Palanisamy UD. Geraniin Protects High-Fat Diet-Induced Oxidative Stress in Sprague Dawley Rats. Front Nutr 2018; 5:17. doi: 10.3389/fnut.2018.00017.

[29] Costa CA, Amaral TA, Carvalho LC, et al. Antioxidant treatment with tempol and apocynin prevents endothelial dysfunction and development of renovascular hypertension. Am J Hypertens 2009; 22:1242-9. doi: 10.1038/ajh.2009.186.

[30] Qin F, Simeone M, Patel R. Inhibition of NADPH oxidase reduces myocardial oxidative stress and apoptosis and improves cardiac function in heart failure after myocardial infarction. Free Radic Biol Med 2007; 43:271-81. doi: 10.1016/j.freeradbiomed.2007.04.021.

[31] Moe KT, Aulia S, Jiang F, et al. Differential upregulation of Nox homologues of NADPH oxidase by tumor necrosis factor-alpha in human aortic smooth muscle and embryonic kidney cells. J Cell Mol Med 2006;10:231-9. doi: 10.1111/j.1582-4934.2006.tb00304.x.

[32] Zhang H, Cui J, Zhang C. Emerging role of adipokines as mediators in atherosclerosis. World J Cardiol 2010; 2:370-6. doi: 10.4330/wjc.v2.i11.370.

[33] Meng R, Zhu DL, Bi Y, Yang DH, Wang YP. Apocynin improves insulin resistance through suppressing inflammation in high-fat diet-induced obese mice. Mediators Inflamm 2010; 2010:858735. doi: 10.1155/2010/858735.

[34] Münzel T, Camici GG, Maack C, Bonetti NR, Fuster V, Kovacic JC. Impact of Oxidative Stress on the Heart and Vasculature: Part 2 of a 3-Part Series. J Am Coll Cardiol 2017;70:212-229. doi: 10.1016/j.jacc.2017.05.035.

[35] Li H, Horke S, Förstermann U. Vascular oxidative stress, nitric oxide and atherosclerosis. Atherosclerosis 2014;237:208-19. doi: 10.1016/j.atherosclerosis.2014.09.001.

[36] Chung JH, Moon J, Lee YS, Chung HK, Lee SM, Shin MJ. Arginase inhibition restores endothelial function in diet-induced obesity. Biochem Biophys Res Commun 2014 ;451:179-83. doi: 10.1016/j.bbrc.2014.07.083.

[37] La Favor JD, Dubis GS, Yan H, White JD, Nelson MA, Anderson EJ, Hickner RC. Microvascular Endothelial Dysfunction in Sedentary, Obese Humans Is Mediated by NADPH Oxidase: Influence of Exercise Training. Arterioscler Thromb Vasc Biol 2016; 36:2412-2420. doi: 10.1161/ATVBAHA.116.308339.

[38] Jang E, Robert J, Rohrer L, von Eckardstein A, Lee WL. Transendothelial transport of lipoproteins. Atherosclerosis 2020; 315:111-125. doi: 10.1016/j.atherosclerosis.2020.09.020.

[39] Chang WC, Yu YM, Hsu YM, Wu CH, Yin PL, Chiang SY, Hung JS. Inhibitory effect of Magnolia officinalis and lovastatin on aortic oxidative stress and apoptosis in hyperlipidemic rabbits.

J Cardiovasc Pharmacol 2006; 47:463-8. doi: 10.1097/01.fjc.000.021.1708.03111.6e.

[40] Kattoor AJ, Goel A, Mehta JL. LOX-1: Regulation, Signaling and Its Role in Atherosclerosis. Antioxidants (Basel) 2019; 8:218-33. doi: 10.3390/antiox8070218.

[41] Rathouska J, Vecerova L, Strasky Z, et al. Endoglin as a possible marker of atorvastatin treatment benefit in atherosclerosis. Pharmacol Res 2011; 64:53-9. doi: 10.1016/j.phrs.2011.03.008.

[42] Chellan B, Sutton NR, Hofmann Bowman MA. S100/RAGE-Mediated Inflammation and Modified Cholesterol Lipoproteins as Mediators of Osteoblastic Differentiation of Vascular Smooth Muscle Cells. Front Cardiovasc Med 2018; 5:163. doi: 10.3389/fcvm.2018.00163.

[43] Chaabane C, Coen M, Bochaton-Piallat ML. Smooth muscle cell phenotypic switch: implications for foam cell formation. Curr Opin Lipidol 2014; 25:374-9. doi: 10.1097/MOL.000.000.0000000113.

[44] Li M, Wang ZW, Fang LJ, Cheng SQ, Wang X, Liu NF. Programmed cell death in atherosclerosis and vascular calcification. Cell Death Dis 2022; 13:467. doi: 10.1038/s41419.022.04923-5.

[45] Shan R, Liu N, Yan Y, Liu B. Apoptosis, autophagy and atherosclerosis: Relationships and the role of Hsp27. Pharmacol Res 2021;166:105169. doi: 10.1016/j.phrs.2020.105169.

[46] Xu YJ, Zheng L, Hu YW, Wang Q. Pyroptosis and its relationship to atherosclerosis. Clin Chim Acta 2018;476:28-37. doi: 10.1016/j.cca.2017.11.005.

[47] Liu Z, Yao X, Jiang W, et al. Advanced oxidation protein products induce microglia-mediated neuroinflammation via MAPKs-NF-κB signaling pathway and pyroptosis after secondary spinal cord injury. J Neuroinflammation 2020; 17:90. doi: 10.1186/s12974.020.01751-2.

[48] Hersek İ, Köroğlu MK, Coskunlu B, Ertaş B, Şener G, Ercan F. Apocynin ameliorates testicular toxicity in high-fat diet-fed rats by regulating oxidative stress, Clin Exp Health Sci 2023, 13: 75-83. doi:10.33808/clinexphealthsci.1035133

[49] Zhaolin Z, Guohua L, Shiyuan W, Zuo W. Role of pyroptosis in cardiovascular disease. Cell Prolif 2019;52:e12563. doi: 10.1111/cpr.12563.

[50] Di Pietro N, Formoso G, Pandolfi A. Physiology and pathophysiology of oxLDL uptake by vascular wall cells in atherosclerosis. Vascul Pharmacol 2016;84:1-7. doi: 10.1016/j.vph.2016.05.013.

MARMARA
MEDICAL JOURNAL

Original Article

https://dergipark.org.tr/tr/pub/marumj

The association of ZIC5 gene rs965623242 polymorphism with neural tube defects

Ebru ONALAN[1], Yasemin ASKIN[1], Tugce KAYMAZ[1], Mehmet SARACOGLU[2], Ahmet KAZEZ[2], Tugba ONAL SUZEK[3], Vahit KONAR[4]

[1] Department of Medical Biology, Faculty of Medicine, Firat University, Elazig, Turkey
[2] Department of Pediatric Surgery, School of Medicine, Firat University, Elazig, Turkey
[3] Department of Bioinformatics, Graduate School of Applied and Natural Sciences, Mugla Sitki Kocman University, Mugla, Turkey, Faculty of Science
[4] Department of Biology, Faculty of Science, Amasya University, Amasya, Turkey

Corresponding Author: Tugce KAYMAZ
E-mail: tugcekaymaz.92@gmail.com

Submitted: 27.09.2021 **Accepted:** 26.02.2024

ABSTRACT

Objective: This study aims to evaluate the effects of the rs965623242 reference single nucleotide polymorphism (SNP) on the ZIC5 gene in patients with neural tube defect (NTD).

Patients and Methods: One hundred sixty-eight controls and one hundred sixty-eight NTD patients were included in the study. Deoxyribonucleic acid (DNA) isolation from peripheral blood samples was carried out for all participants. rs965623242 polymorphic region was amplified by polymerase chain reaction (PCR) and then sequenced.

Results: In the 5' untranslated region (UTR) of the first exon, guanine (G) to adenine (A) base change was detected in the 38th base of NM_033132.5. G to A base change was determined as *GG* genotype in 117 (69.6%), *AG* genotype in 30 (17.86%), and *AA* genotype in 21 (12.5%) patients. In the control group, *GG* genotype in 107 (63.7%), *AG* genotype in 23 (13.7%) and *AA* genotype in 38 (22.7%) were observed. The statistically significant difference was observed between the NTD and the control groups in ZIC5 genotypes or allele frequencies [p=0.044, odds ratio (OR)=0.49 (0.27-0.88) and p=0.021, OR=0.65 (0.46-0.93), respectively].

Conclusion: ZIC5 rs965623242 polymorphism may have a protective role in the NTD development in the Eastern Anatolian population, in Turkey. Although, these findings demonstrate that the rs965623242 polymorphism is associated with NTD, we do not clarify how its expression is affected during the embryonic period and ongoing processes. We will need advanced ongoing genetic and clinical studies to obtain more detail.

Keywords: Congenital anomalies, Neural tube defect, Spina bifida, ZIC5 gene, Polymorphism

1. INTRODUCTION

Spina bifida, also known as neural tube defects (NTDs), affects around 0.57–13.87% of the population and is the second most frequent birth condition globally [1]. In Turkey, the disease is seen in 1.5% to 6.3% of cases [2]. During the first three or four weeks of pregnancy, the neural tube begins to collapse. Delays in closure lead to NTD. In many parts of the world, there is a significant incidence of non-transferable diseases (NTDs), which varies according to the geographical region, season of pregnancy, gender of the diseased fetus, ethnicity, socioeconomic status of the family, and mother age [3]. The word "spina bifida" refers to a broad category of developmental defects. Spina bifida, meningocele, myelomeningocele, encephalocele, anencephaly, dermal sinus, stretched medulla spinalis, syringomyelia, diastemomyelia, and lipoma are the most prevalent of these abnormalities [4]. According to reports, genetic and environmental variables can have a role in the occurrence of NTD. The neural tube may not close properly as a result of maternal malnutrition during pregnancy, health issues such as high blood pressure, diabetes, obesity, and fever, as well as some medications and environmental contaminants [5].

Parallel to the new techniques used in molecular genetics, several possible gene polymorphisms and mutations that cause NTDs were identified. It is known that genetic research is being done to determine the cause of spina bifida. It has been proposed recently that the ZIC gene family may be involved in neural tube closure and abnormalities. NTD is commonly observed in humans with 13q deletion syndrome, which lends support to this observation. The 13q3.3 minimum deletion region is

How to cite this article: Etem Onalan E, Askin Y, Kaymaz T, et al. The association of RS965623242 polymorphism of ZIC5 gene with neural tube defects. Marmara Med J 2024: 37(2):248-255. doi: 10.5472/marumj.1493354

ISSN: 1309-9469

http://doi.org/10.5472/marumj.1493354
Marmara Med J 2024;37(2): 248-255

where the ZIC2 and ZIC5 genes are located [6]. The human genome has five ZIC genes: ZIC1, ZIC2, ZIC3, ZIC4, and ZIC5. ZIC genes participate in neural crest induction, suppression of neurogenesis, and mediolateral segmentation during mouse brain development [7, 8].

Mice lacking ZIC2 showed signs of a broad range of NTDs, including spina bifida aperta, spina bifida oculus, anencephaly, and exencephaly [9–11]. In the Xenopus genus, neural crest development is known to be induced by the ZIC5 gene [12]. It has been demonstrated that ZIC5 deficiency in mice results in a variety of abnormalities, including NTDs and craniofacial abnormalities including hypoplasia. Despite evidence that the ZIC5 gene has a role in neural tube closure and neural crest development in experimental animals, ZIC5 gene mutation screening has not been carried out for human patients with neural tube defects [13]. The cerebellar chain-finger transcription factors encode the ZIC2 and ZIC5 genes. Every zinc finger motif has two histidines in the alpha (α) helix area, two tetrahedral structures in the beta (β)-sheet region, and a zinc atom in the center. The ZIC5 gene has three exons. In all five genes, the first intron-exon limit was maintained. In addition, the boundary of the second intron-exon is conserved in ZIC1, ZIC2 and ZIC3 but not in ZIC4 and ZIC5 [14-16].

Research indicates that the ZIC5 gene plays a role in both the etiopathogenesis and neurulation processes of NTD [12, 13]. There is no information in the literature about the relationship between the likelihood of acquiring neural tube abnormalities and mutations or polymorphisms in the ZIC5 gene. As a result, we looked into the ZIC5 gene's rs965623242 promoter polymorphism in patients with NTD and contrasted the findings with those of controls who resided in Turkey's Eastern Anatolian region.

2. PATIENTS and METHODS

After the approval of the Non-Interventional Research Ethics Committee of Firat University (Decision number: 158/9, dated 02.06.2011) was obtained, the study was carried out by obtaining verbal and written consent from the families. 168 patients who underwent surgery with the diagnosis of NTD at Fırat University Hospital Pediatric Surgery Clinic and 168 control individuals participated in the study between June 2011 and September 2016. Care was taken to collect the samples used in the study from similar geographical regions. For the genotype analyses, blood samples taken for the routine preoperative biochemistry tests from all participants, who were admitted to the outpatient clinic due to circumcision and trauma, were used. In the selection of control subjects, the criteria of absence of any congenital anomaly and genetic disease in the family, and similar age, gender, and region of residence were taken into consideration. Blood samples were collected into biochemistry tubes coated with ethylenediaminetetraacetic acid (EDTA) and for the genotyping analysis, they were conserved at – 20°C. An anamnesis form including each patient's demographic characteristics and clinical history was filled. The type of defect in the patients was recorded. The participants were asked about maternal age, whether there were similar cases in the family, and whether there was any consanguineous marriage. To reveal possible teratogenic causes (besides birth anamnesis); drug usage in the mothers' periconceptional period, whether or not the use of vitamin B12 and folic acid, and whether they had a feverish illness during the 3rd-4th weeks of pregnancy were asked. After a detailed examination of the patients, whether there was any other nervous system anomaly or other system anomalies accompanying spina bifidia was recorded.

DNA extraction

Genomic DNA extraction from blood samples was performed using Wizard® Genomic DNA Purification Kit (CAT # A1120, Promega, USA), designed for the DNA isolation from 300 µL of blood. After the samples were thawed and kept at room temperature, the isolation process followed the manufacturer's protocol and some modifications were made to the isolation protocol. 900 µL of cell lysis solution was added into the 1.5 mL tubes and then 300 µL blood was added into each tube after pipetting it 5-6 times. The tubes were kept at room temperature for 10 minutes and centrifuged at 15,000 x g speed for 20 seconds at 4°C temperature. After centrifugation, the supernatants were discarded, leaving approximately 10-20 µL of liquid at the bottom of the tube. The tubes were vortexed at high speed for 15-20 seconds, 350 µL of nuclei lysis solution was added into each tube and the vortexing process was performed again. After the tubes were centrifuged at 13.00x g speed for 1 min at 25°C temperature, the supernatants were discarded and the remaining liquid at the bottom of the tubes was pipetted 5-6 times with a Pasteur pipette to break down the white cells. To precipitate proteins in the blood, about 120 µL of precipitation solution was added to the nuclear lysate at room temperature. After vortexing the tubes vigorously for 10-20 seconds, small, different brown shades of protein clusters were seen. The samples were centrifuged at 15,000 x g for 3 minutes at 25°C temperature. 300 µL of isopropanol and the supernatants were added respectively into the fresh 1.5 mL centrifuge tubes. After the tubes were shaken thoroughly, DNAs were seen as white residue at the bottom of the tubes. The samples were centrifuged at 15,000 x g for 1 minute at 25°C temperature. 900 µL of 70% ethanol was added into each tube and the tubes were shaken gently. The centrifugation process was repeated at 15,000 x g for 1 minute at 25°C temperature. After the DNA washing process was completed, the tubes were placed on the clean paper as the tubes' mouths were faced upwards, so ethanol was exactly removed. Tubes were allowed to air dry for 5-10 minutes and 100 µL of DNA rehydration solution was added to each tube. The tubes were incubated at 37°C for 60 minutes to rehydrate the DNA and then stored at 2-8°C temperature. DNA concentration and purity were analyzed by a nanodrop device (Maestrogen, MaestroNanodrop, USA), and then DNA concentration was diluted to 1-10 ng.

http://doi.org/10.5472/marumj.1493354
Marmara Med J 2024;37(2): 248-255

Conventional polymerase chain reaction (PCR), DNA sequencing and genotyping

To evaluate the polymorphisms for the *ZIC5* gene, complete sequences of genes were obtained by using the Ensembl genome database [17]. Primers used to perform amplification of the *ZIC5* gene promoter region on human DNA, were designed with the help of a free primer designation tool [18] and purchased from the Sentebiolab (Ankara, Turkey). The nucleotide sequence for the forward (F) primer is 5′-CAGGCCAGGCTCAAACTTCTGCA-3′ and for the reverse (R) primer is 5′-GGGGCTCCATCAGAACTACACAATCA-3′. PCR conditions were set according to the protocol described by Zhang et al [19]. After the optimization process, the PCR protocol was adjusted to our laboratory conditions. The PCR reaction mix was prepared by using 8 µL of template DNA, 5µL of 10X PCR buffer, 5 µL of 25 mM $MgCl_2$, 0.5 µL of Taq DNA polymerase, 5 µL of 2.5 mM deoxyribonucleotide triphosphates (dNTPs), 0.5 µL of Taq DNA polymerase and 2µL each of 20 pmol of F and R primers. The total volume was completed with 50 µl of nuclease-free water. PCR denaturation step was carried out for 5 minutes at 95°C and 30 seconds at 95°C, the annealing step for 30 seconds at 58.4°C, the elongation step for 40 minutes at 72°C, and the extension step for 7 minutes at 72°C. The total PCR reaction consisted of 36 cycles and all steps were performed sequentially. To determine the specificity and quality of the DNA amplification process, PCR products were run on the 3% agarose gel. For the electrophoresis process, 5X Tris/Borate/EDTA (TBE) buffer was used. 6X loading buffer and PCR products were mixed and then loaded into the wells of the gel. 7 µL of 100 base pair (bp) DNA marker (Fermentas) was loaded into the first and last wells of the gel to determine the size of the bands. The gel was run at 60 V at room temperature for 1 hour and finally, it was visualized under ultraviolet (UV) light. A 431 bp product was obtained as a result of amplification of the *ZIC5* gene region containing the rs965623242 polymorphism (Figure 1).

A 401 bp product

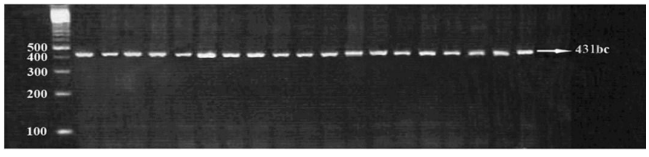

Figure 1. *Control of the PCR products by agarose gel electrophoresis. 100 bp of DNA marker and 431 bp PCR products belonging to exon 1 of the ZIC5 gene were obtained by 2% agarose gel electrophoresis with ethidium bromide (EtBr) staining. Forward (5'-CAGGCCAGGCTCAAACTTCTGCA-3') and reverse (5'-GGGGCTCCATCAGAACTACACAATCA-3') primers were used to amplify the promoter of ZIC5 gene..*

Polymerase chain reaction products were sent to the RefGen Gene Research and Biotechnology laboratory (Ankara, Turkey) for the sequencing process. The sequencing results were compared with a DNA baser program to determine whether polymorphism existed. For bioinformatics analysis of the ZIC5 gene variants, DIANA tools [20], miRDB [21], 1000 Genomes [22], The Exome Aggregation Consortium (ExAC) [23], the Single Nucleotide Polymorphism Database (dbSNP) of the [24] and Variation Viewer [25] were utilized.

Statistical Analysis

All descriptive and inferential statistical analyses were performed with IBM SPSS version 22.0 software (Chicago, IL, USA). Data are presented in counts, percentages, mean, and standard deviation (SD) values. The Kolmogorov-Smirnov test was conducted to determine whether the data were distributed normally. The deviation from Hardy-Weinberg equilibrium (HWE) was verified by using the Chi-square (χ^2) test which was also used to make a comparison between groups, for the analysis of the association between two qualitative variables and allele and genotype frequencies. The magnitude of the association between ZIC5 rs965623242 polymorphism and NTD was expressed with the help of odds ratio and 95% confidence interval (CI). Demographic, clinical, and laboratory data were compared using the χ^2 test, Student's t-test, and one-way ANOVA test. To decide the statistical significance or insignificance of the results, the p-value was accepted as < 0.05.

3. RESULTS

Demographic, clinical, and laboratory results of all subjects are indicated in Table I. 69.7% of the patients are from Elazig province and 31.3% from its surrounding provinces in the Eastern Anatolia Region of Turkey. Sex ratio of the children was 79 (47%) for females and 89 (53%) for males in the control group and 98 (58.3%) for females and 70 (41.7%) for males in the NTD group. The mean age of the children was 2.38±2.83 years [3.28 ± 4.21 for females (1 month-17 years old) and was 3.24 ± 4.15 years for males (1 month-14 years old)] for the control group and 2.22±3.13 years (2.24 ± 3.37 years for females and 2.38 ± 3.14 years for males) for the NTD group. There was no statistically significant difference in terms of the mean age of children and mothers between the control and NTD groups (p>0.05).

Table I. *Demographic, clinical, and laboratory findings for each group*

Parameters	NTD (n=168)	Control (n=168)	p-value
Age (years)	2.22 ± 3.13	2.38 ± 2.83	NS
Female/male	98/70	79/89	NS
Meningosel/ Meningomyelosel	10/158	——	——
History of the other baby with NTD in the family	21 (12.5%)	0 (0%)	0.0000
Consanguinity between parents	46 (27.4%)	16 (9.52%)	0.0001
Iron supplements used during pregnancy	25 (14.8%)	30 (17.9%)	NS
Mother's age during pregnancy (years)	27.35 ± 5.31	26.22±5.68	NS

NTD: Neural tube defect, NS: Non-significant. Results are expressed as mean ± standard deviation (SD). p < 0.05 was considered significant when compared with the control group.

http://doi.org/10.5472/marumj.1493354
Marmara Med J 2024;37(2): 248-255

Genotype and allele distributions

All samples were successfully sequenced and the sequencing results are indicated in Figure 2a. The specific DNA sequence obtained from the sequencing analysis is illustrated in the Figure 2b.

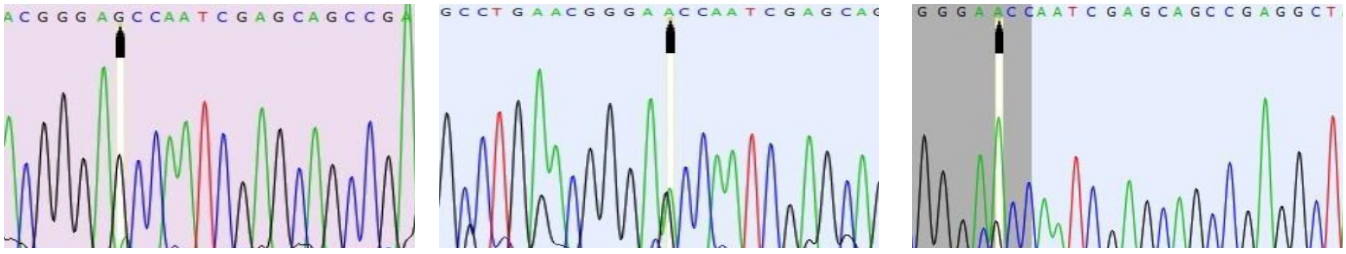

(A) GG genotype (B) GA genotype (C) AA genotype

Figure 2a. *Typical raw data for rs965623242 (G>A) polymorphism obtained by using Sanger sequencing instruments. Polymorphic nucleotide was represented with a black arrow. G nucleotide was the ancestral allele and A nucleotide was the polymorphic allele. (a) Single "G" peak shows a GG homozygous genotype. (b) The presence of both "G" and "A" peaks indicates a G/A heterozygous genotype. (c) Single "A" peak demonstrates a AA homozygous genotype. GenBank accession number of ZIC5 gene was NG_053065.1.*

3'-CGGCCGCAAGCACGGGGGCGAATCCCCGCTGGGTCGAGGGCCTGAACGGGAG/ACCAATCGAGCAGCCGAGGCTACTGCCA
ATCACGCGGCTCCCTCCAATCCCACCCGTGCCATTTCCAAAATCTCGGTCCCACTGTGCAGCTCAAATGTGGTGTTCACTCTGCCAATC
GCTGGAGGATAGAGTGGGAACAGGAATAAGCAGAGTTAAGAGGCCAGGACAAAAGAAGTTAAAGAGCGCCCAATACATAC-5'

Figure 2b. *5' untranslated region (UTR) sequence of ZIC5 gene. The genomic position of rs965623242 polymorphism was NC_000013.10:g.100624126C>T, which is located in the 5' UTR of the ZIC5 gene.*

The distribution of genotypes and allele frequencies of *ZIC5* gene variants are presented in Table II. All SNPs were analyzed in the HWE in NTD and control subjects (p>0.05). Between the patient and control groups, statistical significance was detected in genotype distributions and allele frequencies of the analyzed SNP (p=0.044, OR=0.49 (0.27-0.88) for patients; p=0.021, OR= 0.65 (0.46 – 0.93) for controls). Genotype distribution of rs965623242 *G>A* SNP was determined in 117 (69.6%) NTD patients for wild-type genotype, 30 (17.86%) for heterozygote genotype, and 21 (12.5%) for polymorphic genotype. Furthermore, for rs965623242 *G>A* SNP, 107 (63.7%) of control subjects were homozygous for wild type genotype, 23 (13.7%) were heterozygous, and only 38 (22.7%) were polymorphic homozygous. Allele frequencies in NTD patients were 0.79 for the wild *G* allele and 0.21 (12.5%) for the polymorphic A allele. The frequency of wild type allele was 0.71 and that of the polymorphic allele was 0.29, which represented 22.7% of the examined control subjects. The frequency of the AA genotype in NTD patients (12.5%) was significantly lower compared to control male subjects (22.7%).

Table II. *Genotypes and allele frequencies of ZIC5 gene variant i.e. rs965623242 in control and NTD groups.*

rs16835198	NTD (n=168)	Control (n=168)	p and OR (95% CI) values
Genotypes			
GG	117 (69.6%)	107 (63.7%)	**0.044**
GA	30 (17.86%)	23 (13.7%)	0.71 (0.39-1.26)
AA	21 (12.5%)	38 (22.7%)	
Alleles			
G	0.79	0.71	**0.02**
A	0.21	0.29	0.65 (0.45-0.92)

NTD: Neural tube defect, OR: Odds ratio, CI: Confidence interval, NS: Nonsignificant. χ2 and Fischer tests were performed. χ2 analysis of the genotypes and alleles for NTD subjects was performed versus control subjects. Results are expressed as percentages. p < 0.05 was considered significant when compared with the control group.

http://doi.org/10.5472/marumj.1493354
Marmara Med J 2024;37(2): 248-255

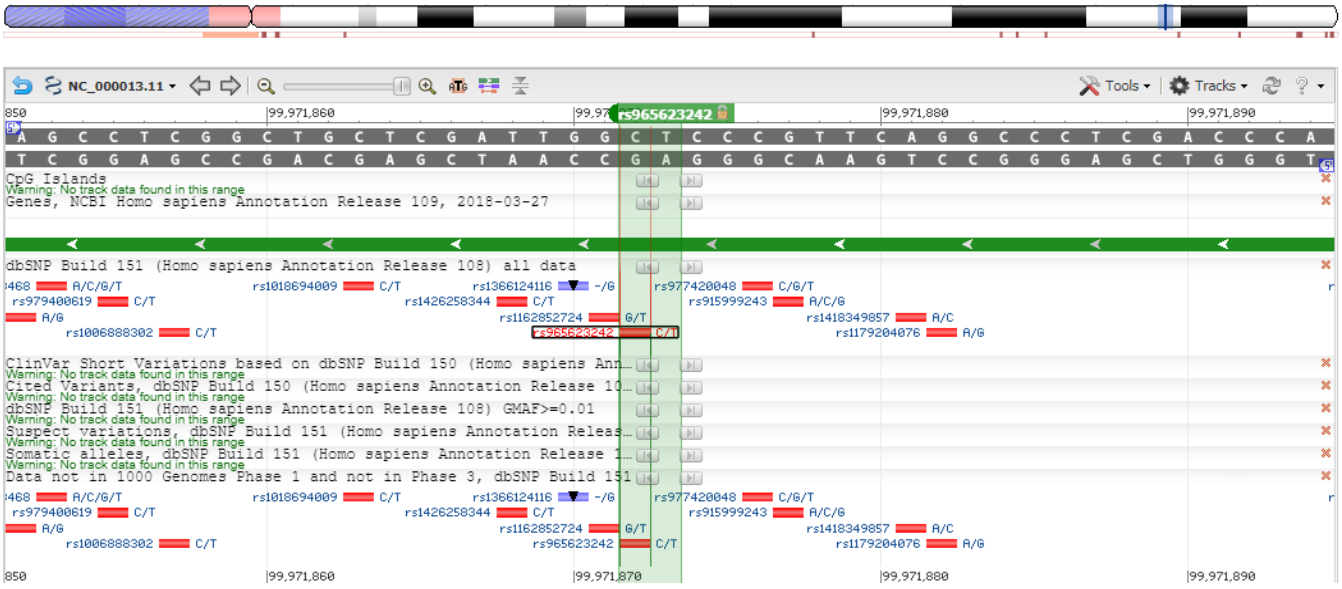

Figure 3. *Reference SNP (rs) reports [26].*

As of the submission date, no report of this variant's allele frequency has been found in the Turkish population or any other populations. Potential microribonucleic acid (miRNA) binding sites of the polymorphic region were investigated using DIANA tools and miRDB [20,21]. It was predicted that miRNA binding sites which were not determined, were found in the polymorphic region. Reference SNP reports are illustrated in Figure 3.

4. DISCUSSION

In the current study, we examined the rs965623242 polymorphism in the 5'-UTR region of the *ZIC5* gene in the formation of NTDs. The decreased frequency of the rs965623242 AA genotype may be a protective factor rather than a risk factor for NTD. This is the first study worldwide to examine this polymorphism in terms of such birth defects.

In our literature review, however, we could not find any study on the effects of this polymorphism on NTD and other neurological diseases. However, two studies are searching for the relationships between *ZIC2* gene polymorphisms and NTD. In the first of these, Brown et al. [27], screened for the polyhistidine tract polymorphism in the *ZIC2* gene in 192 NTD patients but they did not find any association between this polymorphism and NTDs. In other studies, Costa Lima et al. [28], similarly analyzed the same polymorphism in 138 NTD patients and their families, but they also did not find a significant relationship between the mentioned polymorphism and NTD. Recently, two important studies have been conducted that may be indicative of the pathogenic effects of the *ZIC5* gene, especially on fetal development. In the first study, a match between rare copy number variations (CNV) in the *ZIC5* gene and abnormal voluntary movement was identified in a mouse model of global developmental disorder [29]. In the second study, a Whole Exome Sequencing (WES) study was performed in couples with recurrent miscarriages, and missense, non-pathogenic changes were detected in the *ZIC2* and *ZIC5* genes in the patient group [30]. In the present study, the polymorphic variant appears to be protective for NTD. However, the mechanisms underlying the conservation of the rs965623242 polymorphism remain unknown. A small part of SNPs have significant effects on the phenotypes, while most of them have no or very limited effects [31]. SNPs can convert an amino acid to another one (nonsynonymous), be silent (synonymous) or be seen in a noncoding region. Although the promoter activity, messenger ribonucleic acid (mRNA) conformation and translational effects of the rs965623242 polymorphism are not yet known, our bioinformatics analysis showed that this region did not coincide with any miRNA or transcription factor binding sites [20, 21]. Although the transcriptional effects of the rs965623242 polymorphism in the *ZIC5* gene have not been revealed by luciferase reporter experiments, the phenotypic effects of the *ZIC5* AA genotype can be explained by the effects of the *ZIC5* gene on cell proliferation. The central nervous system (CNS) develops from a special region of the ectoderm layer called the neural plate, which is located in the dorsal midline of the embryo. Since the rate of cell division is faster along the edges of the neural plate than in the middle section, the neural plate thickens, expands and takes the shape of a groove during the development of the neural tube [32]. In this process, regulation of the cell division rate is critical. It has been demonstrated that high expression of the *ZIC5* gene accelerates the progression of lung, liver, melanoma and colorectal cancers, increasing cell proliferation through the activation of signaling pathways such as CCNB1/CDK1, Wnt/β catenin, FAK/STAT3 and

http://doi.org/10.5472/marumj.1493354
Marmara Med J 2024;37(2): 248-255

CDK1/CDC25c, while its suppression has antiproliferative and antineoplastic effects [33-38]. Recently, the *ZIC5* gene has been shown to play a role in induction along with Wnt downstream signals and Notch upstream signals [38]. Prevention of neuronal closure (NC) induction occurs through early embryonic exposure to ketamine, which inhibits notch-targeted gene expression, including the *ZIC5* gene [40]. Based on the effects of the *ZIC5* gene on cell proliferation, the AA genotype may cause low expression levels, and NC problems by producing a negative effect on the cell division along the edges of the neural plate.

In the present study, the *G* allele frequency was 0.71 and the *A* allele frequency was 0.29 in the control group. However, in the literature reviews, the frequency of the *T* allele was reported as 3/125568 in the TOPMED project [41] and 0/2188 in the Alfa Project [42]. In our study, unlike these two projects, the frequency of the *T* variant allele was found to be higher in the population of Elazig and its surrounding provinces. Different geographically separated populations may be exposed to different selective environmental conditions, but population-specific selection may result in an increase in population differentiation of the target locus. Nevertheless big differences in rare allele frequencies (RAF) caused by geographical region differences are more prone to be caused by *allelic surfing* which is defined as genetic drift during population expansion after a bottleneck, rather than natural selection. By looking at our findings in the genetic epidemiological scope, it is necessary to investigate the RAF differences that occur in NTD susceptibility variants and can be explained by natural selection or allele surfing [43-45].

The most interesting aspects of the current study are that the frequency of the rs965623242 polymorphism in our society is defined regionally, the frequency in our society is higher than in other societies and, the NTD and *ZIC5* gene relationship is revealed for the first time at the polymorphism level. The most important limitations of our study are that it was performed in a small cross-sectional patient group and only promoter polymorphisms were analyzed. Although it was scheduled to sequence the entire gene at the beginning of the current study, serious problems were experienced in duplicating the target region despite many primer combinations being tried. For this reason, we continued to work with the promoter region primers that worked best. In line with our experience, it is recommended that the gene region contains a high percentage of GC and that it be sequenced by amplifying it in very small regions.

Conclusion

In conclusion, since, multifactorial events including environmental and genetic factors are very important for the etiology of NTD, reporting the prevalence of this variant in different populations and revealing the disease relationships are very important. The effects of factors such as maternal age, health problems (e.g. obesity), consanguinity degree, drugs used by the mother during the pregnancy and maternal nutrition on the functioning of this allele are also unknown. To determine whether rs965623242 and the other polymorphisms in the *ZIC5* gene are susceptible to NTD disease, genetic studies including a higher number of patients in both the Turkish population and other populations are needed.

Compliance with Ethical Standards

Ethical approval: The study was approved by the Non-Interventional Research Ethics Committee of Firat University with approval number 58/9 and date 02.06.2011.

Conflict of interest: There are no conflicts of interest related to this article.

Financial disclosure: This study was supported by the Fırat University Scientific Research Projects Coordination Unit (FUBAP) under project number TF.11.58.

Author contributions: EO: Design, Project administration, statistical analysis Conceptualization, Writing-Reviewing and Editing, Investigation, YA: Methodology, Validation, Resources, Visualization, MS and AK: Patient selection and exclusion, Methodology, VK: Validation, Resources, Visualization, TK: Drafting and revision of the manuscript.

REFERENCES

[1] Nikkila A, Rydhström H, Kallen B. The incidence of spina bifida in Sweden 1973-2003: The effect of prenatal diagnosis. Eur J Public Health 2006; 16: 660-2. doi: 10.1093/eurpub/ckl053.

[2] Sanri A, Karayel M, Abur U, et al. Frequency and risk factors of neural tube defects in Samsun province. Croat Med J 2018; 40: 413-20. doi:https://doi.org/10.7197/223.vi.441516.

[3] Tinkle MB, Sterling BS. Neural tube defects: A primary prevention role for nurses. J Obstet Gynecol Neonatal Nurs 1997; 26: 503-23. doi: 10.1111/j.1552-6909.1997.tb02153.x

[4] Neyzi O, Ertugrul T. 3rd ed. Pediatri 2, Istanbul, Turkey: Nobel Tıp Kitabevleri, 2002:1338-41.

[5] Akan N. Nöral tüp defektli bebek doğurma riski azaltılabilir. Cumhuriyet Üniversitesi Hemşirelik Yüksekokulu Dergisi 2002; 6: 42-48.

[6] Brown S, Russo J, Chitayat D, Warburton D. The 13q-syndrome: the molecular definition of a critical deletion region in band 13q32. Am J Hum Genet 1995; 57: 859-66.

[7] Merzdorf CS. Emerging roles for zic genes in early development. Dev Dyn 2007; 36: 922-40. doi: 10.1002/dvdy.21098.

[8] Grinberg I, Millen KJ. The ZIC gene family in development and disease. Clin Genet 2005; 67: 290-6. doi: 10.1111/j.1399-0004.2005.00418

[9] Elms P, Siggers P, Napper D, Greenfield A, Arkell R. Zic2 is required for neural crest formation and hindbrain patterning during mouse development. Dev Biol 2003; 264: 391-406. doi: 10.1016/j.ydbio.2003.09.005.

[10] Klootwijk R, Groenen P, Schijvenaars M, et al. Genetic variants in ZIC1, ZIC2, and ZIC3 are not major risk factors for neural tube defects in humans. Am J Med Genet 2004; 124A: 40-7. doi: 10.1002/ajmg.a.20402.

[11] Nagai T, Aruga J, Minowa O, et al. Zic2 regulates the kinetics of neurulation. Proc Natl Acad Sci 2000; 97: 1618-23. doi: 10.1073/pnas.97.4.1618.

[12] Nakata K, Koyabu Y, Aruga J, Mikoshiba K. A novel member of the Xenopus Zic family, Zic5, mediates neural crest development. Mech Dev 2000; 99 : 83-91. doi: 10.1016/s0925-4773(00)00480-9.

[13] Inoue T, Hatayama M, Tohmonda T, Itohara S, Aruga J, Mikoshiba K. Mouse Zic5 deficiency results in neural tube defects and hypoplasia of cephalic neural crest derivatives. Dev Biol 2004; 270: 146-62. doi: 10.1016/j.ydbio.2004.02.017.

[14] Ali RG, Bellchambers HM, Arkell RM. Zinc fingers of the cerebellum (Zic): Transcription factors and co-factors. Int J Biochem Cell Biol 2012; 44: 2065-8. doi: 10.1016/j.biocel.2012.08.012.

[15] Sakai-Kato K, Umezawa Y, Mikoshiba K, Aruga J, Utsunomiya-Tate N. Stability of the folding structure of Zic zinc finger proteins. Biochem Biophys Res Commun 2009; 384: 362-5. doi: 10.1016/j.bbrc.2009.04.151.

[16] Mizugishi K, Aruga J, Nakata K, Mikoshiba K. Molecular properties of Zic proteins as transcriptional regulators and their relationship to GLI proteins. J Biol Chem 2001; 276: 2180-8. doi: 10.1074/jbc.M004430200.

[17] ZIC5 gene, https://www.ensembl.org/Homo_sapiens/Gene/Summary?g=ENSG000.001.39800;r=13:99962.964.99971767;t=ENST000.002.67294, 05.02.2023

[18] Primer design, https://eu.idtdna.com/pages, 02.03.2011

[19] Zhang Y, Liu T, Meyer CA, et al. Model-based analysis of ChIP-Seq (MACS). Genome Biol 2008; 9: R137. doi: 10.1186/gb-2008-9-9-r137.

[20] ZIC5 gene, rs965623242, http://diana.imis.athena-innovation.gr/DianaTools/index.php?r=site/page&view=software),referans, 22.05.2020

[21] miRNA binding site, http://mirdb.org/, 22.05.2020

[22] ZIC5 gene, rs965623242, https://www.internationalgenome.org/, 21.10.2020

[23] ZIC5 gene, rs965623242, https://exac.broadinstitute.org/, 22.11.2020

[24] ZIC5 gene, rs965623242, https://www.ncbi.nlm.nih.gov/snp/, 25.11.2020

[25] ZIC5 gene, rs965623242, https://www.ncbi.nlm.nih.gov/variation/view/, 25.11.2020

[26] ZIC5 gene, rs965623242, https://www.ncbi.nlm.nih.gov/snp/rs965623242#history, 25.11.2020

[27] Brown LY, Hodge SE, Johnson WG, Guy SG, Nye JS, Brown S. Possible association of NTDs with a polyhistidine tract polymorphism in the ZIC2 gene. Am J Med Genet 2002; 108: 128-31. doi: 10.1002/ajmg.10221.

[28] Costa-Lima MA, Meneses HN, El-Jaick KB, Amorim MR, Castilla EE, Orioli IM. No association of the polyhistidine tract polymorphism of the ZIC2 gene with neural tube defects in a South American (ECLAMC) population. Mol Med Rep 2008; 1: 443-6.

[29] Shaikh TH, Haldeman-Englert C, Geiger EA, Ponting CP, Webber C. Genes and biological processes commonly disrupted in rare and heterogeneous developmental delay syndromes. Hum Mol Genet 2011; 20:880-93.

[30] Mou JT, Huang SX, Yu LL, Xu J, Deng QL, Xie YS, Deng K. Identification of genetic polymorphisms in unexplained recurrent spontaneous abortion based on whole exome sequencing. Ann Transl Med 2022; 10: 603. doi: 10.21037/atm-22-2179.

[31] Wang L, Shen H, Liu H, Guo G. Mixture SNPs effect on phenotype in genome-wide association studies. BMC Genom 2015; 16: 3. doi: 10.1186/1471-2164-16-3.

[32] Botto LD, Moore AC, Khory MJ, Erickson DJ. Neural-tube defects. N Eng J Med 1999; 1509-19.

[33] Dong C, Li X, Li K, Zheng C, Ying J. The expression pattern of ZIC5 and its prognostic value in lung cancer. Cancer Biother Radiopharm 2021; 36: 407-11.

[34] Zhao Z, Wang L, Bartom E, et al. Beta-Catenin/ Tcf7l2-dependent transcriptional regulation of GLUT1 gene expression by Zic family proteins in colon cancer. Sci Adv 2019; 5: eaax0698.

[35] Satow R, Inagaki S, Kato C, Shimozawa M, Fukami K. Identification of zinc finger protein of the cerebellum 5 as a survival factor of prostate and colorectal cancer cells. Cancer Sci 2017; 108: 2405-12.

[36] Sun Q, Shi R, Wang X, Li D, Wu H, Ren B. Overexpression of ZIC5 promotes proliferation in non-small cell lung cancer. Biochem Biophys Res Commun 2016; 479: 502-9.

[37] Liu L, Hu X, Sun D, Wu Y, Zhao Z. ZIC5 facilitates the growth of hepatocellular carcinoma through activating Wnt/beta-catenin pathway. Biochem Biophys Res Commun 2018; 503: 2173-9.

[38] Maimaiti A, Aizezi A, Anniwaer J, Ayitula, Ali B, Dilixiati M. Zinc finger of the cerebellum 5 promotes colorectal cancer cell proliferation and cell cycle progression through enhanced CDK1/CDC25c signaling. Arch Med Sci 2021; 17:449-61.

[39] Nyholm MK, Wu SF, Dorsky RI, Grinblat Y. The zebrafish zic2a-zic5 gene pair acts downstream of canonical Wnt signaling to control cell proliferation in the developing tectum. Development 2007; 134: 735-46. doi: 10.1242/dev.02756.

[40] Shi Y, Li J, Chen C, et al. Ketamine modulates Zic5 expression via the Notch signaling pathway in neural crest induction. Front Mol Neurosci 2018; 11: 9. doi: 10.3389/fnmol.2018.00009.

[41] https://topmed.nhlbi.nih.gov/topmed-whole-genome-sequencing-project-freeze-5b-phases-1-and-2 Accessed

[42] https://www.ncbi.nlm.nih.gov/snp/docs/gsr/alfa/

[43] Excoffier L, Ray N. Surfing during population expansions promotes genetic revolutions and structuration. Trends Ecol Evol 2008; 23: 347-51. doi: 10.1016/j.tree.2008.04.004.

[44] Hofer T, Ray N, Wegmann D, Excoffier L. Large allele frequency differences between human continental groups are more likely to have occurred by drift during range expansions than by selection. Ann Hum Genet 2009; 73: 95-108. doi: 10.1111/j.1469-1809.2008.00489.x.

[45] Novembre J, Di Rienzo A. Spatial patterns of variation due to natural selection in humans. Nature Reviews Genetics 2009; 10: 745-55. doi: 10.1038/nrg2632.

MARMARA
MEDICAL JOURNAL

Case Report

https://dergipark.org.tr/tr/pub/marumj

MYH9-related diseases in the differential diagnosis of chronic immune thrombocytopenic purpura

Simge HOROZ BICER[1], Mehmet Fatih ORHAN[2]

[1] Department of Pediatrics, Faculty of Medicine, Sakarya University, Sakarya, Turkey
[2] Division of Pediatric Hematology and Oncology, Department of Pediatrics, Faculty of Medicine, Sakarya University, Sakarya, Turkey

Corresponding Author: Mehmet Fatih ORHAN
E-mail: drfatihorhan@gmail.com

Submitted: 13.09.2023 **Accepted:** 20.12.2023

ABSTRACT

Myosin heavy chain 9 (MYH9)-related platelet disorders (MYH9-RD) belong to the group of inherited thrombocytopenias characterized by giant platelets and Döhle bodies. The process leading to the diagnosis of MYH9-RD in a 13-year-old male patient, followed by the diagnosis of chronic immune thrombocytopenic purpura (ITP), is described. The patient had thrombocytopenia with increased mean platelet volume since he was a little boy. Low CD41, CD42 and CD61 levels were detected in blood tests sent to complete missing diagnostic tests. Platelet aggregation tests were also abnormal. The requested genetic test revealed a heterozygous mutation in the MYH9 gene. The patient's audiogram and kidney functions were normal. In conclusion, because MYH9-RD appears to be rare, it is of great importance to maintain a high index of suspicion when managing patients diagnosed with chronic ITP. Additional complaints and findings should be considered at every outpatient clinic examination to make a more accurate diagnosis and prevent unnecessary treatments.

Keywords: Thrombocytopenia, Chronic ITP, MYH9, Mean Platelet Volume, Children

1. INTRODUCTION

Myosin heavy chain 9 (MYH9)-related platelet disorders (MYH9-RD), which have been previously described in four inherited syndromes (Epstein syndrome, Fechtner syndrome, Sebastian syndrome, May-Hegglin anomaly), are a group of hereditary thrombocytopenias characterized by giant platelets and Döhle body [1]. Diagnosis of May-Hegglin and Sebastian syndromes is based on congenital macrothrombocytopenia and characteristic leukocyte inclusions [2]. In contrast, Epstein and Fechtner syndrome diagnosis was defined in patients with additional features such as cataracts, hearing loss, and nephropathy, which usually lead to end-stage renal disease [3]. The disease locus mapped to chromosome 22q12.3-q13.2 in 1999, and a year later, mutations in the MYH9 gene were identified in all four conditions [4]. It was designated as MYH9-RD (OMIM155100) [5]. The MYH9 gene (22q13.1) encodes the heavy chain of the nonmuscular myosin A isoform of class II (myosin-9), a cytoskeletal contractile protein. Myosin-9 is found in most cell types and tissues. There are heterozygous pathogenic variants due to mutations in the MYH9 gene. MYH9-RD is a rare disease with a worldwide prevalence of 1-9:1 million. Mild forms are discovered by chance, and severe conditions are often misdiagnosed. Therefore, the prevalence may be higher than observed. Platelet transfusion should be considered for active bleeding that cannot be stopped otherwise, for life – or organ-threatening bleeding, and bleeding at critical sites. Eltrombopag or platelet transfusion can be used to prepare affected individuals for elective surgery [6]. Antifibrinolytic agents and desmopressin are used to treat bleeding. Hearing loss, kidney complications, and cataracts are treated standardly. People with severe hearing loss benefit from a cochlear implant [7].

In this case, we report a patient's clinical manifestations and management with a c.5593-4G-A mutation in the heterozygous MYH9 NM_002473.5 gene.

2. CASE REPORT

A 13-year-old male patient came with complaints of nosebleeds and easy bruising accompanied by thrombocytopenia. No bleeding, petechiae, purpura or ecchymosis was observed on

How to cite this article: Bicer Horoz S, Orhan FM. MYH9-related diseases in the differential diagnosis of chronic immune thrombocytopenic purpura. Marmara Med J 2024: 37(2):256-258. doi: 10.5472/marumj.1487461

ISSN: 1309-9469

http://doi.org/10.5472/marumj.1487461
Marmara Med J 2024;37(2): 256-258

the patient's examination. It was learned that the patient had no history of bleeding more than usual during circumcision. No other features were found in his background. The patient's father had kidney stones.

When the patient's past examinations were examined, it was seen that he had thrombocytopenia with an increase in MPV since 2015. In the peripheral smear, 70% of the neutrophils, 30% of the lymphocytes and 30% of the erythrocytes were normochromic normocytic. Platelets were generally large in each field of the peripheral blood smear, with an average of seven single and clustered platelets in some areas. When the platelet count was 95,000/mm3, MPV was 11 fL. the hemogram was examined in a citrate tube, considering the patient's ethylenediaminetetraacetic acid (EDTA) phenomenon. However, it was observed that thrombocytopenia did not improve. A qualitative platelet disorder panel was analyzed by flow cytometry to exclude Bernard Soulier syndrome due to its mild thrombocytopenic course. Flow cytometry analysis of platelets revealed low CD41, CD42b and CD61 values. Platelet function tests were repeated for Glanzman and Bernard Solier syndrome. In the PFA-100 analysis performed to evaluate bleeding time, the closure time with collagen/ADP and collagen/epinephrine was over 180 seconds; this value was longer than expected. Platelet aggregation was positive with ristocetin. The platelet aggregation test was inadequate for collagen, ADP and epinephrine. With the current results, grey platelet syndrome or MYH9-related macrothrombocytopenia was considered in the patient. Genetic testing was requested because our hospital could not view the electron microscopic image. As a result of genetic analysis, a heterozygous mutation was detected in the MYH9 gene. The result was determined as NM_002473.5 c5593-4G>MYH9-associated thrombocytopenia.

After the patient was diagnosed with macrothrombocytopenia genetically linked to MYH9, an audiogram was taken to detect sensorineural hearing loss and no hearing loss was detected. Renal functions were normal, and nephropathy was not observed. The patient is being followed closely for possible complications in the future.

3. DISCUSSION

In MYH9-RD, the presence and severity of spontaneous bleeding are related to the degree of thrombocytopenia. Most affected individuals do not bleed spontaneously; Fatal bleeding is rare. Symptoms can develop at any time between infancy and adulthood [8]. 72% of patients are diagnosed before the age of 35. Kidney damage begins with proteinuria and microhematuria and gradually progresses to end-stage renal disease (ESRD) [9].

MYH9-RD is a rare disease with approximately 300 cases reported in the literature [10]. The cause of some of the patients followed up with a diagnosis of chronic ITP may be such rare diseases. While investigating the etiological causes of the patient we have been following with the diagnosis of chronic ITP for years, we detected c.5593-4G-A heterozygous mutation in the MYH9 NM_002473.5 gene. Although, various modifications have been associated with the development of nephritis, they were not detected in our patient [9]. Although, sensorineural hearing loss is associated with some platelet defects, it was not detected in our patient [11]. MYH9-RD is inherited in an autosomal dominant manner. The mother or father of the case we identified did not have thrombocytopenia. Denovo mutation is detected in approximately 35% of index cases without family history [12].

In conclusion, although MYH9-RD is rare, the index of suspicion should be kept high in every new complaint or finding in patients. They should be followed up with the diagnosis of chronic ITP, and further examinations should be performed to determine why thrombocytopenia develops.

Compliance with Ethical Standards:

This research was conducted ethically by following per under Helsinki World Medical Association Declaration.

Patient consent: The patient gave her consent for clinical information relating to his case to be reported in a medical publication.

Conflict of interest statement: The authors have no conflict of interest to declare.

Funding sources: This research did not receive any specific grant from funding agencies in the public, commercial, or notfor-profit sectors.

Authors contributions: The authors confirm contribution to the paper as follows: SHB and MFO: Study conception and design and draft article preparation, SHB and MFO: Data collection, SHB and MFO: Analysis and interpretation of results. All authors reviewed the results and approved the final version of the manuscript.

REFERENCES

[1] Althaus K, Greinacher A. MYH9-related platelet disorders. Semin Thromb Hemost 2009;35:189-203. doi:10.1055/S-0029.122.0327/ID/21/BIB

[2] Marques MI, Carrington Queiró L, Prior AR, Lopo Tuna M. MYH9-related disorders: a rare cause of neonatal thrombocytopaenia. BMJ Case Rep 2018;2018. doi:10.1136/BCR-2018-224510

[3] Tabibzadeh N, Fleury D, Labatut D, et al. MYH9-related disorders display heterogeneous kidney involvement and outcome. Clin Kidney J 2018;12:494-502. doi:10.1093/CKJ/SFY117

[4] Kelley MJ, Jawien W, Ortel TL, Korczak JF. Mutation of MYH9, encoding non-muscle myosin heavy chain A, in May-Hegglin anomaly. Nat Genet 2000;26:106-8. doi:10.1038/79069

[5] Favier R, Raslova H, Kremlin-Bic L, Roussy G. Progress in understanding the diagnosis and molecular genetics of macrothrombocytopenias. Br J Haematol 2015;170:626-39. doi:10.1111/BJH.13478

[6] Estcourt LJ, Malouf R, Doree C, Trivella M, Hopewell S, Birchall J. Prophylactic platelet transfusions prior to surgery for people with a low platelet count. Cochrane Database Syst

Rev 2018;2018:CD012779. .doi:10.1002/14651858.CD012779.PUB2

[7] Economou M, Batzios SP, Pecci A, et al. MYH9-Related Disease. J Pediatr Hematol Oncol 2021;34:412-5. doi:10.1097/mph.0b013e318257a64b

[8] Fernandez-Prado R, Carriazo-Julio SM, Torra R, Ortiz A, Perez-Gomez MV. MYH9-related disease: it does exist, may be more frequent than you think and requires specific therapy. Clin Kidney J 2019;12:488-93. doi:10.1093/CKJ/SFZ103

[9] Gokcay Bek S, Eren N, Ergul M. Difficult diagnosis of myosin heavy chain 9 related platelet disorder. Kocaeli Medical Journal 2020;9:120-3. doi:10.5505/KTD.2020.33602

[10] Orphanet. MYH9 related disease MYH9 related disorder.. https://www.orpha.net/consor/cgi-bin/Disease_Search.php?lng=EN&data_id=18198&Disease_Disease_Search_diseaseGroup=MYH9relateddisease&Disease_Disease_Search_diseaseType=Pat&Disease(s)/group%20of%20diseases=MYH9-related-disease—MYH9-related-disorder-&title=MYH9-related-disease—MYH9-related-disorder-&search=Disease_Search_Simple Accessed July 30, 2023.

[11] Verver E, Pecci A, De Rocco D, et al. R705H mutation of MYH9 is associated with MYH9-related disease and not only with non-syndromic deafness DFNA17. Clin Genet 2015;88:85-9. doi:10.1111/CGE.12438

[12] Economou M, Batzios SP, Pecci A, et al. MYH9-related disease. J Pediatr Hematol Oncol 2021;34:412-5. doi:10.1097/mph.0b013e318257a64b

MARMARA
MEDICAL JOURNAL

Case Report

https://dergipark.org.tr/tr/pub/marumj

Isolated internal carotid artery dissection after a motorcycle accident: A case report

Morteza ASHRAFI[1,2], Sayed Mahdi MARASHI[3], Foroozan FARESS[3], Morteza TAHERI[1], Bahman MOHAMADI[1], Hamid OWLIAEY[4]

[1] Department of Neurosurgery, School of Medicine, Iran University of Medical Sciences, Tehran, Iran
[2] MAHAK Hematology Oncology Research Center (MAHAK-HORC), MAHAK Hospital, Shahid Beheshti University of Medical Sciences, Tehran, Iran
[3] Department of Forensic Medicine, School of Medicine, Iran University of Medical Sciences, Tehran, Iran
[4] Department of Forensic Medicine and Clinical Toxicology, Islamic Azad University, Yazd Branch, Yazd, Iran

Corresponding Author: Sayed Mahdi MARASHI
E-mail: marashi.mh@iums.ac.ir

Submitted: 08.11.2023 **Accepted:** 19.01.2024

ABSTRACT
Extra cranial carotid artery dissection is one of the most important complications associated with blunt head and neck trauma. It is a major cause of ischemic stroke in young adults. We report a case of internal carotid artery dissection which caused transient hemiparesis, horizontal gaze to right and anisocoria in a 19-year-old male motorcyclist involved in a collision. Unenhanced brain computed tomography scan showed well defined infarction in the right frontotemporoparietal area. Digital subtraction angiography showed complete occlusion of the proximal cervical right internal carotid artery. Moreover, intimal dissection was observed in distal cervical left internal carotid artery which did not limit blood flow to the brain. A stent was placed at the site of dissection in the left internal carotid artery. Intravenous heparin was commenced to avoid further thrombosis. He was discharged home 40 days after the accident with oral anticoagulation. Extra cranial carotid artery dissection is a rare condition which may happen after a non-significant neck trauma. Accordingly, the diagnosis of a cervical vascular dissection requires strong clinical suspicion.
Keywords: Case report, Carotid artery, Traumatic dissection, Cerebral infarction, Traffic injuries

1. INTRODUCTION

Extra cranial carotid artery dissection is one of the most important complications associated with blunt head and neck trauma [1]. However, this event is not common and is frequently associated with non-life threatening injuries; which can be missed on initial examination in the emergency room [2]. Compression against the spine in case of cervical rotation and extension may cause carotid dissections [3]. It is a major cause of ischemic stroke in young adults [1,3].

Motor vehicle accident is the most significant risk factor for carotid artery dissection in previously healthy patients. Inconveniently, most patients remain asymptomatic until the occurrence of cerebral ischemia and define focal neurological deficits usually for longer than 24 hours [4].

Here, we report a case of traumatic carotid dissection; the aim is to attract suspicion regarding this entity as a potentially under-recognized condition behind minor traumatic medical complaints.

2. CASE REPORT

We report the case of a 19-year-old male motorcyclist involved in a collision. He was brought to the emergency room by ambulance. At arrival he was agitated and uncooperative. Following administration of 2 mg midazolam intravenously he became slightly sedated and the initial examinations were done. His vital signs were as follows: blood pressure, 115/80 mm Hg; pulse rate, 85 beats/min; respiratory rate, 12 breaths/min and SpO2, 96%. The initial physical examination revealed multiple abrasions in the upper and lower limbs as well as his right shoulder and an abrasion on the penis, without other significant findings. He underwent extended focused assessment with sonography in trauma (eFAST) and computed tomography (CT) scan of the brain, neck, chest and abdomen which appeared normal. The patient's medical history was procured from his father, who subsequently arrived at the emergency department. The patient had no notable past medical history and was not on any specific medications. Furthermore, there was no record of familial diseases. However, the patient has a history of alcohol intake. Another examination was performed 6 hours after admission. He was

How to cite this article: Ashrafi M, Marashi SM, Faress F, Taheri M, Mohamadi D, Owliaey H. Isolated internal carotid artery dissection after a motorcycle accident: A case report. Marmara Med J 2024: 37(2):259-262. doi: 10.5472/marumj.1487503

ISSN: 1309-9469

http://doi.org/10.5472/marumj.1487503
Marmara Med J 2024;37(2): 259-262

alert and conscious and complained of pain in the neck and right pelvic bone. However, his neck, chest, abdominal, pelvic and back examinations were unremarkable. The patient was discharged and advised to visit a neurosurgery clinic for further evaluation with cervical spine magnetic resonance imaging (MRI).

Two days after discharge, he was transported to our emergency department for weakness, lethargy and dizziness. He also complained of transient hemiparesis, however there were no obvious neurological deficits on examination. His pupils were midsized and reactive to light bilaterally. A brain CT scan was performed, which did not have any specific point. He was transferred to the general ward for further management. The next day, his family announced that he had taken some opium the night before due to pain and insomnia. Therefore, a toxicology consultation was requested. The patient had acceptable vital signs including blood pressure, 95/60 mm Hg; pulse rate, 53 beats/min; respiratory rate, 13 breaths/min and SpO2, 98%. A horizontal gaze to right and anisocoria with right side pupil 4 mm and left side pupil 2 mm in the ambient light were observed. He also had left hemiparesis. The blood glucose level was 185 mg/dl and he had a normal venous blood gas analysis (pH, HCO3-, and PCO2 were 7.43, 23.4 mmol/L and 35.3 mmHg, respectively). These findings were more compatible with a structural problem of brain rather than opium poisoning.

Unenhanced brain CT scan showed well defined infarction in the right frontotemporoparietal area as well as right to left midline shift (Figure 1). The patient underwent decompressive craniotomy and admitted postoperatively to the intensive care unit to provide integrated clinical treatment. Transthoracic echocardiography was performed the next day to exclude cerebral embolic event associated vegetations or mitral valve disease. There was normal sinus rhythm, ejection fraction was 60, and there was no structural abnormality in cardiac chambers.

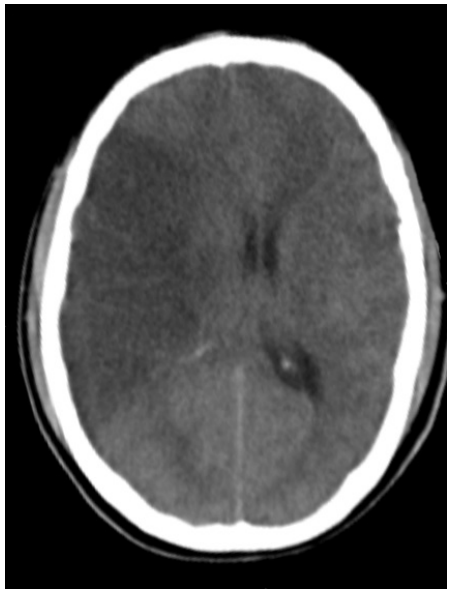

***Figure 1**. Unenhanced brain CT scan. Note the ischemic area in the right frontotemporoparietal region as well as right to left midline shift.*

Computed tomography angiography (CTA) of extracranial carotid arteries demonstrated normal internal, external and common carotid artery of both sides, without any signs of stenosis or filling defect. Both vertebral arteries were normal as well. Nevertheless, digital subtraction angiography (DSA) showed complete occlusion of the proximal cervical right internal carotid artery (Figure 2).

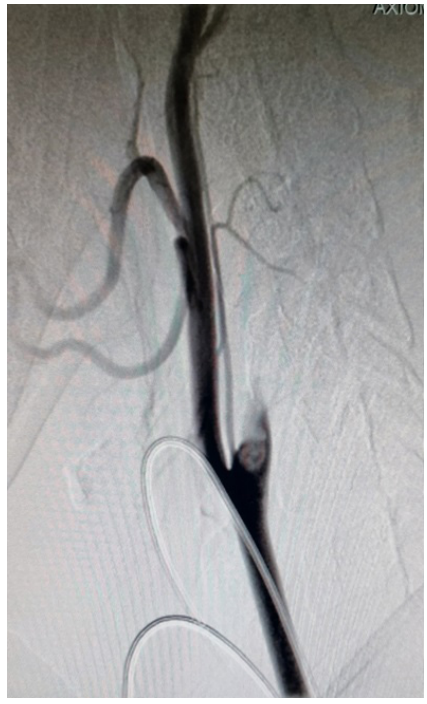

***Figure 2.** Digital subtraction angiography. Note the occlusion of the right internal carotid artery, distal to the carotid bifurcation*

The stopped blood flow was consistent with the massive right ischemic stroke. Moreover, intimal dissection was observed in distal cervical left internal carotid artery which did not limit blood flow to the brain. A stent was placed at the site of dissection in the left internal carotid artery. Intravenous heparin was commenced to avoid further thrombosis. He was discharged home 40 days after the accident with oral anticoagulation with aspirin and clopidogrel for 3 months.

He was last visited 4 months after the accident, at which time he was alert and oriented. His cranial nerve examination revealed a visual acuity of hand motion in right eye and left-sided seventh nerve palsy. He had left hemiparesis which was more severe at the lower limb. He was referred to a rehabilitation facility for prolonged neuromotor rehabilitation. Timeline of symptoms, diagnosis, and treatment of the patient are given in Table I.

http://doi.org/10.5472/marumj.1487503
Marmara Med J 2024;37(2): 251-262

Table I. *Timeline of the patient's examination and therapy*

Hour/Day	Event	Investigation/ Treatment
Hour 0/Day 0	Collision involving a motorcyclist. agitation, uncooperation. acceptable vital signs, abrasions in the upper and lower limbs and penis.	Bedside eFAST scan – normal. CT scan of the brain, neck, chest and abdomen – normal
Hour 6/Day 0	Haemodynamically stable, conscious, complain of pain in the neck and right pelvic bone.	Neck, chest, abdominal, pelvic and back examinations – unremarkable. Discharged and advised to visit a neurosurgery clinic for further evaluation with cervical spine MRI in 7 days
Day 2	Readmission due to weakness, lethargy, dizziness and transient hemiparesis.	Neurological examination – normal. Brain CT scan – unremarkable. Admission in general ward for observation
Day 2	Family's account of him consuming opium the previous night due to pain and insomnia.	Toxicology consultation.
Day 3	Visit on ward by toxicologist. Acceptable vital signs, including respiratory rate, 13 breaths/min and SpO2, 98%. Horizontal gaze to right, anisocoria, left hemiparesis.	Blood glucose, 185. Normal venous blood gas analysis. Brain CT scan – infarction in the right frontotemporoparietal area as well as right to left midline shift. Decision for decompressive craniotomy. Admission in ICU
Day 4	Ongoing review.	Transthoracic echocardiography – ejection fraction 60, no structural abnormality in cardiac chambers. CT angiography – without any signs of stenosis or filling defect in internal, external and common carotid arteries.
Day 12	Ongoing review.	Digital subtraction angiography – complete occlusion of the proximal cervical right internal carotid artery and intimal dissection in distal cervical left internal carotid artery without limitation of blood flow to the brain.
Day 14		Stent placement at the site of dissection in the left internal carotid artery. Intravenous heparin to avoid further thrombosis.
Day 40	Ongoing review. Approved for discharge by neurosurgery team.	Refer to a rehabilitation clinic. Reviewed in clinic in about 80 days.
Day 120	Reviewed in neurosurgery clinic.	Scheduled for cranioplasty. Refer to a rehabilitation clinic.

3. DISCUSSSION

Dissection of the cervical carotid artery in the context of blunt head or neck trauma is a potentially devastating injury due to the considerable huge ischemic stroke in young adults. On average, symptoms of ischemic stroke appear in 2 days; however, this can be delayed up to about 4 months [5]. It is a rare condition that makes up approximately 0.08 to 0.4% of all traumatic injuries [6]. The main mechanisms of the injury include rotation and extension of the neck. Unexpectedly, even a non-significant neck trauma may cause cervical carotid artery dissection [1,7].

During the acute phase, the clinical presentation may remain subtle, unless the dissection is complicated with thrombus formation and subsequent infarction of the underlying brain [4]. Unfortunately, it is impossible to identify a damage mechanism based on the history taken from the patient, especially after traffic accidents. Accordingly, the diagnosis of a cervical vascular dissection requires strong clinical suspicion. On physical examination, the neck should be evaluated for petechiae or bruising, and auscultation for neck bruits should be performed. Bedside ultrasound imaging can help in assessment of cervical artery dissection, nevertheless it is not a sensitive test for small intimal tears [1,8,9]. Unfortunately these were not done in our case.

Digital subtraction angiography is the gold standard protocol for the diagnosis of cervical artery dissection; hence, CTA has a sensitivity of 66-98% in comparison with DSA [10]. CTA could not find culprit lesion in our case, but the DSA showed complete occlusion of the proximal cervical right internal carotid artery. The stopped blood flow was consistent with the massive right ischemic stroke. Of course, this delayed diagnosis did not help to change the prognosis of our patient.

The best action should be taken in the shortest possible time, in managing the emergency patient. Therefore, cervical CTA can be helpful in high-speed accidents, where the vascular damage is considered [11]. Doppler sonography is also useful in the diagnosis of changes in the flow profile with a sensitivity of 79% and a specificity of 94% in comparison with CTA [12]. If the findings were positive, the best possible therapy for the patient may be implemented after consultation with a vascular neurologist.

Fully alert and well-oriented patients benefit from antiplatelet drug therapy. In contrast, patients suffering from progressive

http://doi.org/10.5472/marumj.1487503
Marmara Med J 2024;37(2): 251-262

neurological symptoms may benefit more from surgical treatment. However, due to its perioperative morbidity and mortality, open surgery is currently advocated for potentially life-threatening conditions. Minimally invasive stenting has become an extremely effective and safe method for vascular repair, instead [1]. However, our patient was conscious at the time of discharge after the initial visit; it seems that he was not well informed about neurological red flags at that time, as his neurological exam was initially unremarkable.

He was returned to the hospital with weakness, lethargy and dizziness; but a complete neurological exam was not performed due to the history of opium consumption. While, there were obvious neurological deficits, including hemiparesis, anisocoria and horizontal gaze, brain CT scan showed massive infarction in the right frontotemporoparietal area and midline shift. Therefore, he had lost the golden time for the diagnosis and treatment due to delayed referral. However, according to the DSA, intimal dissection in the distal cervical left internal carotid artery was diagnosed and treated using stent placement and anticoagulant therapy.

In conclusion, we consider that without proper diagnosis and treatment, this lesion could cause a similar stroke on the left side in the future. ICA dissection is a differential diagnosis to consider in trauma patients presenting with hemiparesis. Numerous case studies of traumatic ICA dissection can be found in the existing medical literature [1-3,6,7,11]. The patient in our case study was brought to our emergency department two days after his accident, presenting symptoms of weakness, lethargy, and dizziness. He also reported experiencing transient hemiparesis. Despite the patient's initial CT scan presenting as normal, medical professionals should have considered the potential for an ICA dissection given the patient's complaints. It would have been prudent to conduct an angiography prior to the onset of a massive CVA.

Compliance with Ethical Standards

Ethical standards: This work was conducted ethically by following per under Helsinki World Medical Association Declaration.

Patient consent: The patient gave his consent for clinical information and images relating to his case to be reported in a medical publication.

Conflict of interest: The authors declare that they have no conflict of interest.

Authors' contributions: MA, SMM and MT: Design, FF, SMM and BM: Supervision, MT, MA and SMM: Resources-Materials, FF, SMM, BM, MT and MA: Data collection and and/or processing, FF, SMM, HO,MT, MA and BM: Analysis and/or interpretation, MA, SMM and MT: Literature search, HO and SMM: Writing the manuscript, MA, SMM and MT: Critical review. All authors approved the final manuscript to be submitted.

REFERENCES

[1] Brand S, Teebken OE, Bolzen P, et al. Traumatic dissection of carotid arteries caused by high energy motorcycle accident [Article in German]. Unfallchirurg 2012;115:930-5. doi:: 10.1007/s00113.011.2078-7

[2] Molacek J, Baxa J, Houdek K, Ferda J, Treska V. Bilateral post-traumatic carotid dissection as a result of a strangulation injury. Ann Vasc Surg 2010;24:1133.e9-11. doi: 10.1016/j.avsg.2010.02.042.

[3] Biller J, Sacco RL, Albuquerque FC, Demaerschalk BM, Fayad P, Long PH, et al. Cervical arterial dissections and association with cervical manipulative therapy: a statement for healthcare professionals from the american heart association/american stroke association. Stroke 2014;45:3155-74. I: 10.1161/STR.000.000.0000000016

[4] Biffl WL, Ray CE Jr, Moore EE, et al. Treatment-related outcomes from blunt cerebrovascular injuries: importance of routine follow-up arteriography. Ann Surg 2002;235:699-706. doi: 10.1097/00000.658.200205000-00012.

[5] Baumgartner RW, Arnold M, Baumgartner I, et al. Carotid dissection with and without ischemic events: local symptoms and cerebral artery findings. Neurology 2001;57:827-32. doi: 10.1212/wnl.57.5.827.

[6] Wachal K, Koczewski P, Gabriel M, Kociemba W. Isolated internal carotid artery dissection in a long-distance runner. Wideochir Inne Tech Maloinwazyjne 2016;11:304-8.

[7] López-Sánchez M, Ballesteros-Sanz MA, Pérez-Ceballos A, González-Fernández C, López-Espadas F. Traumatic dissection of the internal carotid artery by a safety belt: a report of two cases [Article in Spanish]. Med Intensiva 2009;33:353-7.

[8] Wachal K, Koczewski P, Gabriel M, Kociemba W. Isolated internal carotid artery dissection in a long-distance runner. Wideochir Inne Tech Maloinwazyjne 2016;11:304-8. Wachal K, Koczewski P, Gabriel M, Kociemba W. Isolated internal carotid artery dissection in a long-distance runner. Wideochir Inne Tech Maloinwazyjne 2016;11:304-8.

[9] Benninger DH, Baumgartner RW. Ultrasound diagnosis of cervical artery dissection. Front Neurol Neurosci 2006;21:70-84.

[10] Galyfos G, Filis K, Sigala F, Sianou A. Traumatic Carotid Artery Dissection: A Different Entity without Specific Guidelines. Vasc Specialist Int 2016;32:1-5.

[11] Rutman AM, Vranic JE, Mossa-Basha M. Imaging and management of blunt cerebrovascular injury. Radiographics 2018;38:542-63.

[12] Petetta C, Santovito D, Tattoli L, Melloni N, Bertoni M, Di Vella G. Forensic and clinical issues in a case of motorcycle blunt trauma and bilateral carotid artery dissection. Ann Vasc Surg 2020;64:409.e11-409.e16.

[13] Tsivgoulis G, Sharma VK, Lao AY, Malkoff MD, Alexandrov AV. Validation of transcranial Doppler with computed tomography angiography in acute cerebral ischemia. Stroke 2007;38:1245-9